Cracking in the welding of cupro-nickel alloys

By: Adrian Duncan MSc AMIM

A thesis submitted to

THE UNIVERSITY OF ASTON IN BIRMINGHAM

For the award of Doctor of Philosophy

June 1985

SUMMARY

Cracking in the welding of cupro-nickel alloys

Adrian Duncan PhD June 1985

University of Aston in Birmingham

The problem of variation in weld crack susceptibility caused by small variations in alloy and impurity elements for the 70-30 cupro-nickel alloy has been investigated. Both wrought and cast versions of the alloy have been studied, the main techniques employed being the Varestraint test and weld thermal simulation.

In the wrought alloys, cracking has been found to occur mainly in the weld metal, whilst in the cast alloys cracking is extensive in both weld metal and heat affected zone. The previously reported effects of certain impurities (P,S,Si) in increasing cracking have been confirmed, and it has also been shown that Ti and Zr may both have a crack promoting effect at levels commonly found in cupro-nickels, whilst C can interact with several of the other elements investigated to produce a beneficial effect.

The testing carried out using the weld thermal simulator has shown that a relationship does exist between hot ductility and weld cracking. In particular, the absence of the peak in ductility in the range 1100°C-900°C on cooling from a temperature near to the solidus is indicative of a highly crack susceptible alloy.

Principal practical implications of the investigation concern the relationship of weld metal cracking to alloy composition, especially the level of certain impurities. It would appear that the upper limits permitted by the alloy specifications are unrealistically high. The introduction of lower impurity limits would alleviate the current problems of variability in resistance to cracking during welding.

Key words: Cupro-nickel alloys

Welding

Cracking

CRACKING IN THE WELDING OF CUPRO-NICKEL ALLOYS

A thesis submitted to the University of Aston
in Birmingham for the degree of PhD.

June 1985

DECLARATION

I, the undersigned, hereby declare that no part of the work described in this thesis was done in collaboration, and that the work has not been submitted for any other award.

A. Duncan

Adrian Duncan

CRACKING IN THE WELDING OF CUPRO-NICKEL ALLOYS

CONTENTS

LIST OF TABLES (APPENDIX A)

LIST OF FIGURES (APPENDIX B)

1. INTRODUCTION

Cupro-nickel alloys, of both the 70-30 and 90-10 varieties, have found steadily increasing use in seawater systems, particularly over the last twenty years. The areas of application include most pipework systems for carrying sea-water. In particular, the use of the alloys is widespread in naval vessels, where the higher cost is acceptable in return for better performance and reliability. In recent years, the alloy has also become attractive for offshore oil platforms, where the high cost of downtime (currently £2.5 million/day) and difficulty of repairs at sea are important considerations.

Clearly, the major properties required from a material which is to be used in such demanding environments are resistance to corrosion and erosion in moving sea water. These requirements are amply met by cupro-nickels containing 1-2%Fe. A typical piping system consists of a mixture of wrought material i.e. tubes and various cast components e.g. valve bodies. This provides a further material requirement, in that the alloy must be easily produced in both wrought and cast forms. Again, cupro-nickel appears to fit this requirement. A third important property possessed by cupro-nickel is its anti-fouling characteristics. This ability to remain free from marine organisims which adhere to steels has made the use of cupro-nickel clad hulls a possibility for future ships.

One factor which has posed some difficulty in the application of these alloys has been the problem of cracking during welding. In

particular, the variation in welding response between different heats produced to the same specification has been a cause for concern. Welding is needed both for the production of cast/wrought fabrications, and for repair welding of castings, and clearly the ability to produce consistent welds is essential to the further development of these alloys.

The considerable practical importance of the alloys has resulted in a number of investigations of the cracking problem. The heat to heat differences have been attributed to small variations in the impurity element content, and a number of elements which cause cracking in other copper alloys have been shown to contribute significantly to this e.g. P, S, Si. In addition to investigations of cracking using various weld configurations and cracking tests, studies of the hot tensile properties of the alloys have also been carried out. These have demonstrated the ductility-dip characteristic of many face-centred cubic alloys, and the dependence of the size and shape of the dip on the presence of certain impurities e.g. Bi, Pb.

However, the work which has been carried out has left a number of important gaps in the development of an overall picture of the problem. The work on cracking has concentrated largely on elements, such as those mentioned above, known to cause cracking in many copper alloys. Less common impurites, or elements which may be intentionally added in small quanitities e.g. Ti or Zr for grain size control, appear to have been overlooked. The same criticism can also be levelled at the use of hot tensile techniques. In addition, a further difficulty with this work has

been the problem of establishing any widely applicable criteria for relating hot ductility to cracking. It is to the investigation of these areas that this work will be dedicated.

The first section of this thesis consists of a review of literature concerned with cracking and hot ductility of cupro-nickel alloys, supplemented by brief coverage of applications of the alloys and relevant test techniques. This review is concluded with a summary which details the current state of knowledge and the gaps which this work seeks to fill. The experimental work described herein consists of parallel weld cracking tests and hot ductility determinations. These are carried out on a series of alloys with controlled variation of a number of compositional variables within specification limits, utilising factorial experimental designs. Effects of these elements are assessed using linear regression analysis, metallographic studies and plots of mechanical properties against temperature.

The results obtained have enabled the effects of a number of elements on cracking and hot ductility to be determined. A relationship between hot ductility and cracking has also been established.

2. LITERATURE REVIEW

2.1. Introduction

The problem of cracking in the welding of cupro-nickel alloys (both 70-30 and 90-10) has been recognised for many years, and a number of investigations have been carried out [1-9]. The first investigator to recognise the importance of trace elements on the crack susceptibility of these alloys was Witherell [1]. He proposed that elements having a low solid solubility in copper and those which form low melting point eutectics with copper were chiefly responsible for cracking of the segregation type, as defined by Hemsworth et al. [10].

For a number of years following this work, no further investigation was carried out, but a resurgence of interest occurred, coinciding with the development of various high strength cast 70-30 alloys [2,3,11]. A number of elements were recognised as having a deleterious effect on resistance of the alloys to one or both types of cracking (segregation and ductility dip). Predominant amongst the elements having deleterious effects are Si[1,2,4,5] P [1,5-8] S[1,6,8] Pb[1,5,6], Cr[3,6,11] and Bi[1,6]. Other elements proposed at various times as crack promoters are B, Cd, Se, Te[1], C[6], Mn[7] and Ag[9]. Detrimental interactions which have been determined are P-Fe, Sb-Fe, P-Sb[7] and Pb-Si[5]. Certain elements have been suggested as crack inhibitors, notably Nb[2,4], and also V[4]. Two elements, Ti[4,5] and Sb[1,7] have been found capable of acting as inhibitors and promoters in different circumstances.

Complementary to the cracking studies, the hot ductility properties of the alloys have also been established in a number of investigations[12-17]. Most notable amongst these has been the work done by Chubb, Billingham and their associates[12-15]. Their attention was concentrated on the effect of alloy and impurity elements on the intermediate temperature ductility dip in cast alloys. Elements shown to cause a loss in ductility were Ni[12,13], Fe[13], Si[13], Al[13], Pb[14,15], Bi[15] and Se[15] One element, Mn, was shown to produce an improvement in hot ductility properties. Middleton[18] found that Ni and Zr were both responsible for reducing hot ductility, whilst Lupton and Thompson[16] attributed an improvement in ductility above 700°C to the presence of Nb. Recent work by Evans and Jones[17] established that failure in hot ductility samples could be traced to cavities nucleated at manganese sulphide inclusions.

Although a considerable amount of information has been generated regarding both cracking and hot ductility, little has been achieved in the efforts to quantitatively relate one to the other. An attempt by Lupton and Thompson[16] to follow up earlier work[4] which had shown Nb, V and Ti to reduce cracking in Si-containing alloys met with limited success. V and Ti had no effect on hot ductility, and Nb, although reducing the depth of the ductility trough, did not eliminate it entirely. Holsberg[11] also made use of both weld tests and hot ductility determinations in his investigations. However, his Cr and Fe strengthened alloys did not exihibit cracking in the HAZ, and he was unable to carry out weld testing on the Be containing alloy. Consequently, no correlation between HAZ cracking and hot ductility could be made.

The total of these efforts has been to generate a large amount of information regarding the effects of various alloy and impurity elements. However, many questions remain unanswered regarding the differences in elemental action between wrought and cast materials, interactions between various elements and the relationship between cracking and the results of hot ductility testing.

2.2. Properties and uses of cupro-nickel

2.2.1. Properties

The potential for using alloys of the 70-30 Cu-Ni type for applications requiring resistance to sea water corrosion has been realised for over 60 years. However, the basic alloy is limited in its use because of low strength and poor resistance to erosion. This latter is a particular problem in contaminated sea water, or where turbulence leads to a high entrained air content. This problem was investigated by Bailey[19], who concluded that the addition of Fe in the range 0.3-4% produced an alloy resistant to impingement attack. Increasing Mn content also reduced this type of corrosion, but the effect of Mn was masked at Fe contents in excess of 0.3%. However, he found that the range of Fe contents was further restricted by the problem of deposit attack, which under certain conditions was rapid and extensive in alloys containing 2% or more Fe. He therefore concluded that the optimum range of Fe contents was 0.5-1%. The level of Fe proposed by Bailey is reflected in the composition of wrought 70-30 Cu-Ni alloys currently in use.

Mn is also present in cupro-nickels, acting as a deoxidiser and desulphuriser. Additionally, Mn also makes a small contribution to corrosion resistance, and aids fluidity both in casting and welding.[20] Use of Mn in this way can be detrimental if S content is high. MnS stringers may be formed in the wrought material, and these assist the fracture process by providing sites for cavity nucleation.[17]

The 70-30 Cu-Ni alloy, listed as the British Standard,[21] designated CN107, contains 0.4-1.0%Fe and 0.5-1.5%Mn. In addition, a special 70-30 Cu-Ni alloy (CN108) is available, for use in situations where erosion is a particular problem. This alloy contains 1.7-2.3%Fe and 1.5-2.5%Mn.

Whilst the erosion and corrosion resistance of the cupro-nickel alloys make them extremely attractive for use in moving sea water applications,[22,23] this group of alloys possess a further important property which enhances their usefulness. This is anti-fouling, the ability of the material to almost totally prevent growth of marine organisms on its surface. The importance of this has been shown previously,[24-26] and relates largely to the increase in turbulent flow which this type of growth produces.

The strength of the basic 70-30 Cu-Ni alloy, with Fe and Mn additions as outlined above, compares favourably with many copper alloys, with UTS $\approx 420 Nmm^{-2}$ and yield stress $\approx 200 Nmm^{-2}$. This level of strength is adequate for the majority of areas in which the alloy might find use. However, investigations of various alloying elements and the use of heat treatment have been carried

out in an effort to develop higher strengths for special applications, whilst retaining good corrosion resistance.[11,27] Badia et al[27] varied Cr up to 4%, and found that by air cooling from the annealing temperature, a spinodal decomposition occurred, causing substantial hardening. Subsequent work by Peterson[3] showed that a maximum Cr level of 2.8% was consistent with good weldability, and this alloy had a yield strength of $350Nmm^{-2}$. Significantly, this strength could be achieved with little variation in a range of thicknesses because of the nature of the spinodal decomposition. The decomposition reaction was studied in greater detail by Bower et al,[28] who looked at alloys in the range 9-56%Ni and 2.5-16%Cr. Their work showed that alloys whose composition lay in the centre of the ternary miscibility gap underwent the spinodal reaction.

The Cr containing 70-30 Cu-Ni alloy was also investigated by Holsberg,[11] who additionally looked at alloys strengthened by Fe and Be. The Fe-modified alloy, with a nominal Fe content of 5.25%, achieves a yield strength similar to that of the Cr-modified alloy. The strengthening mechanism is different, however, utilising a complex thermal treatment consisting of annealing, followed by a double stabilising treatment. No second phase is precipitated, but instead a continuous and periodic compositional variation appears throughout the structure. The Be-modified alloy contains the element at a nominal level of 0.5%, giving a yield strength of the order of $620Nmm^{-2}$. This alloy is strengthened by a precipitation hardening mechanism, the precipitate being a complex copper-nickel-beryllide.

Overall, the 70-30 Cu-Ni is extremely useful for seawater applications. However, some serious limitations do exist, and these will be discussed in the following section.

2.2.2. Limitations of cupro-nickel alloys

Whilst the metallurgical properties of the 70-30 Cu-Ni alloy are encouraging, there are several practical problems which must be overcome. The most significant of these are:

1. The need for a compatible casting alloy with similar strength, to facilitate the construction of complete systems from the 70-30 alloy.

2. The high cost of an alloy containing 30% Ni, which would make it desirable to achieve similar properties in an alloy with lower Ni content. This is due in part to the high price of Ni, but also to the inability to manufacture the high Ni alloy in traditional copper foundaries, because of its higher melting point.

3. The variable weldability of alloys produced within any particular specification. This is the subject of the present work.

The major problem to be overcome in producing a cast 70-30 Cu-Ni alloy is the attainment of sufficient strength. The basic 70-30 alloy, in the wrought form is strengthened only by work hardening. In practice, however, the alloy is normally used in

the annealed condition, as welding would have the effect of annealing during fabrication. Despite this fact, the alloy in the as-cast state has a considerably lower strength (yield stress $\simeq 100 Nmm^{-2}$) than its wrought counterpart. This significant difference is explained largely in terms of the marked segregation to which these alloys are subject. Distribution coefficients as large as 2.4 have been reported,[29] and this would indicate regions containing as little as 12.5% Ni. This is likely to result in a considerably lower overall strength.

The problem of producing a compatible casting alloy has been tackled by a number of investigators.[2,30-33] As previously discussed in connection with the wrought alloys, Cr, Fe and Be have all been shown to improve strength, and these have also been studied in cast alloys. An early attempt to look systematically at the problem was made by Vanick.[30] He looked at the effect of a number of alloy and impurity elements in cast cupro-nickel, and concluded that increasing Fe, Si, C (up to 0.15%) and Al all provided increased strength, whilst increasing S and Pb caused a decrease in tensile properties. Shepherd[31] used a Si-containing alloy, and found that 1%Si produced a yield stress of $480 Nmm^{-2}$. Nb was also present in his alloy, contributing a further strengthening effect, although its prime function was to improve weldability. The Nb-Si containing alloy was also favoured by Calvert,[2] who used an alloy containing 1.2-1.4%Nb and 0.35-0.55%Si. French and Evans[32] modified a standard 70-30 Cu-Ni alloy with 0.5% Be, and were able to achieve a yield stress of $570 Nmm^{-2}$. Ansuini and Badia [33] varied a number of elements; Cr, Si, Ni, Fe, Mn, Nb, Ti, Al, Zr and C. The main objective of their

work was to develop a Cr-Si strengthened alloy. With 1.4-2.0%Cr, 0.3-0.6%Si and Ni at the optimum level of 30%, good toughness and a yield stress of $350Nmm^{-2}$ can be obtained. Furthermore, it was observed that increases in Fe, Mn, Nb, Ti and Al, all of which would normally increase strength, had no effect on the Cr-Si containing alloy. This alloy (IN 768) is the most widely used 70-30 casting alloy, containing, in addition to Cr and Si, 0.7%Fe, 0.6%Mn, 0.05%Ti and 0.1%Zr.

As stated above, the high cost of Ni is also an important factor in the selection of these alloys. Whilst this may be acceptable in some applications, it is clearly desirable to seek an acceptable level of properties in a lower Ni alloy i.e. the 90-10 alloy. An early investigation of the 90-10 alloy was carried out by Bailey.[19] He proposed a 90-10 alloy containing 1.3-2%Fe, and concluded that this had a corrosion resistance compatible with 70-30 Cu-Ni alloys of lower Fe content (0.3-0.5%).

The other important consideration in the 90-10 Cu-Ni is strength, particularly in the development of a casting alloy. This problem has been tackled by a number of investigators.[20,34-37] The approach taken by Townsend[3,4] was to model his 90-10 casting alloy on the Nb-Si strengthened 70-30 alloy which had previously been developed.[2] However, the Nb was found to reduce ductility, unlike its effect in the 70-30 Cu-Ni, and so the final alloy contained Si alone as a strengthener. This gave a yield strength of $300Nmm^{-2}$.

The alloy produced by Guha et al[35] is a complex alloy, relying

chiefly on Al as a strengthening agent. The use of a cast Cu-Ni-Al alloy is hampered by its poor impact strength, and this was attributed to excessive precipitation of Ni_3Al during slow cooling. Precipitation also made the alloy difficult to weld. The properties of the alloy were improved by reducing Al content from 3% to 2%, and adding 5%Fe and 10%Mn. Final Ni content was 14%, and the yield stress value 290Nmm^{-2} in the as-cast condition, with the possibility of improving this substantially by a low-temperature heat treatment.

This alloy was further developed by Dimbylow and Jones,[36] who added 0.3%Ti. This improves weldability by reducing the grain size, and allows Mn to be kept low (8%). 0.3%Ti is the optimum value; above this, ductility will drop off. This alloy has an improved yield strength of 325Nmm^{-2}.

Bagley and Brook[37] utilised Mn and Fe as their alloying elements, although Be, Ti and B were all assessed for their strengthening effect. Mn produces solid solution hardening up to a maximum content of 15%Mn, above which insoluble NiMn is formed. The final level of Mn selected was 10-12.5%, additional strength being obtained by the use of 7%Fe. Alternatively, Fe may be partially replaced by Co (up to a maximum of 2%), which will reduce the risk of forming a continuous brittle phase, whilst retaining the required strength. This alloy requires an ageing treatment to develop its strength, and in the aged condition has a yield stress of 460Nmm^{-2}.

The range of work which has been carried out on development of

cupro-nickel alloys has shown that by suitable alloying additions, high strength wrought and cast versions of both 70-30 and 90-10 alloys can be produced. Mechanical properties and corrosion resistance are excellent, but despite many investigations, weldability is often poor and variable from heat to heat.

2.2.3. Welding Processes

Cupro-nickel alloys, of both the 90-10 and 70-30 varieties are weldable by all of the common arc-welding processes,[38] and recent research[39,40] has shown that several of the more modern processes can also be applied successfully to these alloys. The most commonly used processes are the inert gas processes, MIG and TIG, and these have now virtually replaced the traditional manual metal arc and gas welding techniques for all copper alloys, including the cupro-nickels.[41,42] However, manual metal arc is retained for certain purposes. It can be useful in joining dissimilar metal combinations e.g. cupro-nickel to steel, where alternating current MMA can overcome the problem of arc deflection.[38] The MMA process has been used by Scott[6] in a buttering technique designed to eliminate cracking in the welding of high strength cast 70-30 Cu-Ni. The buttering technique may also be used on steel which is subsequently to be welded to cupro-nickel.[43]

Two other arc processes which have found limited use to date for joining cupro-nickel but have considerable potential, are plasma arc [44] and submerged arc.[45,46] A number of other techniques

have been successfully employed for the joining of Cu-Ni to steel. These include explosive welding, [47] laser welding [39] and ultrasonic welding.[40] Resistance welding is also a suitable method for joining of cupro-nickel sheet.[38]

2.2.4. Uses of cupro-nickel

As discussed in Section 2.2.1, cupro-nickel displays a combination of properties which make it very attractive for use in a seawater environment. The most significant of these are good resistance to corrosion and erosion, a reasonable strength level and anti-fouling properties.

The traditional use, and still the most important, is the construction of seawater piping systems, condensers and heat exchangers.[14,38,42,44,46]. These are installed both in ships and static installations which rely on seawater for cooling. In the latter, the cooling water is often silt laden, and the erosion resistance of cupro-nickel is particularly important. Any seawater system of this type is obviously a mixture of wrought components, i.e. tube, and various castings, e.g. valve bodies. Clearly for the alloy to be useful, it must be readily weldable. Cupro-nickel is also widely used for pipework systems in the chemical plant and petroleum industries.[14,38,46]

More recently, a new use for cupro-nickel alloys has been investigated; namely, the construction of complete hulls from either Cu-Ni or Cu-Ni clad steel.[26,40,49-51] In normal vessel operation, the roughness of a conventional steel hull increases

rapidly due to a combination of corrosion and fouling by marine organisms. It has been demonstrated by Parker[52] that for every 10μm increase in surface roughness, the hull efficiency is reduced by 1%. Cupro-nickel hulls remain largely free from both corrosion and fouling, and so can be economically justified for certain types of ship, in spite of their high initial cost.[53,54]

Gilbert[24] has suggested that cupro-nickel might find use in a number of applications on offshore production platforms, including seawater pipelines, heat exchangers, hydraulic and pneumatic control lines and cladding of splash zones. Again, the high initial cost is offset, in this case by the cost of lost production time and the difficulty of carrying out repairs in situ.

2.3. High temperature cracking in welding of metals

2.3.1. Definition of crack types

The literature contains considerable work on the cracking of cupro-nickels and other alloys during welding. However, the value of much of this work is reduced, and comparison of results obtained by different authors made more difficult, because of the considerable confusion over the terminology used. Hot cracks, hot tears, fissures, super-solidus cracks and sub-solidus cracks have all been used to describe cracking in both weld metal and heat affected zone (HAZ), sometimes more than one term being used in a single paper.

Hemsworth et al[10] proposed a classification for high temperature cracks, based on their microstructural characteristics. This divides cracking into two major types: Type 1, separations along boundaries decorated by films of second phases resulting from microsegregation (solidification cracking in the weld metal and liquation cracking in the HAZ); Type 2, the cracking of migrated grain boundaries free from films but subject to failure because of the intermediate temperature range ductility dip in some alloys.

The two main types are then further subdivided, each into three categories. These six categories are illustrated in Fig. 1, together with the form of cracking in either casting or hot working which is synonymous with the welding crack.

Type 1A, weld metal solidification cracking, is the term which should be applied when the crack path is intimately associated with the solidification microstructure, and not because it is presumed that the cracking occurred only in the interval of solidification. Cracking may occur along the solid impurity films after completion of solidification. It may be along cell boundaries, grain boundaries or between dendrites. Type 1B, HAZ liquation cracking, is defined as pertaining to solid metal which has been heated to a temperature range just below the solidus of its bulk metal matrix, but in which pockets of liquid occurred for some reason. It does not necessarily occur while the liquid films are present, but is associated microstructurally with liquation and film formation. Type 1C, weld metal liquation cracking, is similar in its nature to HAZ cracking. However, the

situation in this case is complicated by the possible presence of type 1A cracking, produced during the original solidification of the weld. In order to simplify definition of the crack type, Hemsworth et al suggested that cracking only be classified as type 1C when type 1A was completely absent. In practice, this would mean that if cracking was found in as-deposited weld metal, and the extent of cracking was increased when this material was reheated, then all of this cracking would be defined as type 1A. Cracking would only be designated as type 1C if it appeared solely in reheated weld metal and no cracking was found in the as-deposited weld metal.

Type 2 cracking is ductility-dip cracking, occurring along grain boundaries free from films. It is associated with low ductility below the rapid recrystallisation temperature. Type 2A is ductility-dip cracking in the HAZ. Type 2B, ductility-dip cracking in as deposited weld metal, occurs in newly migrated grain boundaries, and the crack path cuts across the solidification structure. Type 2C, ductility-dip cracking in reheated weld metal, can be distinguished from Type 2B only when the cracking along migrated boundaries is confined to the reheated regions.

This system of crack classification is an extremely useful tool in the study of cracking during welding, and since its publication has been utilised by many other investigators. However, one anomally does arise with cast cupro-nickel alloys. This can be seen in several investigations,[18,55,56] where intermediate temperature cracking has been reported. This

cracking has been found to pass through the inter-dendritic regions, and has been associated with either the lower inherent strength of this material, or the presence of solid particles or films which are easily fractured. This cracking clearly does not fit into the pattern of high temperature cracking described by Hemsworth et al.[10] Whilst the mechanism of cracking is one of segregation, the temperature at which the cracking occurs is below the recrystallisation temperature, in common with ductility-dip cracking. The latter seems to be the more important factor, and so this type of cracking will be classed as ductility-dip cracking in this present study.

2.3.2. Theories of cracking

As outlined in the preceding section, considerable confusion has existed over the terminology used to describe high temperature cracking in welds, and this confusion has spread even to those investigators who have proposed theories of cracking. In order to simplify this review, suggested theories will be surveyed separately for segregation cracking and ductility dip cracking.

2.3.2.1. Segregation cracking

Segregation cracking, as defined earlier, includes both solidification cracking and liquation cracking. However, for the purpose of discussing mechanisms, these two sub-types can be considered together. They are very similar, because the situation which arises from the liquation of films is identical to that occurring during the last stages of solidification.

One explanation of this type of cracking is to be found in the skrinkage-brittleness theory, the development of which is largely attributed to Singer and his colleagues.[57-61] The essential feature of this theory is that at a certain stage during growth, the primary dendrites come into contact and interlock. This is the coherence temperature. Further cooling of the metal will result in the development of contraction strains, and ultimately cracks in the metal. It is therefore evident that cracking only occurs in the brittle range between the coherence temperature and the solidus. The extent of cracking is proportional to the width of this brittle temperature range.[57] In a separate study,[59] the tensile properties were related to the cracking behaviour. The extent of the temperature range above the solidus over which the alloys possess a finite strength yet have no appreciable ductility is proposed as one of the principal factors determining hot cracking susceptibility. Further support for the theory was contained in an investigation of various levels of alloying elements added to Al.[58] The addition of a small amount produces considerable increase in cracking, but subsequent additions gradually reduce the extent of cracking. This is consistent with the theory, because the brittle temperature range increases rapidly with alloy content up to the solid solubility limit, and then gradually decreases beyond this.

An alternative theory of cracking was proposed by Pellini and his co-workers.[23,75,127] This was referred to as the strain theory of hot tearing. Pellini[62] reasoned that hot cracks could not occur as early in the solidification process as had been proposed in the previous theory. The strain theory predicts that this is

not possible because the shrinkage strains are uniform, and are not sufficiently large to cause cracking at this stage. Instead, cracking can only occur in the last stages of solidification, when much of the alloy is solid, and only liquid films persist. At this point, high localised strains are present, causing fracture of the liquid films; this is the mechanism of crack formation. The effect of impurity elements is explained in terms of their tendency to form low melting point segregates.[62,63] These often exist in the liquid state well below the bulk solidus of the material, and therefore are extremely susceptible to the very high strains which may exist at these temperatures.

Both of the early theories had been developed primarily to cover high temperature cracking in castings, although both groups of authors suggest that their work is equally applicable to high temperature cracking in the welding situation. However, Pellini[62] states that the time for which the liquid film exists is crucial, as the separation developed in the films is additive with time. Clearly, the time involved in weld metal solidification is extremely short compared with casting. For a similar level of cracking to be developed, the rate of strain must be very high, and it is not clear whether such strain rates would be achieved in normal welding operations.

In an attempt to reconcile some of the differences between the two theories, and also to look specifically at welding rather than the casting process, Borland[64] produced his "Generalised theory of super-solidus cracking in welds". In common with the previous work, he found that the quantity and distribution of

liquid around the grain boundaries during cooling through a critical temperature range was the factor controlling cracking. Additionally, he proposed an explanation of the physical factors controlling this distribution, and the way in which the distribution affected crack susceptibility. The main factor influencing distribution of liquid is the ratio of the interphase energy to the grain boundary energy of the solid. This ratio, referred to as τ must be greater than 0.5 during the solidification process; if it were less than this, liquid would penetrate between existing grain boundaries and destroy cohesion. If τ is in the range $0.5 < \tau < 0.57$, then wetting of the grain faces will be almost complete (a low dihedral angle) and only small solid bridges will exist. This is clearly an ideal condition for cracking to occur. For values of $\tau > 0.57$, dihedral angle is larger, and the liquid phase will be confined to grain edges and corners. This virtually eliminates the possibility of cracking.

The non-equilibrium conditions which exist in rapidly cooled alloys (i.e. welding cooling rates) cause most solid solutions to have a value of τ slightly greater than 0.5. The non-equilibrium conditions result in the initial value of τ at the liquidus temperature being retained throughout solidification, rather than τ progressively increasing as the temperature falls. Rapidly cooled solid solutions are therefore inherently susceptible to cracking. This is particularly true of alloys which have a large gap between coherence and solidus temperatures (crack susceptible range), a gap which increases in step with the freezing range of the alloy. This last point is in agreement with

the observation of the effects of alloying elements by Pumphrey and Lyons.[58]

The crack susceptible range (C.S.R.) increases with increasing solute content until the solidus temperature is not further depressed (limit of solid solubility). Beyond this point, the coherence temperature will continue to fall, while the solidus temperature remains constant, and the size of the C.S.R. will be reduced. This is consistent with the explanation in terms of τ values, which will remain just above 0.5 for compositions below the solubility limit, but will increase more rapidly as this limit is exceeded and a eutectic composition approached.

Two important predictions thus emerge from this theory. Firstly, alloying elements which increase crack susceptibility when increased from zero to the solid solubility limit, will bring about a reduction in C.S.R. when alloy content is further increased. This may be an explanation for the contradictory effects attributed to certain alloy and impurity elements in cupro-nickel by different investigators. Secondly, impurity elements which exhibit no solid solubility will possess very high values of τ, and these alloys will not be crack susceptible.

2.3.2.2. Ductility-dip cracking

Ductility-dip cracking may be subdivided into the three types discussed earlier, but for the purpose of considering the cracking mechanism, no distinction between the sub-types is made.

An important contribution to the understanding of the cracking mechanism was made by Rhines and Wray.[65] Their investigation involved brass and several nickel-copper alloys, and they were able to determine both the temperature range and the cracking mechanism involved. They were also able to demonstrate that the processes involved in brittle failure at intermediate temperature and normal testing speeds are the same as these involved in brittle creep rupture.

Rhines and Wray proposed the initial nucleation site for cracks as being four-grain intersections, where cavities are formed. (In current nomenclature, these are referred to either as w-type cracks or triple point Zener cracks). Provided these cracks continue to lie in a shearing grain boundary, they will grow rapidly and link with other similar fissures, leading to the extreme loss of ductility which is evident in many metals in the intermediate temperature range. The occurrence of low ductility only in a relatively narrow temperature range, between the recovery and recrystallisation temperatures of the alloy concerned, is also explained. At low temperatures, the tendency for triple point crack formation is low, and so ductility remains high due to the normal work hardening processes. When the temperature is raised further, formation of triple point cracks occurs, and this produces the observed low ductility. As the recrystallisation temperature is approached, the grain boundaries will begin to move away from cracks which form, and once this has occurred the crack will no longer be able to grow and so will not be effective in reducing ductility. This results in a maximum ductility at the temperature where recrystallisation is complete.

A subsequent investigation by Izumi and Harada,[66] also using 70-30 brass revealed similar relationships between ductility and temperature. However, they extended the work to look at the mechanisms responsible for the initial nucleation of the W-type cracks in more depth. This was explained in terms of locking of dislocations brought about by the presence of solute atoms. This produces a condition where slip propagation from grain boundaries becomes very difficult. A pile-up of dislocations at the grain boundary thus occurs, and when this reaches a critical level, local grain boundary migration takes place, resulting in a corrugated grain boundary. A second consequence of the difficulty of deformation of the material inside the grain is that grain boundary sliding will take place preferentially. Where this occurs on a previously corrugated grain boundary, W-type cracks can form at the tip of any corrugation. This leads to a far larger number of potential crack nucleation sites than that predicted by Rhines and Wray, and would be consistent with the very severe loss of ductility observed in the temperature range over which the mechanism operates.

The two previous studies had both taken a purely qualitative view of the problem. A semi-quantitative approach was used by McKeown[67] who carried out his study on α aluminium bronze, an alloy known to be susceptible to ductility dip cracking during welding. Like Rhines and Wray, he proposed triple points as the crack nucleation sites, and his explanation of how cracks form here by the Zener mechanism is shown in Fig. 2. At temperatures in the ductility trough range grain boundary sliding occurs by movement of dislocations along the boundary. The stress

concentration which this develops can be relieved in two ways; deformation of the grain interior or migration of grain boundaries. As outlined above, deformation of grains is difficult, and migration of boundaries only becomes significant at higher temperatures i.e. recrystallisation. Consequently, a well defined region exists in which triple point cracks can develop and ductility is severely impaired.

The criterion for triple point cracking under these conditions has been quantified by McLean.[68]

He stated that cracking occurs if

$$\sigma^2 > \frac{12\,\gamma\,G}{\pi L},$$

where σ = applied shear stress

γ = new surface energy per unit area

G = shear modulus

L = length of sliding interface

Clearly, for any given alloy composition, γ and G are constant. The shear stress necessary to cause separation is therefore dependent only on L, which in turn is closely related to grain size, i.e. small grain size is beneficial. Whilst McKeown was unable to demonstrate this for his aluminium bronze, ample evidence has been obtained to show that a large grain size is detrimental in cupro-nickels, particularly the cast alloys.[56]

Within the scope of the present study, concerned with the effect of impurity elements, γ will be the only variable affecting shear stress needed for separation. The formula predicts that a drop in γ will result in a lower stress for the separation to occur, and the effect of many impurities is to markedly reduce γ . It has been shown by Powell and Mykura,[69] using Auger analysis, that copper containing small quantities of bismuth (0.02%) has a diatomic layer at grain boundaries which is almost 100% Bi. This would drastically reduce surface energy, and so increase the likelihood of cracking. It would also be entirely consistent with the severe loss of intermediate temperature ductility which Bi produces in cupro-nickels.[13-15]

Three major studies have been undertaken to determine the mechanism of cracking in the intermediate temperature range for cupro-nickels.[17,18,55] These are discussed in more detail in section 2.6, but are outlined briefly here. Middleton[18] directed his efforts largely to cast cupro-nickel alloys. The heavily segregated dendritic structure which these alloys possess leads to a loss of intermediate temperature ductility due to easy crack propagation through the soft interdendritic regions. Work carried out by Middleton on high purity wrought alloys confirmed the mechanism established by Izumi and Harada,[66] and provided a more detailed explanation of slip mechanisms in terms of stacking fault energies. Bradley[55] also supported the explanation proposed by Middleton, and looked in greater detail at the mechanism by which zirconium improved the hot ductility of cupro-nickel, attributing this to the formation of a precipitate which inhibits grain boundary sliding. Evans and Jones[17] used a

commercial purity wrought cupro-nickel, and found that cracks were initiated from cavities formed at MnS inclusions by a number of different mechanisms.

Another important aspect of the intermediate temperature cracking problem is the importance of strain rate. This has been the subject of conflicting reports. Both Rhines and Wray[65] and Bradley[55] reported an increase in strain rate as producing improved intermediate temperature ductility. This would indicate good ductility at the high strain rates normally found in welding. However, in contrast to this, Yeniscavich[70] and Middleton[18] found increased strain rate produced a decrease in ductility, which would be in agreement with the cracking problems encountered in welding.

In summarising the theories regarding ductility dip cracking, two major points seem to emerge:

1. The nucleation of the cracks is brought about by a grain boundary shearing mechanism which operates when the grain interior has higher strength than the boundaries. This will result in the formation of W-type cracks, either at triple points, or at second phase particles in the boundary, or at corrugations in the boundary.

2. The role of impurity elements. In some cases these play a well defined role in the cracking process e.g. MnS inclusions creating cavities. However, many investigators, whilst reporting the effects of impurites

in decreasing ductility have found fracture surfaces apparently free from impurity elements. This seemingly contradictory state of affairs may in part be explained by the work of Powell and Mykura,[69] in that the quantity of impurity present may be such as to be only detectable by the more advanced surface analysis techniques.

2.4. Measurement of cracking

When measurements of cracking are to be carried out to determine the effect of either metallurgical or mechanical factors during welding, it is important that the technique used meets a number of criteria. Krammer et al,[71] in their review of weld cracking tests available at that time, proposed that the ideal cracking test should incorporate the following features.

1. Ability to show a direct correlation with actual fabrication and service behaviour;

2. Reproducibility of results with freedom from variation due to the human element;

3. Sensitivity to small changes in a test variable;

4. Ability to show the effects of several welding variables;

5. Economical preparation of specimens and running of tests;

6. Applicability to all welding processes.

After looking at over thirty weld cracking tests which had then been developed, they concluded that none met all of these requirements.

In general terms, for cracking to occur during the welding process, two factors are involved; the material must be susceptible to cracking, and the stresses and strains present must be in excess of those the material can withstand at the temperature involved. The first of these depends on metallurgical factors, in particular composition, cooling rate, growth rate of solidification front, and, in the case of HAZ cracking, the thermal history of the material. The second factor may also depend to some extent on metallurgical variables, in particular the stresses that are generated by phase transformations, but in most situations the dominant stress/strain effects will be due to thermal expansion and contraction of the material. The magnitude of stresses will depend on a number of variables, notably heat input and section thickness. However, the very complex stress system which normally exists will make it extremely difficult to calculate the stress existing at a certain point and time. As will be seen subsequently, this last point is of considerable importance when considering the merits of various weld cracking tests.

The simplest type of welding test is one that uses a standard welded joint, and relies on the use of thick plates (minimum thickness 12mm) to subject the weld metal to stress. This can

take a number of forms, including restrained butt, tee-joint fillet and cruciform fillet. This type of test is often ideal as a quality control, when the conditions can be set such that an alloy which shows crack free behaviour in the test will also perform satisfactorily in production welding. It is cheap and easy to carry out, not requiring any technically qualified personnel or special jigs. The restrained butt and fillet tests have been used in a number of investigations of the effect of impurities in cupro-nickel.[1,3-6,72] Another test which can be classed with these welded joints is the Hot Cracking Susceptibility Test developed at IITRI.[73,74] Although this test only uses an arc melted spot, and not a weld as such, the restraint is developed purely by contraction strains in a thick section. This test was designed specifically for use on cupro-nickel valve bodies, and has the advantage that it can be carried out without destroying the component.

However, for research purposes this type of test has a number of disadvantages. These include the difficulty in achieving a very high level of strain, and the relatively large quantity of material consumed (except in the IITRI test), which may be extremely costly if using an expensive experimental alloy. The dimensions of the test pice are chosen to suit each particular investigation, and so results from one set of tests are not easily compared with those from another, because of the varying degrees of restraint present. As a consequence of this, heavy section restrained welds may have a place in investigative work because of their similarity to the fabrication situation, but should be used in conjunction with another weld cracking test in

which the factors are more accurately controlled.

A second group of weld cracking tests exist which derive restraint from the shape of the plate, often by utilising a slotted plate. This group includes the LeHigh, Tekken, NRL, Houldcroft and Huxley tests. The LeHigh test piece[75,76] (Fig. 3) has a central groove as a weld preparation, and the length of slot is varied to vary the restraint. The minimum depth of slot at which cracking does not occur is a measure of the hot crack susceptibility of the weld metal. The Tekken crack test[77,78] uses a similar test piece, but the extent of hot cracking is determined by measuring the proportion of the weld which is cracked. The National Research Laboratories test[79,80] uses a plate which is slotted longitudinally (Fig. 4), and the weld is made along this slot. The weld starts at the point of most severe restraint, and the design of the test piece is such that restraint reduces as the weld progresses. Eventually the restraint will fall below the level required to cause centre-line cracking of the weld, and the length of the crack will be a measure of the crack susceptibility of the material. The Houldcroft[81] (and modified Houldcroft[82]) tests also use a specimen designed to produce decreasing strain as the weld proceeds, in this case by progressively increasing the length of slots cut in the side of the specimen (Fig. 5). Again, the length of the centre-line crack is the measure of crack susceptibility. The Huxley test[83] is basically similar to the Houldcroft, but uses equal length slots (Fig. 6). The cracking tendency is expressed using the mean crack length as a percentage of the distance between slots.

This group of tests clearly has advantages over the straightforward restrained butt and fillet tests. In particular, the use of a standardised test piece should ensure good reproducibility of results. However, some disadvantages are associated with these tests. The time (and cost) involved in producing the test pieces is considerably increased, because of the need to cut a number of slots. Additionally, the strain in these tests is transverse, and this causes predominantly centre-line cracking. This is satisfactory if only weld metal cracking is of interest, but in many cases there is also a requirement to study HAZ cracking. Finally, the restraint is still being supplied by the bulk metal, and so in common with the restrained butt and fillet welds, the level of strain at any particular point is not easily quantifiable.

In an attempt to overcome this last problem, several tests have been developed which impose a strain by a mechanism completely external to the test piece. These include the Murex test, RBS test (Reverse Bend Severity or modified Murex) and the Varestraint test and its several derivatives. The first of these to be developed was the Murex test.[84] The weld is a downhand fillet made in the vee formed between two test plates (Fig. 7). As the welding proceeds, the lower plate is rotated at a fixed angular velocity through a total angle which is selected for the material being tested. The strain rate decreases continuously throughout the duration of the test. A centre-line crack is initiated at the start point of the weld, and at some subsequent point the strain rate will fall below that required to give further propagation of the crack. The length of the crack is thus

a measure of the crack susceptibility of the alloy. The RBS test[85,86] is very similar to the Murex, except that the arrangement of plates is different (Fig. 8). Both tests meet the criteria of being able to control the strain, but retain the disadvantage of not being suitable for producing HAZ cracking.

The Varestraint test was devised by Savage and Lundin[87,88] as a means of evaluating hot cracking. The name is an abbrevation of the more descriptive VAriable RESTRAINT, referring to the capability for producing a carefully controlled and easily variable augmented strain in the testpiece. The test employs a bead on plate welding technique, and the strain is provided by bending the testpiece over a former when the welding reaches a pre-determined point. The operation of the Varestraint testing device is shown schematically in Fig. 9.

The claim was made by the authors that their test met the six criteria set out by Krammer et al[71] (see above) for the ideal weld cracking test, and little doubt exists that it does in some measure meet all of these. Additionally, the Varestraint test is extremely versatile, and can be used to look at a number of aspects of the weld cracking problem. Firstly,this test is capable of detecting cracking in both the weld metal and HAZ. This gives the Varestraint a considerable advantage over the majority of the tests outlined above, which were confined purely to the detection of cracking in the weld metal. This obviously relates more nearly to the practical fabrication situation where HAZ cracking is often a problem.

Secondly, the Varestraint can be used to look at variations in either composition or welding parameters. A particular benefit of the Varestraint when changing welding parameters is that the effect of, for example, varying heat input on crack susceptibility can be investigated independently of the changes in restraint which this would normally produce. A third advanatge of the test is its ability to indicate the distribution of cracking with temperature, and in particular provide a simple means of determining the extent of the crack susceptible temperature range. This is possible because the straining of the whole test region occurs at one instant in time, and providing the temperature distribution around the weld is known, the temperature of formation of any crack can be established. Finally, the threshold value of strain which must be exceeded for any particular combination of alloy and welding parameters can be obtained.

The Varestraint test has been used for assessing crack susceptibility of a number of materials, for example HSLA steels[89], high alloy steels,[88] stainless steels,[90] and Nimonics.[91] The Varestraint test has also been used in several investigations of cracking in cupro-nickel alloys.[6,8,9,11,92]

The Varestraint test was the first of a family of welding tests, all employing the principle of an externally applied augmented strain, and all based to some extent on the Varestraint. The most closely related is the Sub-Scale Varestraint test.[91,93] Whereas the full size test requires a test-piece 305 x 50mm, and either 6.5mm or 12.5mm thick, the sub-scale test uses a testpiece 150 x

25 x 3.2mm. This test has therefore been employed for assessing the crack susceptibility of sheet materials, and also for the testing of extremely expensive materials, for example niobium and tantalum base alloys.

A further development intended for the testing of either sheet materials or costly alloys is the Spot Varestraint or TIG-A-MA-JIG test.[91,94] This test permits a further reduction in specimen size by employing a stationary arc. Another important variation from the Varestraint is that the augmented strain is not applied by drawing the testpiece over a former, but instead a punch of the required radius is forced into the testpiece from below, immediately following arc extinction. A view of the testing device is shown in Fig. 10.

The final derivative of the Varestraint to be considered is the Transvarestraint test[95,96]. The only significant use of this test to date has been the study of centreline cracking in submerged arc welding. The Transvarestraint also has it origins partly in the Murex test (described above), and in the test developed by Brockhurst and Muir.[97] The Varestraint itself is unsuitable for this purpose as it develops mainly transverse cracks. The layout and principle of operation of the Transvarestraint is shown in Fig. 11. The weld is carried out along a joint preparation, which has the apex of a "roof-top" shaped former directly beneath it. When the arc reaches the point where it passes from the testpiece proper to the run-off tab, the plate is bent over this former, the extent of augmented strain being controlled by the angle of this former.

It is therefore clear that the Varestraint family of cracking tests offer a range which renders them useful for studying the whole spectrum of weld hot cracking. Additionally, the ability to vary the level of strain over a range from 0.25% to 10% (approximate values, depending on design details of equipment) allows testing of alloys of any crack susceptibility to be carried out.

2.5. Cracking in the welding of cupro-nickel alloys

A number of studies of varying depth have been carried out to determine the effect of various alloy and impurity elements on the crack susceptibility of cupro-nickel. The number of elements proposed as either crack promoters or inhibitors is in excess of twenty. Whilst the effects of certain elements, for example, P, Si and S, are known, there remains disagreement amongst investigators as to the levels which will adversely affect crack resistance. Additionally, there are a number of elements which have been proposed to have an effect on crack susceptibility, but where there has been insufficient investigation to confirm this. Several elements, for example Ti, Sb and Mn, may act as either promoter or inhibitor, depending on alloy composition and condition, and level of impurity present.

In an attempt to clarify this seemingly complex situation, the consideration of elemental effects is divided into four sections, using 70-30 and 90-10 alloy types, and cast and wrought conditions. A very limited amount of work has been carried out on the 80-20 alloy, and this is included with results from the 70-30 alloy.

2.5.1. Cracking in wrought 70-30 cupro-nickel

As outlined above, P has been suggested as a very common cause of cracking in cupro-nickel alloys, and in particular, in the wrought 70-30 alloys, is responsible for segregation cracking. Witherell[1] investigated the effect of varying P in the parent plate, and found that a maximum level of 0.02% could be tolerated if liquation cracking was to be avoided. This level has also been adopted as a maximum in certain specifications and recommendations for both plate and welding wire.[45,46] Taylor and Burn[98] looked at the 80-20 alloy, and concluded that P should be kept at the lowest possible level, without quoting a specific maximum level. In a more recent investigation,[7,99] a considerably lower level of P (0.006%) was used. This level of P was shown to cause cracking in reheated weld metal. Subsequent investigations of the same alloy to determine the extent of microsegregation[29,100] revealed that in the weld metal the P content of the cracked region was as high as 0.032%, and in the partially melted region up to 0.023%. This severe segregation suggests an explanation for the crack promoting effect of the apparently low level of P present in the alloy investigated.

A second element which is widely thought to be a crack promoter in cupro-nickel alloys is Si. It is a particularly important element as it appears at significant levels in several of the high strength cupro-nickels. However, only two investigators have shown that Si does have a detrimental effect in the wrought 70-30 alloy. Townsend[101] investigated the Nb-Si strengthed alloy, and proposed a maximum Si level of 0.3%, in order to avoid ductility

dip cracking. However, this was in the presence of 1.3% Nb + Ta, known to reduce the cracking tendency of these alloys. Petersen[3] also looked at a high strength alloy, but in this case the Cr-strengthened (IN-732) type. He found that Si was responsible for solidification cracking in the weld metal, and suggested a maximum of 0.6% Si in order to avoid this. No Si limit has been firmly established for the unalloyed 70-30 Cu-Ni, but current welding wire specifications use a limit of 0.15%.[46]

In common with Si, S is usually thought of as contributing to both segregation and ductility dip cracking in cupro-nickel. Also in common with Si, there is little evidence for the wrought 70-30 alloy to show how true this is, or what levels of S might be involved. Dawson[102] suggests that whilst S can be a cause of HAZ cracking during welding, the S limit imposed by the need for the material to be hot workable will be adequate to avoid this problem. Taylor and Burn[98] found that a level of 0.03% S was sufficient to cause segregation cracking in the 80-20 alloy. The lack of conclusive evidence on the level of S causing cracking is reflected in the specifications, which vary from 0.01% max[45] to 0.08% max.[21]

An element known to cause cracking of both segregation and ductility dip types in many copper alloys is Pb. Witherell[1] found that up to 0.05% Pb could be tolerated, but that beyond this liquation cracking resulted. In the 80-20 alloy, 0.06% Pb caused segregation cracking.[98] An increase in Pb levels from 0.001% to 0.003% has been linked with ductility dip cracking in reheated weld metal.[103] The relatively high level of Pb which

Witherell proposed as acceptable may be due to the shortcomings of the analysis techniques available at that time. The normally recommended Pb limit is 0.01%.[21,45,48] However, even a low nominal Pb level may result in high local levels due to segregation. A nominal level of <0.02% gave maximum concentrations of 0.18% in weld metal[27] and 0.06% in partially melted regions.[100]

Bi, Se and Te are three elements which are frequently associated with intermediate temperature cracking in copper alloys, and their effect on the wrought 70-30 cupro-nickel was assessed by Witherell. He found that Bi and Se were not detrimental up to the maximum contents evaluated (0.003% and 0.05% respectively), but that a maximum of 0.02% Te could be tolerated if cracking was to be avoided. However, these figures must be considered with caution, because of the limitations of chemical analysis outlined above.

The two alloying elements present in all cupro-nickels for the reasons given in section 2.2.1., are Mn and Fe. These have generally been considered as having little effect on crack susceptibility during welding, although Mn was known to act as a scavenger, particularly of S, and so reduce cracking in this way.[104] However, the series of investigations carried out by Savage and his colleagues[7,29,99,100] showed that Mn alone could be responsible for an increase in cracking, and that both Mn and Fe figured in interactions with other elements. The interactions found to be significant included both P-Fe and Sb-Fe which were found to be detrimental to crack resistance, and Sb-Mn which was

shown to be beneficial. Segregation of both elements was also determined. A nominal 0.87% Mn was increased to as great as 1.94% at weld metal cracks, and 1.02% in the partially melted region. Fe was present at a nominal level of 0.52%, and was as low as 0.1% in weld metal cracks and 0.16% in the partially melted region. Typical levels of Fe and Mn in the 70-30 alloy are 0.4-1.0% and 0.5-1.5% respectively.[21]

Another important group of alloying elements are those which are used to produce strengthening, and in the case of the wrought 70-30 cupro-nickel, these include Be, Cr and Nb. The Be containing alloy was investigated by Holsberg.[11] He used an alloy containing 0.5%Be, found that this alloy suffered to a considerable extent from ductility dip cracking, and could not be classified as weldable. Holsberg also investigated a Cr-strengthened alloy (IN732) containing 2.8%Cr, and in contrast to the Be alloy, found no cracking in the parent plate. However, cracking was produced in the weld metal. The findings for the HAZ confirm the earlier work of Petersen,[3] who found that HAZ cracking was absent from alloys containing up to 3.75%Cr. The two investigations were not in agreement, however, regarding the acceptable level of Cr in the weld metal, as Petersen had suggested that a level of 2.75% (almost equal to Holsberg's) would produce weld metal free from cracking. The Nb-Si strengthened alloy has not been investigated widely in the wrought form, as most attention has been focussed on this alloy in the cast state (discussed in the next section). However, Townsend[101] showed that increasing Nb content would bring about a reduction in the crack susceptibility of the alloy. Nb was also

shown to bring about a reduction in ductility dip cracking by Smith,[105] who believed that this was due to removal of C by a scavenging action of the Nb. He proposed a minimum level of 0.3% Nb as an effective crack inhibitor.

A small group of scavenger elements is added intentionally to cupro-nickel alloys. This group includes Nb, and also Ta, Ti and Zr. Smith also investigated Ta, and concluded that it also was a scavenger of C, and so reduced ductility dip cracking, at a minimum level of 0.72%. In contrast, Ti and Zr are reported to be scavengers of O_2 and N_2, and are added to weld metal to eliminate porosity.[38,106] In their investigation of the 80-20 alloy, Taylor and Burn[98] found that 0.2-0.3%Zr was likely to cause cracking in the weld metal. No definite effect of Ti on cracking in the wrought 70-30 alloy has been found, but in practice the Ti content of weld metal is limited to a maximum of 0.5%.[46]

There are a number of other elements which may be present in cupro-nickel, exceptionally as a deliberate addition, but more normally as an impurity. C is a particularly common element in cupro-nickel. However, no investigation has taken place to assess its effect on cracking in the wrought 70/30 alloy, although its presence has been associated with cracking, particularly of the ductility dip type.[105,107] A maximum content of 0.06% is specified,[21] presumably to avoid the clearly deleterious presence of free graphite which occurs at higher levels. Zn is also found in most commercial cupro-nickels. In the wrought 70-30 alloy, an increase in Zn from <0.006% to 0.02% has been found to cause an increase in ductility dip cracking by Bower.[103] A

local increase in Zn level due to segregation has been associated with cracking by Savage et al.[29,100] An alloy having a nominal Zn content <0.005% was shown to have Zn as high as 0.066% in the weld metal and 0.043% in the partially melted region. Another element which may be found in cupro-nickel alloys is Sb. The effect of this on cracking in the wrought 70-30 alloy was investigated by Casteras,[7,99] who demonstrated that a very small increase in Sb (from <0.002% to 0.0025%) could produce a significant decrease in cracking in the weld metal. Mg has also been shown to reduce weld metal cracking, because of its ability to bring about desulphurisation.[104] Other elements which may be present in cupro-nickel and have been shown to cause cracking in the wrought 70-30 alloy are Ag[9] and Al.[101]

In summary, it can be said that P, Si, S and Pb are the major crack promoters in the wrought 70-30 cupro-nickel alloy and Te, Be, Cr, Zr, Zn and Ag are crack promoters of less importance. The most widespread form of cracking is of the segregation type, appearing both as solidification cracking in the weld metal and liquation cracking in the HAZ. However, a significant number of reports of ductility dip cracking in the HAZ have also been made. Nb is the most important crack inhibitor, and Sb, Mg and Ta also act as inhibitors. Finally, the effects of Mn, Fe, Ti and C have not been firmly established.

2.5.2. Cracking in cast 70-30 cupro-nickel

A considerable proportion of the cracking in the wrought 70-30 alloy is found in the weld metal, as shown in the previous

section. The relatively low level of cracking in the HAZ of the wrought material is attributed largely to the homogeneous structure. However, in the cast alloy a highly segregated structure exists in the parent material, i.e. a similar structure to the weld metal. This results in a much greater level of cracking in the HAZ of cast alloys, particularly of the ductility dip type, which is virtually absent from the wrought alloy. It should also be borne in mind that, for reasons discussed previously, all cast cupro-nickel alloys contain additional elements to increase strength, and these additions are frequently from within the crack promoting group of elements.

Despite these important differences, many of the elemental effects described in the previous section also apply to the cast 70-30 alloy. P is one example of this. Lee et al[8] examined the effect of 3 levels of P in the Nb-Si strengthened alloy, using the Varestraint test. Increased segregation cracking (both weld metal and HAZ) correlated with increasing P content. Surprisingly, however, the ductility dip cracking was found to be most severe in an alloy containing 0.003%P, intermediate in an alloy containing 0.03%P and least in an alloy with 0.015%P. This was explained in terms of cracking at films of high S content in the low P alloy. Scott[6] also investigated the Nb-Si strengthened alloy, and found a conflicting, but more probable, relationship between P content and ductility dip cracking; an increase in P from ≈ 0 to 0.01% was associated with an increase in cracking. Vanick[30] suggests a maximum P content of 0.005% in the same alloy in order to ensure freedom from cracking in welding. In his review of weldability of cast cupro-nickels,

Dimbylow[20] states that P is a cause of cracking in both the Nb-Si strengthened 70-30 alloy, and in its major competitor the Cr-Si hardened alloy. The same author[23] suggests that a maximum level of 0.01% P can be tolerated if segregation type cracking is to be avoided.

The presence of Si for strengthening in both of the commercially available cast 70-30 alloys has led to this being the most widely investigated of the alloy and impurity elements. Si has been clearly established as causing increased cracking.[2,20,23,30,21,33,73,74,101,108-110] Owing to the need to have a high Si level for good strength and a low Si level for crack free welding, much of the investigation has centred around the search for an optimum Si level, and also the relationship between Si and Nb. Only one investigation has been carried out into the effect of Si when it is present as an impurity rather than an alloying element. This was done by Vanick[30] who proposed a maximum of 0.1% Si if the alloy was to remain free from cracking during welding. If this is accepted as a realistic value, it becomes clear that to produce a high strength alloy (requiring a minimum of ~0.3% Si), a further alloy modification will be needed. This is most commonly a Nb addition. Early development work of the Nb-Si alloy by Shepherd[31] suggested that an alloy containing Si up to 1.5% would be welded without cracking if it also contained 2% Nb, and that, in general, any alloy with Nb > Si could be welded. However, such high levels of Si have been found unacceptable by subsequent investigators. Calvert[2] proposed two possible alloy compositions; 0.5-0.7% Si and ≃ 0.65% Nb for low restraint welds, and 0.35-0.55% Si and

1.2-1.4% Nb in more severely restrained conditions. The latter composition was also favoured by Townsend,[101] who found that crack free welds could be produced provided the welding conditions were carefully selected. Freedom from cracking in the HAZ of a casting containing up to 0.55% Si has also been established more recently by Sahoo and Campbell.[110] The improvement in resistance to cracking brought about by the presence of Nb has been explained by Dimbylow and Dawson. They proposed a mechanism involving the formation of Nb_2Ni_3Si particles throughout the structure, resulting in a fine grain size and consequent reduction in crack susceptibility. Work carried out at IITRI[73] sought to produce a formula which would relate Si and Nb contents to cracking. This was expressed as a cracking index, which is actually a measure of resistance to cracking:

$$\text{Cracking index} = \frac{\text{Nb} + \text{Fe}}{5 \times \text{C}} + [40 - (65 \times \text{Si})]$$

However, a subsequent report[74] admits that this formula has shortcomings, particularly that it does not take account of other elements known to have a marked effect on cracking susceptibility. The presence of Fe in the formnula, having an equal crack inhibiting effect to that of Nb is also somewhat surprising. This would require further work in a programme which more clearly accounted for other variables, in order to substantiate it.

The Cr-Si hardened alloy (now designated IN768) was developed by

Ansuini and Badia.[23] One of the original criteria was for a weldable cast 70-30 alloy, and they determined maximum levels of 0.6% and 2.0%, for Si and Cr respectively, to avoid HAZ cracking. In a recent investigation of the same alloy using the Varestraint test, Sahoo and Campbell[110] found that the extent of ductility dip cracking in the HAZ increased dramatically for Si levels above 0.45%. In a similar investigation, but using butt welds in 25mm plate, Dickerson and Zanis[111] found that both liquation cracking and ductility dip cracking occurred in the HAZ if Si >0.5% was present. However, difficulties with highly restrained welds in practice have led to recommendations for Si levels of only 0.3%, in order to completely avoid HAZ cracking.[108]

A second impurity which has been shown to have a detrimental effect on the crack resistance of the cast 70-30 cupro-nickel is S. Dimbylow,[20] and Lee et al[8] have shown that ductility dip cracks pass through regions of high S content. In the development work on the Nb-Si alloy, both Shepherd[30] and Townsend[101] proposed maximum S contents of 0.02%. However, this was subsequently shown to be too high by Scott,[6] who was able to correlate this level of S with increased ductility dip cracking.

Pb is also known to be a cause of cracking in these alloys. The original limit suggested by Shepherd was 0.02%, but this seems to be excessive, particularly when considered in the light of the extent of segregation present (discussed in previous section). A more realistic maximum of 0.01% was proposed by Townsend, but even this was made to look high by Scott's findings; a significant increase in ductility dip cracking being associated

with a rise in Pb content from 0.001% to 0.005%.

Ductility dip cracking is also caused by increase in Bi level. Both Townsend and Dimbylow found that 0.001% was the level of Bi which could be tolerated if cracking was to be avoided. However, Scott again showed that this level was associated with increased ductility dip cracking as compared to a level of Bi <0.0001%. Safe limits for Se and Te were also determined by Dimbylow, these being 0.01% and 0.005% respectively.

A limited amount of investigation has been carried out into the effect on welding of elements which act as scavengers and deoxidisers. Zr has been reported as reducing the tendency for cracking in the cast 70-30 alloy,[23] with the minimum level required for this being quoted as 0.05%[33] or 0.1%.[20] The effects of Ti have been reported by Dimbylow[20] and are somewhat more complex. In some respects, Ti is beneficial, in that it will produce a fine grain size, which in turn leads to reduced cracking during welding. However, the presence of TiO_2 particles will provide sites for cracks to nucleate, and in this way Ti may exhibit a deleterious effect. There is also a level of Ti (~0.5%) above which intermetallic compounds may form with Ni, and these will also lead to increased cracking. In practice, this level of Ti is unlikely to be exceeded in the bulk material, but may be locally in the cast material due to segregation.

Of the remaining alloy and impurity elements which may be found in the cast 70-30 cupro-nickel, the most widely investigated has been C. Early work by Vanick[30] suggested that provided the C

level was not so great as to cause the formation of flake graphite, then it would not bring about any increase in crack susceptibility. A level of 0.1%C was proposed as a suitable maximum. However, this hypothesis was based purely on the need to avoid segregation cracking. The importance of ductility dip cracking had not been realised at that time, and consequently much lower carbon limits have been suggested by subsequent investigators. Townsend[101] proposed a limit of 0.015%C to avoid this problem. This value is supported by work carried out at IITRI.[73] C was varied mainly in the range 0.01%-0.02%, and the equation developed for cracking (see above) indicated that C was acting as a crack promoter. However, a second phase of the work using similar materials[74] reversed this original finding, and showed C to be a crack inhibitor over this range of compositions. Further evidence that C is associated with increased ductility dip cracking has been furnished by Scott[6] who varied C levels between 0.001% and 0.02%. Scott[92] has also suggested that a beneficial interaction might exist between C and Cr.

Al also occurs as an impurity in most cupro-nickels. Vanick found that a maximum level of 0.05% Al could be tolerated if cracking was to be avoided. More recently, attempts have been made to strengthen the cast 70-30 alloy with 0.5% Al, but both Dimbylow[20] and Townsend[101] concluded that this alloy was extremely susceptible to ductility dip cracking. Other elements which are known to increase the tendency for cracking are Zn and Sn,[30] the latter being particularly troublesome if present in combination with P. Mg has been shown to be a crack inhibitor in these alloys.

Overall, the cast 70-30 cupro-nickel alloy seems to be subject to cracking of both the segregation and ductility dip types. In practice, however, the latter seems to be of greater importance, probably because it generally occurs at a lower level of a particular impurity. This contrasts with the wrought 70-30 alloy, where segregation cracking was the more severe. The major elements thought to be responsible for ductility dip cracking are P, Si, Cr, S, Pb, Bi, C and Al, although Se and Te are also known to be harmful. Nb, and to a lesser extent Zr and Mg, have been shown to reduce crack susceptibility, whilst the complex effect of Ti is not clearly established.

2.5.3. Cracking in wrought 90-10 cupro-nickel

The extent of cracking found in the wrought 90-10 cupro-nickel is generally less than in the 70-30 alloy, and the investigations carried out are few in number and date back many years. The effect of several elements in promoting segregation cracking was investigated by Witherell.[1] He determined the maximum level of several impurities which could be tolerated. His work was confined to liquation cracking in the HAZ, as welding was carried out using a 70-30 filler metal. The maximum levels for crack free welding which he determined were 0.02%P, 0.008%Bi, 0.02%Se, 0.03%Te, 0.02%Cd and 0.02%Pb. These levels appear high when considered in the light of more recent work carried out on other cupro-nickel alloys, but no further evidence is available to confirm this. However, current specifications do call for a maximum of 0.01%Pb in the 90-10 alloy.[21]

Pb was also one of the elements investigated by Pease and Kihlgren,[5] although they considered it in terms of a synergistic effect with Si rather than in its own right. However, implicit in their work was an assumption that Pb levels as high as 0.05% in the weld metal would not create a crack susceptible alloy. At this Pb level, the maximum Si level which can be tolerated is 0.15%. However, if Pb is limited to 0.02%, Si can be increased safely to 0.3%, and at 0.01% Pb, an alloy containing 0.4%Si can be welded without cracking. Pease and Kihlgren also investigated two other impurity elements. S was found to be a crack promoter, and a maximum of 0.01% proposed, although the authors admit that this may be a conservative figure. This admission is reflected in the BS 2871 limit of 0.05%S.[21] They also looked at the effect of Ti, which was used in the weld metal to eliminate porosity. Levels of Ti above 0.15% caused solidification cracking in the weld metal.

Hawthorne[72] also found that Ti caused cracking in the weld metal, although his maximum level for crack free welding was 0.29%. The second element considered by Hawthorne to affect cracking was Si. A Si strengthened alloy containing 0.5% was made completely unweldable by the extent of solidification cracking, and a reduction in Si content to only 0.12% was required to overcome this problem.

It is clear that the major cracking problem is the wrought 90-10 alloy is segregation cracking, and that in general the alloy is less susceptible than the wrought 70-30. Pb, S, Si, and Ti are the main elements which have been shown to be responsible for increased cracking.

2.5.4. Cracking in cast 90-10 cupro-nickel

As with the wrought alloys, the amount of research into cracking in the cast 90-10 alloy is small compared with its 70-30 counterpart. Much of the investigation of the effect of alloy and impurity elements centres around high strength alloyed 90-10. This is due primarily to the very low inherent strength of the cast 90-10 alloy.

In common with the cast 70-30, the main cracking problem in the cast 90-10 alloy is ductility dip cracking in the HAZ. A number of common crack promoters have been assessed by Dimbylow and Dawson,[20,112] and the maxima which can be tolerated without cracking have been established. These levels were 0.01% for S, Pb, Se, P and As, 0.005% for Te and 0.001% for Bi. Dimbylow also studied Mn, which is present in the cast 90-10 cupro-nickel alloy at levels up to 15%. In particular, the level of Mn in the aluminium strengthened alloy was investigated. Mn was found to reduce the very severe problems of HAZ cracking which arose, and at levels of 7% Mn or greater this cracking was eliminated. The effect of Mn was also investigated by Cuha et al,[35] again using an alloy containing ~2.0%Al. Their findings were similar revealing that a slightly higher level of Mn (9%) was required if cracking during welding was to be avoided. The structure of the Al hardened alloys has been studied by Dimbylow.[23] Ni-Fe-Al intermetallics are found in the form of a discontinuous precipitate at the grain boundaries, whilst an Fe-Ni phase is present at the dendrite centres. Ni_3Al is found in both interdendritic and grain boundary regions. The improvement

brought about by Mn is explained in terms of modification of the precipitates at the grain boundaries. Cr also can improve crack resistance, possibly due to its grain refining effect.(113)

Jordan[14] directed his attention toward a number of elements which he expected to act as crack inhibitors in the cast 90-10 alloy. The elements he chose were Nb, Ti, V and Zr and the alloy investigated was strengthened with 0.2%Si. Nb clearly reduced the extent of ductility dip cracking in the HAZ, and a formula was developed relating the minimum Nb required to Si content:

$$\%Nb = 1.55\%Si - 0.1$$

This predicts a requirement for 0.21%Nb in the alloy containing 0.2%Si. Similar tests on alloys containing the other additions revealed a need for additions of up to 0.2%Ti and 0.2%V if cracking was to be avoided. However, the tests on Zr containing alloys were inconsistent and it was impossible to determine the effect of this element on HAZ cracking.

In summarising the effects of impurity and alloying elements on cracking in cast 90-10 cupro-nickel, it can be said that S, Pb, Se, P, As, Te and Bi are all crack promoters, whilst Nb, Ti, V and Mn appear as inhibitors.

2.6. High temperature cracking and ductility of cupro-nickel alloys

2.6.1. Principles of hot ductility testing

A serious problem which confronts the researcher in many areas of welding metallurgy is the small volumes of metal with which he must deal. This represents a particular difficulty when the object of the study is microstructural changes or the causes of cracking. In order to overcome this problem, a number of simulation techniques have been developed. These have been largely aimed at simulating the thermal cycles undergone by the heat affected zone (HAZ) of the parent plate, or reheated weld metal.[9,114-117] Clearly, it would be of great advantage if a technique could be devised which allowed the simulation of weld metal. This presents considerable difficulties, because of the need to contain the metal whilst in the molten state. However, several simulators have been produced which are capable of taking a small volume of metal into the molten regions, thus simulating as-deposited weld metal. The earliest of these was that developed by Sopher,[118-119] which used a specimen heated by an induction coil and contained the molten region in a close fitting ceramic tube. Cremisio and Koffler[120] utilised the simulator developed by Nippes (described below), and were able to maintain the integrity of the molten region purely by use of surface tension effects. More recently, Homma et al[121] used a single turn induction coil to melt a very narrow region and were able to retain this in position by a combination of surface tension and electromagnetic forces.

However, although these investigators have produced useful results, the vast proportion of simulators constructed have been intended purely for HAZ work. Of these, the most widely used has been that constructed by Nippes et al[114] and its various derivatives. A schematic diagram of this apparatus is shown in Fig. 12. The apparatus consists of a specimen held between two water-cooled jaws. Heating current is provided from the secondary of a resistance welding transformer connected across these jaws. A thermocouple is attached to the centre of the specimen, and the output taken to a control circuit, which adjusts the transformer output to ensure that this matches the desired thermal cycle.One of the jaws is fixed, and the other attached to a hydraulic system, which permits loading of the specimen for tensile testing.

If the technique of simulation is to be usefully applied to the welding situation, then it is necessary to know how the properties of strength and ductility measured in this test relate to the crack susceptibility in welding. This is obviously dependent on which type of cracking is under consideration. Considering the somewhat simpler case of Type 2 (ductility dip) cracking first, there seems to be general agreement that this can be closely related to the level to which ductility falls at the intermediate temperature minimum.[12,16,23,65,122,123] However, for Type 1 (segregation) cracking, the situation is more confused, and a number of parameters have been suggested.

Yeniscavich[70,124] listed a total of five parameters from the hot ductility test which various investigators had used and

attempted to assess the relative importance of these. The criteria concerned are applicable to tests carried out on cooling. It had been established by Nippes et al[70] that the loss in ductility of an alloy was more severe on cooling than on heating. The "on cooling" situation also relates more nearly to the practical welding operation, as the tensile stresses necessary to cause cracking will normally occur during the cooling part of the thermal cycle. The first criteria discussed by Yeniscavich is the minimum arbitrary ductility. This is often set at 20%, and if the ductility falls below this value at any stage during cooling, then the alloy is classed as crack susceptible. This may permit separation of crack-resistant and susceptible alloys in certain cases,[25] but is of limited value because of its arbitrary nature.

The second criteria, one of those proposed by Nippes et al, is the recovery rate of ductility. This is concerned with the slope of the ductility temperature curve at temperatures approaching the zero ductility temperature (ZDT). If it is steep, the alloy is crack resistant. This parameter was also favoured by Thompson and Genculu.[126] Again, this criteria is useful for comparing alloys, but the definition of the slope required for crack resistance is somewhat arbitrary. Related to this is another parameter, the recovery rate of ultimate tensile strength. Rapid recovery of UTS is also indicative of a crack resistant alloy.

The criteria which was favoured by Yeniscavich was the zero ductility range. This is defined as the temperature difference between the melting point and the point at which ductility starts

to recover on cooling from the peak temperature. A similar criterion was suggested by Williams,[127] who utilised the temperature range between zero ductility and the zero strength temperature (ZST) arguing that this is the region in which cracking would occur. The evidence to support this is that shrinkage strains in welding are normally only of the order of 0.5%, and so any measurable ductility would be sufficient to resist cracking. However, the work of Chubb et al[12-15] on ductility dip cracking is not in agreement with this, and suggests that alloys may crack at temperatures at which they exhibit 3-4% reduction of area. This can only be explained by strains larger than this value, which will frequently occur in the practical welding situation due to mechanical restraint.

The final criteria listed by Yeniscavich is the mid-temperature ductility dip. This is clearly related to Type 2 cracking, and so is not considered as an alternative to the previous four criteria.

Yeniscavich also reviewed the testing parameters which might affect the results of hot ductility testing. The most important of these is peak temperature. A number of authors[115,127,128] have shown that the ZST provides a more suitable peak temperature than the ZDT. Phillips and Jordan[129] found that a marked loss of ductility only occurred when the temperature went above the ZST and approached within 12°C of the melting point. Yeniscavich found that regardless of the criteria used to assess cracking, the alloy appeared more crack sensitive as the peak temperature was increased.

Other test parameters also affect the hot ductility. Yeniscavich found that increasing strain rate decreased the ductility, although, as discussed in Section 2.3.2.2., the effect of varying strain rate is the subject of considerable disagreement. The other factor which he found as significant was the cooling rate. An increase in cooling rate also produces a drop in ductility, whereas ductility is improved if the test piece is held at the test temperature for ten seconds prior to testing.

It therefore seems necessary to use the highest possible peak temperature (limited by bulk melting), and a thermal cycle representative of actual welding conditions. A high strain rate is also required, regardless of the effect it has on ductility, in order that testing is completed as rapidly as possible after the heating current is switched off.

2.6.2. Effect of impurity elements on hot ductility of cupro-nickel

Much of the hot ductility testing carried out on cupro-nickel alloys has been directed towards the intermediate temperature ductility dip region, rather than the high temperature zero ductility region. This is most probably explained in terms of the difficulty in relating the latter to weld cracking, as outlined in the previous section. In turn, this has led to a large proportion of the work being carried out on cast alloys, as it has been shown that these are most susceptible to HAZ ductility dip cracking [56] whereas the wrought alloys are chiefly subject to weld metal cracking.

The most extensive investigation of ductility of the cast alloys is that carried out by Chubb and his colleagues.[12-15,123] They investigated the effect of varying Ni, alloying elements and impurity elements. Ni was found to have a significant effect, in that alloys containing >15% Ni had an inherent loss of ductility at intermediate temperatures. In contrast, those alloys with lower Ni content, provided they are of high purity, do not display a significant ductility loss. This led to a decision to concentrate the remainder of their programme on alloys of the 90-10 type.

The most important alloying elements, particularly in the cast 90-10 alloy, are those which can provide strengthening and three of these were investigated; Fe, Si and Al. All were found to cause a substantial loss of ductility in the intermediate temperature range. However, this problem could be overcome by additions of Mn (minimum of 5%), which has a beneficial effect on the intermediate temperature ductility. The presence of impurities, even at extremely low levels, also has a very significant effect on the ductility of the alloys. Gavin et al[15] established maximum limits for a number of impurities which would ensure a minimum ductility of 20%. These levels were Bi <0.002%, Te <0.0045%, Pb <0.012% and Se <0.0015%. The effect of S was much less marked, and levels up to 0.075% could be tolerated. The cumulative effect of these impurities was also recognised, and this was expressed in the form of a bismuth equivalent composition (BiE), given by the formula:

$$BiE = Bi + 0.7Te + 0.4Pb + 0.2Se + 0.1S$$

This allows the behaviour of any alloy to be predicted by relating it to one containing Bi only.

These results were also reported by Dimbylow,[20,23,122] who generally chose to adopt slightly lower impurity limits, presumably to make allowance for cumulative effects without actually utilising the formula. Additionally, he proposed As and P as impurities which would reduce intermediate temperature ductility, and suggested maximum limits for both of these of 0.01%. Dimbylow further established two elements as improving the mid-temperature ductility. These were Zr and Ti. Zr has also been reported as having this effect by a number of other authors.[18,55,130,131] A third element capable of producing this effect is Nb.[4,16] This capability for improving ductility has been attributed to one of two mechanisms. Zr and Ti both produce a grain-refining effect and, as decreasing grain size produces a marked increase in ductility, may be operating in this manner. Ti and Nb are both scavengers, combining readily with such impurities as C, P, Si or S, and thus preventing deleterious effects which might otherwise arise.[4,18,20] It seems likely that in practice both mechanisms operate together to produce the overall effect.

A small number of other elements have also been reported as being detrimental to the ductility of the alloys. In the Be strengthened wrought alloy, the Be has been shown to cause loss of ductility,[11] and also in the wrought alloy, Ag has been reported to be detrimental.[9] In the cast 90-10 alloy Sb causes a marked reduction in intermediate temperature ductility.[41]

Only very limited work has been carried out to determine the effect of variation in composition on the ductility at high temperatures. Holsberg[11] found that in both the Be- and Cr-strengthened alloys, the addition of the alloying element in both cases resulted in an increase in the zero ductility range. It has also been reported that P produces a similar effect.

2.6.3. Mechanism of intermediate temperature ductility loss in cupro-nickel alloys

Whilst the effect of various alloying and impurity elements is of great practical significance, the understanding of the physical mechanisms involved in these ductility changes is also of vital importance.

The loss of ductility at temperatures near to the solidus is generally considered to be caused by liquation of low melting point material, being either a second phase or a heavily segregated region. These mechanisms were discussed in detail in Section 2.3.2, and no further comment need be made here. However, a number of investigations have been undertaken to determine the causes of low ductility in the intermediate temperature range for cupro-nickel alloys (550°C-750°C), and these are detailed below.

The first significant investigation was carried out by Middleton,[18] who examined both wrought and cast 70-30 Cu-Ni alloys. In the wrought alloy, he proposed that the loss of ductility was caused by the formation of voids at grain boundaries. These result from a pile-up of dislocations at the

boundary producing a serrated interface, and the subsequent sliding of this interface to form the voids. This same mechanism was also reported by Lupton and Thompson,[16] but for the cast 90-10 alloy. Bradley[55] and Dimbylow[122] have both pointed out that grain boundary sliding is produced by dislocation climb, a process which is diffusion controlled and consequently only becomes energetically favourable above 450°C. This temperature corresponds with the onset of ductility loss in the cupro-nickel alloys.

However, in the cast alloy, Middleton proposed a theory which differed somewhat from his wrought alloy, and also from the other investigations of cast alloy. He suggested that crack propagation, rather than being intergranular, was interdendritic. This occurred because the Ni depleted interdendritic regions were of lower strength, and already contained voids produced by shrinkage during solidification. A third possible mechanism of ductility loss has been proposed by Evans and Jones,[17] who found that MnS inclusions at grain boundaries were a possible source of voids which reduced ductility.

Despite these differences about the reason for the loss of ductility, all of the above investigators have been in agreement as to the causes of the recovery in ductility which occurs as the temperature is further increased. This is attributed to the onset of dynamic recrystallisation, which permits the movement of grain boundaries away from voids which form, and thus renders them harmless.

The various alloy and impurity elements which may be present in cupro-nickel alloys can be divided into groups, depending on their effect on the constitution of the alloy. Ni itself suppresses the onset of recrystallisation to a higher temperature so resulting in an extension of the low ductility region.[13] However, in a high purity alloy, Ni levels of up to 15% do not cause any reduction in intermediate temperature ductility. Other major alloying elements, including Fe, Si and Al, will reduce ductility by a mixture of segregation, if present at a sufficient level to produce second phase precipitation effects. Impurity elements divide into two types. Those which are present as second phase particles were found by Gavin[123] to have little effect on ductility. The elements which he found to be most deleterious were those present in solid solution, and heavily segregated to grain boundary layers. These layers were only one or two atoms thick, and required Auger Electron Spectroscopy for their detection. The effect of these heavily segregated layers is to cause a drop in grain boundary energy. This will lead to poor intergranular cohesion, allowing easier sliding and loss of intermediate temperature ductility by the mechanisms outlined above.

Another important group of elements are those which have been shown to reduce ductility dip cracking during welding. Lupton and Thompson demonstrated that Nb produced precipitation in the grain boundary which would reduce sliding, and so was able to effect a ductility improvement in this way. Bradley found that Zr brings about an improvement in ductility by a combination of two mechanisms; grain refining, and the formation of a Ni_5Zr

precipitate at grain boundaries, which again reduces sliding. In contrast, Dimbylow reported Zr as working by a grain refining effect only, and also Ti as operating in the same way.

Conflicting explanations of the mechanism by which reduced grain size improves ductility have also been given. Middleton, in keeping with his explanation in terms of dislocations suggests that increasing grain size increases the number of dislocations per unit strain, which in turn leads to decreased ductility. Dimbylow, however, following on from Gavin's work, proposes that a reduced grain size gives increased boundary area, leading to dilution of segregated impurites. This produces an increased boundary energy, making decohesion less likely and improving the ductility.

2.7. Summary

From the preceding review of published work, a number of important points can be seen to have been adequately investigated, whilst many others have received little attention or have been the subject of conflicting reports. Consideration will now be given to these latter areas.

Widespread agreement exists as to the crack promoting effects of a number of common impurities, including P, S, Si and Pb. However, in many investigations the level of impurity used was somewhat higher than that commonly found in commercial alloys. Whilst these levels would undoubtedly cause increased cracking, they seem to be of limited relevance to the problem of cracking

when alloys are within specification. A requirement therefore exists for determination of the effects of these impurities when at the maximum level permitted in the specification.

In contrast to this group of elements, a second group exists whose effects on cracking are much less clearly defined. Prominent amongst these are the elements which are frequently added in small quantities (typically up to 0.25%) to achieve a variety of deoxidation, scavenging and grain refining effects. These elements include Ti, V, Zr and Nb. Of these, Nb has been widely investigated and is known to be a crack inhibitor. However, Ti and Zr, which are added to many commercial alloys, appear to have a dual effect. In certain circumstances, they may act to produce a reduction in cracking, whereas in other situations their effect is to increase cracking. The way in which these two opposing effects arise remains an area for which a satisfactory explanation is required. The effect of C, which is another common impurity in cupro-nickels, also requires further clarification.

The importance of interactive, additive and synergistic effects is an area which has been the subject of very few investigations. The only exception to this has been the relation between Nb and Si, which has been well established because of its importance in the Nb-Si strengthened alloys. The relationship between various impurity elements and that between impurity elements and potential crack inhibitors also requires further investigation.

Whilst the importance of determining the effect at certain levels

of each element is clearly the prime objective from the practical point of view, an increased understanding of other areas is also needed. In particular, a correlation between variation in hot tensile properties and both composition and cracking behaviour would be extremely useful, as it would enable the hot tensile test to be used more widely for prediction of welding behaviour. This is an area which to date has received little attention in cupro-nickel alloys. Indeed, it is a problem which has not been completely solved for any alloy system.

Finally, the mechanisms of cracking must be determined, and the way in which various alloy and impurity elements relate to these mechanisms clarified. An understanding of these mechanisms is clearly essential if the effect of impurities on cracking is to be fully understood, and suitable treatments or additions are to be developed which will reduce cracking tendency.

It is therefore with the intention of making a contribution to the solving of these problems that this programme of work is undertaken. Each of the points outlined above will be accounted for in the investigation. The upper levels of impurity elements have been selected such that they fall within the levels allowed by the common specifications. From the less widely studied elements, C, Ti and Zr have been selected for inclusion, whilst the use of the factorial design permits the determination of interactions. Finally, use will be made of metallographic and fractographic studies to provide information regarding cracking mechanisms.

3. EXPERIMENTAL TECHNIQUES AND RESULTS

3.1. Introduction

The primary objective of this research was to establish the effect of impurity elements on cracking in the welding of cupro-nickel alloys. In particular, the problem of varying welding response between heats within specification required investigation, and the composition of experimental alloys was selected to take account of this. Two parallel techniques were used. Susceptibility to cracking was measured by use of the Varestraint weld cracking test, and in certain cases this was supplemented by the use of restrained butt welds. In order to determine tensile properties (in particular ductility) at high temperatures, and also to generate fracture surfaces for subsequent examination, the weld thermo-mechanical simulator was used.

3.2. Selection of compositions and alloy manufacture

3.2.1. Selection of alloy compositions

From the review of published literature, it was evident that over twenty different elements have been proposed by various investigators as affecting either one or both of weld cracking behaviour and hot ductility response. This clearly represented a greater number of variables than could be included in this investigation, and consequently a careful decision was needed as to which elements to include and which to omit. A number of

factors were taken into account:

1. All alloys produced needed to be reasonably representative of commercial alloys likely to be used in practice.

2. The most important elements to investigate were those whose effects are least well known.

3. Information about interactions between pairs of elements was required wherever possible.

4. If the alloy is to be tested in the wrought condition, the impurity levels must not be so high as to make hot working impossible.

At this stage, it was also necessary to settle on the basic alloy to be tested (i.e. 70-30 or 90-10). Additionally, selection of a suitable experimental design was needed.

It was decided to base all experimental designs for the various stages of the programme on the factorial design principle. In its simplest form, the factorial experiment has each of the independent variables at two levels, and the total number of experiments is made up by using all possible combinations of high and low levels. For independent variables, this type of design gives 2^n experiments. This technique has several advantages over the traditional type of experiment where variables are changed individually.

1. The same information can be obtained from a smaller number of tests, thus reducing cost and time taken.

2. Alternatively, if the number of tests is fixed for some reason, either better precision can be obtained or more variables investigated.

3. Information regarding interactions is obtained. Certain variations on the factorial experiment may also be used, and one of these, the fractional factorial design, was utilised in the first stage of the current programme. In a full factorial design, all possible interactions between all variables are given. However, in practice, three factor and higher interactions are usually small and consequently of little real significance. If this situation is anticipated, then extra variables may be included without increasing the number of tests, using a fractional design. This is achieved by using a technique known as confounding, where a variable or interaction thought to be significant is linked with an interaction which is negligible. The two can then no longer be distinguished, but as the one is negligible, any measured effect can be attributed to the other. The actual technique by which this is carried out will not be detailed here, but, in common with other factorial designs, is covered in great depth by Davies.[132]

The decision was made to concentrate the main part of the experimental programme on the wrought 70-30 Cu-Ni alloy. The high

cost of producing experimental alloys within close composition limits dictated that a total of 32 experimental alloys would be available for this part of the programme. Consequently it was decided to produce an initial batch of 16 alloys, in which a number of elements would be varied. The results obtained from these would then point to specific areas of interest, which could be investigated in more detail using two smaller experimental designs of 8 alloys each.

Input from industry via INCRA suggested six elements which were of most concern to fabricators; P, Pb, S, Bi, C and Si. Next came the task of developing a suitable design. For six variables in 16 experiments, a fractional factorial is required; a quarter replicate of 2^6. However, an investigation of the various designs available revealed that only the main effects would be given by this design (no interactions). Further investigation of possible designs revealed that an extra two variables could be added, without increasing the number of alloys required, and still leaving all main effects clear. It was decided to adopt this course, the two elements chosen being Zr and Ti, often added as grain refiners, but whose effects on weld cracking have been the subject of conflicting reports. The final design for this first stage of the programme, a one sixteenth replicate of 2^8, is shown in Table 1.

Having selected the experimental design, the actual levels of each element had to be fixed. In general, the lower level was chosen to be either 0 or the lowest level which could be consistently achieved by the chosen production route. The high

levels were based on the maximum levels permitted in the major British and American specifications. For elements which do not have a specified maximum, levels were taken which approximated to the high levels found in commercially available alloys. In certain cases, the high levels were reduced slightly because of reservations regarding the hot workability of alloys containing several impurities at high level. (These reservations were later seen to be unnecessarily cautious). The final levels selected are shown in Table 2.

The second and third groups of experimental materials both consisted of 8 alloys, representing a full factorial with 3 elements being varied (P, Ti, C and S, Zr, C respectively.) The elements for inclusion in these stages of the programme were chosen on the basis of the results from the first group of alloys, a choice which is explained fully in a subsequent section. Two alloys (H1 and H3) were common to both series of alloys. Full factorial designs were chosen as these were able to provide information about interactions. These simple designs have the added advantage that actual physical effects, as determined from metallographic and fractographic studies, can be more easily attributed to a particular element or interaction.

In addition to the main programme on the wrought cupro-nickels, a series of eight cast 70-30 alloys was also investigated. Again, a full factorial design using 3 elements was used, the elements being Pb, Bi and S (in line with reports of problems in welding these alloys from MoD). The reasons for this choice of design are the same as those detailed for the second and third series above.

3.2.2 Manufacture of experimental alloys

In order to facilitate the testing programme outlined above, the production of experimental alloys to these composition limits was necessary. If the work was to produce a valuable final result, the levels of the intentionally varied impurities and also of the other alloy and impurity elements had to be controlled as tightly as possible.

The wrought alloy material was all produced by INCO Alloy Products, a slightly different procedure being utilised for the first series of alloys to that for the subsequent two. The sixteen alloys of the first series were cast as 100kg melts from a basic lined HF induction furnace. Each alloy was split into two 50kg taps before final additions were made. High purity copper and nickel raw materials from single batches were used. Melting was carried out under a layer of charcoal. After tapping into the ladle, 0.02%Ca was added to deoxidise the melt and then the impurity additions were made by wrapping them in copper foil and plunging beneath the surface of the melt.

Each alloy was cast into two 25kg ingots measuring 250 x 100 x 100mm. One ingot of each alloy was taken and one face machined to remove the as-cast surface. This was then reduced to 6mm thickness for Varestraint testing, the machined surface being needed because it would be free from major casting defects which might affect cracking results. The second ingot was reduced to 12.5mm thickness, this being required for preparation of 10mm diameter simulator specimens. In both cases, reduction was

carried out by forging and rolling at 950°C, followed by annealing at 850°C. Final analysis of these alloys is given in Table 3(a).

A broadly similar procedure was used for production of the second and third series experimental alloys, but subject to the following modifications. The variations in C content which arose in the first series prompted the selection of a vacuum melting unit for these further alloys, and this in turn led to the production of each alloy as an individual 25kg melt. The second alteration to the procedure was also made as a consequence of information obtained from the first series alloys. It was clear that the greatest proportion of cracking occurred in the weld metal. It therefore seemed appropriate to use a weld metal type structure for the simulator tests, and the nearest structure which it was practical to achieve was a cast structure. Therefore a 35mm long section was cut from the bottom of the ingot for this purpose before any hot work was carried out. The analysis of the second and third series alloys are shown in Table 3(b). It can be seen in Table 3(b) that alloy H2 varies considerably in Fe and Mn content from the other alloys. Owing to the problems that variation in alloy content had caused in statistical analysis of the first series alloys (see Sect. 3.3.1.2.), a replacement for this alloy was produced, shown in Table 3(b) as alloy P1.

The series of cast cupro-nickels of the IN768 type (30%Ni, 0.4-1%Fe 0.4-1%Mn, 0.2-0.4%Si, 1.5-2%Cr) were manufactured by BNF Metals Technology Centre. The alloys were air melted without flux cover or degassing and sand cast to give ingots of approximately

20kg. The pouring temperature of the melts varied from 1300 to 1440°C. As can be seen in Fig. 13, the ingots were cast 105mm wide 55mm thick and 160mm high, with a sleeved hot top feeder attached to the top of the 105mm x 55mm section. The feeder, approximately 100mm thick and 100mm high, was connected across the whole width of the section, the intention being to obtain sound, porosity free ingots. Analysis was determined by BNF from separately cast test bars. A check analysis for each alloy was carried out by AMTE Dockyard Laboratory, on material removed from the ingots themselves. Both sets of results are shown in Table 3(d). An acceptable level of agreement exists between the analysis and, with the exception of alloy K8, the compositions were suitable for the investigation. Alloy K8 had a Bi level of 0.01%, and was replaced by N2. Samples were needed from each ingot to provide Varestraint, restrained butt weld and hot ductility test pieces. Details of the sectioning of the ingots to achieve this are given in Fig. 13.

3.3. Determination of weld crack susuceptibility

The largest proportion of the weld crack susceptibility determinations were carried out using the Varestraint weld cracking test. The single most important advantage of this test for the present programme was its ability to introduce various levels of augmented strain. This was particularly important as the statistical analysis applied to the crack length data required all alloys to be cracked, but was found to operate more accurately if excessive cracking could be avoided. By way of contrast, the restrained butt weld produced a constant (but

unknown) strain, and was expected to have two advantages; producing a greater extent of cracking in the HAZ, and being more nearly related to the practical welding situation.

3.3.1. Varestraint testing

The origins of the Varestraint (shortened from VAriable RESTRAINT) test, developed by Savage and Lundin (87,88) were desribed in Sect. 2.4. The apparatus used in this research works on exactly the same principle, as shown in Fig. 9; a schematic view is shown in Fig. 14.

The test piece used was 300mm x 50mm x 6.5mm. One end of the test piece was clamped to the top of the variable radius die block, and the other end held firmly in a loading yoke. This yoke is connected to a large pneumatic cylinder, capable of exerting a maximum load of 135kN.

The specimens used in the majority of the tests were in the form of hot rolled plate and consequently had a heavy coating of mill scale. This was removed prior to welding by either grit blasting or rotary scratch brushing treatments, followed by pickling in 50% nitric acid. A final degreasing was carried out just prior to welding, this latter treatment also being applied to specimens with either cold rolled or machined surfaces. Scrupulous attention to cleanliness was vital, as contamination could have led to porosity or increased cracking due to P and S contained in cutting oils.

The welding technique used in the standard Varestraint test is a bead on plate weld. This arrangement was used in the current programme, the welding process used being automatic TIG. The welding torch incoporated a closed loop arc length control system, which allowed a constant arc voltage to be maintained regardless of plate profile. The welding conditions used were d.c. electrode -ve, 210A, 11V, travel speed 2.1mms^{-1} and shielding gas Helishield 2 (75%He,25%Ar), flow rate 45 1min^{-1}. (The choice of shielding gas is explained in the next section).

The weld was initiated on the centreline of the testpiece at a point near to the loading yoke. As the arc passed the end of the radius section of the die block, rapid downward movement of the yoke was initiated by a limit switch. This movement continued until the test piece had been bent to conform to the die block. The arc was allowed to proceed a minimum of 25mm further and was then extinguished. The specimen was left under load for 5min. in order to ensure that crack propagation was complete and then removed for examination. The experimental set up is shown in Figs. 15-16.

When the test piece had cooled, it was first straightened using a mandrel press, care being taken to ensure that the press did not make contact directly with the cracked region of the surface. A section was then removed for crack measurement; the full width of the specimen, and extending 25mm in either direction from the position of the arc on completion of bending (see Fig. 17). This section was then etched using 50% nitric acid.

Crack measurements were made on all specimens on the etched surface using a Nikon Shadowgraph, at a magnification of 20X. The Shadowgraph projects an image on to the screen at the required magnification, and measurements of crack length can then be made directly on the screen. Accuracy on the screen was ±0.25mm, so accuracy of the actual crack length measurements was ±0.0125mm. The measured crack lengths were then processed to produce three crack length parameters; maximum crack length (MCL) total crack length (TCL) and sum of five longest cracks (SFL). The first two of these criteria were amongst those used by Savage and Lundin; the usefulness of the latter was evident from the results obtained by Scott.[92] These three crack parameters then provided the basis for statistical analysis and other assessment of relative crack susceptibility of the alloys.

3.3.1.1. Preliminary Varestraint testing

Prior to commencing work on any of the main experimental alloys, it was necessary to carry out a series of preliminary tests to investigate a number of factors:

1. Strain level,
2. Effect of straightening the specimen after the test,
3. Reproducibility of results

These tests also offered the opportunity to eliminate any practical problems which might arise.

The need to carry out these preliminary tests also offered a chance to test out the type of factorial design and analysis which would be later applied to compositional variables. Consequently, a full factorial using the four levels of strain available at that stage (1.8%, 3%, 4% and 6%) and two levels of straightness (i.e. straightened or unstraightened) were used. Two replicates were used to give a measure of reproducibility (i.e. two tests for each combination of conditions), giving a total of 16 tests. The tests were carried out on a commercial purity alloy.

When Varestraint testing was commenced, the shielding gas was argon. An immediate problem with porosity was observed. This was attributed to atmospheric gases entering the cooling weld pool after the torch had moved on, and was solved initially by constructing a box which provided a trailing shield, fed by a supplementary gas supply. However, this arrangement was somewhat cumbersome, and on the advice of the gas suppliers,[133] a conventional torch arrangement supplied with Helishield 2 gas was substituted. This gas is a 75-25 He-Ar mixture, and appeared to have the desired effect in eliminating porosity. As the porosity had been confined largely to the alloys where Ti and Zr were both at low level, it seems likely that oxygen and possibly nitrogen are the causes. If this is the case, the improvement achieved by the He based gas is likely to be brought about by the narrower, deeper weld pool generated, which in turn will restrict the amount of the deleterious gases entering the pool.

With this problem eliminated, the series of 16 tests was

completed using the procedure described previously. Cracking results are shown in Table 4. Analysis of variance was carried out on these results, and this revealed that, as expected, increasing strain caused increased cracking, whilst straightening of the bar to facilitate easier measurement had no significant effect on crack length. It was also apparent that better reproducibility of results was obtained with 1.8% and 6% strain than with the two intermediate levels, although no satisfactory explanation could be found for this result. Results of the analysis of variance are given in Table 5.

3.3.1.2. Varestraint testing of first series of experimental alloys

The experimental design and manufacture of these materials, as outlined in earlier sections, produced a set of sixteen alloys of composition as in Table 3(a). The good reproducibility of tests on commercial material at 1.8% and 6% dictated that these strain levels should be used, and the calculation in Appendix C suggested that four tests per alloy would be required. Consequently, two tests at two strain levels for each alloy were proposed. The quantity of experimental material available was large, and so a sample composed entirely of the experimental material was used for each test.

The results of these tests are shown sets 1 & 2 in Table 6, and in Table 7. Cracking was confined mainly to the weld metal. A statistical analysis of these results was then required. Some doubt was attached to the validity of using the analysis of variance technique, since this assumes each of the elements to be

present at either the nominal low or high level. As can be seen from Table 3a, this assumption would not have been justified. The method also fails to account for variations in alloy element content, which are sufficient to affect cracking. The alternative statistical method which was employed was linear regression analysis. This enables the actual content of each element (alloy and impurity) to be used in the analysis.

Linear regression analysis was carried out individually on the results for the two strain levels, and also collectively on all the results. The analysis of the results at 6% strain revealed that none of the impurity elements was significant at a level of 10% or better. An identical result was obtained for the combined results at both levels. However, analysis of the results at 1.8% strain revealed that Pb, P, Zr, and Ti all exhibited a crack promoting effect at a significance level of 10% or better, whilst C appeared to have an inhibiting effect.

Rather than treat these results as an end point in themselves, and give full consideration to the detailed statistical analysis, it was decided to carry out a further four tests on each alloy using a strain level of 1.8%. The results of these tests are shown in Table 6, as sets 3-6. However, 10 successive tests of the third set exhibited anomalously low results owing to equipment problems, and consequently only the remaining five sets were included in the statisitical analysis. For the reasons discussed above, Mn and Fe, as the major alloying elements, and also Ca, which was added to deoxidise the melt, were all included as variables in this analysis. The results of this analysis are

shown in Table 8. A brief explanation will be given of the column headed "Crack length variation". This figure is the product of regression coefficient and the difference between maximum and minimum compositions for a given element. It is included to simplify visualisation of the relative size of the effects attributed to various elements.

It can be seen that amongst the intentionally varied impurites, P, Si, S, Ti and Zr all appear as crack promoters, with high significance levels. C alone brings about a reduction in sum of five longest cracks, again with a good significance level. Pb does not appear in the results, and the effect of Bi cannot be properly assessed because of its low absolute level. All three alloying elements included in the analysis appear as crack inhibitors. However, the importance of this latter information is limited, as these elements were not varied in any controlled way, and the results are therefore not entirely reliable.

The results obtained for P, S and Si, showing these elements to be crack promoters, were as expected. More surprising were the crack promoting effects of Ti and Zr, and the apparent inhibiting effect of C. Two further series of experiments were therefore planned, each varying one of the unexpected crack promoters, a known crack promoter and carbon. Series 2 thus varied P, Ti and C, whilst series 3 studied S, Zr and C.

3.3.1.3. Varestraint testing of second and third series experimental alloys

The procedure adopted for these tests was identical to that already described except in one detail. The smaller quantities of experimental material available for these alloys dictated that a composite specimen should be used. These were produced by taking a piece of experimental plate 115 x 50mm, and TIG welding suitable lengths of commerical plate to each end to ensure that the test region was in the centre of the experimental plate.

As a strain level of 1.8% had proved satisfactory for the original alloys, this was employed initially on the second series. However, as can be seen from Table 9, this produced cracking in only two of the alloys. Increased strain levels of 3% and 4% were also investigated, but again were insufficient to produce cracking in all alloys, the situation which is ideal for accurate statistical analysis. However, an analysis was carried out on these three sets of results, and the results are shown in Table 10. This reveals that P, Ti and strain are all responsible for increased cracking, whilst a C-P interaction brings about a reduction in cracking. These results also allow a cracking threshold to be established for each alloy, i.e. the strain below which no cracking occurs. This offers an alternative method of ranking their relative crack susceptibility. The ranking of the alloys is shown in Table 11, in order of increasing crack susceptibility, together with the elements they contain at high level. It can be seen that the P containing alloys with their high crack susceptibility form the bottom half of the list.

Similarly, each Ti containing alloy appears below the corresponding alloy without Ti, whilst alloys with crack inhibitor C are above corresponding alloys without C.

To ensure a level of strain where all alloys would crack, 6% was employed for four tests on each alloy. The results of these tests are shown in Table 12 and the linear regression analysis in Table 13. Again, P appears as a crack promoter and a C-P interaction as a crack inhibitor.

For the third series alloys, containing S, Zr and C, the same approach of testing each alloy at a number of different strains was employed, with the addition of a test on each alloy at 1% strain. The results of these tests are shown in Table 14. Again, the bottom half of the list is made up of alloys containing crack promoter S, but the importance of C and Zr is not as clear. Six sets of tests were carried out on each alloy using 6% augmented strain. The results of these tests are shown in Table 15, and the information obtained by regression analysis in Table 16. For the total crack length and sum of five longest crack length parameters, Zr and S are crack promoters individually, but interact to produce an inhibiting effect. Zr also increases maximum crack length, but a reduction is produced by the interaction Zr-C.

3.3.1.4. **Varestraint testing of IN768 alloy**

A number of particular problems arose with the testing of this alloy which had not been experienced with the wrought alloys. The

first of these was the small size of the pieces of the alloy which were available for testing, the maximum size being a 50mm square. This meant that the technique described above, using TIG welding to join the experimental material to commercial plate, was unsuitable, because the region to be subsequently tested would be within the HAZ of the preparatory welds. A technique was therefore developed using electron beam welding to form this joint.

The second problem was related to the strength of the IN768 alloy. This is considerably higher than that of the commercial alloy, even when the material is hot. Consequently, when the straining took place in the Varestraint apparatus, much of the strain was accommodated in the commerical material, with the result that very little bending of the test material took place. This difficulty was overcome by the use of auxiliary bending bars, 15mm x 10mm section. These are placed on top of the test piece at each edge, and ensure uniform bending around the former.

The strain level selected for these alloys was 1.8%, which appeared to be adequate. Although the alloy with all impurities at low level did not crack, some alloys exhibited extensive cracking. In contrast to the wrought alloys, although there was some weld metal cracking, the majority of the cracking was found in the HAZ. The HAZ cracking in these alloys is shown in Table 17.

It seemed probable that in addition to the effect of impurity elements on cracking, grain size was also likely to be an

important factor. As the pouring temperature had varied considerably between alloys, the grain size of each was determined by the linear intercept method. Grain sizes and associated pouring temperatures are shown in Table 18. Linear regression analysis was carried out on the cracking results, using the impurity element contents and grain size as independent variables. Results of this analysis are shown in Table 19. It can be seen that Pb is the most significant of the single element effects in promoting cracking, whilst S and Bi appear to act in combination to achieve the same effect. In contrast, a favourable interaction occurs between Pb and Bi.

3.3.1.5. Varestraint testing of a crack susceptible commercial cupro-nickel alloy

A commercial 70-30 Cu-Ni alloy in the form of 1.6mm TIG filler wire had been reported as crack susceptible in production welding,[103] and a sample was received for assessment. Its composition is given in Table 20, together with that of a similar wire which had not been crack susceptible. In order to test this alloy, six Varestraint pieces were prepared from commercial 70-30 Cu-Ni plate, and slots 25mm long, 19mm wide and 3.6mm deep were machined in the test areas. Weld metal was deposited in these slots by the TIG process at 210A and 11V. After removal of any weld reinforcement, a standard Varestraint test was carried out at 1.8% strain. All six test pieces showed considerable cracking in the weld of the type observed in the experimental alloys. Additionally, very extensive cracking was found in the HAZ, i.e the reheated regions of the weld metal previously deposited.

Cracks up to 3mm in length were found and the crack susceptible zone reached a maximum distance of 7mm from the fusion line. This finding was in marked contrast with the behaviour of the HAZ in the wrought alloys used in this investigation where very little cracking was observed.

3.3.2. Cracking in restrained butt welds (IN768)

In order to try to reproduce more realistically the situation which would exist in an actual welded fabrication, the use of a restrained butt weld test was considered. These tests had been contemplated for all alloys, but were not used for the wrought alloys.This was because the test must use a standard filler wire, and so experimental material would be confined to the HAZ. As the greater part of the cracking of the wrought alloy occurred in the welds, this test would be of little value.

However, in the cast IN768 alloy, the main cracking was in the HAZ. Consequently, a set of restrained butt welds were made between pairs of plates which had previously been anchor welded to a 25mm thick steel base plate to provide restraint. Details of the test piece design are given in Fig. 18. Multirun butt welds were made using a compatible 1.6mm welding wire containing 28.8%Ni, 2.1%Cr, 0.47%Si, 2.16%Mn, 0.15%Fe, 0.06%Ti and 0.22%Al; the balance being Cu. The weld metal was deposited by the MIG process at 350A, 27V and 25$lmin^{-1}$ argon; the root runs being made at 11mms^{-1} and the three filler runs at 8.2mm s^{-1}. After welding, two 25mm sections were taken from the central region of the experimental alloy and measurements made in the HAZ on the

bottom surface of the plate. As in the Varestraint tests, the three parameters of maximum crack length, total crack length and sum of five longest cracks were determined and the data are recorded in Table 21. The order in which these figures rank the crack susceptibility of the alloys is similar to that of the Varestraint results, indicating that the Varestraint is a good pointer to the service behaviour of the alloys. Regression analysis was carried out on these results, and the outcome of this is shown in Table 22.

3.4. Weld thermal simulation

As discussed elsewhere in this thesis, weld thermal simulation is an extremely useful technique in that it allows a substantial volume of material to be subjected to a given thermal cycle facilitating the determination of hot tensile properties and fracture surface examination. In the current investigation, these hot ductility determinations were carried out in parallel with the weld tests already described. Hot ductility tests were carried out for all alloys on cooling from a peak temperature, and for selected alloys were also carried out on heating.

3.4.1. Description and operation of weld simulator

The weld simulator is derived from that developed by Nippes et al[114] and described previously. The apparatus is based on a Mand servo-hydraulic tensile testing machine. The conventional jaws are replaced by water cooled copper jaws with the specimens gripped in copper inserts. This provides good thermal and

electrical conductivity, necessary for rapid heating and cooling of the test piece. A heating current is supplied by connecting the secondary of a resistance welding transformer across the jaws. Feedback for control of temperature is supplied from a Pt/Pt-13Rh thermocouple attached to the centre of the specimen by means of a micro-resistance welder. The whole arrangement of specimen and jaws is contained within a closed box, permitting testing to be carried out in a protective atmosphere when required. This arrangement is shown in Fig. 19.

The execution of a test using the simulator involves first setting up the specimen in the jaws by utilising the movable lower jaw. The specimen is held in position by means of silver steel pins (4.5mm diam) passing through it, and good contact between specimen, inserts and jaws is ensured by the use of two springs. With the specimen correctly positioned, the box is closed and a sequence of evacuate, fill with protective atmosphere, evacuate again and refill with atmosphere is carried out. The atmosphere used is an Ar-8%H_2 mixture, the reducing nature of this giving additional protection against oxidation. With the protective atmosphere present, the specimen is held under a small constant tensile load, and is than heated through the required temperature cycle. At a pre-set temperature, either on heating or cooling, the heating current is switched off, and the lower jaw moved rapidly downwards to carry out a high strain rate tensile test. (The control of both thermal cycle and mechanical testing is described in a later section). A view of the apparatus upon completion of the test is shown in Fig. 20.

3.4.1.1. Determination of thermal cycles

Before any weld simulation work can be carried out, it is essential that suitable thermal cycles are available for the material being investigated. Two possible methods exist for obtaining these, and previous investigations have used both.[134,135] The most simple method is by direct measurement. This can be done by attaching thermocouples to the undersurface of thin plate. For thicker plate, blind holes must be drilled from the underside and thermocouples attached to the bottom of these. Greater care is needed in this case, because of the effect of the holes on heat flow. The alternative to direct measurement is calculation. A number of computer programs have been developed, based on heat flow theory, which permit the calculation of the thermal cycle undergone by any particular point. These have been shown to be adequate by comparison with measured cycles. However, these techniques have only been used for steels to date, and a preliminary investsigation into modifying a program for cupro-nickel suggested this would not be possible because insufficient information was available regarding the variation of specific heat and thermal conductivity with temperature of this alloy.

Tests were therefore carried out to measure thermal cycles directly, using single pass full penetration MIG butt welds between two plates 300 x 200 x 6mm. Welding conditions of 320A, 25V, 1.2mm Monel 67 wire and argon flow rate of 25 $lmin^{-2}$ were used. Heat input was varied by changing welding speed, with values of 8.0, 6.2 and 4.7 mm s^{-1} giving heat inputs of 1.0, 1.3

and 1.7kJmm^{-1} respectively. The joint preparation was a vee with 70° included angle, 1.5mm root face and 1.5mm root gap. Eight chromel-alumel thermocouples were attached to the underside of one of the plates at distances of 0-12mm from the anticipated position of the fusion line, in order to include a range of peak temperatures. The signals were recorded using a PET microcomputer fitted with an analogue to digital convertor. Cycles for three peak temperatures are shown in Fig. 21.

3.4.1.2. Conversion of simulator to computer control

At the commencement of the investigation, the weld simulator employed an analogue control system. The mechanical control, using either load or position control, was based on a system of potentiometers. Control of thermal cycle was achieved by drawing the required cycle on carbon coated paper. This paper was attached to a rotating drum, where a sensor followed the position of the line. The signal from the sensor was compared with that from the thermocouple attached to the specimen, and the error was used to control the heating current supplied by the transformer. Additionally, pen recorders of both X-Y and X-t types and a u-v recorder were available for collection of data.

This control system was somewhat cumbersome and had shortcomings in terms of accuracy and repeatibility. It was therefore decided to replace this with a computer based system. The computer selected was the MACSYM 2 minicomputer, which combined the essential requirements of high speed (up to 4000 samples/sec.), capability for handling a large number of inputs and outputs, and

had the additional advantage that external analogue to digital and digital to analogue convertors were not required. The computer and ancillary equipment can be seen in Fig. 22.

Installation of the computer required a number of hardware changes. The necessary communications between the computer and existing equipment are shown in Fig. 23. These divide into three groups. For mechanical control, inputs from the position transducer and load cell are required, together with an output to the servo-valve amplifier. Temperature control requires input from the thermocouple and an ouput to the transformer control box. Finally outputs to printer, graph plotter and pen recorder are needed for visual presentation of information.

With the hardware modifications complete, development of suitable software was then undertaken. The major program needed was that to carry out the actual testing procedure, but supplementary programs for purposes such as calibration and data handling were also produced. The sequence of events to be carried out by the main program is illustrated in Fig. 24. One of the important features of the MACSYM is its ability to operate in a multi-tasking mode. This allows each of the operations shown in the diagram to be written as a separate task, operating at a rate largely independent of other tasks, and activating or de-activating these as required. The programming language used is MACBASIC (abbreviated from Measurement And Control BASIC), a variant of Basic with additional commands enabling input/output communications to be made with single, simple commands. The program developed is listed in Appendix D.

3.4.1.3. Development of test technique

Prior to this investigation, the use of the simulator had been confined to dilatometric studies and production of simulated HAZ microstructures. For these purposes a simple cylindrical specimen of 10mm diam. had usually been found adequate, and as this was known to give a satisfactory heat distribution, the dimension was adopted for the present study.

A series of tests were then required to set up the various test parameters which were required. The first stage of this operation was the selection of a suitable thermal cycle, combined with choice of program variables to accurately reproduce this. As described in section 3.4.1.1, a range of thermal cycles had been determined with varying peak temperatures. As the welding tests had shown solidification/liquation cracking to be the predominant type, it seemed essential to use a thermal cycle which would take the specimen into the temperature range where this would occur. Consequently, a thermal cycle was initially selected which had a peak temperature of 1180°C, slightly higher than the nominal solidus of the alloy. The thermal cycle is controlled by a PID (proportional-integral-differential) control loop, and by altering the various constants associated with this, a good reproduction of the required cycle was achieved with overshoot limited to maximum 10°C at peak temperature and minimal oscillation. However, on heating a number of specimens through this cycle to test repeatability, it became apparent that the high peak temperature meant that approximately one third failed, due either to overstressing or incipient melting, at the peak

temperature. Therefore, a second thermal cycle was selected, with a peak temperature of 1160°C, and, as this seemed adequate to investigate the liquation cracking problem but had a low failure rate, was adopted for the main programme of testing.

Having established the necessary thermal cycle, attention was directed towards the execution of the tensile test. A requirement existed to carry out tests in the temperature range from 450°C up to the peak temperature. An immediate problem was observed with test temperatures at the lower end of this range. As the strength of the material at these temperatures is only a little less than the strength at ambient temperature, the specimens broke in the area around the hole for the pin, where the section was considerably reduced. In order to overcome this difficulty, the central area of the specimen was reduced to 6mm diameter. The final specimen design is shown in Fig. 25.

The other important factor in the hot ductility test is the strain rate, as demonstrated in section 2.3.2.2. The effect of strain rate is disputed but it is clear that in practice a high strain rate should be used for two reasons:

1. Strain rate is normally rapid in the practical welding situation.

2. The heating current must be shut off prior to the tensile test, and so a high strain rate will minimise any fall in temperature between this point and breaking of the specimen.

The strain rate selected for the tests was 5.2 s^{-1} (equivalent to 78mm s^{-1} for a 15mm gauge length), this being the most rapid rate attainable with the existing equipment.

3.4.1.4. **Temperature distribution**

Before any meaningful results could be obtained from hot ductility testing, checks on temperature distribution both along the length and through the thickness of the specimen were required. Temperature distribution along the length of the specimen was measured by attaching thermocouples at various distances from the control thermocouple. Through thickness distribution was measured by drilling 1mm holes of varying depth into the specimen, attaching the thermocouple to the bottom of the hole by capacitor discharge, and then coating the thermocouple wires with zirconia to avoid short circuiting. The results of these tests are presented in Fig. 26 and 27.

3.4.2. **Hot ductility tests**

After due consideration to the limited number of specimens likely to be available for the majority of the experimental alloys a programme of hot ductility testing was devised which centred around tests on cooling from a peak temperature of 1160°C. Provision was also made for a smaller number of tests on heating and any tests on cooling from lower peak temperatures which might subsequently appear necessary.

3.4.2.1. Hot ductility testing of first series experimental alloys

For each of these alloys, tests were carried out on cooling at intervals of 100°C over the range 450-1150°C. The U.T.S. was calculated by dividing the maximum value recorded on the load cell by the original cross-section area. The reduction of area was measured by taking three measurements across the diameter of each half of the fracture, and using the mean diameter to calculate the reduction. The results for the sixteen alloys of the first series are shown in Table 23, and depicted graphically in Figs 28-43. The plots of U.T.S. against temperature all follow a similar pattern, decreasing steadily from a value of approximately $300Nmm^{-2}$ at 450°C to a nil-strength temperature in the range 1150-1200°C. However, the plots of reduction of area against temperature divide into two distinct types. The majority of alloys exhibit the standard ductility curve; good ductility at low temperatures, decreasing to a minimum around 700°C, increasing again to reach a maximum at approximately 1050°C, and then dropping to zero as the temperature is raised further. In contrast to this, a number of alloys (Figs 32, 37-39) show ductility steadily decreasing as temperature increases, and a complete absence of the maximum around 1050°C. It will be shown later how this lack of ductility can be related to cracking during welding.

The complex way in which impurity elements varied in this series of alloys, according to the one-sixteenth replicate factorial design, meant that information about particular impurities could not be easily obtained from study of one ductility curve or

fracture surface. Therefore, no further hot ductility tests were carried out on these alloys.

3.4.2.2. Hot ductility testing of second and third series experimental alloys

For the majority of these alloys, testing was carried out on cooling at 100°C intervals in the temperature range 450-950°C, 50°C intervals up to 1100°C, and also at 1130°C and 1150°C. Additionally, tests were carried out on a number of the alloys on heating at temperatures of 750°C and higher using the same temperature intervals as above. Finally, in an attempt to ascertain whether the loss in ductility on cooling was due to some change occurring near the peak temperature, a small number of tests (one per alloy) were carried out on cooling from a lower peak temperature of 1050°C. All other test parameters were maintained at their previous values. The results of these tests are shown for the second series alloys in Tables 24-26 and depicted graphically in Figs 44-57. Unfortunately, only S1 amongst the third series alloys had sufficient material available to permit testing on heating. The results for these alloys appear in Tables 27-29 and Figs 58-64.

The retention of a small section of each ingot in the cast state was explained in section 3.2.2. Simulator specimens were prepared from these pieces and put through the same series of tests as that detailed for the wrought alloys above. Results for series 2 alloys are given in Tables 30-32 and Figs 65-76, and those for series 3 in Tables 33-35 and Figs. 77-85.

The comments already made about the variation of reduction of area with temperature in the first series alloys apply equally well to the on cooling ductility of both the wrought and cast versions of the series 2 alloys. However, the behaviour of the alloys on heating shows that all possess good ductility throughout the temperature range, only losing this at temperatures in excess of 1100°C.

In contrast to the first two series, the third series alloys all show the standard type ductility behaviour with a peak at 1050°C, both in cast and wrought forms. Again, ductility is good across the temperature range when tested on heating.

Cast and wrought alloys of both series all show ductility which is similar or improved when tested on cooling from a lower peak temperature. This improvement appears to be most marked in the alloys which exhibited the worst on cooling behaviour from the higher peak temperature.

3.4.2.3. **Hot ductility testing of IN768 alloys**

The procedure used in the testing of these alloys was identical to that used on the first series wrought alloys, tests being carried out at intervals of 100°C on cooling from 1160°C only. The results of these tests are shown in Table 36, and graphically in Figs 86-94. Again, the two types of ductility-temperature relationship are observed, but in these alloys the number showing the high temperature peak is small, and several have a very low ductility across the whole temperature range tested. Data for

alloy K8, which contained the erroneously high Bi content, are included for comparison, although this alloy was not included in the weld cracking tests.

3.5. Metallographic and Fractographic studies

Whilst the cracking studies and hot ductility determinations have been vital in providing quantitative evidence of the effects of various impurity elements, it is essential that metallographic and fractographic studies are carried out in an attempt to ascertain the physical mechanisms by which the various effects and interactions occur. If possible these will be related to quantitative and semi-quantitative measurements of composition in localised areas of material.

3.5.1. Metallographic Studies

Two main areas arise which require metallographic study; the determination of the relationship between cracking and structure in the crack test specimens, and the investigation of any changes undergone by the hot ductility test pieces as a result of passing through the peak temperature.

3.5.1.1. Relationship between cracking and structure for wrought alloys

The initial examination carried out on each Varestraint test piece was made on the as-welded surface at a low magnification. The pattern of cracking exhibited by all wrought 70-30 alloys was similar, varying only in its extent according to composition and

strain level. A typical Varestraint test region is shown in Fig. 95. It can be seen that the crack pattern is approximately radial, and centred around the position of the arc at the moment of application of the augmented strain. It is also clear that the cracking is almost entirely confined to the weld metal. In no case did cracking in the HAZ exceed 10% of the total, and frequently it was considerably less than this.

In order to establish the crack morphology, metallographic specimens were prepared by machining a layer approximately 0.25mm thick from the surface, polishing and etching in acidified ferric chloride. It was important to minimise the amount of material removed as the extent of cracking decreases rapidly with increasing depth. The extent of cracking on a typical sub-surface section is shown in Fig. 96. Examination of these specimens revealed that cracking in the weld metal followed an interdendritic path. This is illustrated in Fig. 97. In many cases, the cracks in the HAZ appeared to be an extension of those existing in the weld metal, as shown in Fig. 98. It will be noted that in both Figs 97 and 98 the cracking appears extremely coarse, and this type of cracking constitutes the majority of the cracking found in the alloys. However, in a number of alloys of the first series (A1, A5, A7, B1, B3, B4, B5), cracking of a much finer nature was observed. This cracking occurred in the HAZ of the parent plate, and the cracks followed the grain boundaries, as shown in Fig. 99.

3.5.1.2. Relationship between cracking and structure for cast alloys

In complete contrast to the wrought alloys, the low magnification examination carried out in the cast alloys revealed that although significant cracking occurred in the weld metal, considerably more cracking was to be found in the HAZ. This is illustrated in Fig. 100. It is also apparent that the crack path is much more irregular than the well defined pattern of cracking found in the wrought alloys.

An identical method of preparation of metallographic specimens was used to that employed on the wrought alloys, minimising the amount of material removed again being an important requirement. Examination of the specimens after etching in ferric chloride revealed a much more clearly defined HAZ than had been apparent in the wrought alloy and the three distinct regions (weld, HAZ and parent plate) are shown in Fig. 101.

The cracking in the weld metal again appears to be associated with solidification structure, following a path through the interdendritic regions (Fig. 102). However, in the plate material, the cracking appears to take different forms between the visible HAZ and the material at a greater distance from the fusion line. In the visible HAZ, the dendritic structure is not as marked as in the weld metal or the parent plate. The cracking in this region is obviously intergranular in nature, and severe in its extent (Fig. 103). The parent plate also exhibits considerable cracking. The dendritic structure of this region is clearly visible but the location of cracking is not as easily

pinpointed. Indeed, it appears that cracking in the parent plate is a mixture of interdenritic and intergranular cracks, as illustrated in Fig. 104.

3.5.1.3. Cracking in restrained butt welds

All of the IN768 alloys exhibited some cracking in the restrained butt weld tests. In each alloy, cracks were evident perpendicular to the fusion line, and typically commencing approximately 0.5mm from the fusion line. These cracks are relatively coarse, and can be seen clearly at low magnification, as in Fig. 105. Additionally alloys L3 and N2, which were extremely crack sensitive, exhibited cracking parallel to the fusion line, again a distance of approximately 0.5mm away. This considerably more extensive crack pattern is illustrated in Fig. 106. Regression analysis results obtained from these welds are given in Table 22.

3.5.1.4. Structural changes in simulated heat affected zones

The pattern of cracking observed in the Varestraint tests carried out on the wrought alloys suggested that the prevalent mechanisms were solidification and liquation cracking. In order to determine whether heating through a peak temperature close to the nominal solidus brought about any adverse changes in the microstructure, a number of test pieces from hot ductility testing were sectioned longitudinally. These were then examined microscopically to look for any differences in structure between the region near to the fracture, and an unheated area of the

test piece. The majority of the sections examined had been heated to a peak temperature of 1160°C, and in both the wrought and cast materials, no changes were detected except for signs of the deformation which had occurred. However, a specimen was also sectioned which had failed prematurely in the simulation test due to overheating and bulk melting. A section taken near to the fractured surface showed signs of a considerable degree of liquation having occurred (Fig. 107).

3.5.1.5. Analysis of cracked regions by energy dispersive analysis (EDA)

In order to establish the importance of the segregation pattern shown by each of the elements and its relation to cracking, an analysis was carried out on the material through which cracks passed in the weld metal for each of the first series wrought alloys. This was done using the EDA attachment of a scanning electron microscope on a polished surface. The compositions measured in these tests are shown in Table 37.

3.5.2. Fractographic Studies

Hot ductility tests were carried out in an Ar-8%H_2 protective atmosphere as described earlier, and so in addition to generating values of reduction of area and tensile strength, produced fracture surfaces suitable for SEM examination. Approximately 30 specimens were examined in this manner, chosen to clarify the following points:

i) The considerable differences in ductility which most

alloys exhibited when tested at similar temperatures on heating and on cooling.

ii) Any differences in mechanism of fracture between wrought and cast alloys of similar composition.

iii) Effect of composition upon fracture mechanism.

In order to simplify comparisons whilst maintaining the number of specimens to be examined at a reasonable level, investigations were confined to the second and third series of wrought alloys and their cast counterparts.

In the wrought alloys, those with P at high levels exhibit poor ductility over a wide range of temperatures up to the melting point, when tested on cooling. Figures 108 and 109 show fracture surfaces of alloy H6 on cooling, at temperatures of 999°C and 1100°C respectively. In both cases the crystalline nature of the fracture surface is clearly visible. By way of contrast, alloys with high P exhibit good ductility when tested on heating. This is illustrated by Fig. 110, alloy H5 tested at 1057°C, exhibiting a fibrous ductile fracture. The ductile type of fracture is exhibited to even higher temperatures on heating in the low P alloys. This can be seen in Fig. 111, alloy H1 tested on heating at 1150°C.

In the third series of wrought alloys, good ductility was exhibited to high temperatures both on heating and on cooling.

The nature of on cooling fracture is shown in Figs 112 and 113. These show fractures at 851°C and 1150°C of alloy S3, and both exhibit a similar fibrous nature.

The cast alloys, in addition to their lower overall ductility are also particularly adversely affected by high levels of P when tested on cooling. In alloy R1, with low P, failure is brittle at temperatures near to the melting point, but ductility improves significantly as temperature falls. The fractures produced at temperatures of 1095°C and 1131°C on cooling are shown in Figs 114 and 115. Unlike the brittle failures in the wrought alloys, these fracture surfaces clearly show a dendritic form. At lower temperatures of 451°C and 849°C, the same alloy on cooling exhibits ductile fracture surfaces (Figs 116 and 117).

The dependence of fracture type on temperature for a high P alloy was considered for alloy R7. This alloy exhibited very low ductility over a wide temperature range. At a temperature of 1130°C (Figs 118) the specimen fractured on cooling had a very smooth fracture surface. This type of fracture has previously been reported as indicative of incipient melting.[136] At a slightly lower temperature (1099°C), the fracture surface has a somewhat unclear structure, which appears to be a more normal dendritic structure (Fig. 119). As test temperature is lowered still further (to 851°C), the fracture produced during testing on cooling has a distinct dendritic appearance (Fig. 120). Below this temperature, the fracture takes on a ductile, fibrous appearance, as evidenced by the fracture at 651°C shown in Fig.

121. The considerably better ductility on heating is shown by the fracture surface produced at 858°C (Fig. 122), which has a ductile appearance, in contrast to the test at a similar temperature on cooling.

The fractures shown by the cast alloys show a similar pattern to the cast alloys of the second series, being mainly dendritic at high temperature and fibrous at lower temperature. Signs of incipient melting, as described above, can be seen in alloy T4, tested at 1150°C on cooling (Fig. 123). Freely solidified dendritic surfaces were observed in alloy T6, in a specimen which had failed on cooling after partially melting on heating through the peak temperature (Fig. 124).

4. DISCUSSION

The results obtained from the experimental work appear to divide conveniently into a number of areas, concerned with the effect of composition on crack susceptibility, the effect of composition on hot tensile properties, and the relationship between crack susceptibility and hot ductility. These will be treated as separate issues in this discussion, but drawn together in a final section which will also seek to consider some of the practical implications of the results.

4.1. Effects of composition on cracking

The information obtained from the cracking tests divides into two main areas. The first of these is the study of the position of cracks and their relationship to macro and microstructure; the second the quantitative relationship between composition and cracking obtained by linear regression analysis.

4.1.1. Crack morphology in wrought alloys

Initial input from industry, particularly fabricators in the USA,[137] had suggested that the major crack type in the wrought cupro-nickels was HAZ cracking. However, Varestraint tests on the first series of experimental alloys revealed that regardless of the level of augmented strain utilised, the cracking was confined almost entirely to the weld metal, as shown in Fig. 95. This pattern of cracking was repeated in all alloys of the second and third series. It has also been shown that the

cracking in the weld metal follows an inter-dendritic path, whilst such cracking as is to be found in the HAZ is intergranular.

These results are perhaps not as contradictory to the alloys' reported behaviour as might at first seem the case. Whilst the input from industry noted above suggested that cracking did not occur in the as-deposited weld, it seems likely that at least some of the cracking reported might be in reheated weld metal. Indeed, the importance of this type of cracking was demonstrated by the tests carried out using the commercial TIG filler wire. The likelihood of weld metal rather than HAZ cracking is also indicated by the structures of the two areas. As has already been demonstrated, the weld metal has a heavily cored structure, and it has been shown previously that the interdendritic regions may contain as little as 10-15% Ni.[56] These regions will clearly have a lower solidus temperature, and also exhibit lower strength at all temperatures making the weld metal crack susceptible. Although the grain boundaries represent areas of weakness in the wrought structure, the extent of segregation is less, and so strength and solidus are not decreased greatly, resulting in better resistance to cracking.

It has not been possible to show conclusively whether the cracking occurs actually during the solidification process, or if fracture of low strength inter-dendritic solid regions is responsible. It seems likely, however, that a combination of the two mechanisms is operating.

4.1.2 Effects of composition on weld cracking in the wrought alloys

The philosophy behind this whole study has been to produce results which would ultimately make a contribution towards improved specifications for weldable cupro-nickel alloys. There is consequently a sense in which this section is the most important. The following sections, whilst being of critical importance to the study of the problem, only make a minor contribution to the solution of the practical problem; they represent a means to an end, rather than being an end in themselves.

The elements involved in this study appear to divide conveniently into three groups, based on a combination of their previously reported effects and the results obtained from the current programme of work.

4.1.2.1. Effect of recognised crack promoters

The first group of elements are those which previous studies have agreed are responsible for producing increased cracking in the welding of cupro-nickel alloys. This group comprises Pb, P, S, Si and Bi, and the crack promoting tendencies of each of these has been reflected to a varying degree in the present study.

Probably the most important of these elements in the current research has been P. This has been varied in both the first and second series of wrought alloys, using a low level of <0.005%

and high levels of 0.015% and 0.03%. The first of these high levels is permitted by all of the common national standards and the second by all except ASTM. Regression analysis carried out on the first series of wrought alloys confirmed P as a crack promoter. This is evident from Table 8, where its effect on TCL and SFL at the 1% significance level and on MCL at the 2% level can be seen.

The effect of P in promoting cracking has previously been attributed both to the formation of low melting liquid films, and to the presence of P enriched solid films. In order to determine the extent of segregation in the weld region, energy dispersive analysis (EDA) was carried out in the cracked areas. These revealed P contents up to 0.1%. A more comprehensive study of segregation was carried out on the same group of alloys by Timothy,[138] and he quoted average enrichment factors in the range 2.6-3.7. Based on the nominal alloy composition, this would indicate P contents in the range 0.04%-0.055%, levels which would be responsible for a considerable drop in the true solidus of the alloy. This in turn would be consistent with the interdendritic type solidification cracking described earlier.

In the second series of wrought alloys three separate assessments of the effects of varying composition on cracking are available; two different regression analyses, and a ranking by means of cracking threshold. Results of regression analysis based on single tests on each alloy at several strain levels are shown in Table 10. Again, P is shown as having a crack promoting effect, whichever crack parameter is considered. In each case,

the significance level is extremely good, at 0.1%, indicating there can be little doubt that P is producing a real effect. Similar trends are also shown by the regression analysis carried out on the results on these alloys using a strain level fixed at 6%. Here also P appears as a crack promoter, having an effect on maximum crack length signficant at the 5% level and on the other crack parameters at the 1% level. The predominant role of P in controlling the cracking in this group of alloys is illustrated most strikingly by Table 11. The alloys are ranked here by cracking threshold (and by average cracking for those with the same threshold). This shows that the four alloys most subject to cracking are those with P at the high level, whilst those with P at low level are considerably more crack resistant.

The effect of P can be summarised as causing increased cracking in the weld metal at levels of 0.015% and above. This is slightly lower than the safe level of 0.02% reported by Witherell,[1] but higher than the harmful level of 0.006% in reheated weld metal reported by Casteras et al.[7,99] P has also been shown to be heavily segregated to the interdendritic regions through which cracks propagate.

Also of considerable importance among the group of impurity elements is S. This was varied in the first and third series of wrought alloys, using a low level of 0.002% and high levels of 0.02% and 0.08%. Once again, the level of 0.02% is permitted by all of the common specifications, and was selected because of initial pessimism about the hot workability of the alloys. When the initial series of alloys had proved these unfounded, the

level of 0.08% was selected as this represents the maximum permitted by BS 2870.

In every case, the high level of S can be associated with increased cracking. In the first series of wrought alloys, regression analysis showed that S had a crack-promoting effect on all three crack parameters, significant at the 1% level (Table 8). The same comments as those made about P (forming low melting films and brittle solid films) apply to S, and EDA in this case revealed S contents up to 0.12% in cracked regions. The results obtained by Timothy[138] also point to S concentrations but with his enrichment factors ranging between 1.1 and 5.1, the corresponding range of S contents is very wide (0.02%-0.1%). As with P, values at the higher end of the range would produce a significant drop in solidus temperature and a corresponding increase in susceptibility to interdendritic solidification cracking.

For the third series of wrought alloys, it was once more possible to examine the effect of S by looking both at regression analysis and cracking thresholds. It can be seen from Table 16 that S is significant at the 2% level in increasing both total crack length and sum of five longest cracks, but does not have any significant effect on the maximum crack length. This latter observation is somewhat surprising, and can be explained only in terms of the increased S content not producing an increase in the width of the crack susceptible zone. Instead, the increased S content produces a large number of potential crack sites, a change which is reflected in the increase in

total crack length.

This conclusive indication that levels of S of 0.02% or greater will cause increased weld metal cracking represents a step forward in understanding cracking in the 70-30 Cu-Ni, as it had previously been reported that S did not make a significant contribution to weld metal cracking in this alloy.(102)

Of all the possible impurities and alloying elements which might occur in cupro-nickels, Si has probably had most attention in previous investigations. It therefore did not seem appropriate to give great importance to this element in the present study, and consequently it appears only in the first series of wrought alloys. Low and high levels of 0.01% and 0.1% respectively were selected, the latter representing a level which typically occurs in commercial alloys. Although the change in Si content appeared to have no effect on total crack length, it was significant at the 1% level in increasing both maximum crack length and sum of five longest cracks.

Measurement of local Si content in cracked regions by EDA indicated that typical levels were around 0.5%, and in one particular case as high as 0.9%. These levels suggest that the solidus temperature of these regions will be reduced considerably, making them likely sites for solidification cracking to occur.

The effect of Si in increasing cracking is in agreement with that previously reported.(3,10) However, both of these

investigations were on high strength cupronickels, and so the level of 0.1% seen to cause cracking in this alloy cannot be directly compared with these earlier results.

The effect of varying Pb levels was investigated in the first series of wrought alloys. Low level was <0.002% and high level 0.01%. This level again represented one permitted by all specifications, and this would appear to be a satisfactory Pb content, as no association with increased weld metal cracking was found.

The final element of this group is Bi. In common with Pb, it was varied only in the first series of wrought alloys. The low level of Bi was <0.0005% and high level 0.002%. Bi levels are not specified in any of the major national standards, but the level selected, although low in absolute terms, is at the high end of the commercial range. Linear regression analysis of the tests on the first series alloys revealed that Bi was responsible for an increase in both maximum crack length and sum of five longest cracks, although in neither case was the significance level particularly good. As can be seen from Table 8, another problem arose in determining the effect of Bi. This was the failure to obtain regression coefficients for the Bi effect, due to a shortcoming in the statistical analysis technique, which makes it difficult to handle very small numbers. The lack of any highly significant effect of Bi on weld metal cracking is consistent with the way in which Bi affects cupro-nickel. It has previously been widely reported as a major source of intergranular ductility dip cracking in the alloy due to grain

boundary segregation. However, in the alloys under investigation here, the major factor controlling cracking is the drop in true solidus temperature. The low Bi contents involved are likely to make only a small contribution to this, hence the limited effect of Bi at this level in increasing solidification cracking.

4.1.2.2. Effect of carbon on cracking

Whilst C is an equally common impurity in cupro-nickel to those in the previous section, its effects seem to be less well understood. It has been suggested that increased C is a cause of ductility dip cracking. However, the only definite detrimental effect of C on the solidification/liquation type cracking is that which occurs if sufficient C is present to cause the formation of flake graphite. This will only be formed at C contents above 0.1%, which are unlikely to occur in normal practice.

Despite the lack of knowledge regarding the effect of C in cupro-nickels, the major specifications limit it to 0.05% or 0.06% in the wrought alloy. C was varied in all three series of wrought alloys. As before, the level was selected to represent the upper limit of the specification; in this case 0.06%. A low level of <0.01% was obtained for the second and third series, which were vacuum melted. However, this had not been possible for the first series alloys, which were melted under carbon, a level of 0.02%C being used.

The importance of C in reducing cracking was initially observed

in the first series of wrought alloys where it was significant in producing a decrease in the sum of five longest cracks (Table 8). This was somewhat surprising in the light of the comments made about C above, and prompted the decision to include C as a variable in the further series of alloys, hoping that this would clarify its effect. Unfortunately, the low atomic number of C prevents the determination of local C content in the cracked regions by EDA.

In the second series of alloys, the importance of C in reducing cracking is vividly illustrated by the cracking threshold figures in Table 11. It can be seen that in each case the cracking threshold is higher for an alloy containing C than for the alloy with other elements the same and C absent. The only exception to this is the pair of alloys containing no other impurities, where the one with C exhibited slightly higher cracking. These cracking figures suggest the occurrence of two conflicting effects. Firstly, when present alone, C is responsible for a small increase in cracking. However, when other impurities (P and Ti) are also added to the alloy, an overwhelming interaction occurs by which C is able to reduce cracking.

Further evidence to support this hypothesis is supplied by the regression analysis carried out. Both Table 10 (results at varying strain level) and Table 13 (at 6% strain) show an interaction between C and P which is highly significant in reducing cracking. Of the two possible interactions suggested above, this seems the less likely, compared with the formation

by Ti of a carbide. However, a careful consideration of the situation yields a possible explanation. A negative interaction (reduction in crack length) between two elements is effectively a statement that when the two are present simultaneously, their combined effect is not as great as the sum of their individual effects. Clearly C and P will not react to form any compound; it therefore seems likely that some substitution of P by less harmful C has occurred, although no definite evidence can be offered for this.

In the third series of wrought alloys, C was varied along with S and Zr. Consideration of the ranking of these alloys by cracking threshold again produces a pattern which indicates the way in which C behaves. In the two pairs of alloys where Zr is present, the C containing alloy is the less crack susceptible of the pair. However, in the other two pairs, with Zr absent, the C containing alloy in each pair is more crack susceptible. This again points to C alone having a small crack promoting effect, whilst when Zr is present this is masked by a crack inhibiting interaction.

The results of regression analysis carried out on the tests at 6% strain confirm these findings (Table 16). In particular, an interaction between C and Zr is shown to be significant in reducing maximum crack length. This interaction is explained in terms of the known effect of Zr in cupronickel, to react with C and other impurity elements. As will be shown in the following section, Zr is responsible for an increase in cracking and any Zr which is tied up by reaction with C will not be available to

participate in this effect.

In summarising these complex effects of C, two major factors emerge. C itself appears to have a small crack promoting effect, particularly when few other impurity elements are present. However, in most alloys investigated this effect is overshadowed by crack inhibiting interactions with Zr, P and possibly Ti.

4.1.2.3. Effects of Titanium and Zirconium on cracking

These two elements do not usually occur as impurities in the cupro-nickel alloys. Rather, their presence in many alloys of this type is the result of a deliberate addition, typically aimed at producing final levels in the range 0.15%-0.25%. These additions are made with a variety of aims, including the prevention of porosity, tying up of harmful impurities, control of grain size (particularly in the cast alloys) and prevention of ductility dip cracking.

As these two elements produce largely beneficial effects, it was for this reason that they were included in the present programme of work. Both were varied in the first series of wrought alloys, using low levels of <0.01% and high levels of 0.2%. The same levels were repeated for Ti in the second series alloys and Zr in the third.

Both Ti and Zr exhibited highly significant effects on all three crack parameters in the first series alloys. Surprisingly, these effects were not to reduce cracking, but in fact to produce an

increase in cracking, as can be seen in Table 8. These effects were clearly of considerable practical importance. It had previously been suggested by Pease and Kihlgren[5] that Ti levels greater than 0.15% could cause weld metal cracking, but except for this isolated report, neither element had been found detrimental.

Attempts to determine the extent of segregation of the elements to the cracked region by EDA gave inconsistent results. However, in certain cases there was considerable segregation to the cracked regions, with Ti up to 0.4% and Zr as great as 0.7% being recorded.

In the second series of wrought alloys, the importance of Ti as a crack promoter was shown clearly by the cracking thresholds of the eight alloys (Table 11). In every case, the alloy containing Ti was more sensitive than the corresponding alloy with the other impurities identical but Ti absent. The same effect was also demonstrated in the regression analysis carried out on the tests at varying strain levels (Table 10).

The effect of Zr as a crack promoter is demonstrated in the third series of wrought alloys. The results of regression analysis on the cracking at 6% strain show Zr as causing a significant increase in all three crack parameters (Table 16). Additionally, interactions of Zr with both of the other elements varied in these alloys occur which act to reduce cracking. The interaction between Zr and C is significant in reducing maximum crack length. This was discussed fully in the previous section

and will not be considered further here. Zr also interacts with S to reduce total crack length and sum of five longest cracks. This information is consistent with the cracking threshold data. In the group of four alloys not containing S, the two with high Zr are more crack sensitive than those with low Zr. However, in the other four alloys where S is high, the two containing Zr are the less crack sensitive, indicating that in this case a substantial interaction between S and Zr is the dominant feature.

The similarities between Ti and Zr, both in their nature and in the manner in which they have affected cracking in this study, dictate that they should be treated together for a consideration of the mechanisms operating. Clearly, when operating singly, particularly in alloys where most other impurities are absent, these elements increase cracking. The results of EDA indicate that in certain cases high levels of Ti and Zr are present in the cracked regions. It is also known that these areas contain a considerably higher proportion of Cu than the nominal 70%; typically, the Cu content of these regions is around 80%. Furthermore, both Zr and Ti form eutectics with Cu (eutectic compositions 4.7% Ti and 9% Zr). Zenkova and Glikman[139] showed that the drop in solidus temperature due to increased Zr in a Cu-Cr-Zr-Ti alloy was responsible for an increase in solidification cracking. It therefore seems likely that Ti and Zr are acting to produce solidification cracking in a similar manner in the cupro-nickel alloys.

In contrast to these single element effects, Ti (in combination

with P) and Zr (in combination with S) both produce interactions which reduce cracking tendency. All of these elements have the tendency to produce increased cracking when present alone. There is likely to be combination between the impurity element and the reactive metal in each case, which will remove both from solution, and in this way the extent of cracking will be reduced. This might also provide an explanation for the wide variation in local Ti and Zr contents found in the alloys of the first series. Each alloy had a different combination of impurity elements and these will have greatly influenced the distribution of Ti and Zr.

There does not appear to be any conflict between these findings and the reasons for Ti and Zr additions outlined at the start of this chapter. Their effect in reducing the maleficient effects of many common impurities has been confirmed. There is also no reason to suppose that the reports of reduced ductility dip cracking achieved by these elements are incorrect.[20,23] This type of cracking is heavily dependent on grain size, and there can be no doubt of the grain control effects achieved by Ti and Zr. However, the effect of Zr in promoting weld metal cracking at a level of 0.2-0.3% has previously been reported by Taylor and Burn,[98] and this appears in good agreement with the present work. Clearly, if the addition of these elements to an alloy is contemplated, then this propensity for increasing solidification cracking in the weld metal must be given consideration.

4.1.3. Crack morphology in cast alloy (IN768)

Unlike the wrought materials, the cast alloy has proved subject to extensive cracking in the HAZ, in addition to a significant amount of cracking in the weld metal. The cracking occurring in the weld metal is again interdendritic in nature. No further comment need be made on this, as the same explanation will apply as that given in Section 4.1.1.

However, the cracking in the HAZ is made up of two distinct types. Close to the fusion line, relatively coarse interdendritic cracking occurs, which appears to be liquation cracking. As with solidification cracking, this can be explained in terms of the lower solidus temperature and lower strength exhibited by the Ni depleted interdendritic regions. Also in common with solidification cracking, it seems likely that a combination of cracking due to presence of liquid films and fracture of brittle solid films is responsible for the overall effect.

In addition to this cracking, further HAZ cracking of an intergranular nature occurs at greater distances from the fusion line. This cracking is apparently of the ductility dip type, as it occurs in regions which have not been subjected to high peak temperatures.

4.1.4. Effect of composition on cracking in cast alloy (IN768)

The programme of work carried out on these alloys was of a much

more limited nature than that undertaken on the wrought cupro-nickels. It consisted of just one series of eight alloys, a full factorial involving Pb, S and Bi at high and low levels. The ability of these elements (particularly Pb and Bi) to contribute to ductility dip cracking in cupro-nickels is well known; the aim of this part of the investigation was to ascertain whether this held true for the Cu-Ni-Cr-Si alloy (IN768) at the particular levels of impurities selected. Low levels were set at <0.002%Pb, <0.005%S, <0.001%Bi and high levels 0.015%Pb, 0.05%S and 0.003%Bi were specified. These values are similar to the ones utilised in the wrought alloy, representing typical values which would be permitted by current specifications. However, in each case the high level is above that allowed by the new proposed specification shown in Table 3d.

As discussed in the previous section, the larger proportion of the cracking was in the HAZ and it was on this that all measurements were made. With all alloys cracking at the strain level of 1.8%, no ranking by cracking threshold was possible, and so assessment of the various impurites was done only by regression analysis, although this was carried out on results both from Varestraint testing and restrained butt welds.

Of the three impurity elements, Pb appears as the most consistent crack promoter. In the Varestraint testing, it produced a significant increase in each of the three cracking parameters (Table 19), and was also responsible for an increase in the sum of five longest cracks in the restrained butt welds (Table 22). This is in agreement with previous investigations

which have demonstrated the detrimental effect of Pb in the cast 70-30 cupro-nickels.[6,30,101]

A significant effect attributed to S is also shown by both weld tests, but these effects are conflicting ones. In the results from Varestraint testing, S is significant in increasing the sum of five longest cracks. However, the results of restrained butt weld tests show that S has a significant effect in reducing both sum of five longest cracks and total crack length. No obvious explanation can be seen for these conflicting results in terms of different mechanisms which might be operating. Despite the fundamental difference in the way in which the strain is generated the nature of the cracking is very similar, as described in the previous section. A more likely explanation is suggested by the poor significance levels; that one of these results (or possibly both) is due to experimental error, and that S has little real effect on the extent of cracking at the level used in these alloys. It has not been possible to confirm the reported effect of S in causing increased HAZ cracking in the cast alloys.[8,20]

It is also clear that Bi does not have any significant single element effect on cracking in either test. However, Bi does appear to be of considerable importance in that it exhibits significant interactions with both S and Pb. The interaction with S is one which increases all three crack parameters, whether measured on restrained butt weld or Varestraint test pieces. The means by which this interaction might occur is not clear. However, given that the levels of Bi and S are both

insufficient to make a significant contribution to cracking when present alone, it seems probable that when present in combination their total level then causes the increase seen in cracking. The interaction between Bi and Pb is of the opposite sign i.e. a reduction in cracking. This type of interaction (a beneficial one between two apparently harmful elements) was attributed in an earlier section to a saturation effect in the sites where the element might cause damage; in this case, with Pb and Bi both present, the total effect would be less than the sum of their individual effects because not all of the impurity would be concentrated harmfully at the grain boundaries.

Brief mention will also be made at this point of the importance of grain size. The original intention was to produce all alloys with a constant grain size. However, this was not achieved in practice, and the best remedial step was to include values of grain size in the regression analysis. In common with variation in S content, this appeared to produce conflicting evidence in the Varestraint (where increased G.S. led to increased cracking) and restrained butt weld tests (where increased G.S. caused decreased cracking). Again, significance levels were not particularly high, and consequently no conlcusions can be drawn on the effect of grain size over the range obtained in these alloys.

4.2. Effect of composition on hot ductility properties

The end product of the series of hot ductility tests carried out on each alloy is a pair of curves representing the variation of

reduction of area and breaking stress with temperature. Attempts to apply any of the criteria proposed by Yeniscavich[70] to obtain a value which might be related quantitatively to cracking were not particularly successful (the one exception to this is discussed fully in section 4.3.). In general, therefore, this review of the relationships between hot ductility results and composition will be based on a qualitative assessment of the hot ductility curves.

4.2.1. Relationship between on-heating and on-cooling ductility

For several of the second and third series wrought alloys testing was carried out on-heating in addition to the normal series of on-cooling tests. Similar tests were also carried out on cast alloys of the same composition.

It is widely accepted that on-heating ductility is generally better than on-cooling, particularly if the latter uses a high peak temperature. The main objective of these tests was to ascertain whether these differences in the temperature-ductility relationship could be related to cracking in any way.

It was evident from the graphs of reduction of area against temperature that the low values of ductility, recorded over a wide temperature range above 800°C for a number of alloys on-cooling, were not evident when the same alloys were tested on-heating. Indeed, all the alloys tested on heating the wrought state had reduction of area maxima of 80% or higher, whilst those tested in the cast state had maxima of at least 45%.

The marked contrast between these results indicates that the poor on-cooling ductilities are a consequence of changes to the structure brought about by heating to the peak temperature. Further evidence for this is given by the single test carried out on each alloy using a specimen which had been heated to a peak temperature of 1050°C. In every case except alloy R7, a value of R.A. greater than 15% was found. Additionally, most of the alloys exhibited improved ductility when tested on-cooling from 1050°C as compared to 1160°C. The only exceptions to this were alloys R1 and R4, where the differences were only small.

Metallographic and fractographic evidence also points to the importance of microstructural changes. Examination of fractures which occurred at high temperature and exhibited zero or low ductility has shown that liquated material was present under these conditions (Fig. 118). Evidence of liquation was also clearly visible on the section taken through the simulator specimen which was accidentally overheated (Fig. 107). However, such a change could not be observed using the microscope in testpieces which had been heated to the correct peak temperature; this may be due to the liquation occurring on too fine a scale to be readily detected by this means.

4.2.2. **Wrought alloys**

As described in the preceding section, the most notable feature of the hot ductility curves is the presence or absence of a substantial rise in ductility in the temperature range 800-1000°C, associated with the onset of dynamic recrystallisation.

A correlation exists between this feature and certain of the compositional variables.

The elements varied in the wrought alloys were divided into three groups for the purpose of considering their effects on cracking, and it seems appropriate to repeat the same division here.

4.2.2.1. Crack promoting impurities

From this group of elements, P had the most substantial effect on cracking, and will be considered first here. Amongst the first series of wrought alloys four completely lacked the rise in ductility mentioned above; A5, B2, B3 and B4 (Figs 32, 37-39). Two alloys exhibit only a small and insignificant rise in ductility; A4 and B1 (Figs. 31 and 36). However, of these six alloys, three contain high level P and three low level, so no useful information on the effect of P was obtained.

Consideration of the effects of various elements in the first series wrought alloys is made difficult because of the complex experimental design used, which makes comparisons between pairs of alloys difficult. P is also varied in the second series wrought alloys, and here the simple experimental design makes for easy, direct comparisons. The four alloys containing P at the low level are H1, P1, H3 and H4 (Figs 44-47). All of these display high ductility (RA > 80%) in the range 900-1100°C. In contrast, of the four alloys containing high P (Figs 48-51), three display low ductility through this region. The exception

is alloy H8 (Fig. 51) which has a maximum reduction of area of 60%. However, even this alloy is considerably less ductile than the corresponding alloy containing low P, but other impurities the same (H4, Fig. 47). It is therefore clear that P severely reduces ductility in the range 900-1100°C, in most cases completely suppressing the ductility recovery exhibited in this range by alloys containing P at a low level.

As discussed earlier, cast versions of each of the series 2 and 3 alloys were produced for hot ductility testing, in an effort to more nearly reproduce the structure existing in the weld metal. The results of the tests on these are shown in Figs 65-68 for the low P alloys and Figs 69-72 for the high P alloys. The pattern which emerges is very similar to that described above for the tests on the wrought material. The low P alloys all exhibit high ductility in the range 900-1100°C. The high P alloys, except for R5 (Fig. 69) show extremely low ductility over a wide range of temperature e.g. alloy R7 (Fig. 71) has RA <5% at all temperatures above 750°C. Alloy R5 containing only P, has considerably lower ductility than the coresponding alloy with all impurities low (R1, Fig. 65). The tests on these cast alloys confirm the effect of P in greatly reducing the ductility in the range 900-1100°C. These results also confirm the reported effect of P in increasing zero ductility range.[7,99]

Attempts to carry out a semi-quantitative analysis on fracture surfaces using an EDA technique were not sufficiently accurate to indicate whether any concentration of impurity elements existed here. However, SEM examination of fracture surfaces

showed that at the very highest temperatures, fractures with little reduction of area exhibited some signs of liquation, whilst at lower temperatures these took on an intergranular appearance. Relating this to the hot ductility curves suggests that two mechanisms are operating in combination. At high temperatures, the drop in solidus temperature brought about by increased P in the alloy is responsible for increased liquation and the poor ductility of the alloy. However, as the temperature of testing is lowered, the effect of P persists, in some cases down to 800°C. This clearly cannot be attributed to liquation, and a more probable mechanism seems to be the fracture of brittle grain boundary films, high in P. The suggestion that these films are produced by enhanced liquation in the high P alloys is confirmed by a consideration of the on-heating ductility curves. Those produced for wrought alloys with high P (Figs 55-57) reveal that the values for reduction of area are very high in the temperature range under consideration. Unfortunately sufficient material was available to carry out similar tests on only one of the cast versions (Fig. 76), and so it was not possible to determine if liquation damage occurred to the cast materials.

The second impurity which has been extensively investigated is S. In the first series alloys, the high level of S seems to produce marginally improved ductility results. Of the six alloys listed above as having poor ductility, only two (B1 and B4, Figs 36 and 39) have high S. However the comment made above about the difficulty of interpreting the results because of the complex experimental design applies equally here, and it appears

sensible not to attach too much weight to this observation.

S is also included in the third series of alloys. Here the low S alloys are H1, H3 (common to second and third series) S1 and S4 (Figs 44, 46, 58 and 61), whilst those with high S are S2, S3, S5 and S6 (Figs. 59, 60, 62 and 63). The first observation from these curves is that none have the form of the high P curves, with the complete absence of ductility increase in the high temperature region. However, a closer inspection of the curves reveals that in three cases an alloy with low S has moderately better ductility than one with other elements the same but S high (H1 and S2, H3 and S5, S4 and S6, Figs 44 and 59, 46 and 62, 61 and 63 respectively). The exception to this is alloys with high Zr and high and low S (S1 and S3, Figs 58 and 60) where little difference in ductility behaviour exists.

Cast versions of these alloys were also tested, and an identical pattern of results was found (Figs 65, 67, 77-82). In the case of alloys R1 and T2, R3 and T5, T4 and T6 (Figs. 65 and 78, 67 and 81, 80 and 82), a more significant drop in ductility was exhibited by the high S alloy of the pair. As with their wrought counterparts, varying S appeared to have little effect on the alloys containing high Zr (T1 and T3, Figs 77 and 79).

A general shortage of material of the third series alloys meant that it was only possible to carry out on-heating tests on one cast high S alloy (Fig. 84). Whilst this did show a marginal improvement over the on-cooling tests, no significance can be attached to this single result.

It appears likely that S acts to reduce ductility in a similar manner to P, by liquation at the highest temperature, and by the action of brittle solid phases at lower temperatures. However, the extent of the effect attributed to S is considerably less than that of P, and it seems that at the level employed in this investigation (0.08%), S does not have an effect which will be of practical importance. It also seems likely that some beneficial interaction takes place between S and Zr in alloys where both are present.

The remaining three elements in this group are Si, Pb and Bi, which were varied in the first series alloys only. The difficulty in extracting the effects of each individual element from the fractional factorial design has already been explained. For each of these three elements, the six alloys which displayed poor hot ductility properties were divided equally between those containing high and low levels of the element. Consequently, no meaningful conclusions can be drawn about the effects of these alloys from the current work.

4.2.2.2. **Effect of C on hot ductility**

Of all the elements varied in the cupro-nickels in this programme of work, C gives the best opportuinity for assessment as it was varied in all three series of wrought alloys.

In the first series alloys, C presents a clearer picture than any of the impurities already dealt with. The six alloys listed above as having poor ductility at high temperatures are all

alloys containing C at the low level except for alloy A5. This would appear to be a significant indication that the high C level is able to produce an improvement in hot ductility.

However, in the alloys of the second series, no clear effect of C emerges. If pairs of alloys with similar compositions but high and low C are compared, it appears that C has little effect, except for alloys H6 and H8, where the higher C alloy has significantly better ductility. Tests were also carried out on the cast equivalents of these alloys, but again the picture was not entirely clear. Three pairs of comparable alloys (R1 and R3, R2 and R4, R6 and R8, Figs 65 and 67, 66 and 68, 70 and 72) showed a moderate improvement in ductility in the alloy containing high C. However, in the fourth pair this relationship was reversed, with the high C alloy (R7, Fig. 71) having very low ductility at all temperatures above 750°C.

The effect of C on the third series alloys proved equally difficult to assess. In the wrought versions of these alloys, any differences between the low and high C alloys were small and of no real significance. In the cast alloys of the same analysis, some effect of C could be seen. For two pairs of alloys (R1 and R3, T1 and T4, Figs. 65 and 67, 77 and 80) the high C alloy exhibited a modest improvement in ductility when compared with the alloy with similar composition but low C. However, for the other two pairs of alloys, no difference due to the change in C level was observed.

It therefore appears that C does make some contribution to an

improvement in hot ductility. However, the results obtained are far from being consistent, showing considerable variation according to the other elements present in the alloy, and also whether the alloy is in the wrought or cast form. The overall effect attributed to C is consequently small compared for example, with that of P, and is therefore likely to be of only limited practical importance.

4.2.2.3. **Effect of Titanium and Zirconium on hot ductility**

These two elements were the subject of considerable attention in this investisgation, each being included as a variable in the first and one of the subsequent series of experimental alloys.

The presence of Ti in the first series alloys appears to have only a slight detrimental effect on hot ductility. Of the six alloys displaying low ductility, four have Ti at the high level (A4, A5, Bi and B2, Figs. 31 and 32, 36 and 37) whilst two have Ti at low level (B3 and B4, Figs. 38 and 39). This does not seem to indicate a highly significant effect of Ti in these alloys.

Ti was also varied in the second series of wrought alloys, but despite the ease of comparison facilitated by the full factorial design, little more information on its effects could be obtained here. The only alloys to show a change in ductility with Ti content were those containing both P and C at high level (H7 and H8, Figs 50 and 51) where the alloy with high Ti had the better ductility at high temperatures. When the cast versions of these same two alloys were tested (R7 and R8, Figs 71 and 72)

the same effect of Ti improving ductility was observed, although smaller in magnitude. In contrast to this however, the cast alloys with high P and low C (R5 and R6, Figs 69 and 70) exhibited a marked loss of ductility when Ti was present at the high level.

An equally inconclusive pattern of results emerged for the effect of Zr. In the first series wrought alloys, a similar pattern emerged to that observed for Ti, i.e. four of the low ductility alloys had high level Zr, whilst the remaining two were low level Zr. As before, this did not provide a basis for any firm conclusion. Furthermore, the variation of Zr in the third series alloys did not give any better results. The only alloys to have their hot ductility affected by change in Zr level were those containing high S and low C, both in wrought and cast forms (S2 and S3, T2 and T3, Figs 59 and 60, 78 and 79). In each case, the increased level of Zr brought about a moderate improvement in ductility at high temperatures.

In summarising, Ti and Zr can be said to be responsible only for minor changes in the ductility of the cupro-nickel alloys at high temperatures. It seems likely that those changes which are observed are the result of an interaction with one or more other elements, thus preventing the simple comparisons drawn here from representing the full picture.

4.2.3. Cast IN768 alloys

Hot ductility tests were carried out on each of the eight

alloys of this type, and also on the ninth alloy (K8) which had been rejected for use in the weld cracking tests because of its erroneously high Bi content. In each case, tests were carried out on-cooling only (Figs 84-92).

A few general comments seem appropriate before discussing the effects of individual elements. The overall level of hot ductility is very poor compared with that displayed by the wrought alloys. With only two exceptions (K2 and L2, Figs. 86 and 90) the ductility of these alloys was worse than any of the wrought alloys. With the same two exceptions, none of the alloys exhibited greater than 15% RA at any temperature above 450°C.

The shape of the ductility temperature curve for alloys K2 and L2 is in agreement with that widely reported previously for this type of alloy. At low temperatures ductility is good but falls to a minimum around 700°C. Above this, ductility rises again, reaching a maximum around the recrystallisation temperature and finally falling off again as the solidus is approached. However, for the remaining seven alloys, a different curve is produced. Once the ductility has fallen in the intermediate temperature range, it remains relatively low (some alloys do exhibit a small increase) right up to the solidus temperature.

The fact that such a large proportion of the alloys tested do exhibit extremely low ductility, and also that they behave very similarly to each other, makes a meaningful assessment of the effect of composition very difficult. However, a closer inspection of the ductility temperature curves reveals that of

the seven showing poor ductility, two do show a modest improvement at high temperature (K6 and L3, Figs. 88 and 91) and this further division of the curves is of considerable assistance in assessing the elemental effects.

Considering first the effect of Pb it is clear that in every case the hot ductility of an alloy containing high Pb is inferior to that of an alloy with other elements at the same level but with low Pb. This difference is particularly marked in the alloys containing Bi at a low level (K2 and K4, L2 and K6, Figs. 86 and 87, 90 and 88) but is much smaller in the presence of high Bi (M1 and M3, L3 and N2, Figs. 92 and 93, 91 and 94). This effect would appear to be consistent with the well documented ability of Pb to reduce ductility in both the intermediate and high temperature ranges,[15] attributed to formation of both brittle solid films and liquated material.

The effect of Bi is very similar to that described above for Pb. Changing Bi from low to high level whilst holding other elements constant produces a significant drop in hot ductility, except for the alloys containing Pb at high and S at low levels (K4 and M3, Figs. 87 and 93) where no change occurs. A further interesting facet of the behaviour of Bi is revealed by comparing alloy K8 (Fig 89) which had the erroneously high Bi level, with alloy N2 (Fig. 94) its replacement with correct Bi level. It is clear that no further loss in ductility is brought about by the increase from 0.005% to 0.01%, confirming the results of Gavin et al[15] that a low level of Bi is sufficient to produce almost complete loss of high temperature ductility.

The effect of the third impurity element (S) is less clear than that of either Pb or Bi. For the pair of alloys without other impurities, increase in S results in a small loss of hot ductility (K2 and L2). However, this pattern is not repeated in other alloys. The alloys containing Pb (K4 and K6, Figs. 87 and 88) and Bi (M1 and L3, Figs 92 and 91) singly are subject to a small increase in hot ductility when S is present at a high level, whilst the alloys containing both Pb and Bi (M3 and N2, Figs. 93-94) appear to be unaffected by change in S level. It therefore appears that S, when present alone, has a very small detrimental effect, but can interact beneficially with both Pb and Bi.

This is in agreement with the tolerance of levels of S up to 0.075% without loss of hot ductility reported by Gavin et al.[15]

4.3. Relationship between cracking and hot ductility

If the results obtained from hot ductility testing are to be of any practical value, then a means of relating them to cracking results is required. In the case of ductility dip cracking, this has conventionally been done by looking at the minimum intermediate temperature ductility, and an acceptable correlation has been produced. However, the major type of cracking produced in this present study is the Type 1, associated with solidification (in weld metal) or liquation (in HAZ). The difficulty of relating this cracking to any parameter measured from the ductility-temperature curve was discussed in

section 2.6.1. A number of possible criteria for assessing the crack susceptibility of an alloy were listed there, and the usefulness (or otherwise) of these in the present study will now be outlined.

1. Minimum arbitrary ductility. As the name suggests, this is an arbitrary value and does not provide a useful basis for a quantitative relationship, as it only divides alloys into crack resistant or susceptible categories. However, as will be seen later, it does relate well to the results obtained in these tests.

2. Recovery rate of ductility. This was easily measured from the curves, and is a possible criteria for relation to cracking.

3. Recovery rate of stress. The small additions of alloy and impurity elements made did not appear to produce any significant change in strength-temperature curves. The differences between alloys in the value of this parameter would therefore be insignificant.

4. Zero ductility range. This could not be calculated as neither zero strength temperature nor solidus temperature could be satisfactorily measured for most of the alloys.

In addition to the selection of a suitable parameter, the need arises to give a more general consideration to the suitability of the hot ductility results for relation to cracking. In

particular, much of the cracking in the wrought alloys had occurred in the weld metal, whereas specimens tested using the weld thermal simulator were producing a simulation of the HAZ. This raises two problems. Firstly, the type of cracking being simulated is liquation cracking, whereas in the real situation it is solidification cracking. Secondly, the structure of the simulator specimen is a wrought one, whereas the weld metal is a "cast" structure. The latter is a particular problem in the cupro-nickels, as the weld has a highly dendritic structure and the wrought alloy is homogenous.

The second problem is the more easily solved, and so this one will be considered first. In the first series of wrought alloys, tests were carried out only on straightforward wrought material. However, during the course of these tests it was realised that a cast material might provide a better simulation of weld metal, even after accounting for the obvious difference in coarseness of structure. As a consequence, when the material for the second and third series tests was prepared, a portion of each ingot was retained in the cast state, and utilised for additional hot ductility tests. The results of these tests have already been described, and their significance in relation both to the tests on the wrought specimens and to the weld cracking in these alloys will be discussed later.

The difficulty in relating the reduction of area in a material of which the bulk remains solid to cracking in a solidifying alloy is less easily overcome. Clearly, the ideal would be to utilise a simulator which has the facility to take the test

piece into the fully molten state, but unfortunately the machine available for this investigation does not have this capability. However, it is possible to demonstrate reasonable grounds for assuming that the elemental factors affecting soldification cracking and liquation cracking (which is effectively being simulated) are similar. The first reason which can be established for this is the similarity of the cracking mechanisms; in both cases failure is associated with the fracture of liquid films or of brittle solid films associated with the solidification structure (see Section 2.3.2.1.). Secondly, the likelihood of elements which are responsible for the one form of cracking also being responsible for the other form has been demonstrated by a number of previous workers both for cupro-nickels and other alloys, e.g. steels.

4.3.1. Hot ductility and cracking in wrought alloys

The correlations existing individually both between composition and cracking and between composition and the hot ductility curve have already been shown. These were seen to exist for a number of elements in the three series of wrought alloys. In many cases the elements affecting cracking and hot ductility were the same ones; P appears to be the most serious crack promoter at the levels used, and also had the most detrimental effect on hot ductility. However, as will now be shown, whilst it has proved possible to relate these factors in a qualitative way, development of a quantitative relationship has proved considerably more difficulty.

In the first series wrought alloys, six were recognised as having inferior hot ductility to the remainder; in particular, the large peak in the ductility curve normally observed in the temperature range 900-1100°C was absent in alloys A5, B2, B3 and B4 (Figs 32, 37-39) and only very small in alloys A4 and B1 (Figs 31 and 36). If these curves are compared to the average values for TCL shown in Table 6, a certain amount of agreement can be seen. For example, if the alloys are divided equally into two groups according to the value of TCL (using TCL = 6.5mm as the boundary), five of these alloys with poor ductility fall in the more crack susceptible group. However, with three of the alloys with good ductility also falling in this group, this point must be treated with some caution. Despite this shortcoming, it does seem reasonable to conclude that if the peak is missing from the ductility curve, the alloy is likely to be subject to cracking. Attempts to develop a quantitative relationship between extent of cracking and recovery rate of ductility did not meet with any success.

In the second series of alloys, hot ductility results were available for material of identical composition in both the wrought and cast states. Again, the hot ductility curves divided into the two distinct types (with and without the peak at high temperature). In general, the wrought and cast versions of each alloy exhibited the same ductility-temperature relationship, although there were two exceptions to this (H5 and R5, H8 and R8, Figs 48 and 69, 51 and 72). If the wrought alloy hot ductility results are compared with the cracking as before, it can be seen that the three alloys which lack the ductility peak

are also the three exhibiting the highest average values of SFL in Table 12. (H5, H6 and H7 Figs 49-51). Unfortunately, an equally clear picture does not emerge from the hot ductility results on the cast specimens. Here the poor ductility is exhibited by alloys R6, R7, R8, (Figs 70-72), whereas the worst cracking corresponds to alloy R5 (Fig. 69), and these three alloys are next worst. It therefore appears that the use of cast simulator specimens does not, as had been hoped, improve the simulation of weld metal, but in fact gives inferior results.

An attempt was again made to produce a quantitative relationship between rate of ductility recovery and extent of cracking. In order to calculate ductility recovery on a consistent basis, it was taken as being the average rate of ductility recovery in the range 0-20%. The values obtained for this parameter for the wrought simulator tests are shown in Table 38. These are plotted against average SFL in Fig. 125. It can be seen that an approximate straight line relationship exists between cracking and recovery rate of ductility for these alloys.

For the third series alloys, information is again available from hot ductility tests in both the wrought and cast states. However, all alloys tested show a substantial ductility peak in the range 900°C-1100°C and it was therefore impossible to develop the type of relationship with cracking which had been shown in earlier series. Attempts to quantitatively relate rate of ductility recovery to extent of cracking met with failure.

4.3.2. Hot ductility and cracking in cast IN768 alloys

The cracking in this group of alloys was predominantly in the HAZ, and so the difficulties described earlier in relating simulator results to weld metal cracking are of no significance here. The cracking in the HAZ appears to be a combination of liquation and ductility dip cracking.

Consideration of the plots of ductility against temperature reveals that the same two types of curve are generated as in the wrought alloys. With the exception of two alloys (K2 and L2, Figs 86 and 90), all materials exhibited extremely low ductility at temperatures from around 750°C up to the melting point. Significantly, alloys K2 and L2 were the ones which showed the least crack susceptibility in both Varestraint and restrained butt weld tests. The low ductility exhibited by the remaining alloys over the wide temperature range is consistent with the extensive cracking of both ductility dip and liquation types which were observed. In common with many of the wrought alloys, development of a quantitative relationship between recovery rate of ductility and crack susceptibility is not possible. However, in this case the problem appears to be largely due to the extremely low values of recovery rate. These are brought about by the intervals of several hundred degrees which many alloys have between 0 and 20%RA, and result in most points occurring close together when plotted.

4.4. Practical implications of this study

The need for this study arose out of a feeling held by many cupro-nickel users and producers that the current national standards were inadequate in terms of the impurity limits specified. It therefore seems right that the major practical implications are those concerned with the levels of alloy and impurity elements.

In order to make a useful assessment of existing impurity maxima, high levels were selected as close to these as possible. It has been shown that levels of 0.025-0.03%P are responsible for severe increases in cracking compared to a low P alloy. Levels of S of 0.08% have also been shown to be detrimental to crack resistance, as have Si levels of 0.08-0.12%. The propensity to cracking of alloys containing these high impurity levels indicates that every effort should be made to keep them low in weldable grades of cupro-nickel.

Whilst the three elements listed above were all expected to increase crack susceptibility, the effect of Ti and Zr in doing the same was more surprising. These elements are generally intentional additions, and so could easily be totally eliminated. However, this may not be a satisfactory answer in all cases, as these elements may be required for grain control, or even prevention of ductility dip cracking. It is therefore necessary that careful consideration be given to the type of cracking likely to occur in a particular situation. Alternatively, the possibility of replacing Ti and Zr by another

element which would not be detrimental to weld metal crack resistance may be considered.

The role of C in interacting with other elements (P, Zr and Ti) to reduce cracking also proved surprising. However, whilst the reality of these interactions is not doubted, it does not seem prudent at this stage to increase C for this purpose. Such a move might lead to increased ductility dip cracking or formation of highly detrimental flake graphite.

The usefulness of the hot ductility test carried out on the weld simulator has also been demonstrated. It has been shown that any alloy failing to exhibit a substantial improvement in the temperature range 900-1100°C will be subject to extensive cracking during welding. This gives a basis upon which crack susceptibility of alloys might be predicted. Indeed, it suggests that specifications might usefully require a test to be carried out at a temperature in this range, with a minimum on-cooling ductility of say 20% needed for the alloy to be acceptable.

5. CONCLUSIONS

5.1. It has been shown that wrought 70-30 cupro-nickel alloys with compositions within most national specifications are subject to weld metal cracking; the extent being a function of the exact composition. A small amount of cracking occurred in the HAZ, but this was largely very close to the fusion line, where it appeared to be an extension of weld metal cracking.

5.2. It has been confirmed that the presence of the impurities P, S and Si increases weld metal crack susceptibility of wrought cupro-nickel alloys, and shown that C operates as a crack inhibitor in combination with P or Zr.

5.3. Ti and Zr, both common additions to commercial cupro-nickels at levels around 0.2%, produce increased weld metal cracking when present in the wrought alloy at this level.

5.4. In the cast 70-30 cupro-nickel (IN768), the predominant form of cracking is in the HAZ (both liquation and ductility dip), although a significant amount of cracking also occurs in the weld metal. Again, the extent of cracking is dependent on precise composition.

5.5. It has been shown that Pb, S and Bi increase HAZ cracking in the cast cupro-nickel alloy IN768, the latter two appearing to act in combination.

5.6. In general, tensile tests carried out during the heating portion of a simulated weld thermal cycle demonstrated that the hot ductility of the cupro-nickel alloys over the temperature range 850-1100°C was invariably high, typically in the range 80-90%RA. However, this was reduced on cooling; some alloys retained moderate to high ductility in the temperature range 1100-900°C with a trough at lower temperatures, whilst other alloys exhibited low ductility (<20%RA) over the entire temperature range 1150-750°C.

5.7. A qualitative correlation appears to exist between crack susceptibility of the alloys and certain features of the ductility - temperature curves. In particular, absence of an improved on cooling ductility, over the range 1100-900°C, can in many cases be associated with a crack susceptible alloy. More explicitly, a proportional relationship seems to exist between the rate of ductility recovery and the extent of cracking for the alloys of the second series.

6. RECOMMENDATIONS FOR FURTHER WORK

6.1. This investigation has demonstrated the previously unreported effect of both titanium and zirconium in promoting high temperature cracking in the cupro-nickels. However, in the series of tests carried out it was possible to use only two levels of each element. A further series of tests using a number of levels of each element would indicate the levels which could be tolerated without increasing cracking.

6.2. Although the present study has successfully shown that a qualitative relationship exists between weld metal cracking and the form of the hot ductility curve, it has been possible to develop a quantitative relationship only for one series of alloys. In order to produce a more definitive correlation, further simulation work is required. This should be directed primarily towards the determination of nil ductility temperature (NDT) and nil strength temperature (NST), which will probably require utilisation of a simulator which is able to take material into the fully molten state.

APPENDIX A
TABLES

Table 1 Experimental Design for 70/30 Cupronickel Alloys for the First Stage of the Programme

Alloy No	High Level Impurities
A1	Pb, P
A2	S, Zr
A3	Pb, Bi, S, Ti
A4	Bi, P, Zr, Ti
A5	Pb, C, Zr, Ti
A6	C, P, S, Ti
A7	Pb, Bi, C, P, S, Zr
A8	Bi, C
B1	Pb, Si, P, S, Ti, Zr
B2	Si, Ti
B3	Pb, Bi, Si, Zr
B4	Bi, Si, P, S
B5	Pb, C, Si, S
B6	C, Si, P, Zr
B7	Pb, Bi, C, Si, P, Ti
B8	Bi, C, Si, S, Zr, Ti

NB Impurities not listed are at a low level

Table 2 Impurity Levels in the Experimental 70/30 Cupronickel Alloys

Element	Low Level	High Level
P	0	0.015
Pb	0	0.01
S	0.002	0.02
C	0.02	0.06
Si	0.01	0.01
Bi	0	0.002
Zr	0	0.2
Ti	0	0.2

Elements in %wt

Table 3a Nominal and Analysed Composition of the first series of experimental 70/30 Cupronickel Alloys

Alloy No		Composition Weight Per Cent (Cu Balance)												
		Ni	Mn	Fe	Pb	S	C	Si	Bi	Zr	Ti	P	Ca	Al
A1	Nominal	30.0	1.0	0.5	0.01	0.002	0.02	0.01	-	-	-	0.015	-	-
	Analysed	29.8	1.02	0.70	0.01	0.004	0.015	0.01	<0.0005	<0.01	<0.01	0.013	0.006	<0.01
A2	Nominal	30.0	1.0	0.5	-	0.02	0.02	0.01	-	0.2	-	-	-	-
	Analysed	29.9	1.09	0.61	<0.002	0.018	0.018	0.01	<0.0005	0.17	<0.01	0.002	0.009	<0.01
A3	Nominal	30.0	1.0	0.50	0.01	0.02	0.02	0.01	0.002	-	0.20	-	-	-
	Analysed	30.3	1.03	0.65	0.012	0.018	0.019	0.01	0.0023	<0.01	0.20	0.002	0.005	<0.01
A4	Nominal	30.0	1.0	0.50	-	0.002	0.02	0.01	0.002	0.2	0.2	0.0015	-	-
	Analysed	29.6	1.02	0.83	<0.002	0.003	0.018	0.01	0.0013	0.14	0.2	0.015	0.002	<0.01
A5	Nominal	30.0	1.0	0.50	0.01	0.002	0.06	0.01	-	0.2	0.2	-	-	-
	Analysed	29.5	1.07	0.64	0.008	0.004	0.05	0.01	<0.0005	0.16	0.19	0.002	0.005	<0.01
A6	Nominal	30.0	1.0	0.50	-	0.02	0.06	0.01	-	-	0.2	0.015	-	-
	Analysed	30.1	1.16	0.62	<0.002	0.02	0.05	0.01	<0.0005	<0.01	0.22	0.014	0.007	<0.01
A7	Nominal	30.0	1.0	0.50	0.010	0.02	0.06	0.01	0.002	0.20	-	0.015	-	-
	Analysed	29.9	1.11	0.64	0.008	0.017	0.045	0.01	0.0023	0.16	<0.01	0.015	0.005	<0.01
A8	Nominal	30.0	1.0	0.50	-	0.002	0.06	0.01	0.002	-	-	-	-	-
	Analysed	29.3	1.02	0.63	<0.002	0.004	0.05	0.01	0.0021	<0.01	<0.01	0.002	0.005	<0.01

continued

Table 3a continued

Alloy No		Composition Weight Per Cent (Cu Balance)												
		Ni	Mn	Fe	Pb	S	C	Si	Bi	Zr	Ti	P	Ca	Al
B1	Nominal	30.0	1.0	0.50	0.01	0.02	0.02	0.10	-	0.2	0.2	0.015	-	-
	Analysed	29.8	1.03	0.67	0.011	0.017	0.027	0.095	<0.0005	0.15	0.22	0.014	0.005	<0.01
B2	Nominal	30.0	1.0	0.50	-	0.002	0.02	0.10	-	-	0.2	-	-	-
	Analysed	30.1	1.11	0.70	<0.002	0.003	0.020	0.12	<0.0005	< 0.05	0.22	0.002	0.006	<0.01
B3	Nominal	30.0	1.0	0.5	0.01	0.002	0.02	0.10	0.002	0.2	-	-	-	-
	Analysed	30.1	1.08	0.71	0.009	0.003	0.020	0.12	0.0019	0.15	<0.01	0.002	0.004	<0.01
B4	Nominal	30.0	1.0	0.5	-	0.02	0.02	0.10	0.002	-	-	0.015	-	-
	Analysed	30.1	1.07	0.65	<0.002	0.02	0.024	0.08	0.0021	<0.01	<0.01	0.013	0.008	<0.01
B5	Nominal	30.0	1.0	0.5	0.01	0.02	0.06	0.10	-	-	-	-	-	-
	Analysed	29.4	1.11	0.72	0.011	0.018	0.043	0.10	<0.0005	<0.01	<0.01	0.002	0.006	<0.01
B6	Nominal	30.0	1.0	0.50	-	0.002	0.06	0.10	-	0.2	-	0.015	-	-
	Analysed	30.2	1.07	0.71	<0.002	0.004	0.057	0.10	<0.0005	0.15	<0.01	0.015	0.005	<0.01
B7	Nominal	30.0	1.0	0.50	0.01	0.002	0.06	0.10	0.002	-	0.20	0.015	-	-
	Analysed	30.5	1.06	0.72	0.01	0.004	0.057	0.11	0.002	<0.01	0.21	0.014	0.006	<0.01
B8	Nominal	30.0	1.0	0.50	-	0.02	0.06	0.10	0.002	0.2	0.2	-	-	-
	Analysed	29.4	1.16	0.72	<0.002	0.017	0.045	0.12	0.0021	0.13	0.20	0.002	0.003	<0.01

Table 3b Composition of the second series of experimental 70/30 cupronickel alloys.

Alloy	Composition %wt (Cu balance)					
	Ni	Fe	Mn	C	P	Ti
H1	29.9	0.72	1.08	0.004	<0.005	<0.003
H2	30.1	0.83	0.80	0.007	<0.005	0.2
H3	29.9	0.72	1.1	0.054	<0.005	<0.003
H4	29.6	0.72	1.11	0.052	<0.005	0.2
H5	29.8	0.71	1.1	0.004	0.025	<0.003
H6	29.9	0.71	1.08	0.002	0.029	0.2
H7	29.9	0.72	1.1	0.06	0.029	<0.003
H8	29.7	0.71	1.11	0.052	0.029	0.2
P1	29.9	0.71	1.22	0.007	<0.005	0.21

Nominal low and high levels. C - 0 and 0.06, P - 0 and 0.03 and Ti - 0 and 0.2

Table 3c Composition of the third series of experimental 70/30 cupronickel alloys

Alloy	Composition % wt (Cu balance)					
	Ni	Fe	Mn	C	S	Zr
S1	29.8	0.71	1.08	0.001	0.002	0.18
S2	29.8	0.70	1.04	0.001	0.064	<0.005
S3	29.8	0.76	1.07	0.001	0.080	0.15
S4	29.6	0.75	1.11	0.044	0.006	0.22
S5	29.0	0.70	1.04	0.043	0.080	<0.005
S6	30.0	0.70	1.07	0.041	0.080	0.22

Table 3d Composition of the Experimental IN768 Alloys

ALLOY DESIGNATION	COMPOSITION % wt											
	Cu	Ni	Fe	Mn	Si	Cr	Zr	C	Ti	Pb	S	Bi
Proposed Specification	Bem	29.0 -33.0	0.4 -1.0	0.4 -1.0	0.2 -0.4	1.5 -2.0	0.05 -0.15	<0.02	-	<0.005	<0.01	<0.002
K2	Bem	30.2 28.92	0.55 0.48	0.45 0.48	0.30 0.35	1.92 1.75	0.07 0.08	0.014 0.013	0.04 0.06	<0.002 <0.002	0.005 0.003	<0.0005 <0.001
K4	Bem	29.7 29	0.55 0.48	0.42 0.48	0.30 0.36	1.90 1.67	0.035 0.03	0.017 0.014	0.025 0.02	0.028 0.03	0.005 0.002	<0.0005 <0.001
K6	Bem	29.8 28.83	0.58 0.49	0.45 0.47	0.29 0.34	1.84 1.65	0.08 0.07	0.017 0.015	0.05 0.07	0.025 0.03	0.035 0.029	<0.0005 <0.001
K8	Bem	29.8	0.55	0.40	0.28	1.70	0.025	0.015	0.015	0.027	0.038	<0.01
L2	Bem	29.3 28.86	0.65 0.52	0.50 0.49	0.30 0.34	1.57 1.57	0.09 0.08	0.009 0.01	0.08 0.09	<0.002 <0.002	0.049 0.049	<0.0005 <0.001
L3	Bem	29.0 28.68	0.65 0.51	0.50 0.49	0.29 0.33	1.56 1.56	0.05 0.07	0.009 0.01	0.07 0.09	<0.002 <0.002	0.051 0.048	0.004 0.005
M1	Bem	29.3 28.67	0.64 0.51	0.55 0.55	0.33 0.37	1.87 1.68	0.06 0.08	0.009 0.01	0.06 0.07	<0.002 <0.002	<0.005 0.002	0.004 0.006
M3	Bem	29.3 28.63	0.60 0.51	0.47 0.50	0.29 0.33	1.52 1.55	0.02 0.06	0.01 0.01	0.03 0.08	0.023 0.03	<0.005 0.002	0.004 0.005
N2	Bem	29.4 28.92	0.68 0.51	0.52 0.53	0.30 0.33	1.83 1.73	0.10 0.06	0.006 0.007	0.025 0.07	0.022 0.02	0.048 0.052	0.005 0.005

Duplicate Analyses.

1. BNF Metals Technology Centre
2. AMTE Dockyard Laboratory
   HM Naval Base, Portsmouth

Table 4 Varestraint crack length data for the commercial 70/30 cupronickel alloy for a range of applied strain levels

	Crack Lengths (mm)								
	Strain	1.8%		3%		4%		6%	
	Flattened	Y	N	Y	N	Y	N	Y	N
Set 1	TCL	13.71	10.8	17.9	15.95	17.14	12.75	17.6	19.88
	SFL	9.27	8.1	11.57	7.87	14.08	9.75	11.22	11.05
Set 2	TCL	9.14	13.18	8.81	21.41	16.53	15.19	17.86	22.43
	SFL	6.71	9.61	8.31	11.98	10.38	11.63	16.2	13.1

Table 5 Summary of the Varestraint Crack Measurements for the Commercial 70/30 Cupronickel Alloy for a Range of Applied Strain Levels

a) Sum of Five Largest Cracks

Strain %	Mean Length mm	Standard Deviation mm	Coefficient of Variation
1.8	8.43	1.31	0.156
3.0	9.93	2.14	0.216
4.0	9.97	3.78	0.379
6.0	12.17	2.00	0.164

b) Total Crack Length

Strain %	Mean Length mm	Standard Deviation mm	Coefficient of Variation
1.8	11.71	2.13	0.182
3.0	16.02	5.31	0.331
4.0	13.12	5.38	0.41
6.0	18.09	2.45	0.136

Table 6 Varestraint Crack Length Data for the First Series Experimental 70/30 Cupronickel alloys tested at 1.8% strain

Alloy	Parameter	Crack Lengths mm						
		Set 1	Set 2	Set 3	Set 4	Set 5	Set 6	Average *
A1	MCL	1.54	1.85	1.6	1.14	1.14	0.84	1.3
	TCL	3.74	4.51	6.46	4.71	5.41	2.06	4.08
	SFL	3.48	4.51	4.98	4.05	4.71	2.06	3.76
A2	MCL	1.55	2.08	1.06	1.2	1.3	1.04	1.43
	TCL	4.63	4.99	3.28	4.23	6.87	5.05	5.15
	SFL	4.63	4.99	3.03	3.83	4.53	3.62	4.32
A3	MCL	1.83	1.58	0.84	1.74	1.71	1.28	1.63
	TCL	6.63	5.82	1.07	7.28	9.62	2.86	6.44
	SFL	5.7	5.22	1.07	5.5	6.54	2.86	5.16
A4	MCL	2.56	1.57	2.09	1.54	1.75	1.94	1.87
	TCL	9.4	9.43	4.34	3.78	9.85	7.78	8.05
	SFL	8.77	5.52	4.34	3.78	6.64	6.36	6.21
A5	MCL	1.58	2.18	1.39	1.96	1.1	1.35	1.63
	TCL	7.14	9.22	1.63	7.06	6.85	2.85	6.62
	SFL	5.18	6.57	1.63	6.58	4.57	2.85	5.15
A6	MCL	2.45	1.38	0.51	2.09	1.47	1.23	1.72
	TCL	7.7	8.19	1.05	8.01	10.63	6.66	8.24
	SFL	6.85	5.48	1.05	6.88	6.19	4.26	5.93
A7	MCL	2.19	2.07	1.02	1.22	1.54	1.32	1.67
	TCL	9.98	7.41	4.18	8.17	7.95	8.7	8.44
	SFL	7.06	5.14	3.81	4.62	5.91	5.22	5.59

*Average values do not take account of set 3 (see Sect. 3.3.1.2)

Table 6 (continued)

Alloy	Parameter	Crack lengths mm						
		Set 1	Set 2	Set 3	Set 4	Set 5	Set 6	Average
A8	MCL	1.51	0.88	1.34	1.63	1.27	1.25	1.31
	TCL	3.52	3.14	4.47	4.85	9.94	5.86	5.46
	SFL	3.52	2.98	3.93	4.69	5.01	4.94	4.23
B1	MCL	3.9	4.26	2.12	3.08	3.06	2.95	3.45
	TCL	12.43	12.48	6.18	14.07	9.61	11.5	12.02
	SFL	11.61	12.24	6.18	10.3	8.52	9.1	10.35
B2	MCL	1.65	1.79	1.83	1.1	1.92	1.49	1.59
	TCL	5.25	5.23	15.26	3.91	9.24	3.23	5.37
	SFL	4.44	4.96	7.37	3.91	6.75	3.23	4.66
B3	MCL	2.23	1.9	1.49	1.93	1.64	0.91	1.72
	TCL	10.85	7.55	8.24	6.02	7.47	4.15	7.21
	SFL	7.08	6.56	4.86	5.35	5.9	3.44	5.67
B4	MCL	2.42	1.62	1.52	1.08	1.96	1.72	1.76
	TCL	7.46	5.17	8.49	6.12	9.53	6.9	7.04
	SFL	6.43	5.17	6.38	4.59	5.91	5.73	5.57
B5	MCL	1.21	1.18	0.8	1.3	0.87	1.42	1.2
	TCL	2.68	4.51	2.38	7.18	3.66	4.11	4.43
	SFL	2.51	3.9	2.38	4.91	3.07	3.83	3.64
B6	MCL	1.38	1.93	1.85	1.67	1.64	1.25	1.57
	TCL	5.43	6.83	6.66	5.62	8.06	4.07	6.0
	SFL	4.86	6.44	6.43	5.17	5.69	4.07	5.25
B7	MCL	1.62	1.25	0.4	1.77	1.12	0.98	1.35
	TCL	7.2	5.62	0.67	4.98	5.75	3.43	5.36
	SFL	6.11	4.77	0.67	4.43	4.18	3.2	4.54
B8	MCL	1.95	1.04	0.42	1.71	0.97	1.32	1.4
	TCL	9.09	7.84	0.85	4.88	5.26	8.72	7.16
	SFL	7.13	4.62	0.85	4.88	3.69	5.76	5.22

Table 7 Varestraint Crack Length Data for the first series Experimental 70/30 Cupronickel Alloys at 6% strain

Alloy	Crack Lengths mm			
	Set 1		Set 2	
	MCL	SFL	MCL	SFL
A1	2.73	7.58	4.0	9.66
A2	3.38	12.97	2.84	9.26
A3	3.19	10.92	2.9	8.81
A4	4.15	17.26	3.13	11.87
A5	2.32	10.27	3.49	12.48
A6	3.28	12.57	3.67	12.8
A7	4.5	16.9	3.39	11.74
AS	3.21	8.97	3.06	10.26
B1	4.85	16.2	3.9	13.78
B2	6.41	20.66	1.48	5.76
B3	5.23	15.97	4.06	13.36
B4	3.71	14.84	2.58	8.8
B5	3.74	13.16	2.57	11.67
B6	4.21	11.33	2.8	10.62
B7	2.82	10.79	3.32	12.25
BS	2.67	9.35	2.46	9.07

MCL = Maximum Crack Length

SFL = Sum of Five Longest Cracks

Table 8 Analysis of regression of the cracking data on alloying and impurity element variables based on five sets of experiments; first series of experimental alloys.

Cracking Parameter	Variable name	Regression coeff,	Standard error	t stat	Significance level	Crack Length Variation
MCL	Ti	2.42	0.56	3.89	1%	0.411
	Fe	-3.14	1.29	2.44	2%	-0.691
	P	26.2	9.30	2.82	2%	0.367
	Si	4.90	1.24	2.84	1%	0.539
	Mn	-7.28	1.51	4.85	1%	-1.02
	S	25.9	8.65	4.21	1%	0.453
	Zr	3.25	0.78	4.00	1%	0.39
		*	*	1.92	10%	*

Multiple correlation coefficient = 0.7 Intercept term = 10.3
Residual error = 0.36 Degress of Freedom = 71

TCL	Zr	12.6	3.46	3.58	1%	1.51
	Ti	7.83	2.48	3.13	1%	1.33
	P	111	40.9	2.84	1%	1.55
	S	8	31.9	2.60	2%	1.45

Multiple correlation coefficient = 0.59 Intercept term = 3.03
Residual error = 0.58 Degrees of Freedom = 75

Cracking Parameter	Variable name	Regression coeff.	Standard error	t stat	Significance level	Crack Length Variation
SFL	Ti	6.41	1.85	3.52	0.1%	1.09
	Zr	7.59	2.56	3.46	0.1%	0.911
	Mn	-13.8	4.31	3.91	1%	-1.93
	Si	15.9	3.50	2.91	1%	1.75
	P	124	26.4	2.72	1%	1.74
	S	67.0	24.5	4.07	1%	1.17
	Fe	-18.1	4.65	2.89	5%	-3.98
	C	-22.6	12.4	1.82	10%	-0.94
	Ca	-405	144	2.00	5%	-2.84
	Bi	*	*	2.04	5%	*

Multiple correlation coefficient = 0.75 Intercept term = 31.6
Residual error = 1.59 Degrees of Freedom = 69
* In certain cases, the low absolute value of %wt prevents accurate determination of these figures.

Table 9 Varestraint crack length data for the second series of experimental alloys tested at 1.8%, 3% and 4% strain.

Alloy	Crack length mm								
	1.8% strain			3% strain			4% strain		
	MCL	TCL	SFL	MCL	TCL	SFL	MCL	TCL	SFL
H1	0	0	0	0	0	0	0	0	0
H2	0	0	0	0.93	0.85	2.85	1.58	7.69	5.62
H3	0	0	0	0	0	0	0	0	0
H4	0	0	0	0	0	0	1.02	3.75	3.75
H5	1.15	2.46	2.46	1.69	4.27	4.27	3.27	16.23	10.46
H6	2.76	7.53	7.33	2.33	9.92	8.82	2.7	17.99	8.35
H7	0	0	0	1.05	2.91	2.91	2.08	7.91	6.21
H8	0	0	0	2.37	7.22	6.83	3.18	12.11	9.16

Table 10 Analysis of regression of weld metal cracking data on impurity content for second series of experimental alloys

Cracking parameter	Variable name	Regression coefficient	Standard error	t-stat	Significance level	Crack length variation
MCL	P	89.3	12.7	7.03	0.1%	2.14
	Ti	2.54	1.21	2.09	10%	0.528
	CP	-682	233	3.05	1%	1.18
	Strain	0.56	0.13	4.23	1%	1.23

Mult. corr. = 0.9 Residual error = 1.28
Intercept term = 1.95 Deg. of Freedom = 19

TCL	P	378	57.8	6.54	0.1%	9.07
	Ti	11.8	5.53	2.13	5%	2.44
	CP	-3550	1020	3.5	1%	-6.14
	Strain	3.12	0.6	5.18	0.1%	6.86

Mult. corr. = 0.9 Residual error = 3.63
Intercept term = -10.5 Deg. of Freedom = 19

SFL	P	262	38.1	6.88	0.1%	6.29
	Ti	9.11	3.64	2.5	5%	1.89
	CP	-2130	670	3.19	1%	3.68
	Strain	1.91	0.4	4.81	1%	4.20

Mult. corr. = 0.9 Residual error = 2.52
Intercept term = -6.5 Deg. of Freedom = 19

Table 11 Ranking of second series experimental alloys by cracking threshold

Alloy	Cracking Threshold (%)	Elements of high level
H1	6	-
H3	6	C
H4	4	C,Ti
P1	3	Ti
H7	3	P,C
H8	3	P,C,Ti
H5	1.8	P
H6	1.8	P,T

Table 12 Varestraint crack length data for the second series of experimental 70/30 curponickel alloys tested at 6% strain

Alloy	Parameter	Crack Lengths (mm)				
		Set 1	Set 2	Set 3	Set 4	Average
H1	MCL	3.29	2.34	1.0	2.59	2.31
	TCL	14.45	8.35	4.75	4.34	7.97
	SFL	12.05	7.25	4.19	4.34	6.96
P1	MCL	3.09	1.85	4.15	4.19	3.32
	TCL	10.5	14.2	14.05	15.55	13.58
	SFL	8.75	7.7	12.25	12.55	10.31
H3	MCL	2.2	3.45	2.54	2.04	2.56
	TCL	16.2	14.75	7.75	5.65	11.09
	SFL	8.65	10.7	7.75	5.65	8.19
H4	MCL	2.09	3.09	2.7	2.5	2.6
	TCL	3.89	6.8	5.8	9.15	6.41
	SFL	3.89	6.79	5.8	7.3	5.95
H5	MCL	4.44	3.15	5.3	3.65	4.14
	TCL	17.85	16.45	23.89	22.35	20.14
	SFL	13.95	10.75	16.05	12.7	13.36
H6	MCL	3.75	3.45	4.34	2.7	3.56
	TCL	11.7	14.75	28.0	21.05	18.88
	SFL	11.69	10.55	16.29	11.85	12.6
H7	MCL	3.2	3.34	3.25	3.4	3.3
	TCL	9.6	15.44	16.2	10.05	12.82
	SFL	9.6	11.85	11.85	10.05	12.84
H8	MCL	2.45	3.84	3.09	3.04	3.11
	TCL	4.55	21.8	15.1	19.9	15.34
	SFL	4.55	14.95	11.79	12.0	10.82

Table 13 Analysis of regression of the cracking data on impurity element variables for second series experimental alloys

Cracking parameter	Variable name	Regression coefficient	Standard error	t-stat	Significance level	Crack Length variation
MCL	P	53.5	16.7	3.2	5%	1.61
	CP	-637	305	2.09	5%	-1.15

Mult. Corr. = 0.55
Intercept term = 2.57

Residual error = 0.802
Deg. of Freedom = 24

TCL	P	470	104	4.52	1%	14.1
	CP	-5910	1900	3.11	1%	-10.6

Mult. Corr. = 0.68
Intercept term - 8.47

Residual error = 5.0
Deg. of Freedom = 24

SFL	P	252	57.5	4.38	1%	7.56
	Cp	-2740	1050	2.61	2%	-4.93

Mult. Corr. = 0.67
Intercept term = 7.09

Residual error = 2.76
Deg. of Freedom = 24

Table 14 Ranking of third series experimental alloys by cracking threshold

Alloy	Cracking threshold (%)	Elements of high level
H1	6	-
H3	6	C
S4	3	C,Zr
S1	1.8	Zr
S6	1.8	C,S,Zr
S3	1.8	S,Zr
S2	1.8	S
S5	1	C,S

Table 15 Varestraint crack length data for the third series of experimental 70/30 cupronickel alloys tested at 6% strain

Alloy	Parameter	Crack Lengths (mm)						
		Set 1	Set 2	Set 3	Set 4	Set 5	Set 6	Average
H1	MCL	3.29	2.34	1.0	2.59	2.38	2.23	2.30
	TCL	14.45	8.35	4.75	4.34	6.13	9.51	7.92
	SFL	12.05	7.25	4.19	4.34	6.13	7.19	6.86
H3	MCL	2.2	3.45	2.54	2.04	2.29	2.13	2.44
	TCL	16.2	14.75	7.75	5.65	8.22	8.96	10.26
	SFL	8.65	10.7	7.75	5.65	7.15	8.63	8.09
S1	MCL	4.0	3.34	3.04	3.75	4.02	4.49	3.77
	TCL	12.35	14.39	8.94	21.1	17.16	17.17	15.19
	SFL	12.35	13.44	8.94	14.1	12.63	15.12	12.77
S2	MCL	3.65	2.95	3.04	2.4	2.34	2.15	2.76
	TCL	25.8	24.8	10.14	15.2	15.09	13.1	17.36
	SFL	13.75	11.85	9.75	9.9	10.47	7.61	10.56
S3	MCL	2.84	2.7	2.09	3.0	2.8	2.52	2.66
	TCL	13.5	15.84	16.2	8.7	15.57	9.04	13.14
	SFL	10.4	9.94	7.9	8.7	9.62	8.17	9.17
S4	MCL	2.29	3.25	2.29	2.79	3.33	2.91	2.81
	TCL	19.7	12.2	13.7	12.75	11.61	18.66	14.77
	SFL	9.6	12.2	8.8	9.35	11.16	11.24	10.39
S5	MCL	2.0	3.04	4.05	2.84	2.91	3.68	3.09
	TCL	12.9	17.0	7.35	18.6	12.31	13.38	13.59
	SFL	9.09	11.4	7.35	11.25	9.56	11.96	10.1
S6	MCL	2.95	2.59	2.9	3.29	2.58	2.87	2.86
	TCL	16.3	9.75	13.39	15.65	12.27	9.89	12.88
	SFL	10.55	8.25	9.55	10.75	9.54	9.38	9.67

Table 16 Analysis of regression of the cracking data on impurity element variables for third series experimental alloys

Cracking parameter	Variable name	Regression coefficient	Standard error	t-stat	Significance level	Crack length variation
MCL	Zr	3.81	1.32	2.86	2%	0.761
	CZr	-68.5	32.1	2.13	2%	-0.822

Mult. corr. = 0.39 Residual error = 0.605
Intercept term = 2.64 Deg. of Freedom = 45

TCL	Zr	20.7	7.77	2.67	2%	4.14
	S	71.4	25	2.86	2%	5.71
	SZr	-324	113	2.86	2%	-5.18

Mult. corr. = 0.44 Residual error = 4.35
Intercept term = 9.78 Deg. of Freedom = 44

SFL	Zr	13.3	3.8	3.49	2%	2.66
	S	30.7	12.2	2.51	2%	2.46
	SZr	-139	55.5	2.51	2%	2.22

Mult. corr. = 0.48 Residual error = 2.13
Intercept term = 7.79 Deg. of Freedom = 44

Table 17 Varestraint crack length data for the IN768 alloys tested at 1.8% strain

Alloy	Parameter	Crack Lengths (mm)				
		Set 1	Set 2	Set 3	Set 4	Average
K2	MCL	0	0	0	0	0
	TCL	0	0	0	0	0
	SFL	0	0	0	0	0
K4	MCL	6.2	3.9	3.8	2.1	4.0
	TCL	49.4	27.5	29.6	16.0	30.6
	SFL	18.9	15.1	15.1	8.6	14.4
K6	MCL	3.7	4.6	5.1	4.6	4.5
	TCL	28.1	30.0	32.6	36.3	31.8
	SFL	15.8	17.3	16.4	19.4	17.2
L2	MCL	0	1.4	2.3	1.1	1.2
	TCL	0	3.0	6.3	3.9	3.3
	SFL	0	3.0	6.3	3.5	4.2
L3	MCL	7.1	8.1	6.5	6.4	7.0
	TCL	47.8	86.3	43.7	62.4	60.1
	SFL	29.5	32.1	21.4	26.3	27.3
M1	MCL	3.5	2.8	2.0	4.2	3.1
	TCL	9.8	10.4	7.2	24.8	13.1
	SFL	9.3	8.4	5.7	13.3	9.2
M3	MCL	6.7	3.8	5.8	3.4	4.9
	TCL	44.5	23.3	27.9	31.3	31.8
	SFL	22.8	14.1	17.1	13.7	16.9
N2	MCL	13.0	9.1	11.8	8.7	10.7
	TCL	125.0	144.0	173.6	167.5	152.5
	SFL	45.1	41.4	50.5	37.9	43.7

Table 18 Grain Size Measurement of the Individual Alloy Ingots and Associated Pouring Temperatures for IN768 alloys

ALLOY	Grain Size (mm)	Pouring Temperature (°C)
K2	4.54	1420
K4	2.29	1415
K6	2.12	1385
L2	2.32	1325
L3	0.50	N.D.
M1	2.41	1440
M3	4.21	N.D.
N2	0.92	1300-1350

N.D. = not determined.

Table 19 Regression Analysis of Varestraint Cracking Data on Composition Variables and Grain Size at 1.8% Augmented Strain for IN768 alloys

Cracking Parameter	Variable	Regression Coefficient	Standard Error	t Statistic	Significance Level	Crack Length Variation
MCL	Pb	145	20.2	7.18	0.1%	3.77
	S Bi	32100	2440	13.1	0.1%	5.16
	Intercept term	-0.32		Multiple Correlation		0.93
	Degrees of Freedom	29		Residual Error		1.24
SFL	Pb	786	99.1	7.93	0.1%	20.4
	S	117	59.8	1.95	10%	5.38
	Pb Bi	-44400	24400	1.82	10%	-4.04
	S Bi	163000	16100	10.1	0.1%	26.3
	Grain Size	3.12	1.11	2.81	10%	12.6
	Intercept term	-15.6		Multiple Correlation		0.97
	Degree of Freedom	26		Residual Error		3.61
TCL	Pb	1510	345	4.37	1%	39.3
	Pb Bi	-197000	86700	2.27	10%	-17.9
	S Bi	386000	72900	5.29	0.1%	62.1
	Grain Size	6.11	3.41	1.79	10%	24.7
	Intercept term	-8.9		Multiple correlation		0.95
	Degree of Freedom.	27		Residual Error		7.16

Table 20 Composition of crack free and crack susceptible 70/30 cupronickel TIG filler wires

Element	Composition % wt	
	Crack free	Crack sensitive
Cu	65	68
Ni	34	30
Cr	0.003	0.02
Zn	<0.006	0.02
Te	<0.03 -	0.03
Sn	0.002	0.003
Pb	0.001	0.003
Bi	<0.0003	0.0005

Table 21 Crack Length Data for IN768 Experimental Alloys from Restrained Butt Welds.

Alloy Designation	Crack Length mm					
	Maximum Crack Length (MCL)		Sum of Five Largest Cracks (SFL)		Total Crack Length (TCL)	
	1	2	1	2	1	2
AXL - K2	1.1	1.6	2.7	3.6	2.7	3.6
AXL - K4	2.1	5.3	7.1	11.6	8.9	11.6
AXL - K6	3.1	2.3	9.3	8.7	11.7	14.2
AXL - L2	1.4	1.7	3.3	3.3	3.3	3.3
AXL - L3	10.4	9.1	26.1	26.9	68.3	74.7
AXL - M1	2.8	2.4	9.9	8.1	14.3	14.9
AXL - M3	2.8	1.4	4.6	3.9	4.6	3.9
AXL - N2	12.6	8.6	43.1	30.6	99.3	69.2

Table 22 Regression Analysis of Restrained Butt Weld Cracking on Composition and Grain Size.

(a) Maximum Crack Length

Independent Variable	Regression Coefficient	Standard Error	t Statistic	Significance Level	Crack Length Variation
S Bi	37100	3770	9.85	0.1%	5.97

Intercept term 1.81 Multiple Correlation 0.94
Degrees of Freedom 14 Residual Error 1.37

(b) Sum of Five Largest Cracks

Independent Variable	Regression Coefficient	Standard Error	t Statistic	Significance Level	Crack Length Variation
Pb	230	76.7	2.99	2%	5.97
S	-171	59.1	2.89	5%	-7.86
PbS	5840	22.80	2.56	5%	6.98
SBi	113000	13500	8.35	0.1%	18.2
Grain Size	-2.34	1.02	2.3	5%	-9.45

Intercept term 21.5 Multiple Correlation 0.98
Degrees of Freedom 12 Residual Error 6.97

(c) Total Crack Length

Independent Variable	Regression Coefficient	Standard Error	t Statistic	Significance Level	Crack Length Variation
S	-254	133	1.91	10%	-11.7
S Bi	325000	30500	10.65	0.1%	52.3
Grain Size	-4.6	2.32	1.99	10%	-18.6

Intercept term 21.5 Multiple Correlation 0.96
Degrees of Freedom 12 Residual Error 6.96

Table 23 Hot ductility and hot strength of the first series wrought alloys on cooling in a simulated weld thermal cycle

Alloy A1

Testing Temperature (°C)	Ductility (% RA)	Strength (Nmm^{-2})
450	37	267
550	47	258
651	28	225
749	28	183
849	35	142
951	63	116
1050	62	85
1149	6	31

Alloy A2

Testing Temperature (°C)	Ductility (% RA)	Strength (Nmm^{-2})
451	73	272
550	61	259
650	65	238
751	72	201
850	74	161
948	90	124
1049	97	94
1150	2	20

Table 23 continued

Alloy A3

Testing Temperature (^{o}C)	Ductility (% RA)	Strength (Nmm^{-2})
451	40	291
549	29	260
649	19	195
749	23	180
851	29	156
949	52	121
1049	59	91
1150	28	29

Alloy A4

Testing Temperature (^{o}C)	Ductility (% RA)	Strength (Nmm^{-2})
451	47	299
551	51	287
651	39	259
750	29	210
850	27	165
950	35	71
1049	9	53
1150	2	12

Table 23 continued

Alloy A5

Testing Temperature (°C)	Ductility (% RA)	Strength (Nmm^{-2})
451	63	268
550	40	271
651	26	239
748	15	176
850	18	143
947	15	96
1051	12	64
1149	1	12

Alloy A6

Testing Temperature (°C)	Ductility (% RA)	Strength (Nmm^{-2})
451	41	287
551	39	267
650	34	250
749	34	208
848	69	169
948	62	122
1049	58	87
1146	3	27

Table 23 continued

Alloy A7

Testing Temperature (^{o}C)	Ductility (% RA)	Strength (Nmm^{-2})
551	31	270
651	22	230
749	13	131
849	16	113
949	34	103
1050	53	87
1150	2	7
1162	2	0

Alloy A8

Testing Temperature (^{o}C)	Ductility (% RA)	Strength (Nmm^{-2})
451	46	281
551	30	246
650	24	223
748	28	192
851	41	149
951	41	109
1051	33	78
1151	1	8

Table 23 continued

Alloy B1

Testing Temperature (^{o}C)	Ductility (% RA)	Strength (Nmm^{-2})
449	39	313
651	35	267
750	31	220
848	27	161
949	43	127
1050	5	45
1150	0	12

Alloy B2

Testing Temperature (^{o}C)	Ductility (% RA)	Strength (Nmm^{-2})
450	58	294
551	31	272
649	21	225
750	17	175
847	15	137
950	11	73
1050	14	63
1150	2	4

Table 23 continued

Alloy B3

Testing Temperature (°C)	Ductility (% RA)	Strength (Nmm^{-2})
451	46	292
550	43	271
650	33	246
749	23	191
851	25	157
950	27	114
1049	18	72
1150	4	2

Alloy B4

Testing Temperature (°C)	Ductility (% RA)	Strength (Nmm^{-2})
451	52	298
551	51	282
650	26	238
849	30	155
951	21	89
1050	20	68
1150	5	3

Table 23 continued

Alloy B5

Testing Temperature (°C)	Ductility (% RA)	Strength (Nmm^{-2})
450	39	296
551	23	262
650	20	216
750	21	178
850	30	154
949	51	110
1050	46	80
1150	6	7

Alloy B_6

Testing Temperature (°C)	Ductility (% RA)	Strength (Nmm^{-2})
450	60	318
551	64	293
649	48	263
751	38	202
849	37	153
949	82	126
1048	59	84
1151	3	29

Table 23 continued

Alloy B7

Testing Temperature (°C)	Ductility (% RA)	Strength (Nmm^{-2})
451	51	310
550	47	290
651	29	256
750	11	137
850	22	141
949	51	120
1050	26	77
1150	1	8

Alloy B8

Testing Temperature (°C)	Ductility (% RA)	Strength (Nmm^{-2})
451	52	304
550	32	271
649	27	250
750	19	192
848	32	162
1050	82	90
1151	4	33

Table 24 Hot ductility and hot strength of the second series wrought alloys on cooling in a simulated weld thermal cycle

Alloy H1

Testing Temperature (°C)	Ductility (% RA)	Strength··· (Nmm^{-2})
451	54	259
551	42	238
650	39	209
851	40	146
951	47	112
999	91	102
1049	73	85
1099	95	75
1130	66	65

Alloy P1

Testing Temperature (°C)	Ductility (% RA)	Strength (Nmm^{-2})
450	69	284
551	51	264
651	35	230
750	43	195
851	62	159
948	82	118
1001	76	94
1050	82	93
1100	79	72
1130	39	66
1150	2	21

Table 24 continued

Alloy H3

Testing Temperature (^{o}C)	Ductility (% RA)	Strength (Nmm^{-2})
450	61	292
551	52	255
648	35	231
748	38	194
848	45	146
948	41	108
1000	80	97
1049	72	85
1099	63	68
1129	57	63
1146	2	16

Alloy H4

Testing Temperature (^{o}C)	Ductility (% RA)	Strength (Nmm^{-2})
450	51	285
551	50	269
650	36	240
749	34	197
850	47	160
950	75	120
999	89	103
1049	87	92
1101	85	74
1129	84	67
1151	0	10

Table 24 continued

Alloy H5

Testing Temperature (°C)	Ductility (% RA)	Strength (Nmm^{-2})
451	66	280
551	45	261
651	37	232
951	29	103
1051	11	45
1146	2	7

Alloy H6

Testing Temperature (°C)	Ductility (% RA)	Strength (Nmm^{-2})
450	68	285
549	58	250
648	40	250
749	14	121
850	11	76
947	10	75
999	13	66
1049	10	40
1100	3	37
1127	0	25
1151	0	9

Table 24 continued

Alloy H7

Testing Temperature (°C)	Ductility (% RA)	Strength (Nmm^{-2})
451	49	303
550	42	282
650	28	250
750	24	143
850	14	107
950	10	57
1000	0	67
1098	5	40
1128	1	29
1152	1	10

Alloy H8

Testing Temperature (°C)	Ductility (% RA)	Strength (Nmm^{-2})
450	40	296
550	65	294
650	40	230
750	35	200
849	40	154
951	41	112
1000	55	96
1049	60	87
1099	49	76
1130	2	28
1143	2	0

Table 25 Hot ductility and hot strength of the second seried wrought alloys on heating in a simulated weld thermal cycle

Alloy H1

Testing Temperature (°C)	Ductility (% RA)	Strength (Nmm^{-2})
453	81	276
545	77	258
639	64	237
760	83	185
863	90	152
961	95	115
1055	98	85
1150	44	56
1172	0	4
1181	0	7
1200	0	7

Alloy H3

Testing Temperature (°C)	Ductility (% RA)	Strength (Nmm^{-2})
763	63	185
857	78	156
956	84	116
1057	91	81
1106	90	71
1153	2	28
1168	0	2

Table 25 continued

Alloy H4

Testing Temperature (°C)	Ductility (% RA)	Strength (Nmm^{-2})
758	60	201
863	81	149
951	91	123
1062	90	85
1114	91	71
1162	12	46
1178	1	6

Alloy H5

Testing Temperature (°C)	Ductility (% RA)	Strength (Nmm^{-2})
453	81	276
545	77	258
640	61	241
749	62	198
858	80	152
949	76	112
1057	78	83
1153	0	21
1169	0	3
1179	0	2

Table 25 continued

Alloy H6

Testing Temperature (°C)	Ductility (% RA)	Strength (Nmm^{-2})
960	92	119
1079	97	80
1109	64	70
1150	3	31
1178	1	1

Alloy H7

Testing Temperature (°C)	Ductility (% RA)	Strength (Nmm^{-2})
739	59	215
856	84	161
952	96	125
1049	89	89
1111	94	72
1156	0	42

Table 26 Hot ductility and hot strength of the second series wrought alloys on cooling from a peak temperature of 1050 ^{o}C.

Alloy	Testing Temperature (^{o}C)	Ductility (% RA)	Strength (Nmm^{-2})
P1	649	44	239
H3	649	56	197
H4	751	48	208
H6	950	89	129
H7	998	81	154
H8	749	70	214

Table 27 Hot ductility and hot strength of the third series wrought alloys on cooling in a simulated weld thermal cycle

Alloy S1

Testing Temperature (°C)	Ductility (% RA)	Strength (Nmm^{-2})
449	66	280
551	60	257
651	52	238
760	39	199
850	44	160
949	82	123
999	85	106
1050	90	85
1097	89	79
1128	1	14
1150	0	12

Alloy S2

Testing Temperature (°C)	Ductility (% RA)	Strength (Nmm^{-2})
451	48	228
551	43	210
650	28	-
751	27	176
850	36	146
946	33	112
1001	50	83
1050	51	77
1100	45	64
1130	22	63
1150	1	20

Table 27 continued

Alloy S3

Testing Temperature (°C)	Ductility (% RA)	Strength (Nmm^{-2})
450	56	261
550	39	241
650	31	209
750	29	186
851	52	131
951	78	117
1000	76	98
1050	62	85
1101	77	77
1130	80	81
1150	75	65
1160	30	59

Alloy S4

Testing Temperature (°C)	Ductility (% RA)	Strength (Nmm^{-2})
551	47	253
651	36	234
751	33	197
850	58	158
948	78	114
1000	82	98
1050	81	83
1100	57	71
1148	25	54

Table 27 continued

Alloy S5

Testing Temperature (°C)	Ductility (% RA)	Strength (Nmm^{-2})
450	47	294
551	30	266
651	33	221
751	25	175
850	30	156
951	38	109
999	54	95
1051	61	80
1098	65	73
1128	7	40
1148	0	3

Alloy S6

Testing Temperature (°C)	Ductility (% RA)	Strength (Nmm^{-2})
451	43	285
550	32	266
650	26	230
751	26	196
849	21	124
949	50	117
999	42	99
1050	61	80
1098	63	74
1129	72	71
1151	31	63

Table 28 Hot ductility and hot strength of the third series wrought alloys on heating in a simulated weld thermal cycle

Alloy S1

Testing Temperature (^{o}C)	Ductility (% RA)	Strength (Nmm^{-2})
862	81	151
951	89	125
1064	94	85
1110	96	77
1148	2	21

Table 29 Hot ductility and hot strength of the third series wrought alloys on cooling from a peak temperature of 1050 °C

Alloy	Testing Temperature (°C)	Ductility (% RA)	Strength (Nmm^{-2})
S1	748	44	209
S2	750	39	189
S5	751	31	200
S6	851	52	149

Table 30 Hot ductility and hot strength of the second series cast alloys on cooling in a simulated weld thermal cycle

Alloy R1

Testing Temperature (°C)	Ductility (% RA)	Strength (Nmm^{-2})
451	64	208
550	53	188
651	36	168
750	35	148
849	37	117
950	61	103
998	62	93
1051	60	80
1095	0	13
1131	0	2
1151	0	5

Alloy.R2

Testing Temperature (°C)	Ductility (% RA)	Strength (Nmm^{-2})
450	76	230
550	52	219
651	38	175
750	33	154
850	31	134
948	57	96
1000	61	96
1050	46	75
1100	17	61
1150	0	5

Table 30 continued

Alloy R3

Testing Temperature (°C)	Ductility (% RA)	Strength (Nmm^{-2})
450	69	248
550	52	223
651	24	187
751	37	180
849	65	161
950	80	103
997	81	84
1051	91	78
1115	84	60
1129	82	59
1148	0	10

Alloy R4

Testing Temperature (°C)	Ductility (% RA)	Strength (Nmm^{-2})
451	71	237
550	30	230
651	21	198
750	27	166
849	50	137
946	56	107
998	77	86
1067	84	73
1101	88	65
1129	67	58
1151	3	29

Table 30 continued

Alloy R5

Testing Temperature (°C)	Ductility (% RA)	Strength (Nmm^{-2})
451	61	235
550	54	220
649	42	203
844	19	106
947	15	83
1000	25	82
1051	40	73
1098	31	64
1128	0	21
1147	0	4

Alloy R6

Testing Temperature (°C)	Ductility (% RA)	Strength (Nmm^{-2})
451	61	239
551	44	227
651	31	188
751	12	90
848	4	62
949	1	18
1000	0	8
1051	0	28
1100	0	17
1130	0	6
1151	0	10

Table 30 continued

Alloy R7

Testing Temperature (°C)	Ductility (% RA)	Strength (Nmm^{-2})
451	59	259
551	65	234
651	23	185
749	2	48
851	1	38
948	3	37
998	0	26
1051	0	26
1099	0	23
1130	0	23
1149	0	9

Alloy R8

Testing Temperature (°C)	Ductility (% RA)	Strength (Nmm^{-2})
451	26	186
551	40	248
650	38	204
750	34	177
849	28	125
951	17	82
1000	19	68
1050	1	27
1097	0	6
1129	1	17
1149	0	20

Table 31 Hot ductility and hot strength of the second series cast alloys on heating in a simulated weld thermal cycle

Alloy R1

Testing Temperature (°C)	Ductility (% RA)	Strength (Nmm^{-2})
948	53	102
1048	62	70
1111	65	58
1149	55	60
1178	1	3

Alloy R2

Testing Temperature (°C)	Ductility (% RA)	Strength (Nmm^{-2})
747	34	165
852	52	138
959	56	102
1052	63	59
1112	68	63
1153	1	18

Table 31 continued

Alloy R3

Testing Temperature (°C)	Ductility (% RA)	Strength (Nmm^{-2})
950	70	99
1056	80	72
1101	78	65
1159	1	11

Alloy R7

Testing Temperature (°C)	Ductility (% RA)	Strength (Nmm^{-2})
759	16	143
858	20	120
951	27	97
1061	48	68
1111	26	56
1149	6	8

Table 32 Hot ductility and hot strength of the second series cast alloys on cooling from a peak temperature of 1050 °C

Alloy	Testing Temperature (°C)	Ductility (% RA)	Strength (Nmm^{-2})
R1	749	30	155
R2	849	47	141
R3	648	29	191
R4	650	19	195
R5	749	35	180
R6	999	17	75
R7	1001	0	42
R8	949	33	93

Table 33 Hot ductility and hot strength of the third series cast alloys on cooling in a simulated weld thermal cycle

Alloy T1

Testing Temperature (^{o}C)	Ductility (% RA)	Strength (Nmm^{-2})
451	35	244
551	32	208
650	18	167
750	16	141
850	31	143
950	55	106
1001	49	84
1050	56	78
1099	1	11
1130	2	14
1146	2	10

Alloy T2

Testing Temperature (^{o}C)	Ductility (% RA)	Strength (Nmm^{-2})
450	24	202
550	24	191
651	22	162
750	20	137
849	19	132
951	17	82
999	35	84
1050	29	70
1099	0	27
1126	0	10
1148	0	0

Table 33 continued

Alloy T3

Testing Temperature (°C)	Ductility (% RA)	Strength (Nmm^{-2})
450	39	215
551	25	189
649	20	160
751	14	139
851	18	125
950	42	107
999	34	85
1051	56	80
1099	49	63
1130	3	28
1150	0	5

Alloy T4

Testing Temperature (°C)	Ductility (% RA)	Strength (Nmm^{-2})
451	52	232
551	32	214
650	21	188
749	20	161
850	35	139
950	50	104
999	47	93
1050	80	73
1115	67	-
1131	42	62
1150	2	27

Table 33 continued

Alloy T5

Testing Temperature (°C)	Ductility (% RA)	Strength (Nmm^{-2})
451	21	244
550	21	197
650	14	163
750	15	156
846	17	130
947	22	98
1001	37	91
1049	27	68
1097	2	22
1130	0	1
1151	0	6

Alloy T6

Testing Temperature (°C)	Ductility (% RA)	Strength (Nmm^{-2})
450	40	255
550	29	208
649	20	167
749	17	151
848	17	121
948	18	81
999	39	81
1050	44	72
1099	12	50
1130	0	14
1151	0	4

Table 34 Hot ductility and hot strength of the third series cast alloys on heating in a simulated weld thermal cycle

Alloy T1

Testing Temperature (°C)	Ductility (% RA)	Strength (Nmm^{-2})
749	38	178
952	64	112
1059	74	78
1107	24	60
1156	1	7

Alloy T2

Testing Temperature (°C)	Ductility (% RA)	Strength (Nmm^{-2})
759	17	135
852	21	127
953	24	90
1056	47	70
1109	22	62
1158	1	5

Table 34 continued

Alloy T4

Testing Temperature (^{o}C)	Ductility (% RA)	Strength (Nmm^{-2})
954	65	106
1050	71	75
1104	72	67
1153	3	29

Table 35 Hot ductility and hot strength of the third series cast alloys on cooling from a peak temperature of 1050 ^{o}C

Alloy	Testing Temperature (^{o}C)	Ductility (% RA)	Strength (Nmm^{-2})
T1	750	37	173
T2	950	27	95
T3	751	22	145
T4	749	21	158
T5	651	17	163
T6	749	25	155

Table 36 Hot Ductility and Hot Strength of the Experimental IN768 Alloys on cooling in a simulated Weld Thermal Cycle

Alloy - K2

Testing Temperature (°C)	Ductility % R.A.	Strength Nmm^{-2}
451	56	350
551	27	288
650	32	301
750	30	217
846	36	163
947	49	115
1051	29	67
1149	0	4

Alloy - K4

Testing Temperature (°C)	Ductility % R.A.	Strength Nmm^{-2}
550	13	242
651	10	202
749	13	136
847	8	79
948	3	64
1049	4	47
1147	0	7

Table 36 Continued

Alloy - K6

Testing Temperature (^{o}C)	Ductility % R.A.	Strength Nmm^{-2}
449	16	256
550	13	197
650	9	174
750	4	99
851	7	98
950	12	89
1044	0	26
1134	3	27

Alloy - K8

Testing Temperature (^{o}C)	Ductility % R.A.	Strength Nmm^{-2}
551	9	147
650	2	101
750	4	74
850	2	53
948	5	80
1049	3	34
1142	0	7

Table 36 Continued

Alloy - L2

Testing Temperature (^{o}C)	Ductility % R.A.	Strength Nmm^{-2}
451	32	321
550	28	292
650	6	188
750	14	141
849	15	118
950	29	107
1051	28	72
1147	0	10

Alloy - L3

Testing Temperature (^{o}C)	Ductility % R.A.	Strength Nmm^{-2}
451	12	261
550	9	228
649	4	121
846	6	106
950	13	99
1047	2	37
1145	0	2

Table 36 Continued

Alloy - M1

Testing Temperature (^{o}C)	Ductility % R.A.	Strength Nmm^{-2}
450	24	310
550	12	223
649	12	192
750	15	171
848	12	132
949	10	95
1046	7	46
1149	0	8

Alloy - M3

Testing Temperature (^{o}C)	Ductility % R.A.	Strength Nmm^{-2}
450	31	302
551	1	66
649	2	108
748	13	48
851	0	23
947	3	62
1045	4	44
1150	1	2

Table 36 Continued

Alloy - N2

Testing Temperature (^{o}C)	Ductility % R.A.	Strength Nmm^{-2}
450	11	211
551	2	130
650	3	97
751	4	99
848	2	66
946	4	85
1047	0	33
1131	0	3

Table 37. Results of Energy Dispersive Analysis carried out in cracked regions of first series alloys. (Elements in wt%).

Alloy	Cu	Ni	Mn	Fe	Pb	S	Si	Bi	Zr	Ti	P	Ca
A1	68.7	30.0	1.96	0.80	0	0	0.27	0	0	0	0.09	0.15
A2	69.7	26.9	1.26	0.50	0	0	0.23	0	0.35	0	0	0.10
A3	68.4	29.3	1.16	0.43	ND	0.11	0.23	ND	0	0.30	0	0.05
A4	69.4	27.0	1.90	0.57	0	0	0.25	0.05	0.28	0.31	0.06	0
A5	69.5	27.8	1.28	0.57	0	0	0.26	0	0.14	0.34	0	0
A6	71.5	25.9	1.26	0.57	0	0.11	0.26	0	0	0.23	0.06	0.08
A7	70.7	24.6	1.35	0.47	0.78	0.11	0.25	0.60	0.70	0	0	ND
A8	68.9	28.8	1.26	0.69	0	0	0.23	0.09	0	0	0	0.05
B1	75.1	22.0	1.69	0.49	ND	0.13	0.25	ND	0.22	0.02	0.05	ND
B2	69.9	27.5	1.16	0.67	0	0	0.40	0	0	0.24	0	0.07
B3	66.8	30.1	1.10	0.79	0.07	0	0.71	0.06	0.31	0	0	0.03
B4	73.0	24.0	1.39	0.70	0	0.12	0.49	0.09	0	0	0.08	0.09
B5	74.0	22.8	1.62	0.43	0.08	0.11	0.90	0	0	0	0	0.05
B6	64.8	32.8	1.02	0.73	ND	0.10	0.17	ND	0.36	0	0.05	ND
B7	70.0	27.4	1.20	0.68	0	0	0.42	0	0	0.25	0	0.07
B8	68.5	28.7	1.08	0.47	0	0.10	0.46	0.07	0.24	0.41	0	0

ND = Not determined

Table 38. Average sum of five longest cracks and recovery rate of ductility for second series wrought alloys.

Alloy	Average SFL/mm	Recovery rate of ductility/$°C^{-1}$
H1	6.96	3.19
P1	10.31	2.00
H3	8.19	3.17
H4	5.95	3.79
H5	13.36	0.14
H6	12.6	0.05
H7	12.84	0.07
H8	10.82	1.05

APPENDIX B
FIGURES

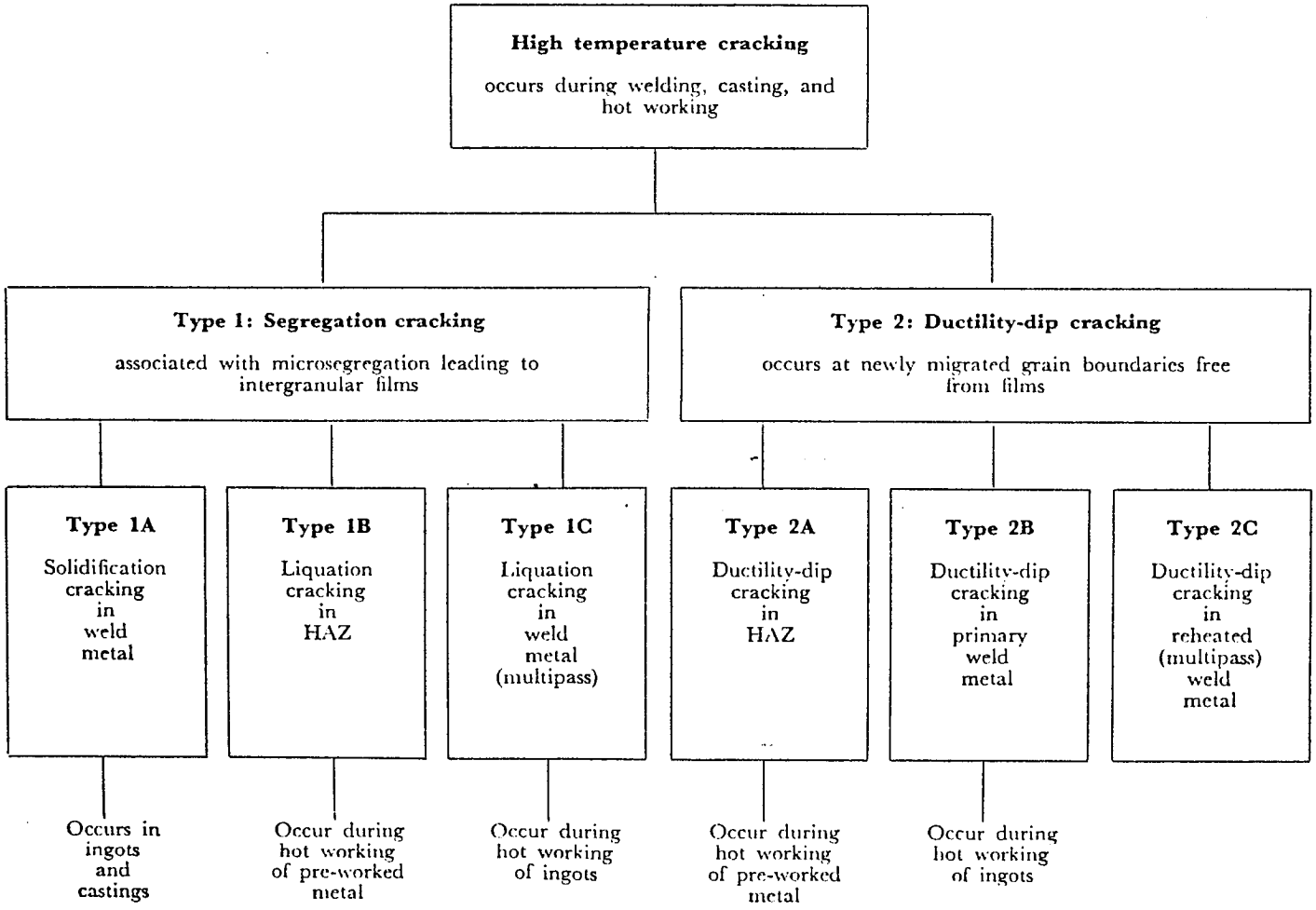

Fig 1. Classification of intergranular welding cracks (after Hemsworth et al) (10)

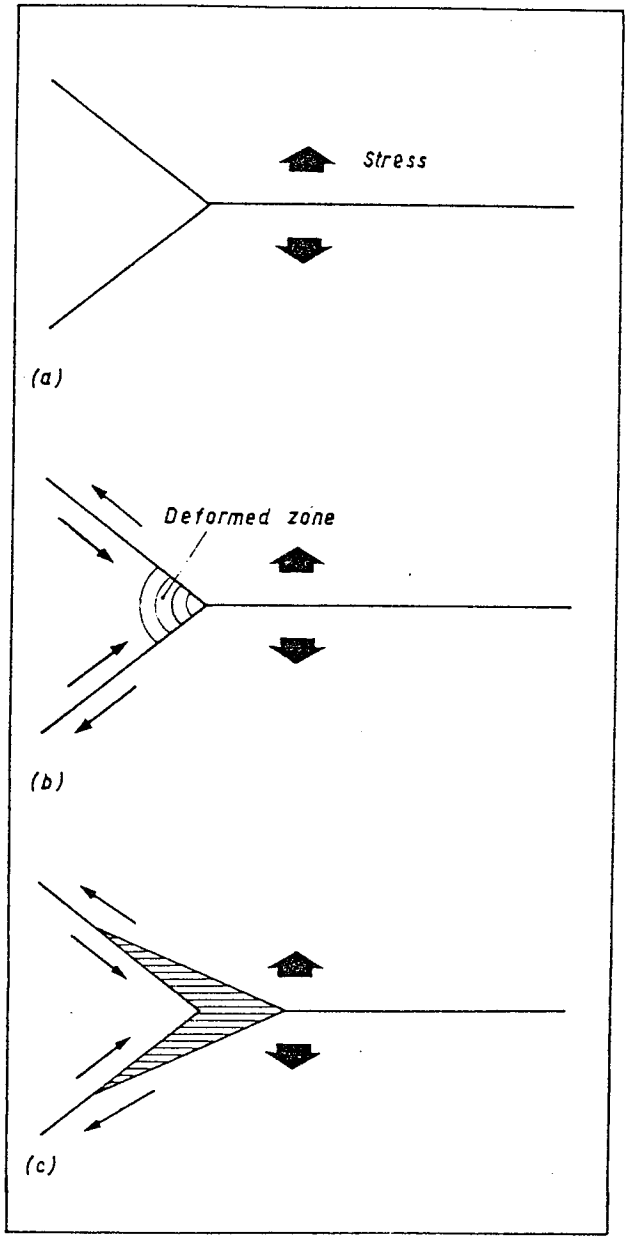

Fig 2. Schematic representation of triple-point Zener crack formation (after McKeown) (67)

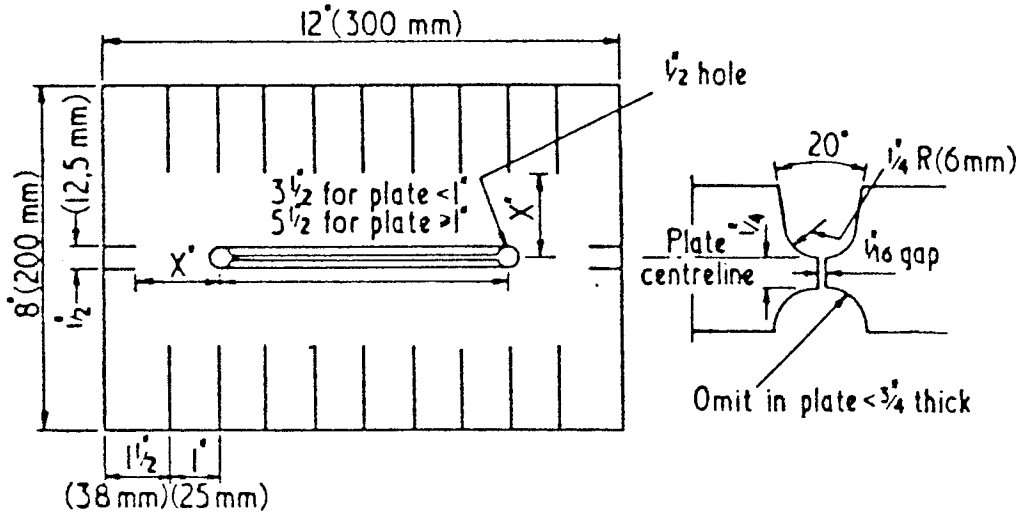

Fig 3. LeHigh restraint test (after Stout et al) (75)

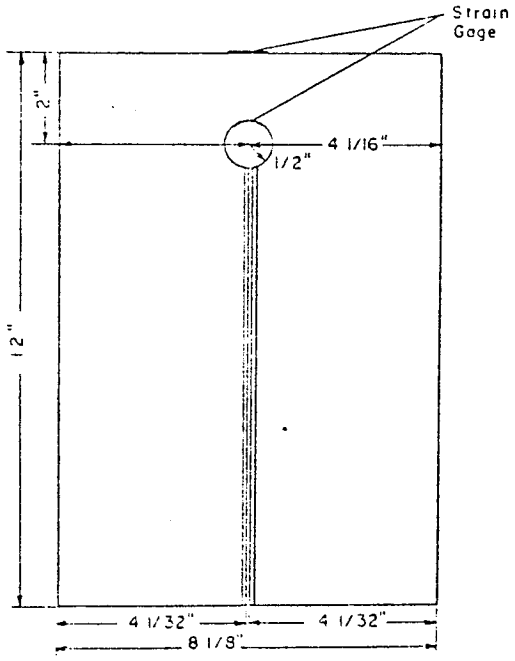

Fig 4. NRL (Type II) slotted test piece (after White et al) (80)

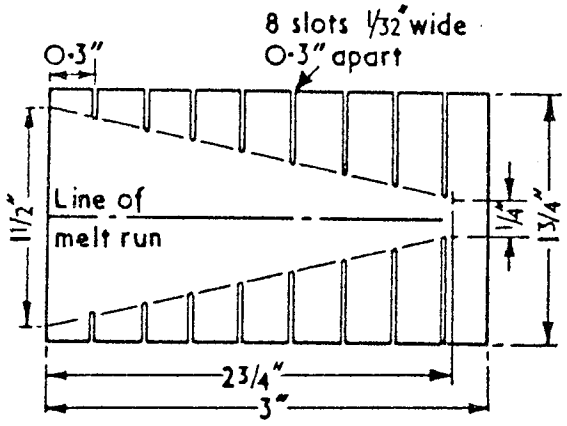

Fig 5. Houldcroft crack test specimen (after Houldcroft) (81)

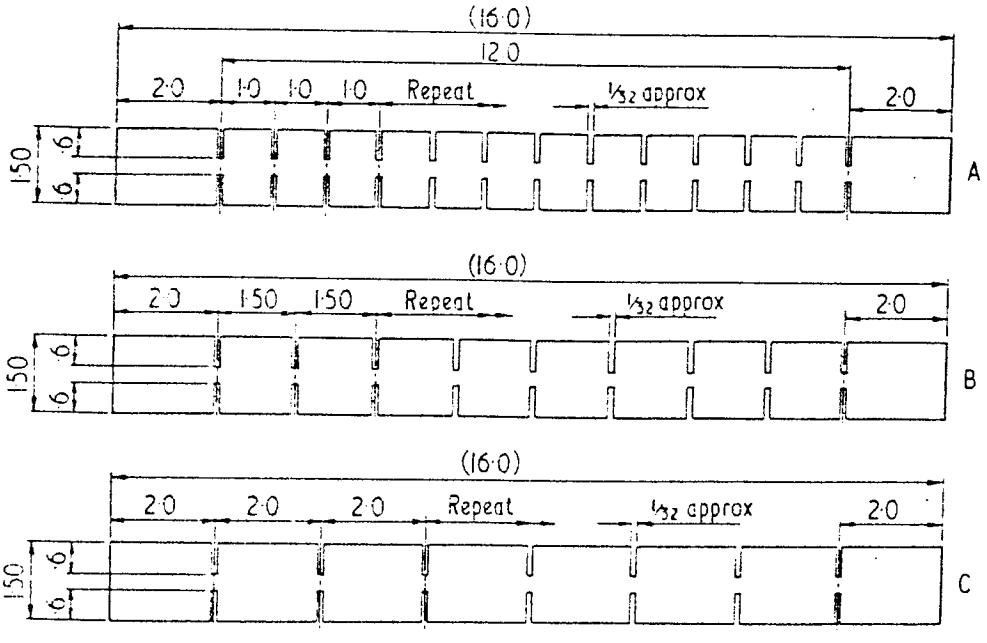

Fig 6. Huxley crack test specimens (after Huxley) (83)

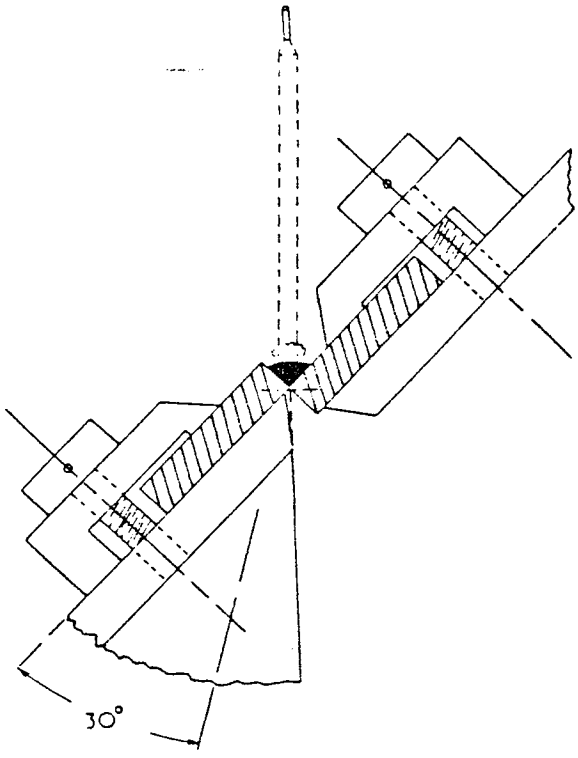

Fig 7. Murex hot cracking test (after Rollason & Roberts) [84]

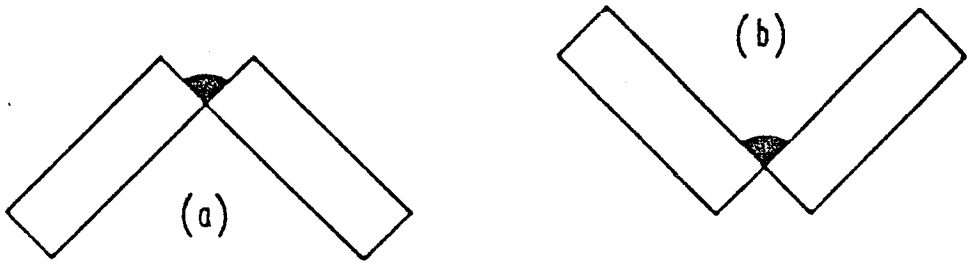

Fig 8. Alternative test piece arrangements for RBS test (after Nakane et al) [85]

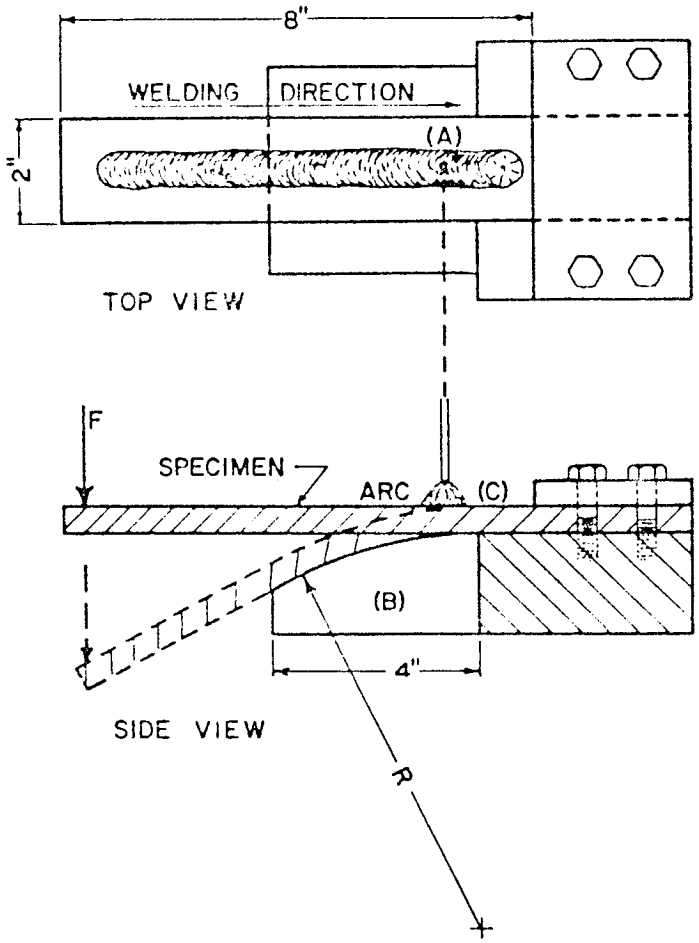

Fig 9. Varestraint test (after Savage & Lundin) (87)

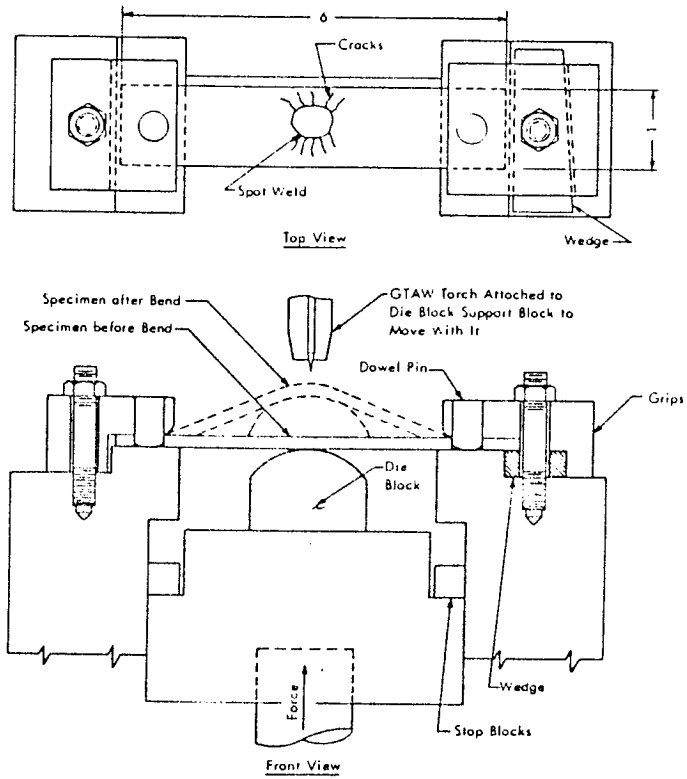

Fig 10. TIC-A-MA-JIG weld cracking test (after Lundin et al) (91)

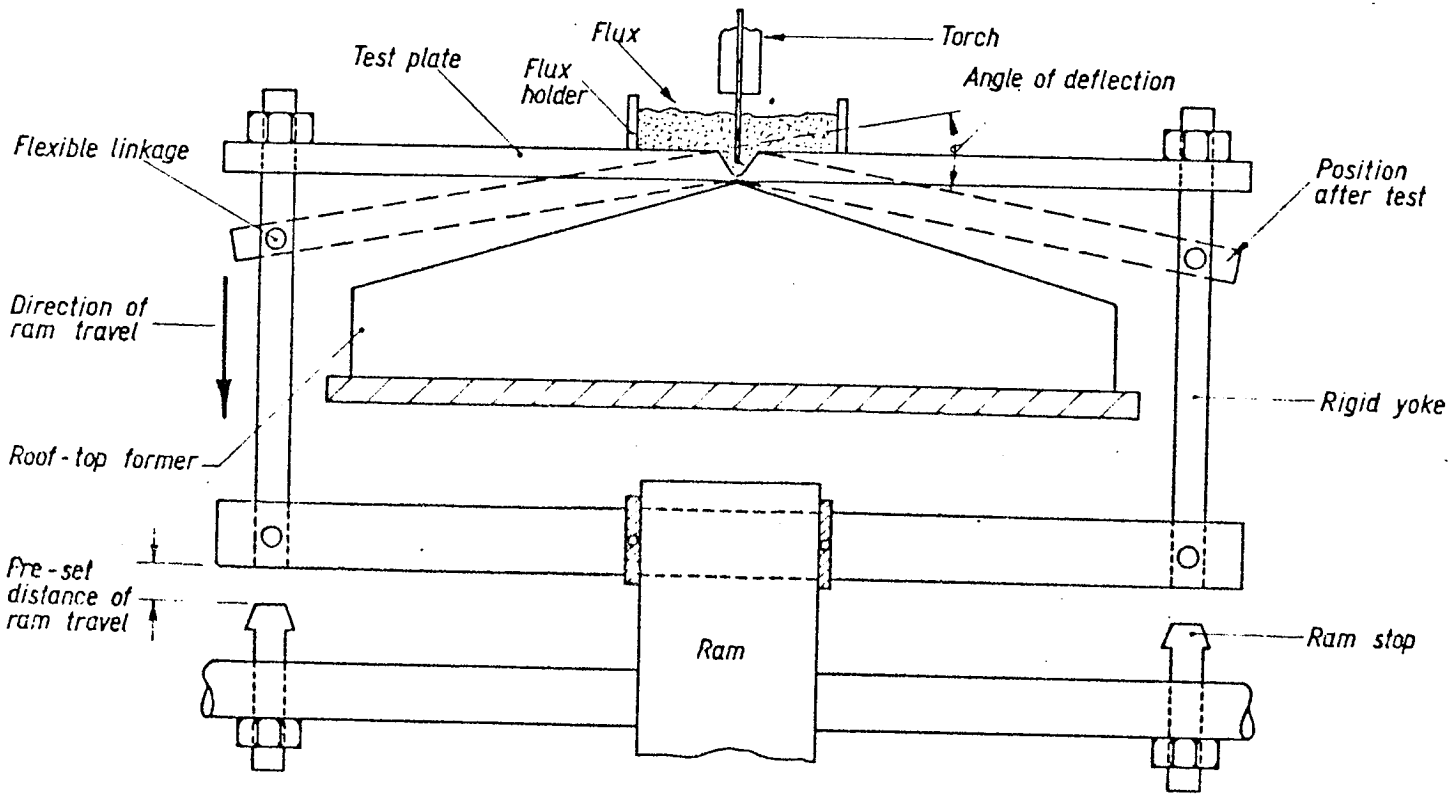

Fig 11. Transvarestraint test (after Garland & Bailey) (96)

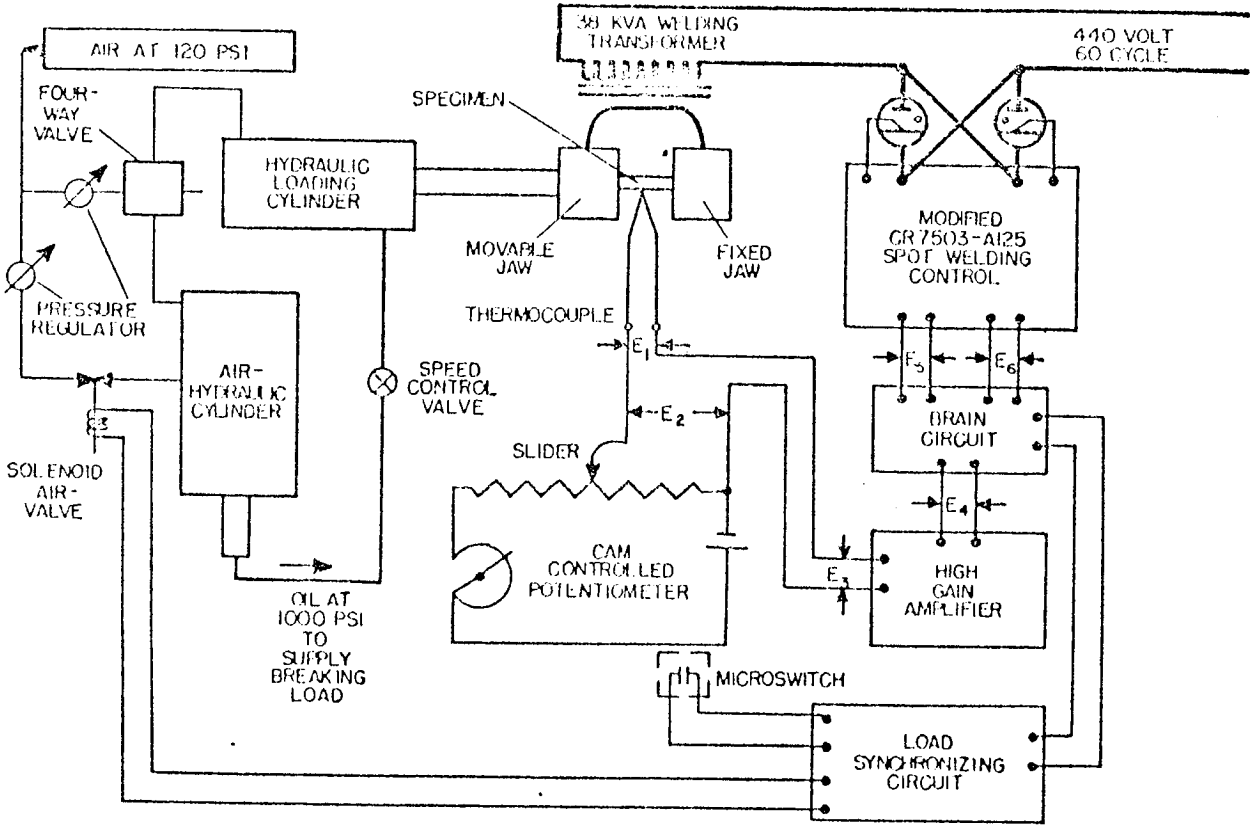

Fig 12. Schematic representation of weld thermal simulator (after Nippes et al) (114)

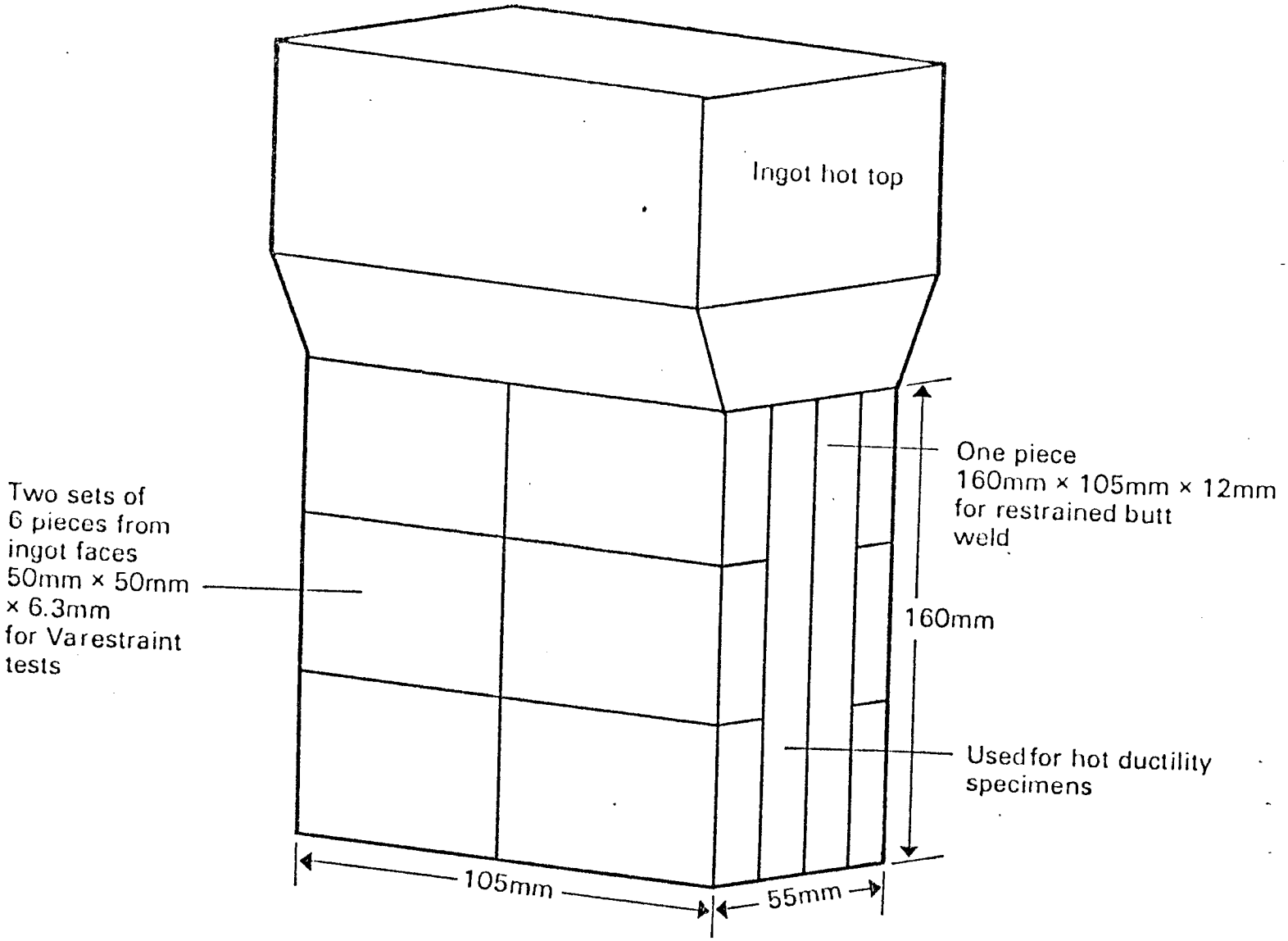

Fig 13. Sections taken from IN768 ingot

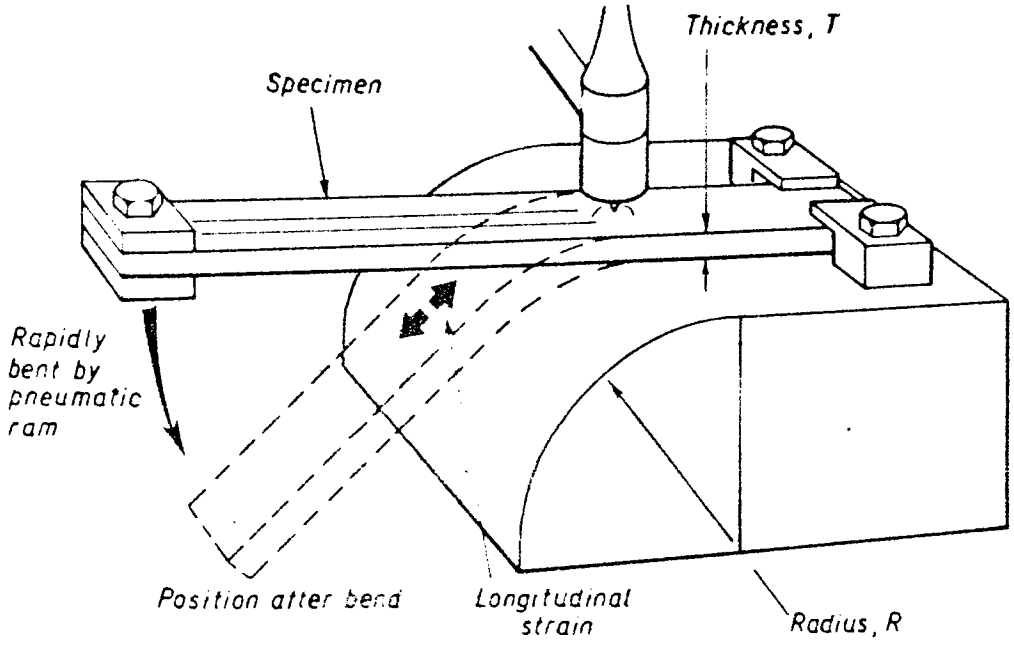

Fig 14. Schematic view of Varestraint test

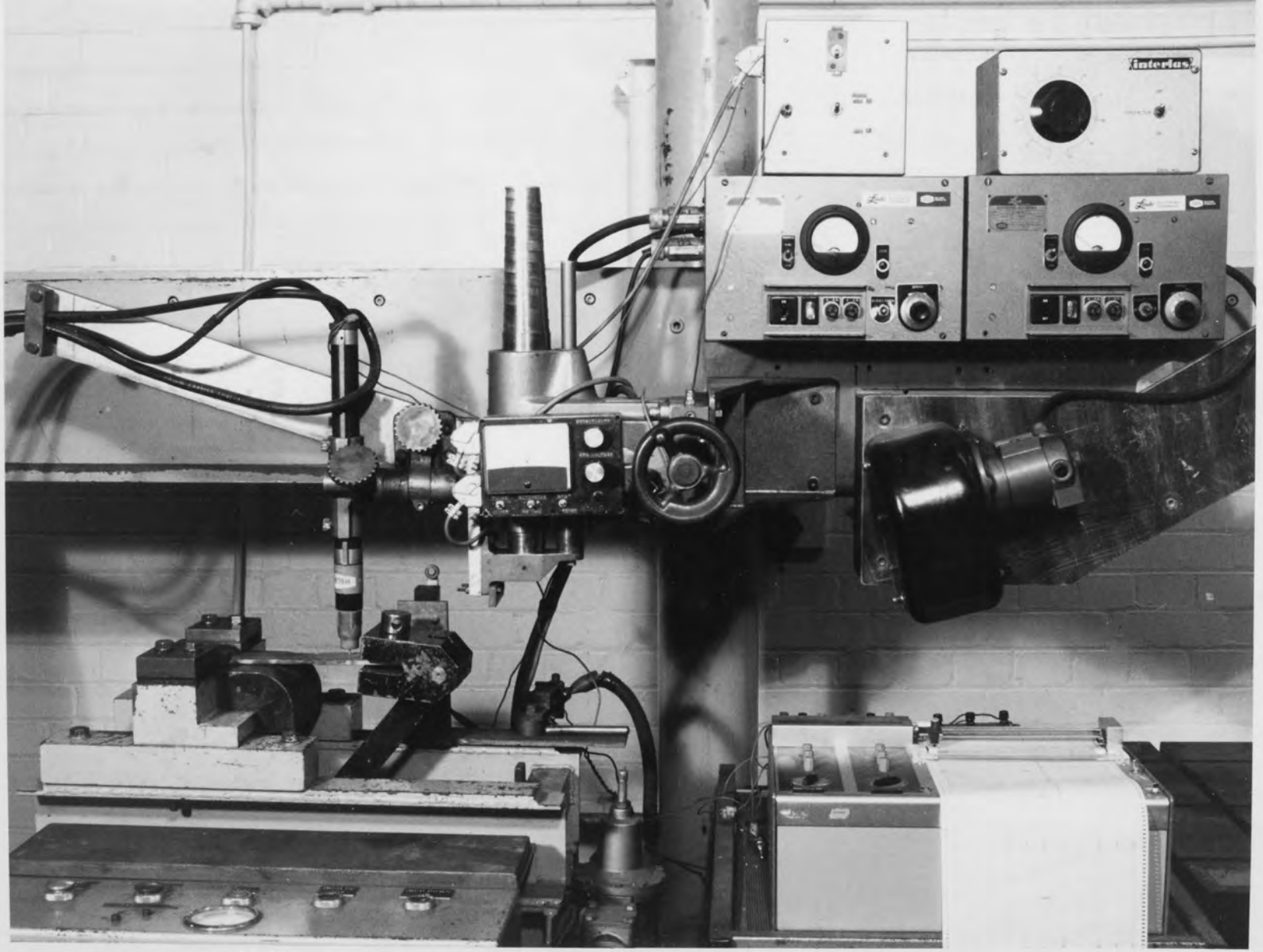

Fig 15. Varestraint apparatus before test

Fig 16. Varestraint after completion of test

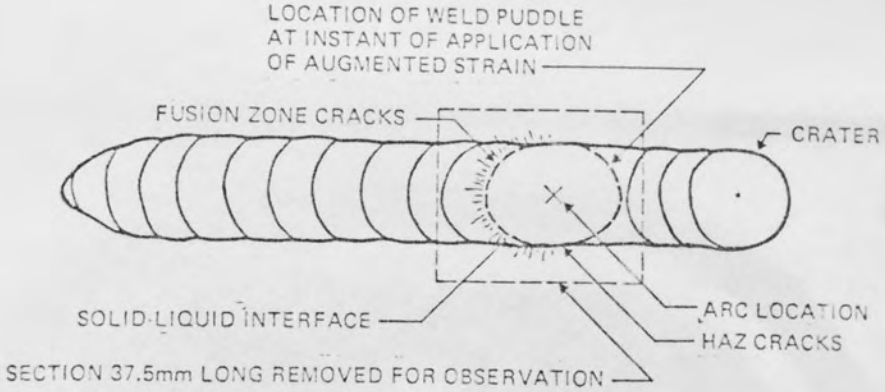

Fig 17. Section removed from Varestraint test piece for crack measurement

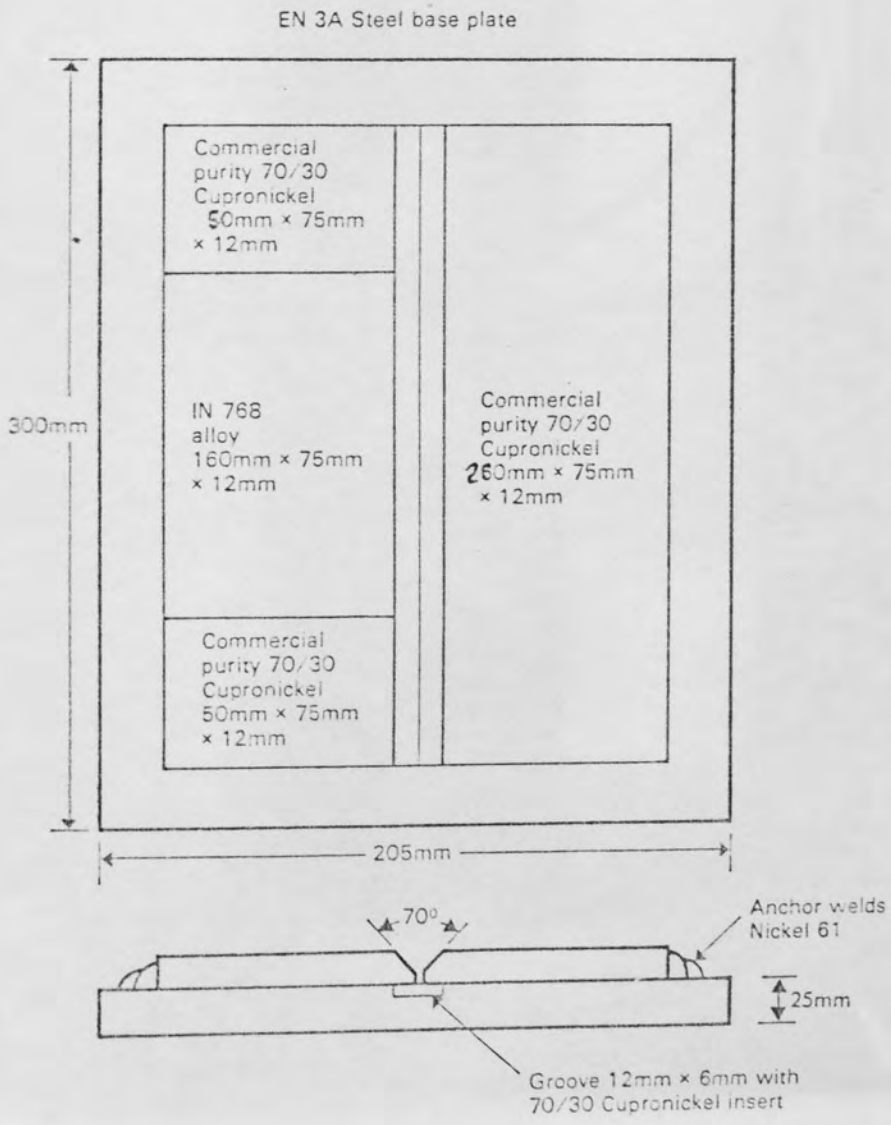

Fig 18. Design of restrained butt weld tests

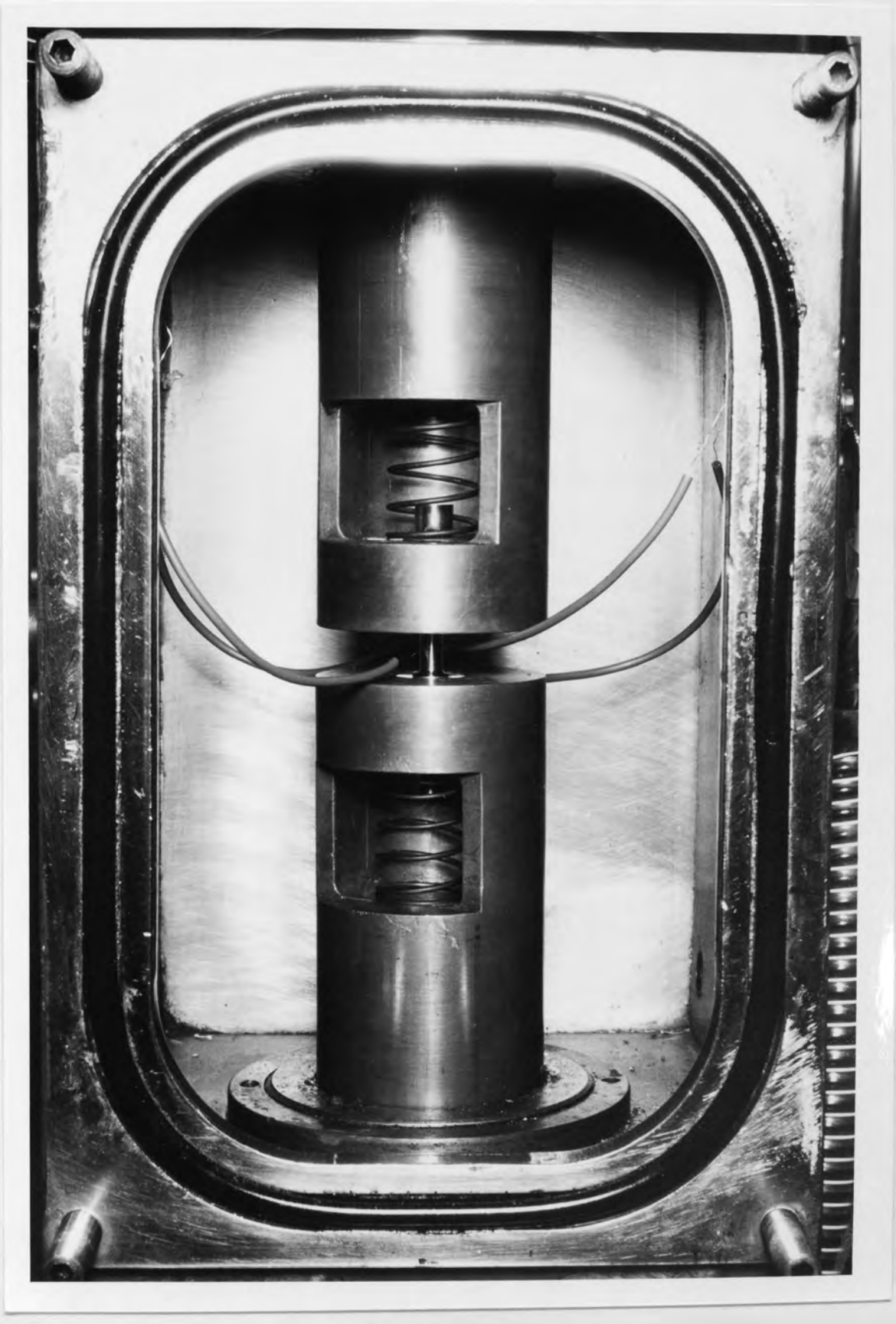

Fig 19. Simulator jaws before test

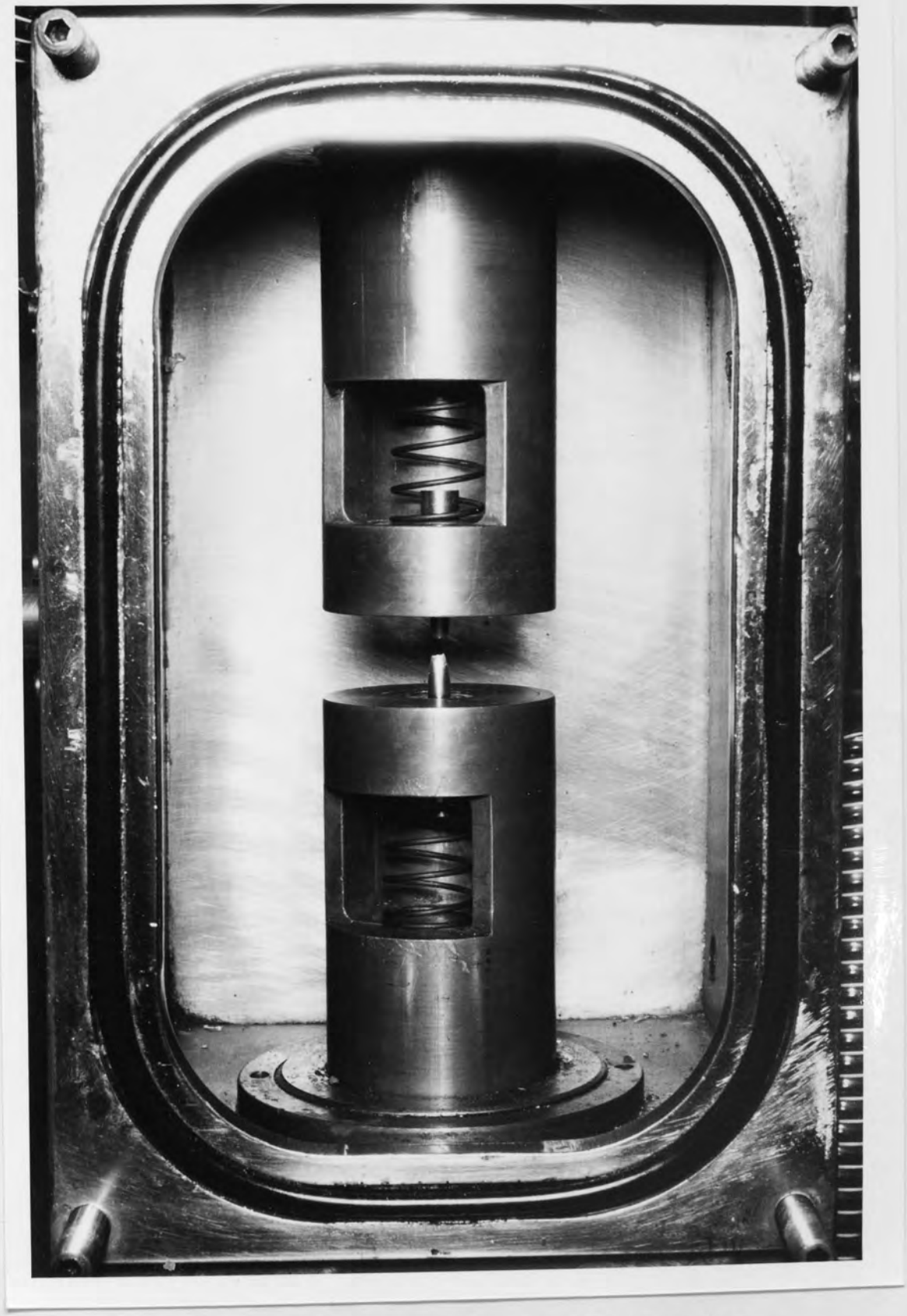

Fig 20. Simulator jaws after completion of test

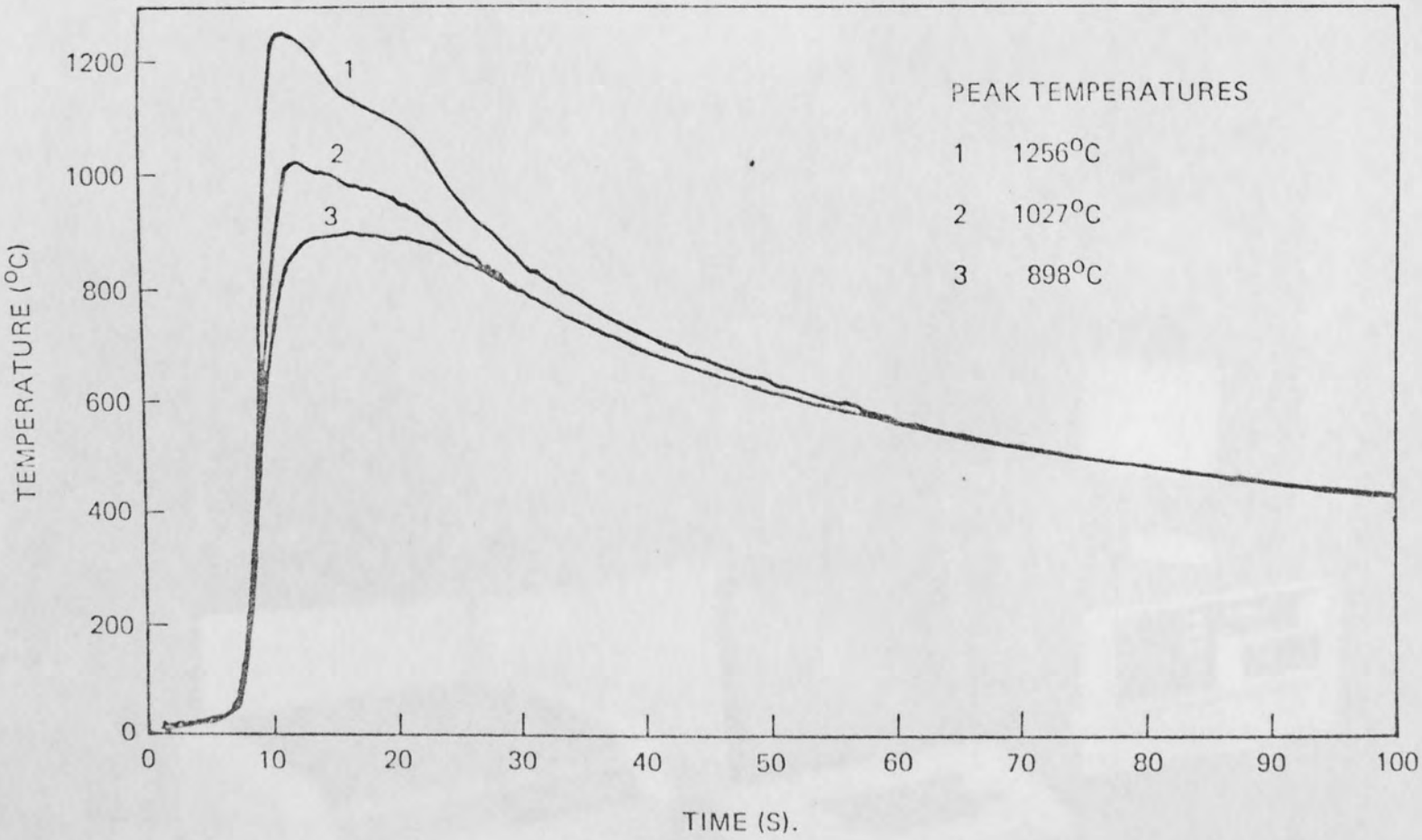

Fig 21. Thermal cycles measured at three different thermocouple positions. Heat input 1.7kJmm^{-1}

Fig 22. General view of weld thermal simulator
and MACSYM mini-computer

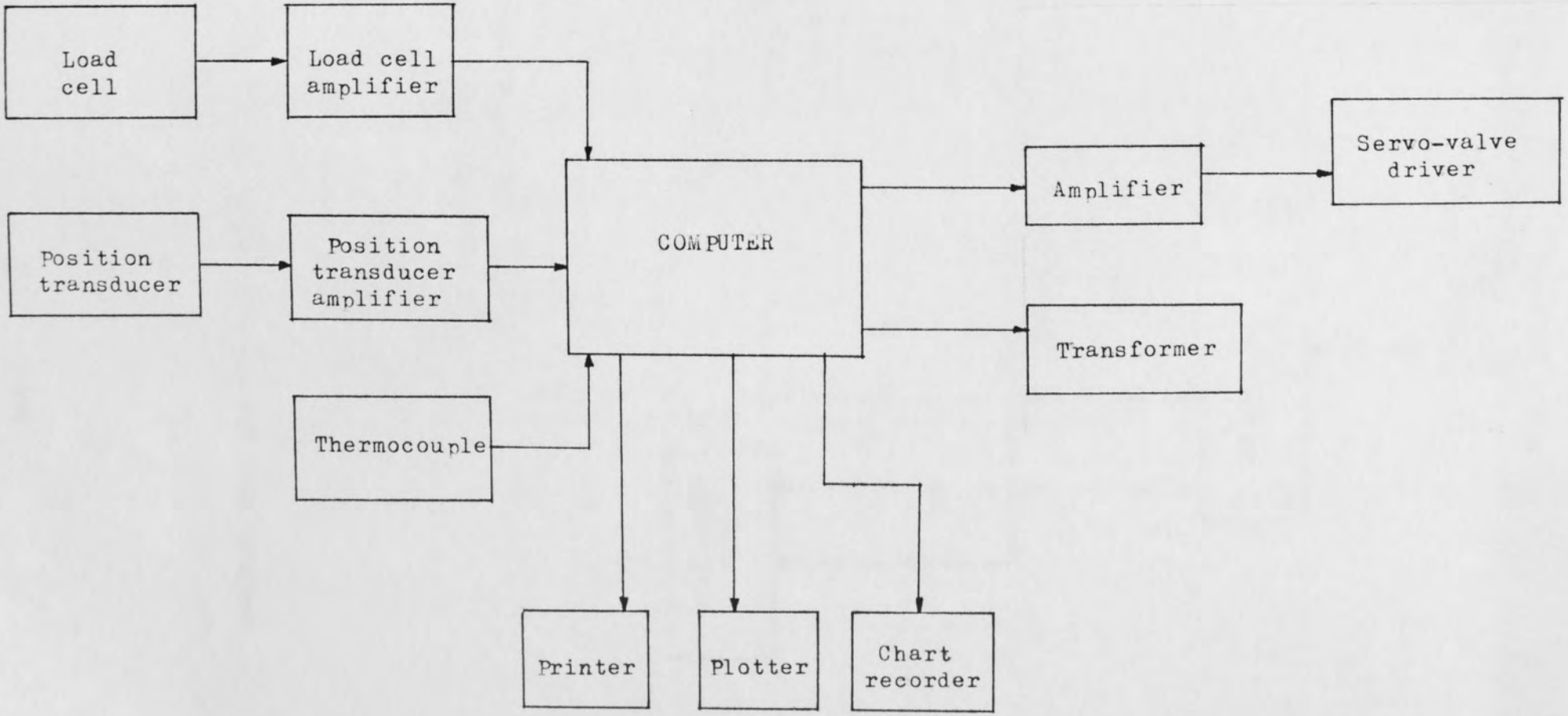

Fig 23. Communications with MACSYM computer

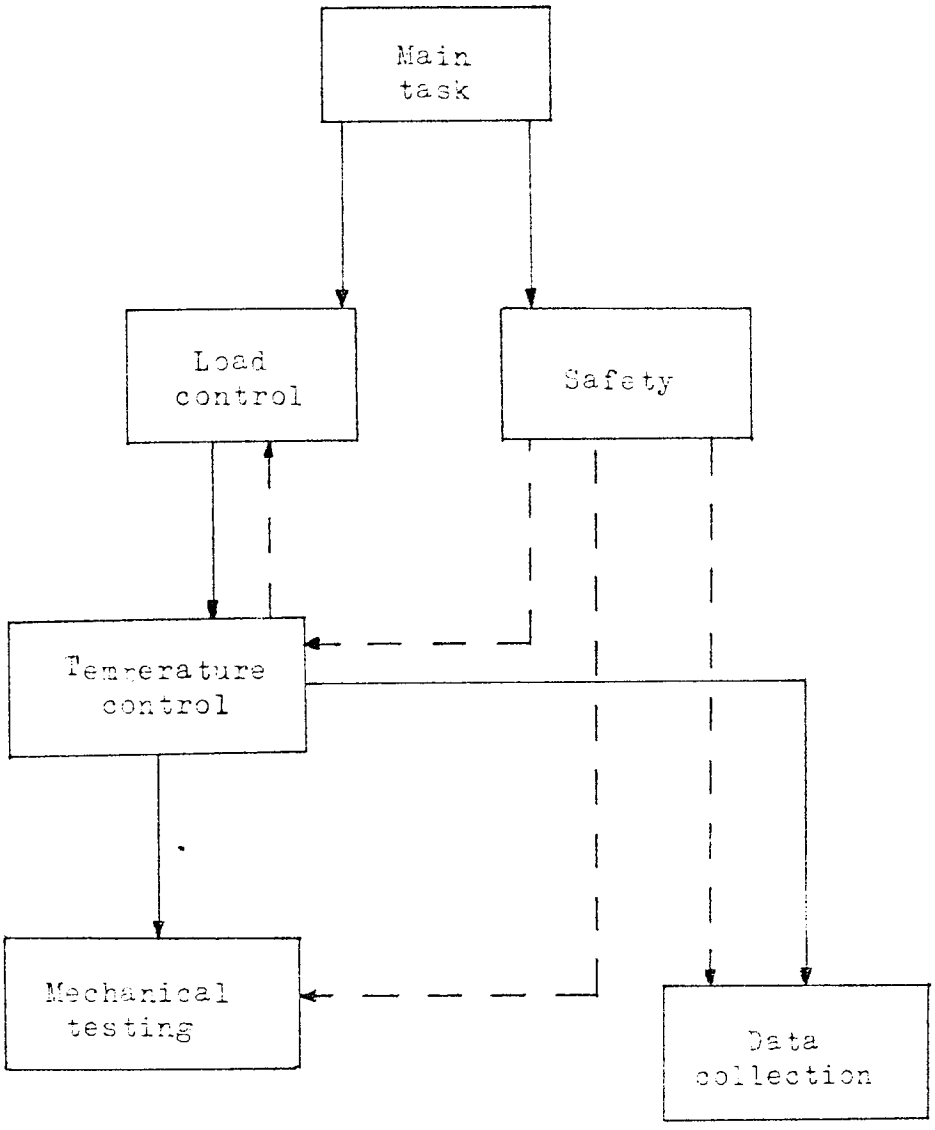

Fig 24. Sequence of tasks for main program

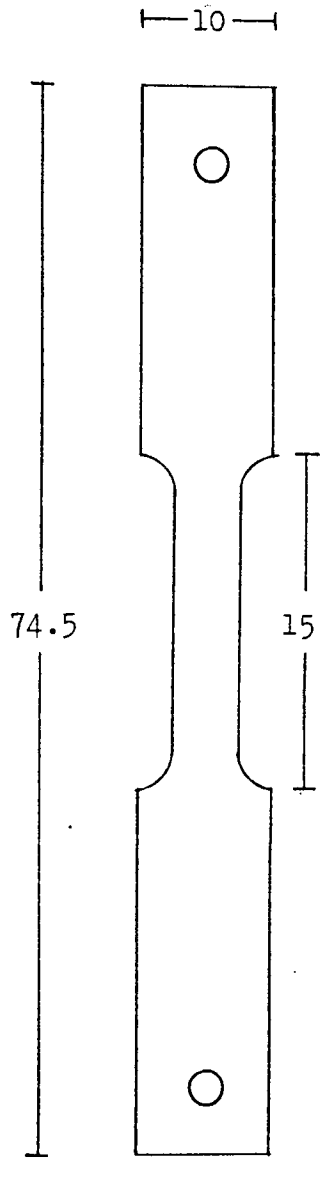

All dimensions
in mm.

Fig 25. Design of testpiece for weld thermal simulation

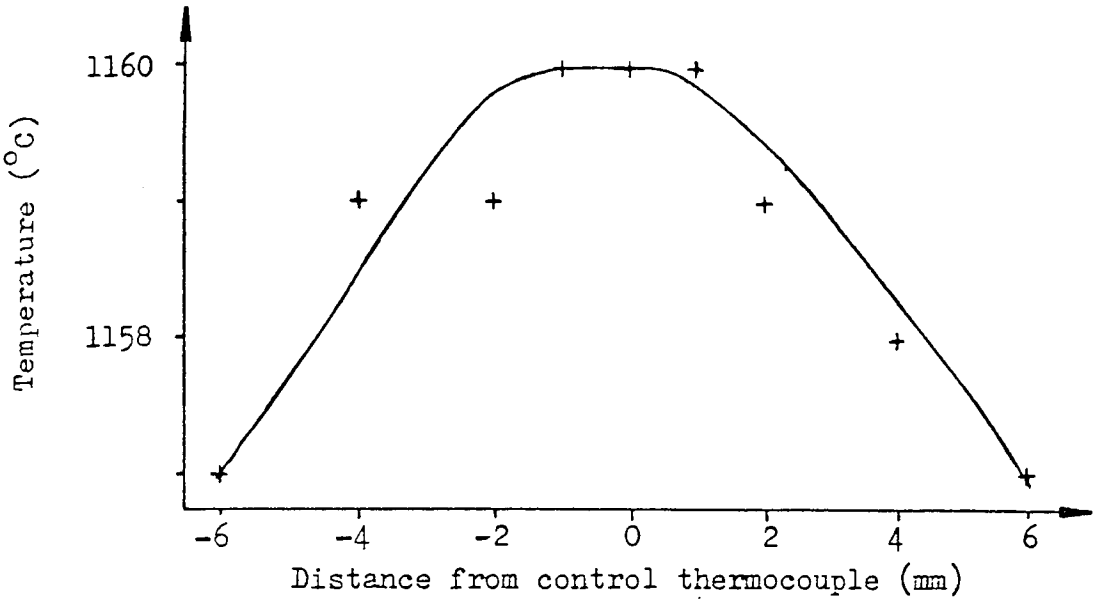

Fig 26. Temperature distribution along length of simulator specimen

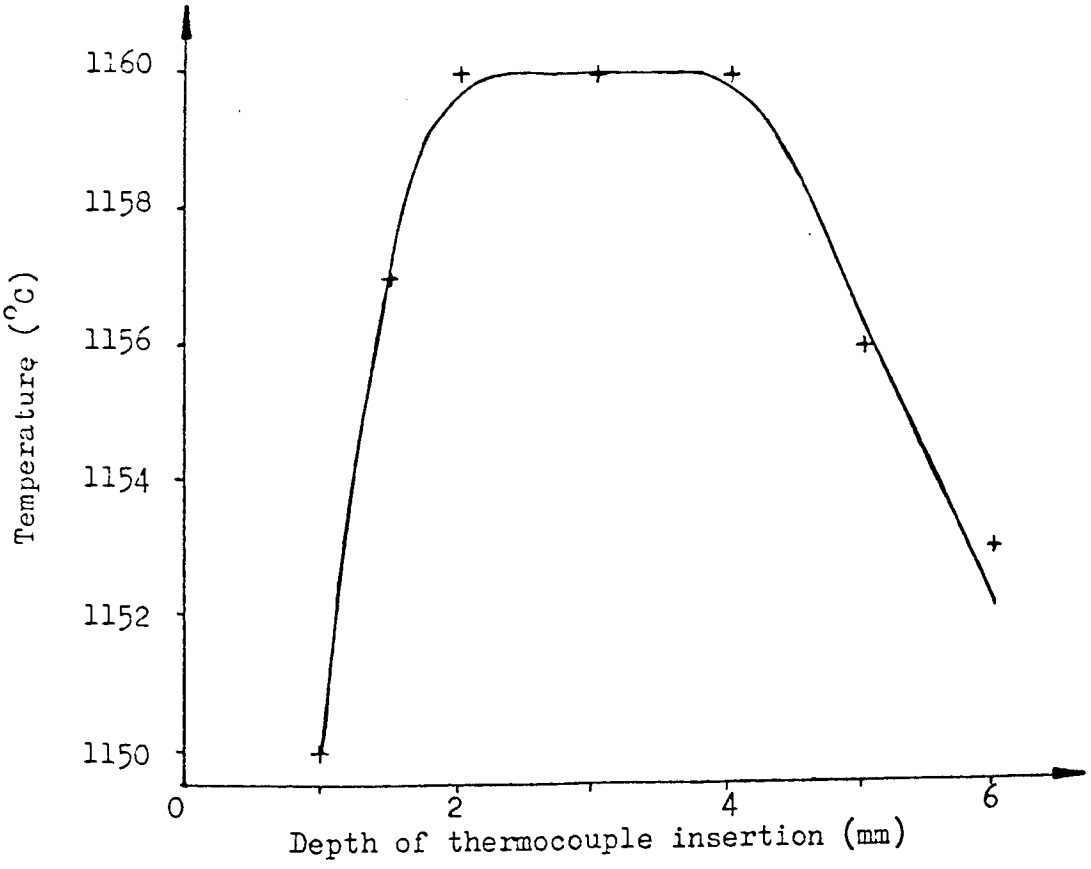

Fig 27. Temperature distribution through thickness of simulator specimen

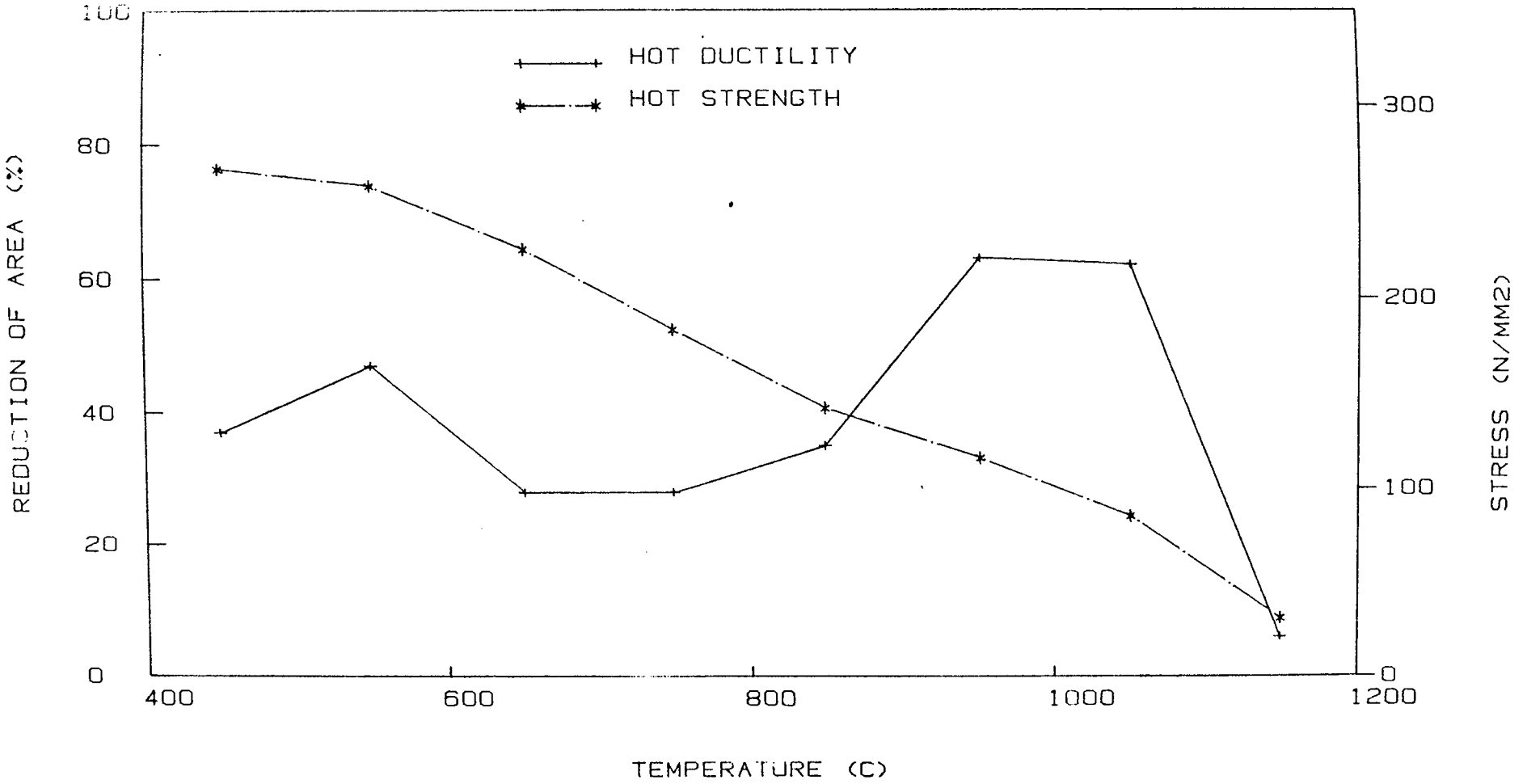

Fig 28. Plot of tensile properties against temperature for alloy A1 on cooling from 1160 C

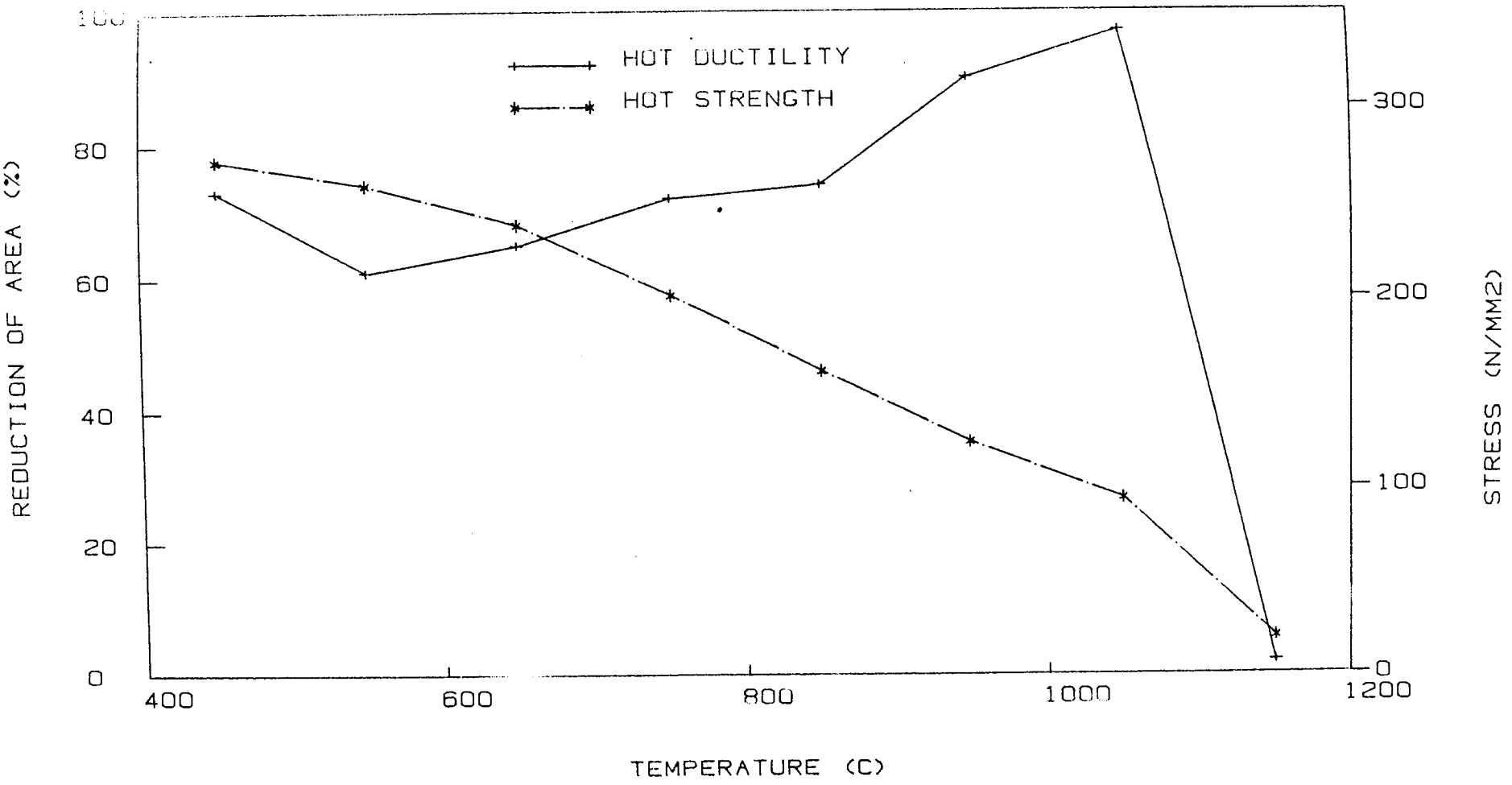

Fig 29. Plot of tensile properties against temperature for alloy A2 on cooling from 1160 C

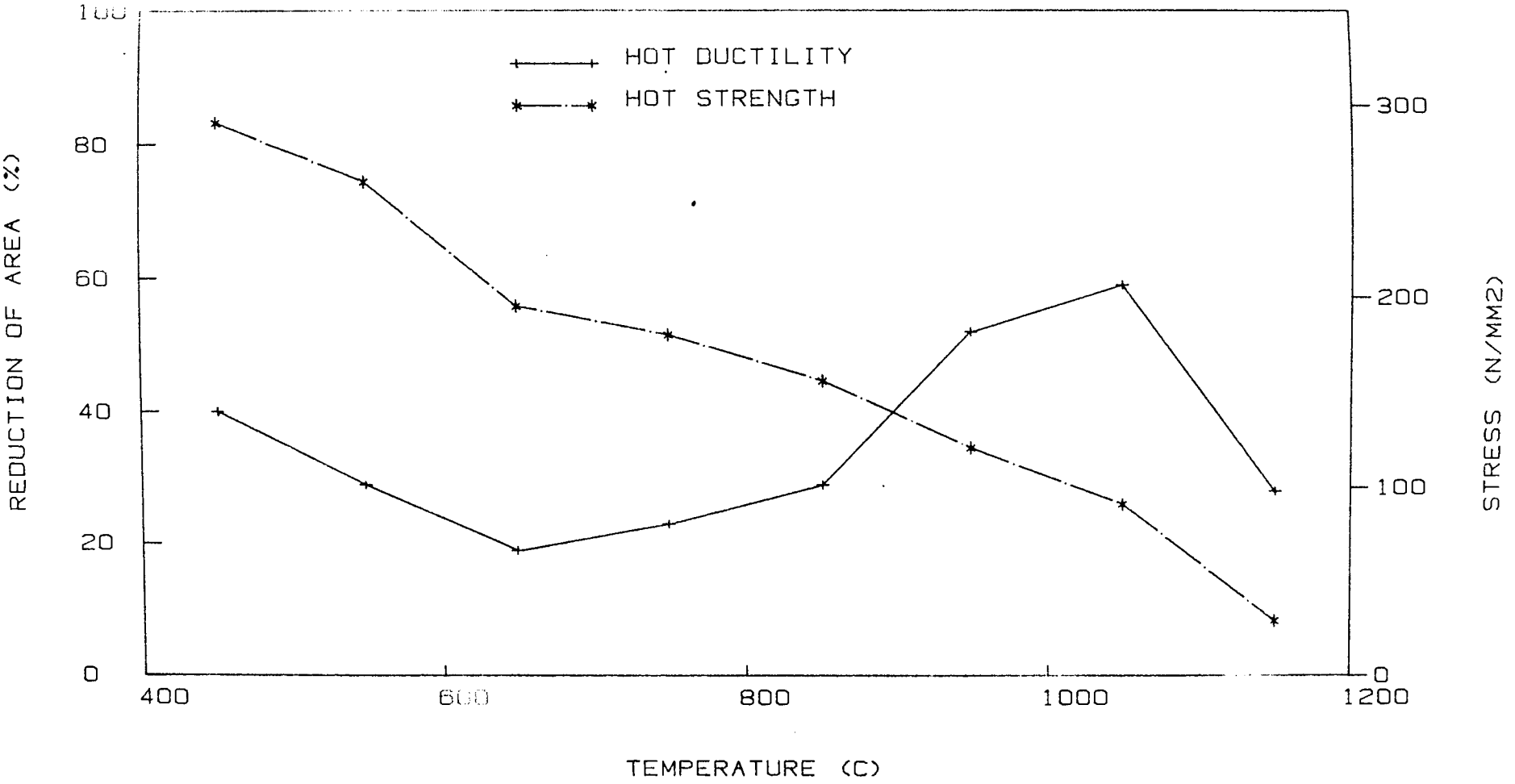

Fig 30. Plot of tensile properties against temperature for alloy A3 on cooling from 1160 C

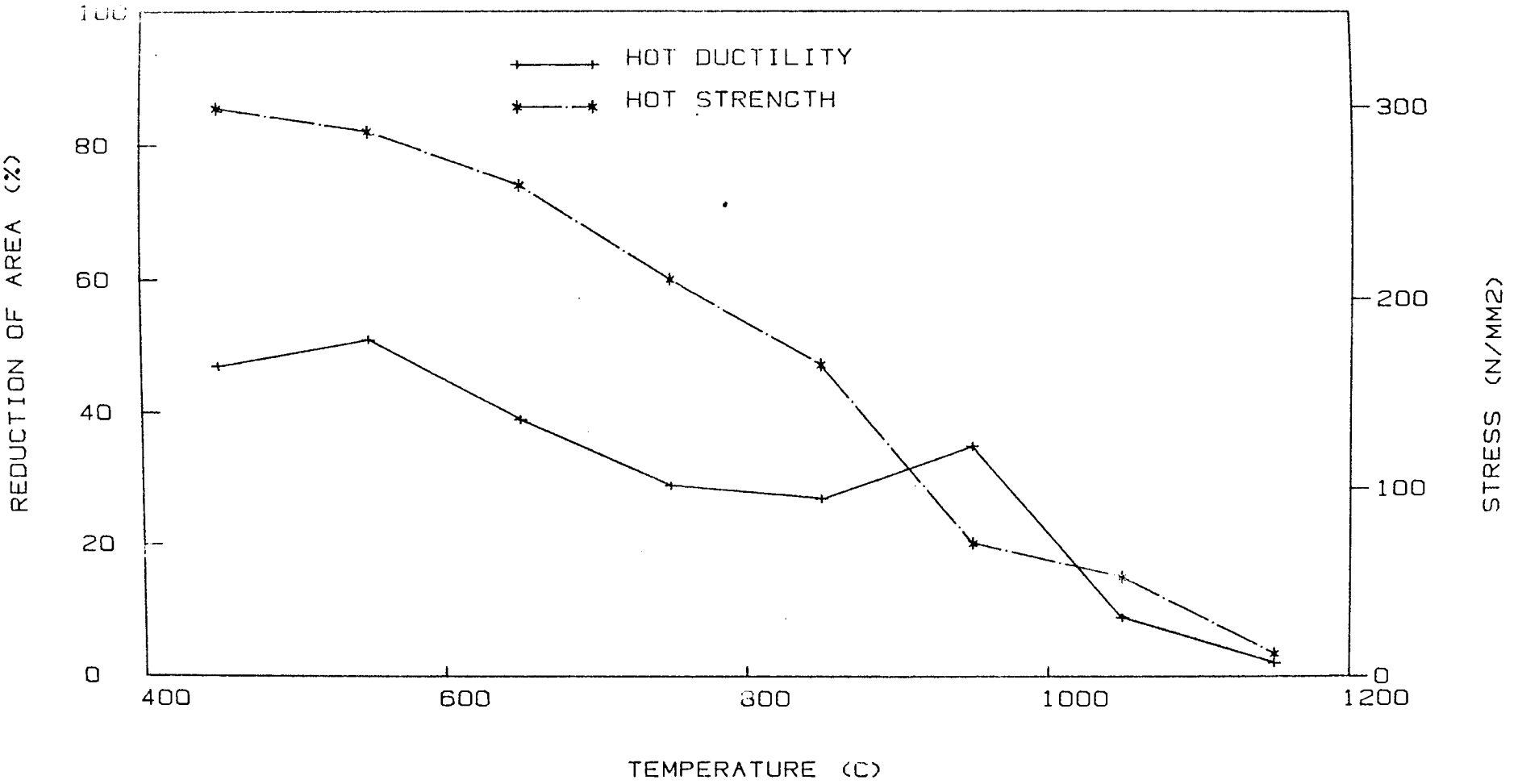

Fig 31. Plot of tensile properties against temperature for alloy A4 on cooling from 1160 C

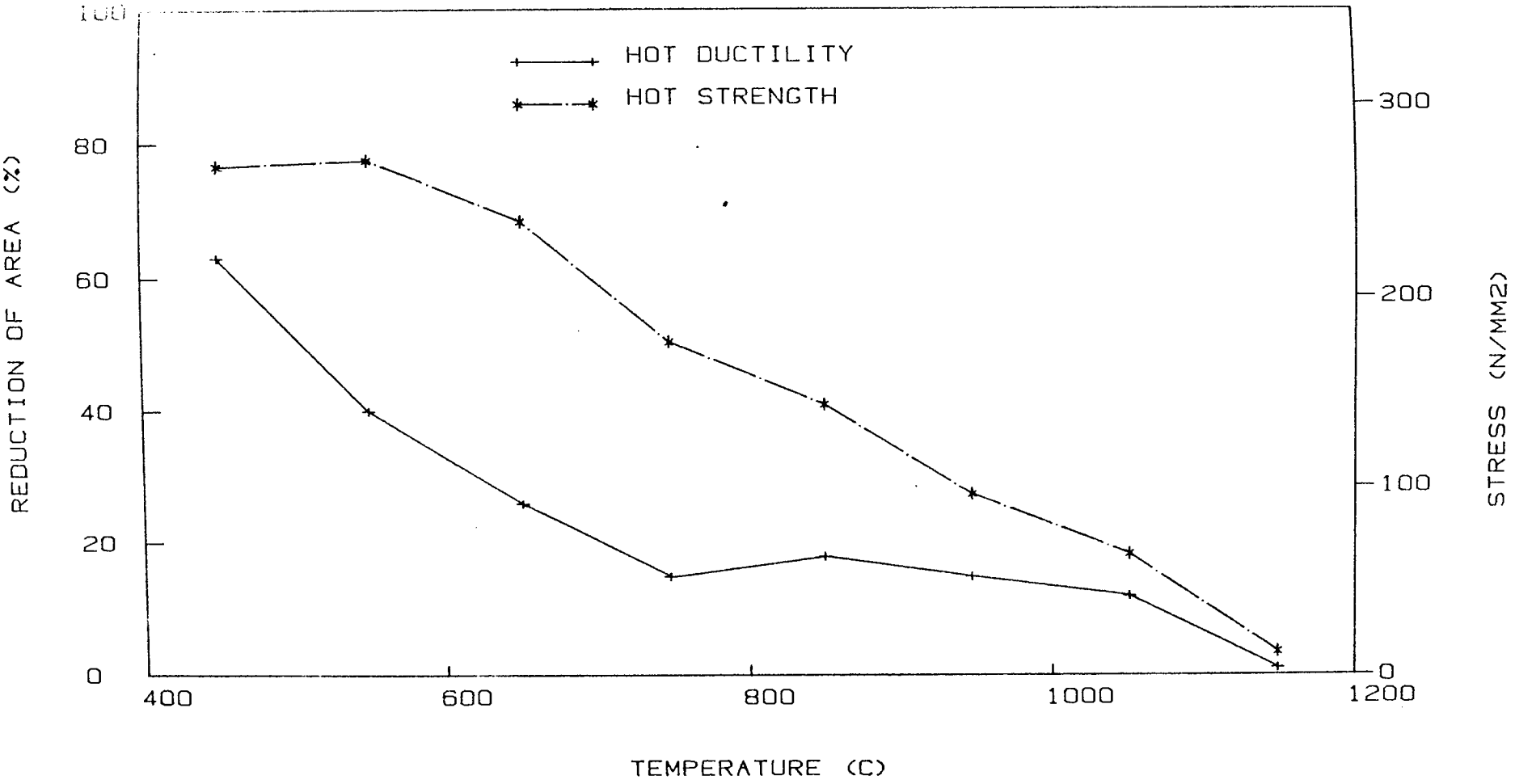

Fig 32. Plot of tensile properties against temperature for alloy A5 on cooling from 1160 C

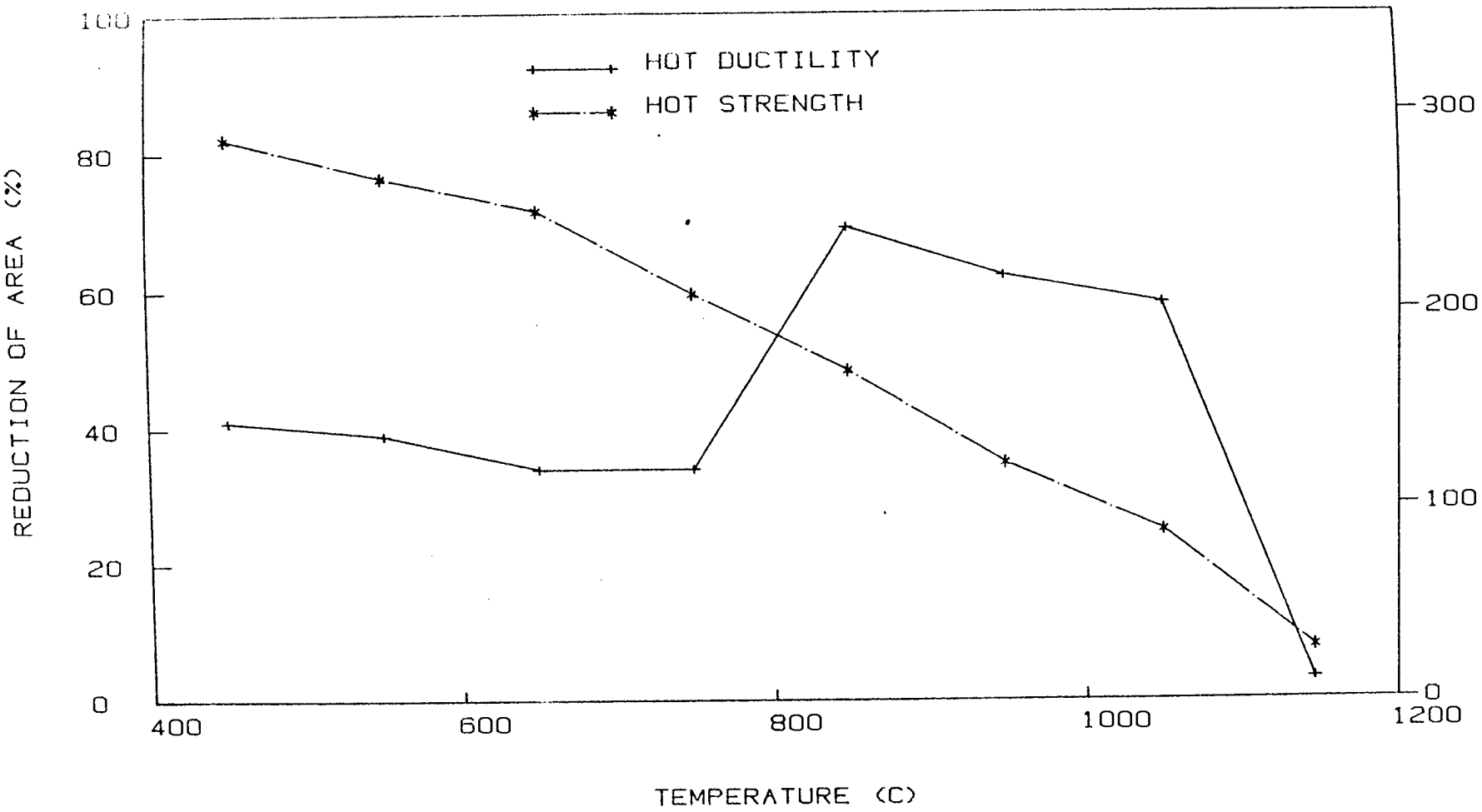

Fig 33. Plot of tensile properties against temperature for alloy A6 on cooling from 1160 C

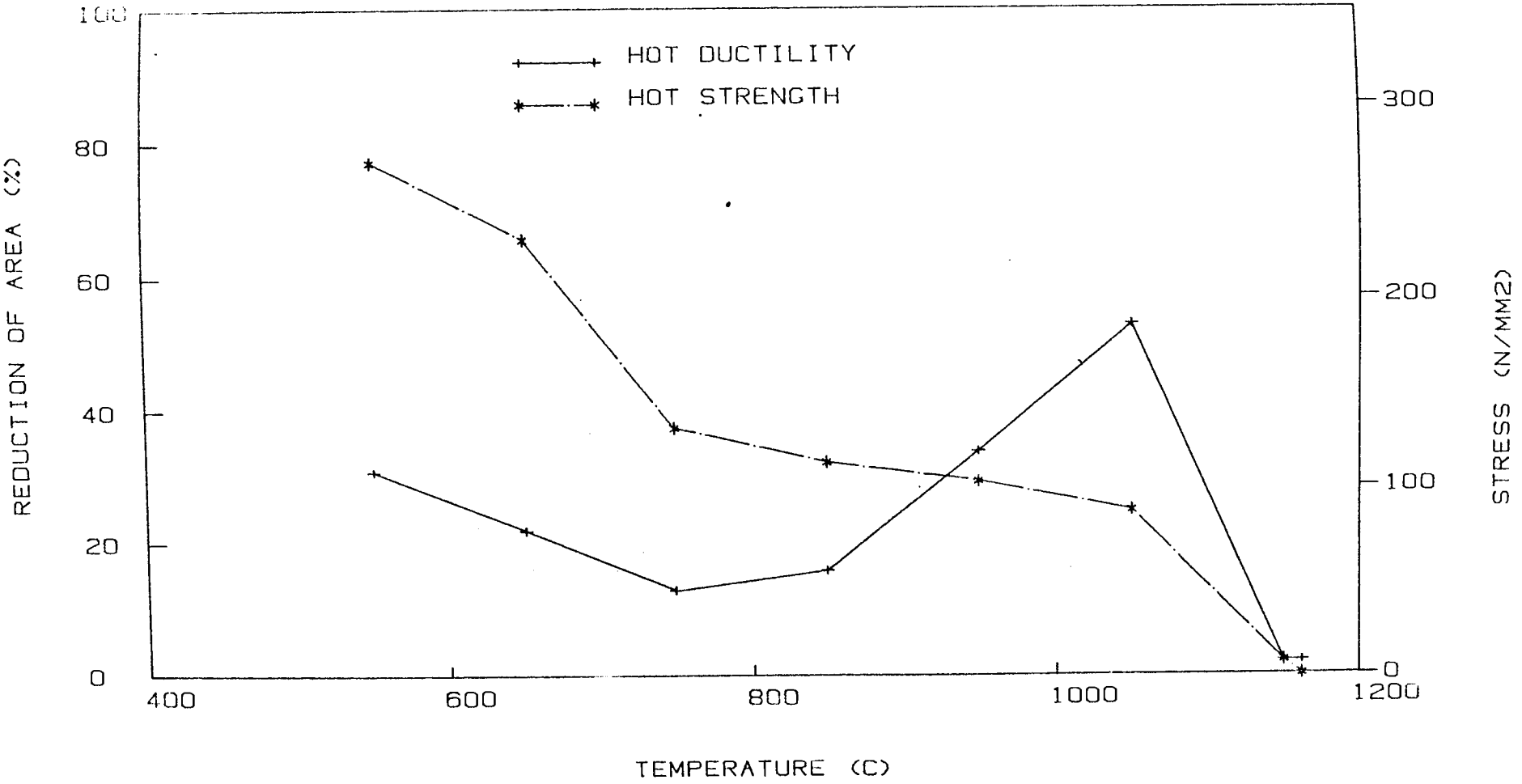

Fig 34. Plot of tensile properties against temperature for alloy A7 on cooling from 1160 C

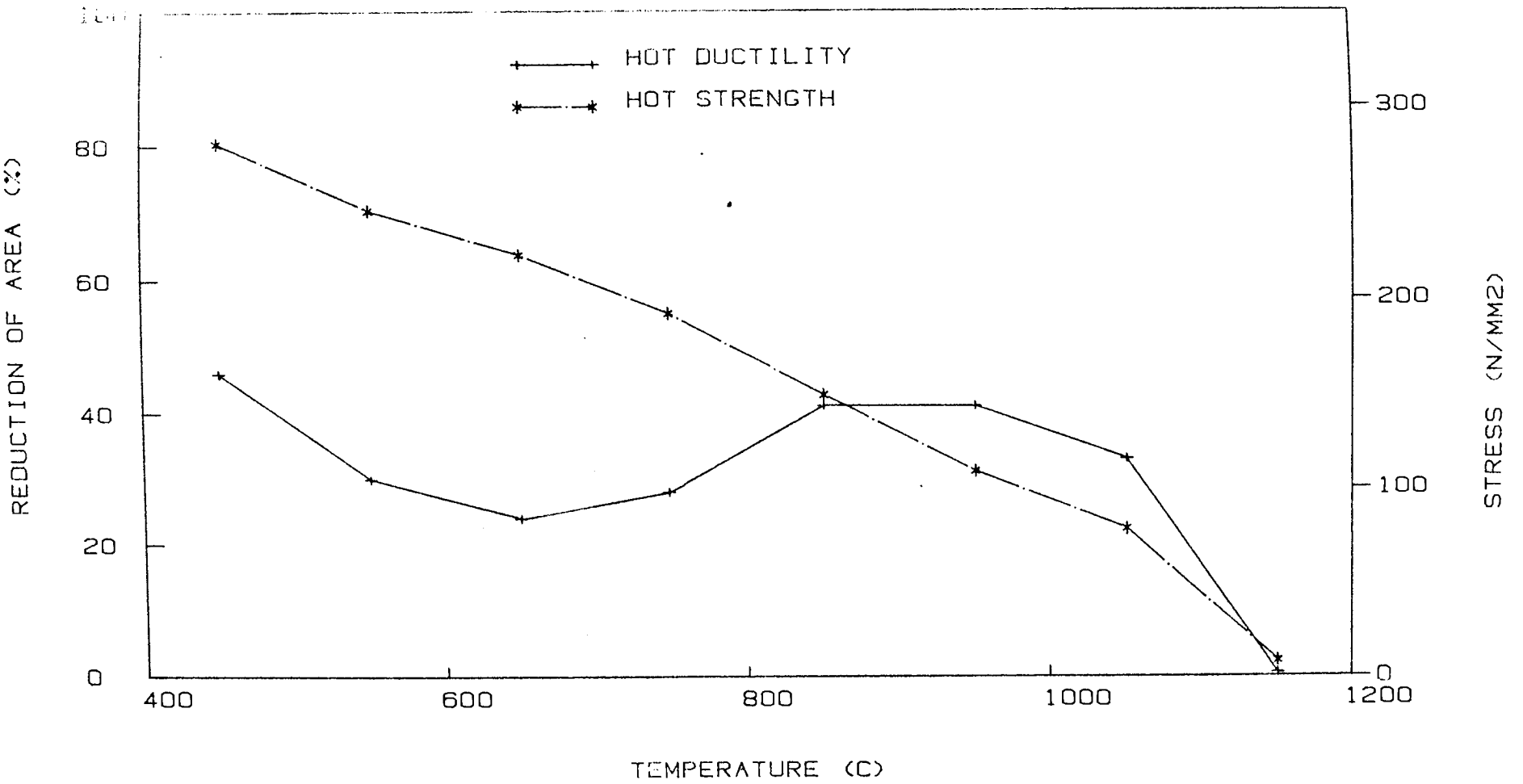

Fig 35. Plot of tensile properties against temperature for alloy A8 on cooling from 1160 C

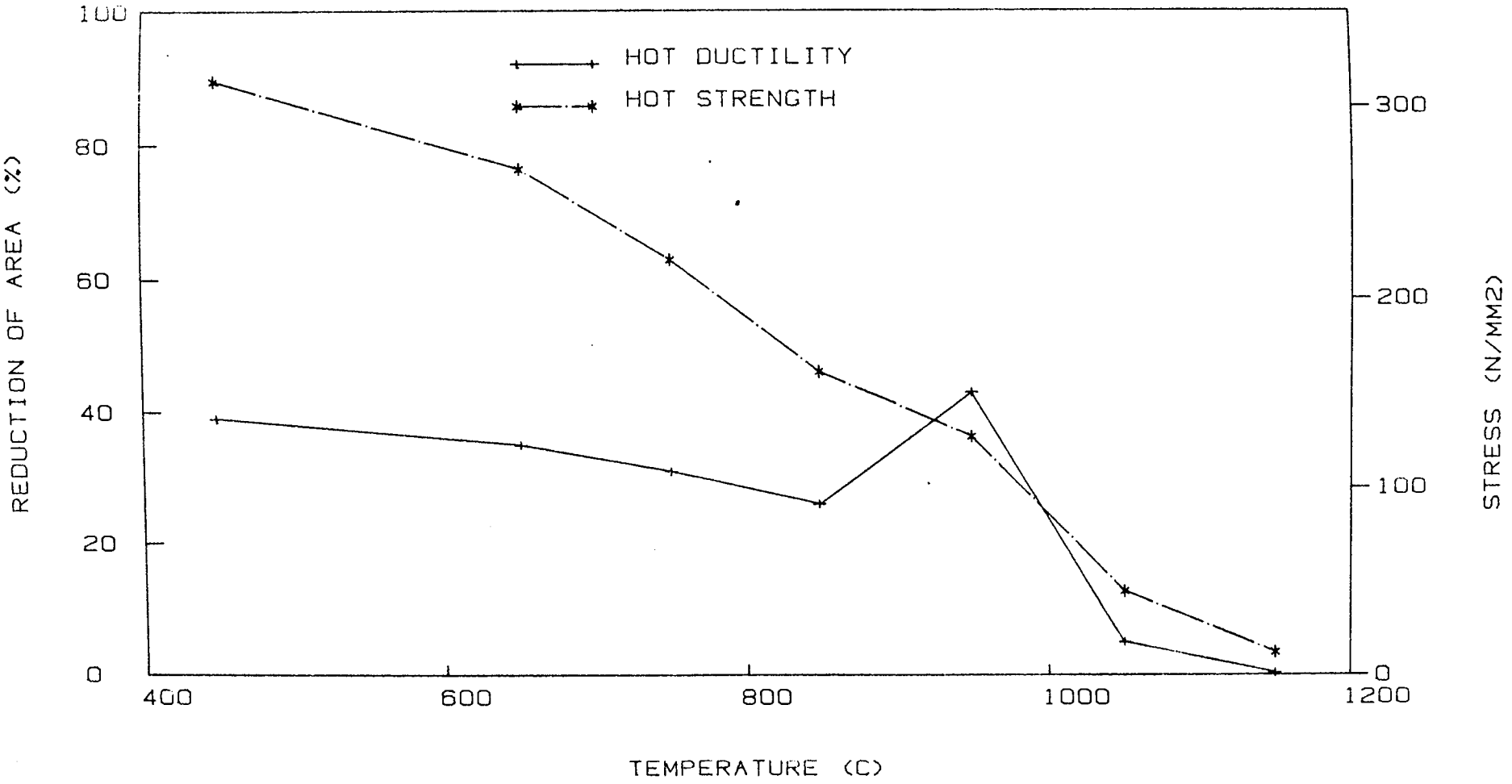

Fig 36. Plot of tensile properties against temperature for alloy B1 on cooling from 1160 C

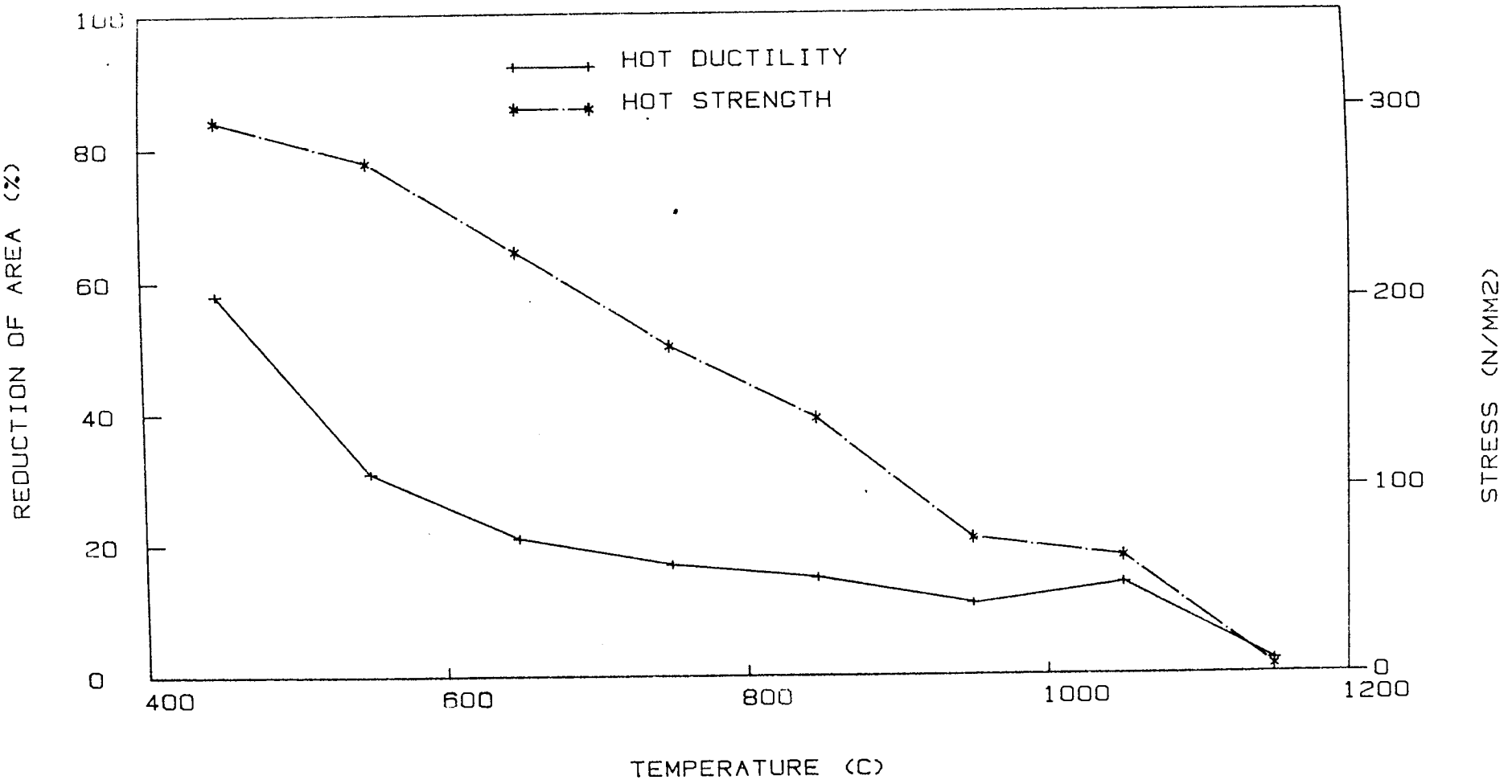

Fig 37. Plot of tensile properties against temperature for alloy B2 on cooling from 1160 C

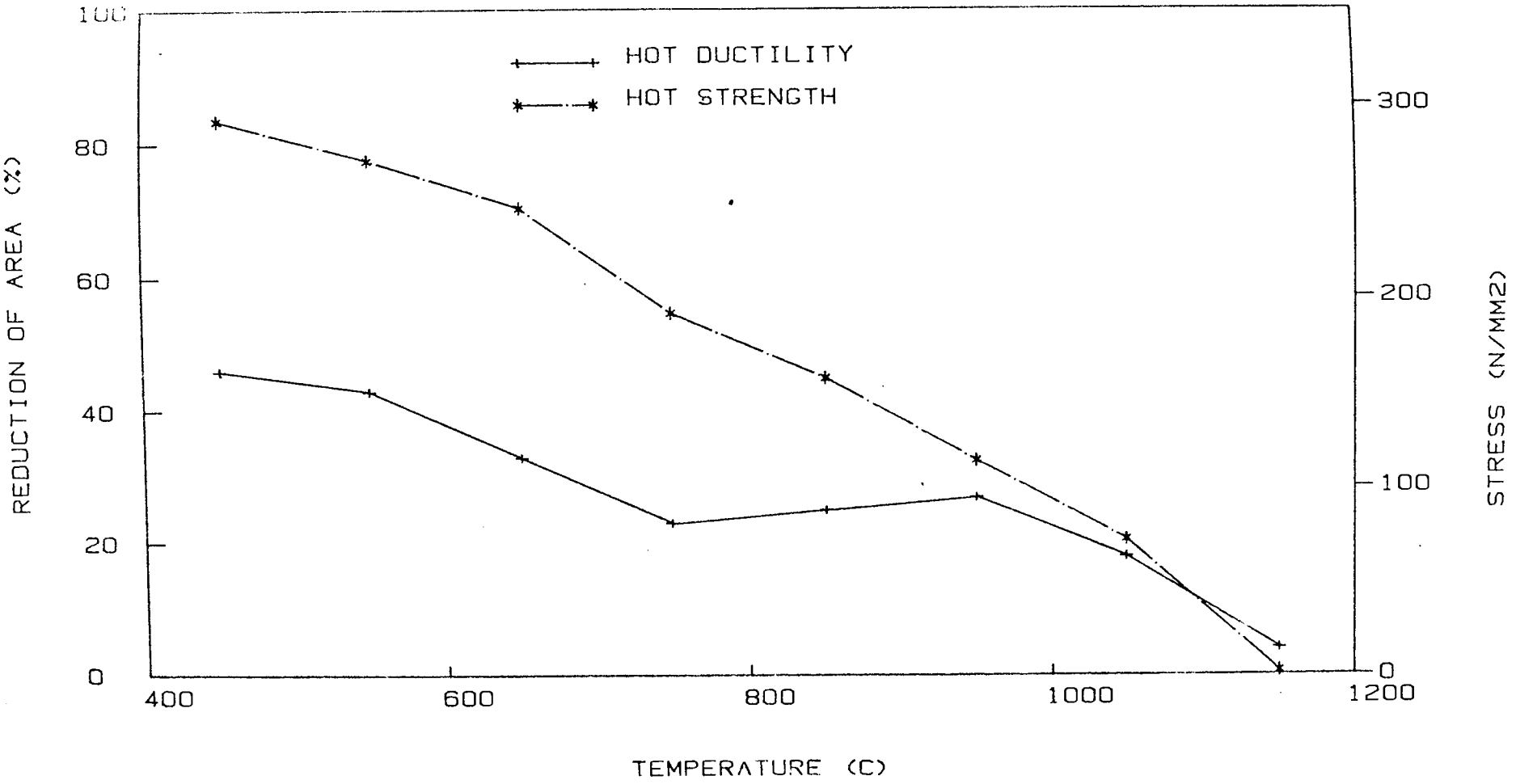

Fig 38. Plot of tensile properties against temperature for alloy B3 on cooling from 1160 C

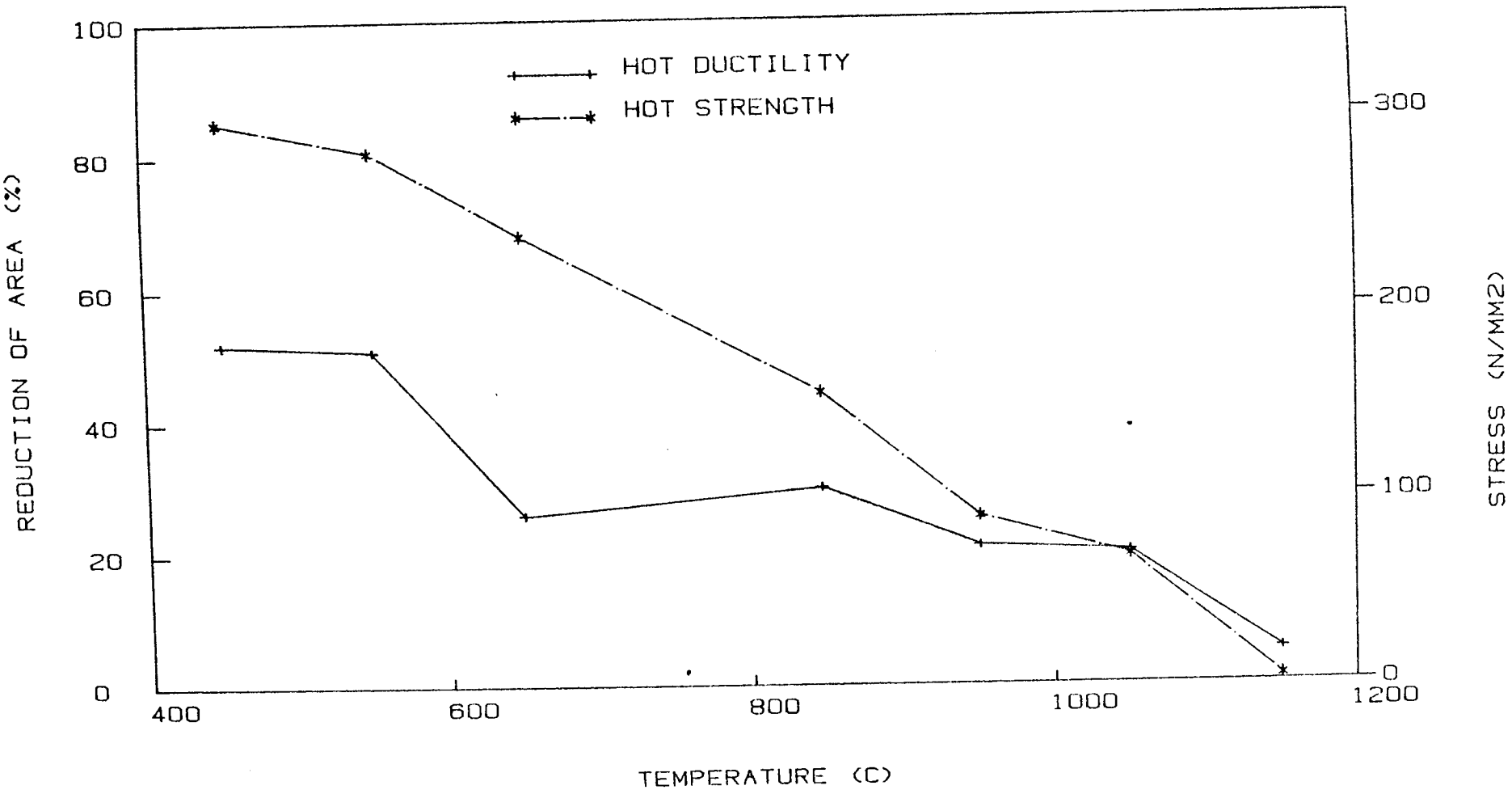

Fig 39. Plot of tensile properties against temperature for alloy B4 on cooling from 1160 C

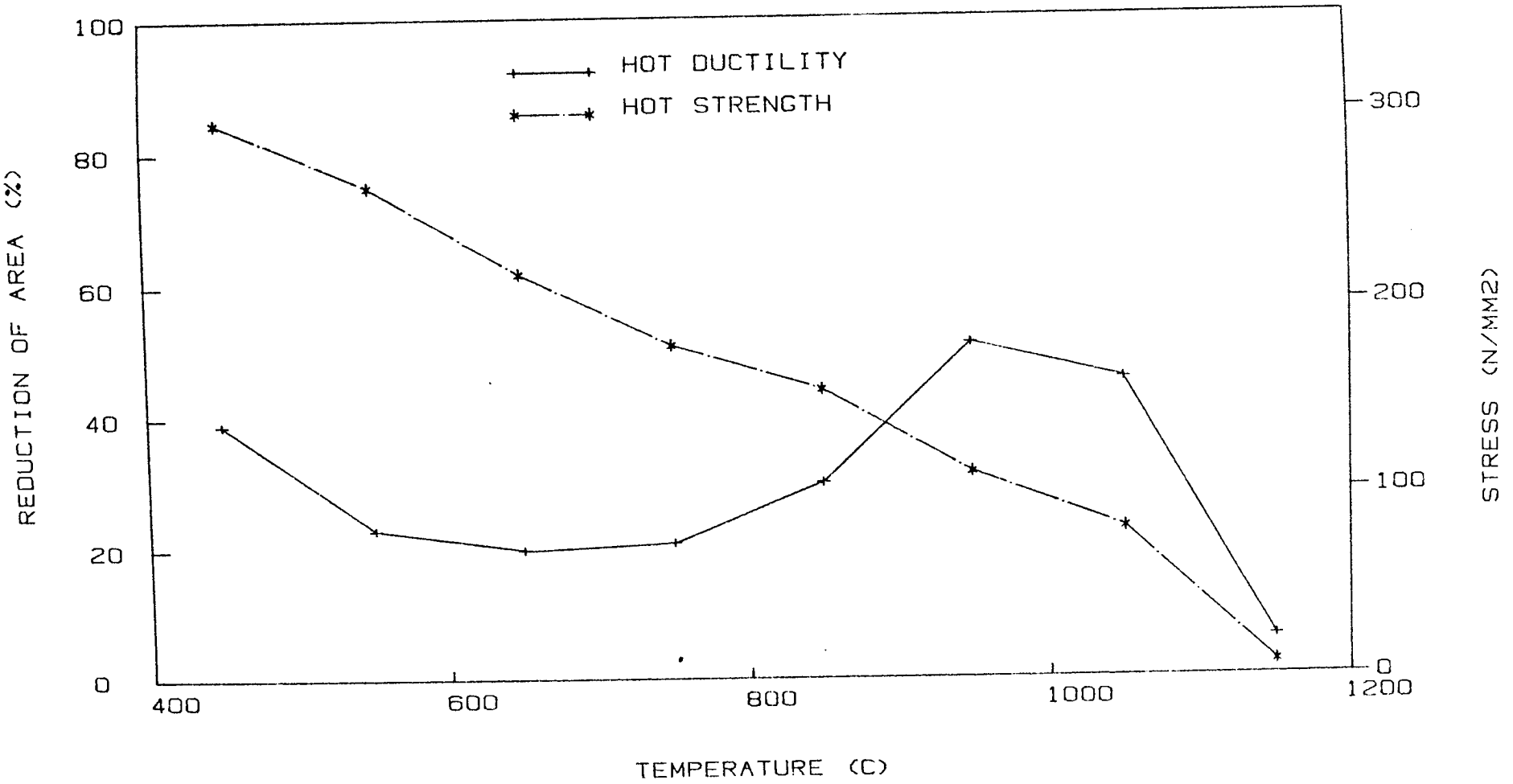

Fig 40. Plot of tensile properties against temperature for alloy B5 on cooling from 1160 C

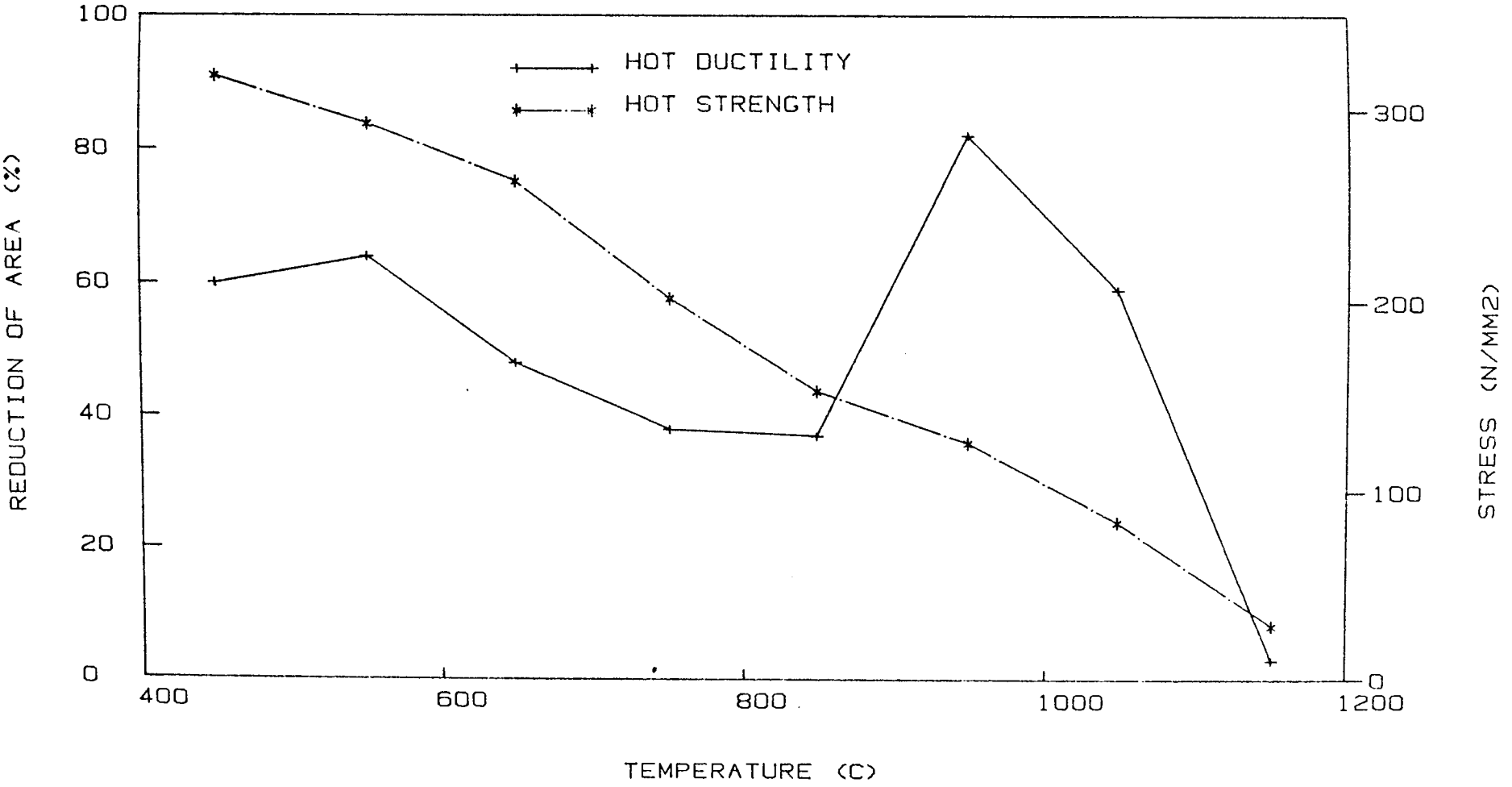

Fig 41. Plot of tensile properties against temperature for alloy B6 on cooling from 1160 C

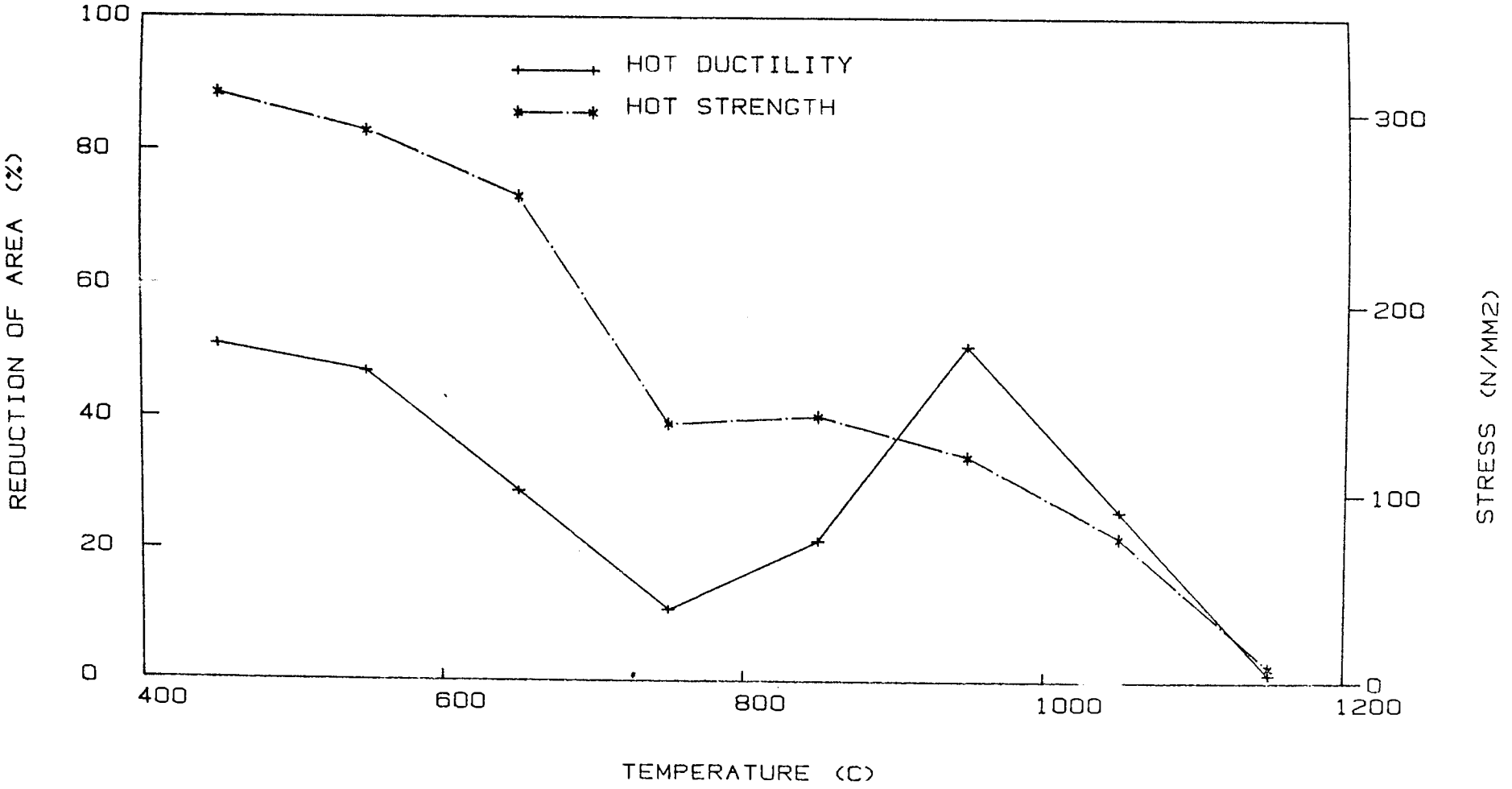

Fig 42. Plot of tensile properties against temperature for alloy B7 on cooling from 1160 C

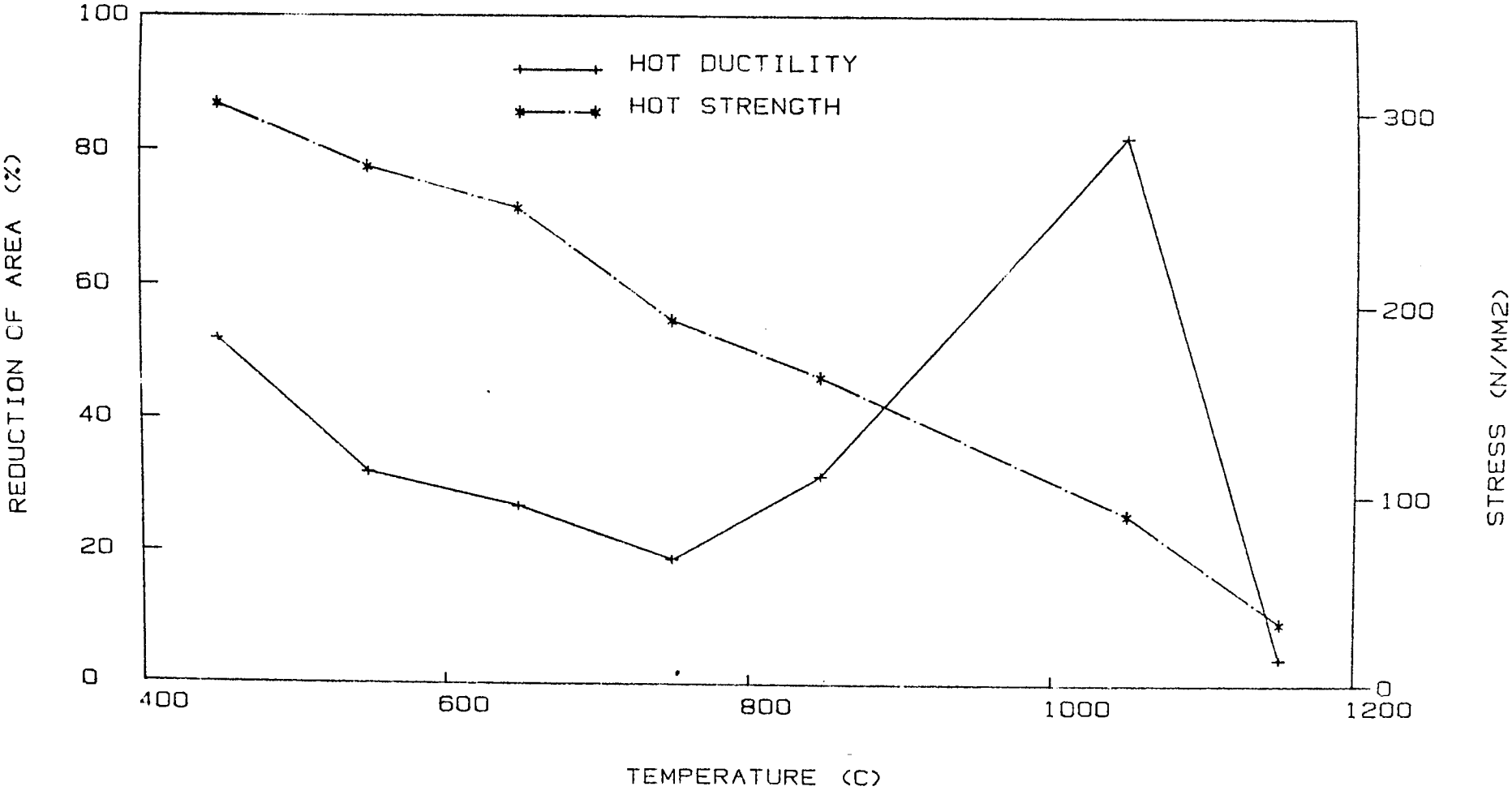

Fig 43. Plot of tensile properties against temperature for alloy B8 on cooling from 1160 C

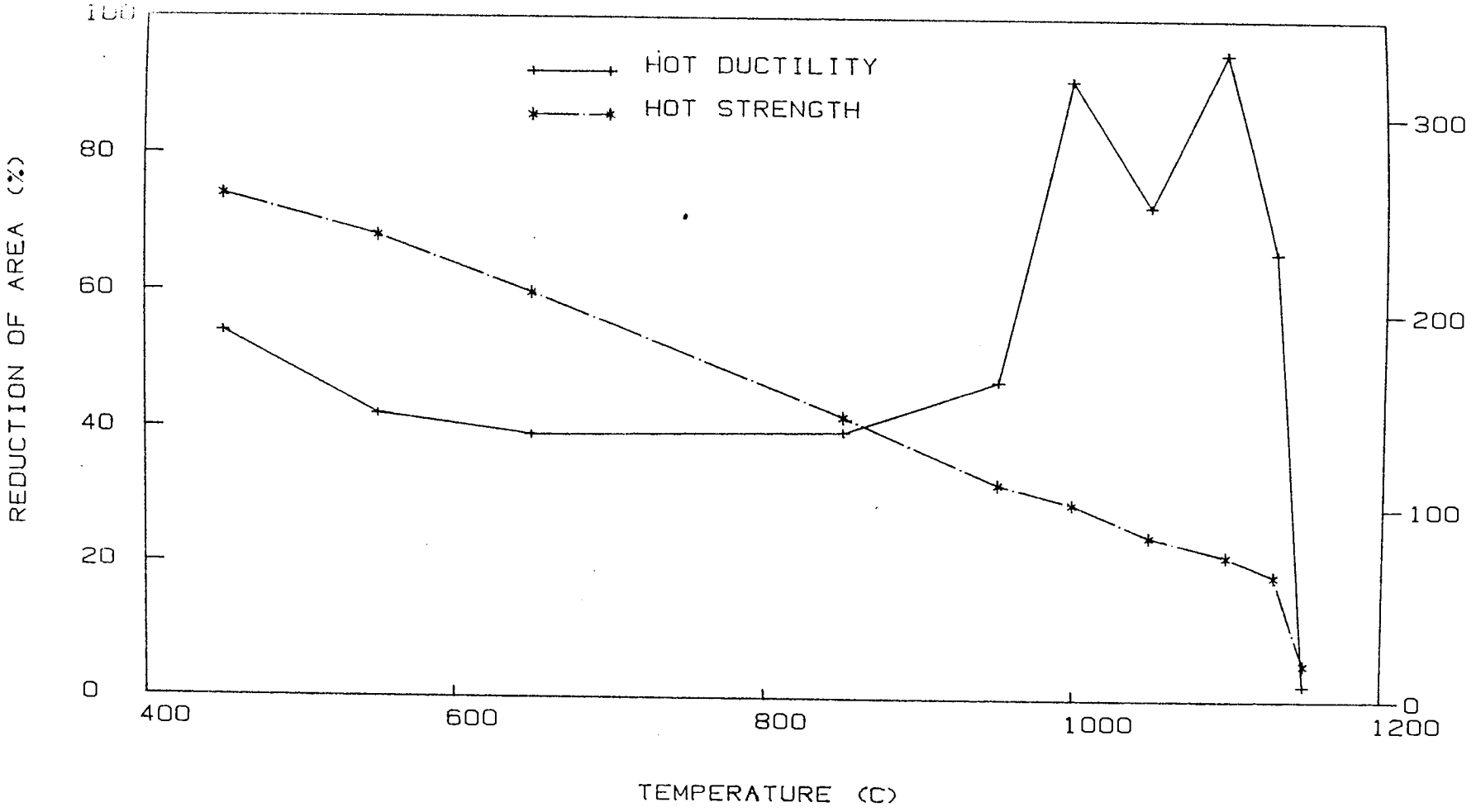

Fig 44. Plot of tensile properties against temperature for alloy H1 on cooling from 1160 C

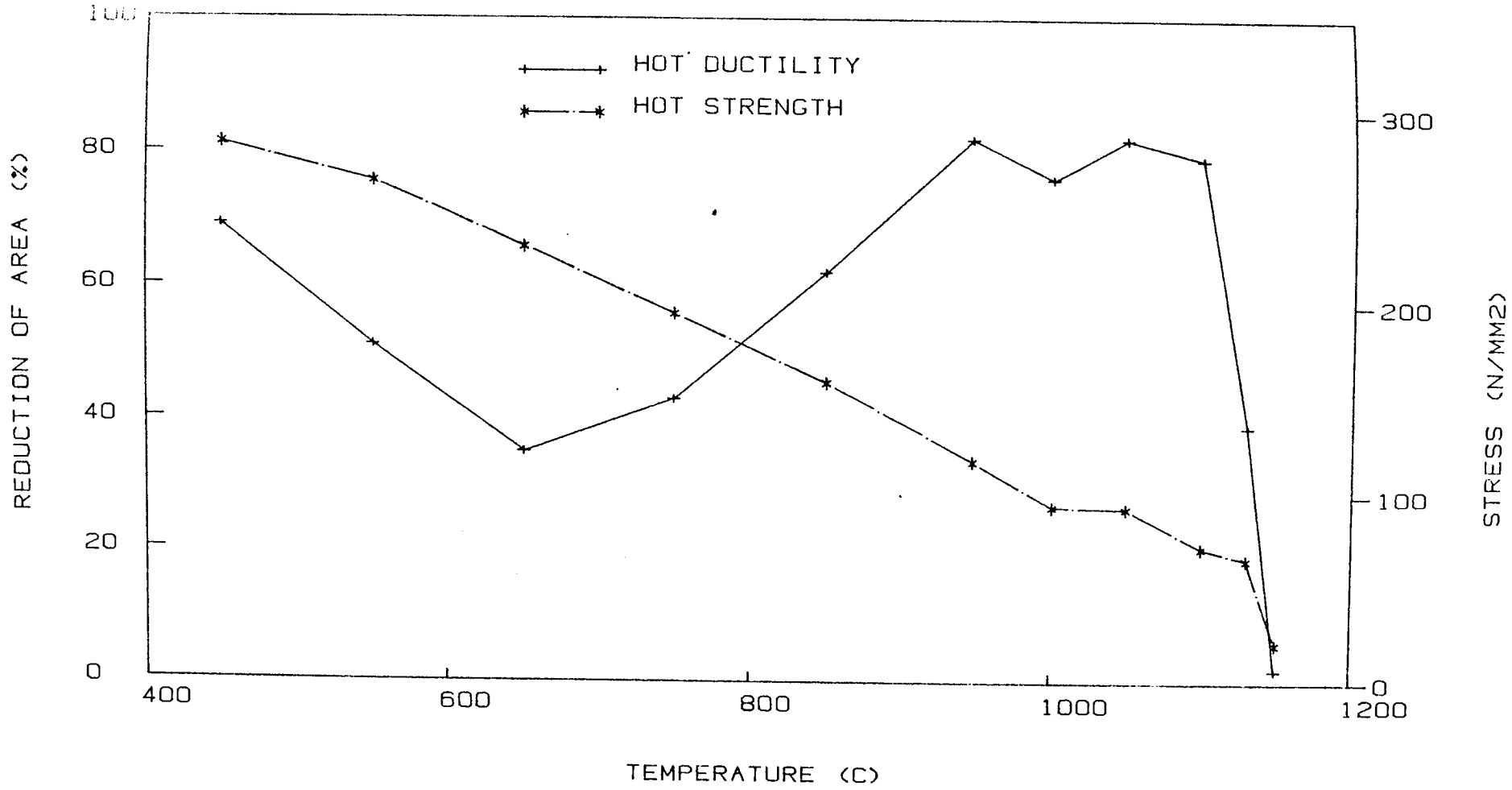

Fig 45. Plot of tensile properties against temperature for alloy P1 on cooling from 1160 C

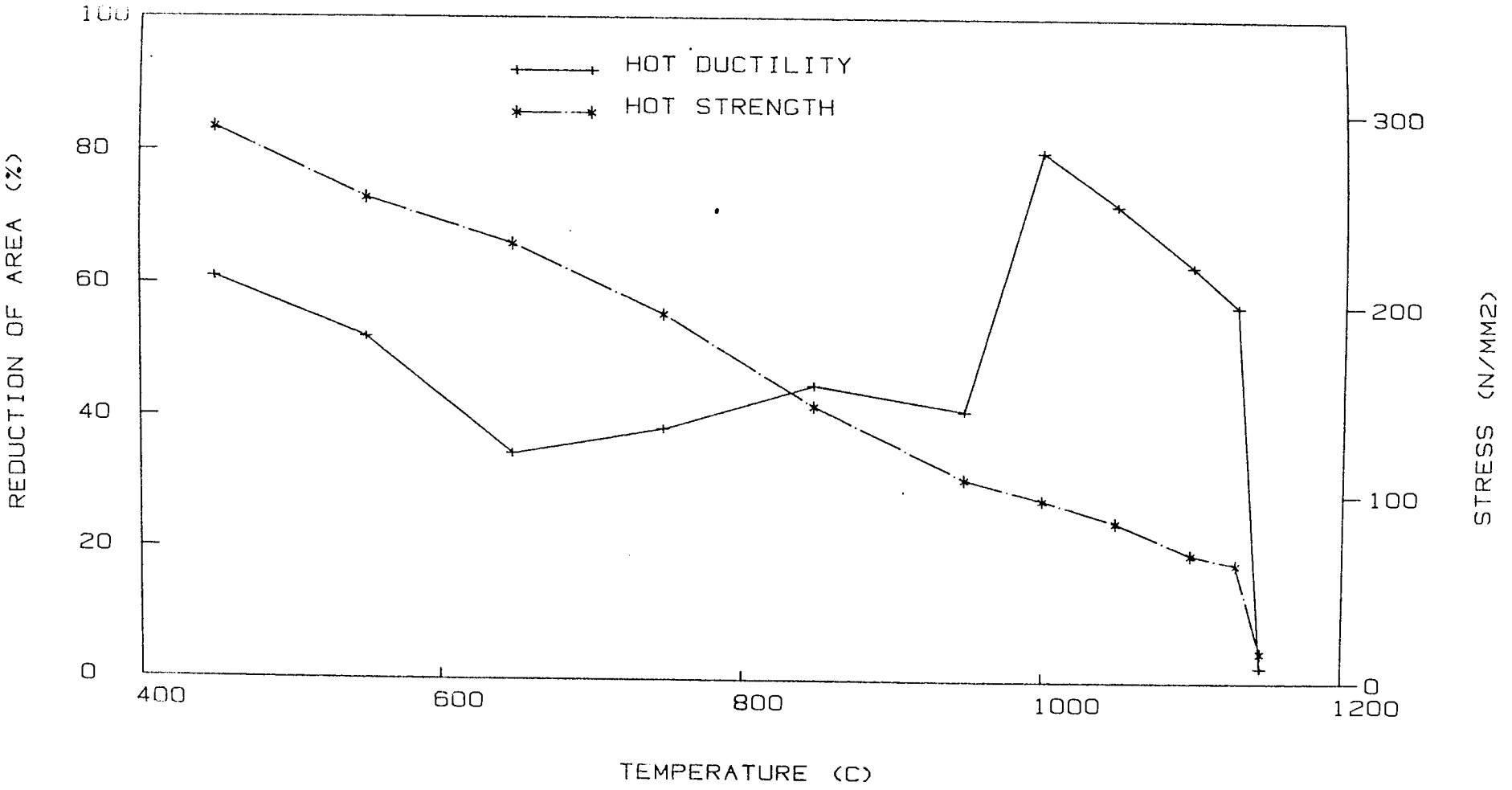

Fig 46. Plot of tensile properties against temperature for alloy H3 on cooling from 1160 C

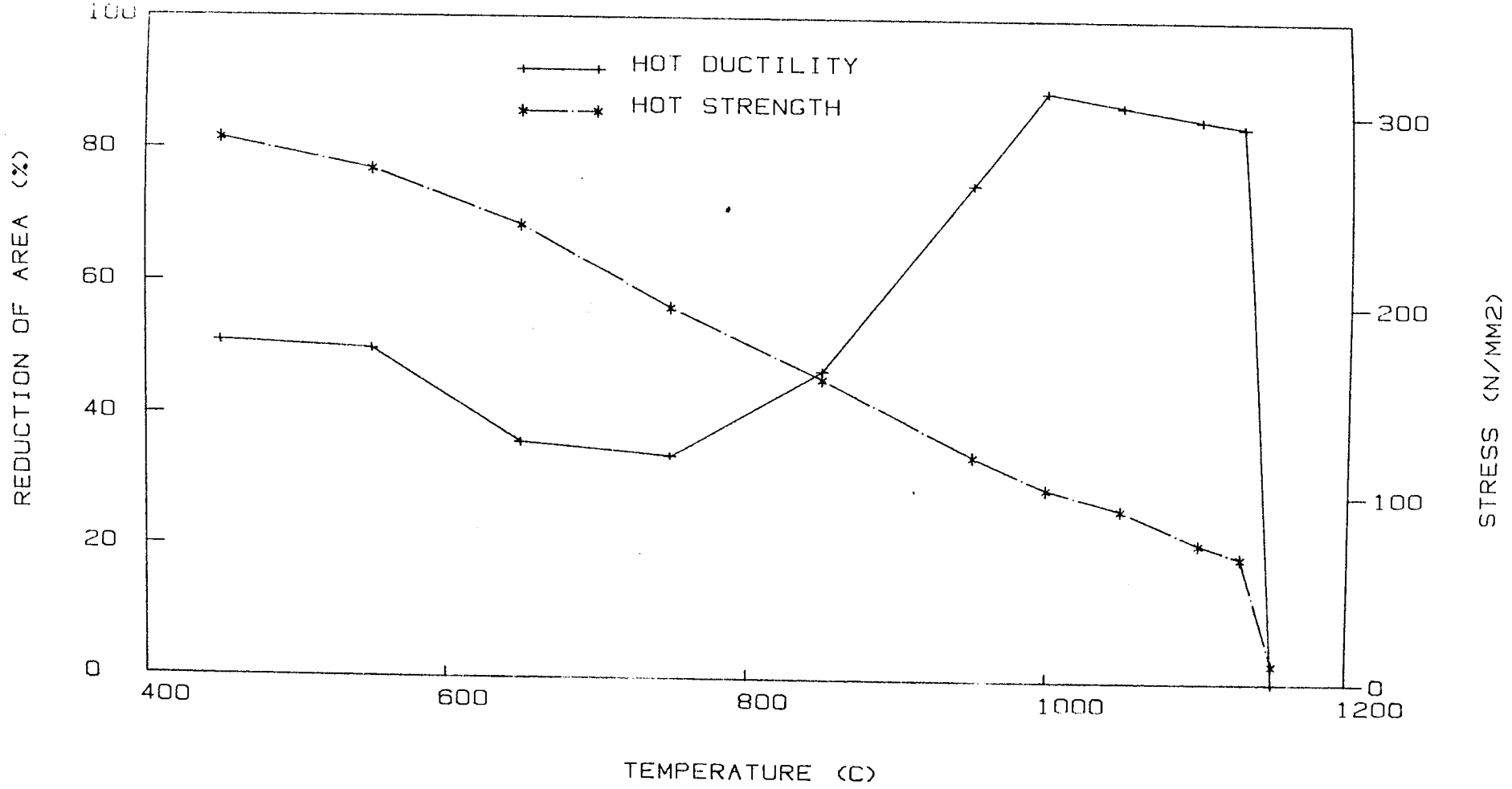

Fig 47. Plot of tensile properties against temperature for alloy H4 on cooling from 1160 C

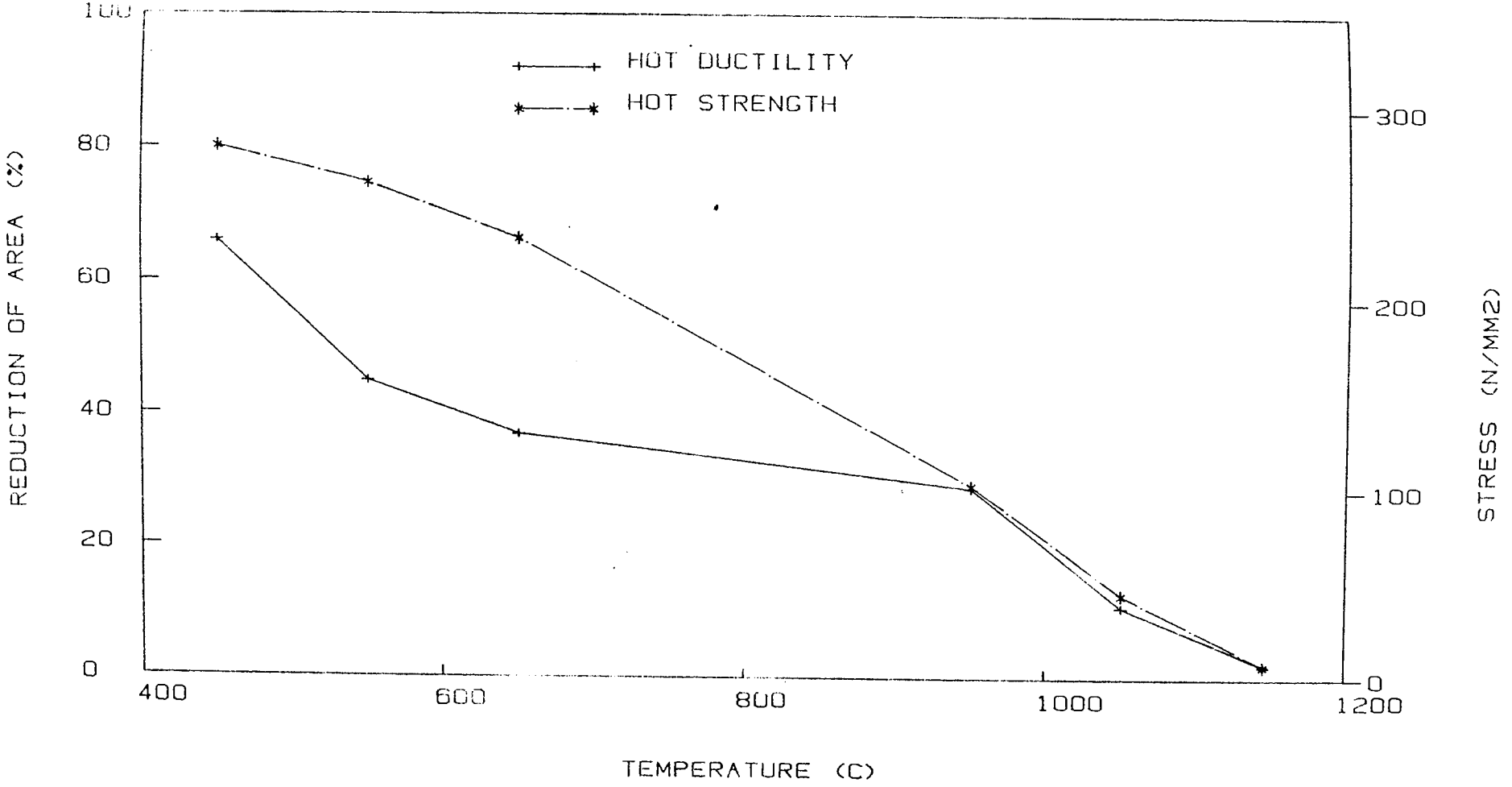

Fig 48. Plot of tensile properties against temperature for alloy H5 on cooling from 1160 C

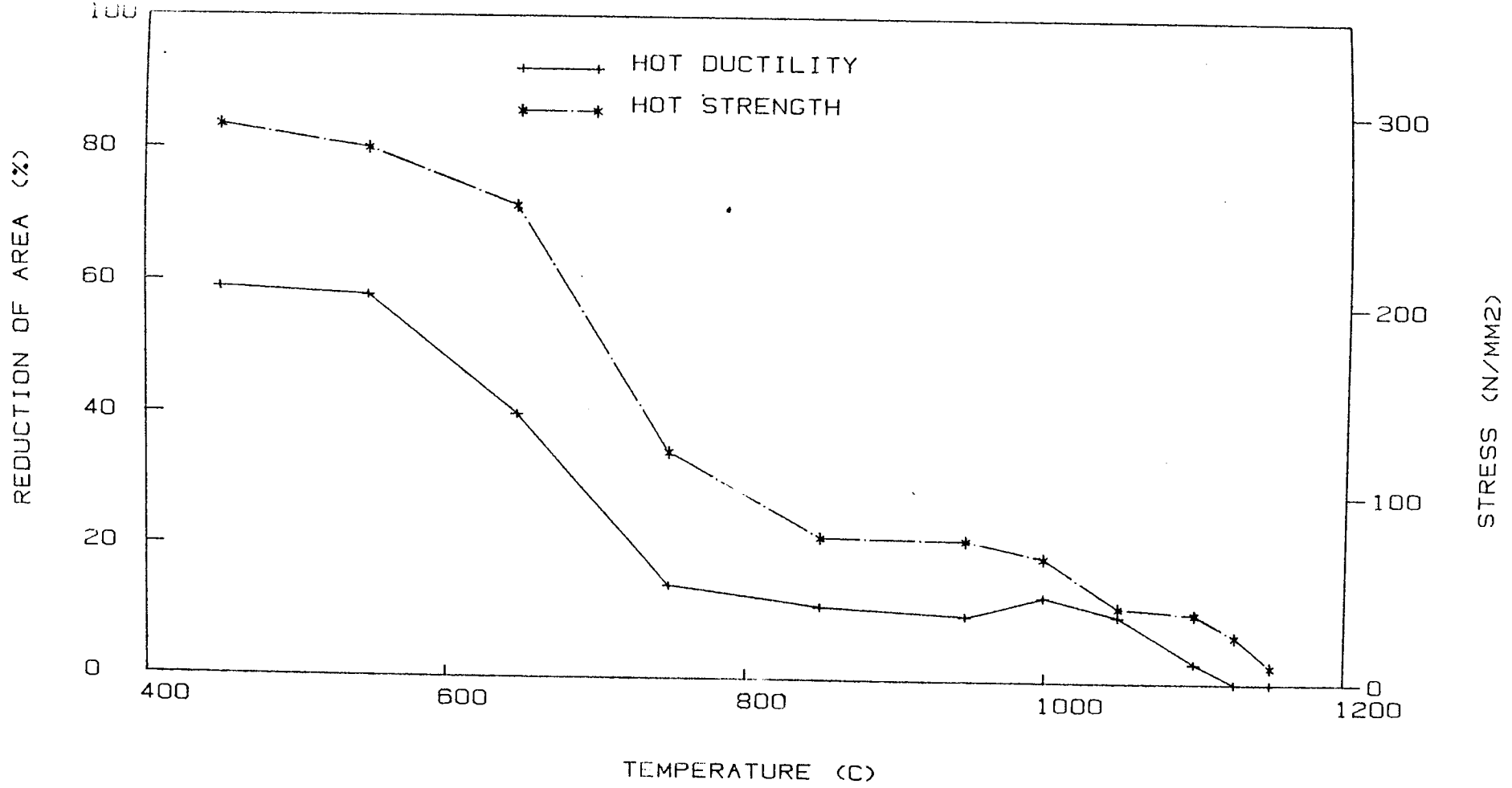

Fig 49. Plot of tensile properties against temperature for alloy H6 on cooling from 1160 C

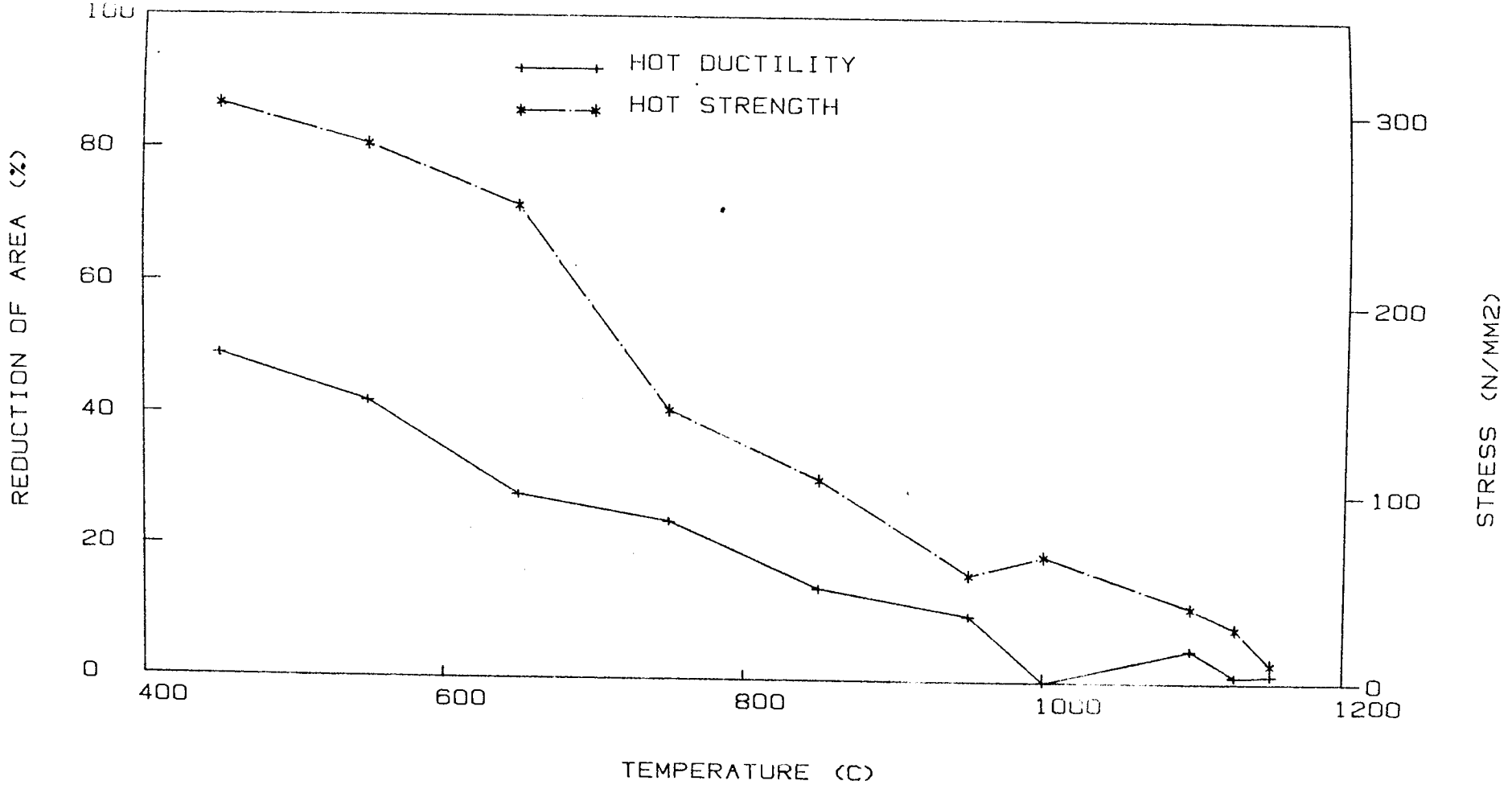

Fig 50. Plot of tensile properties against temperature for alloy H7 on cooling from 1160 C

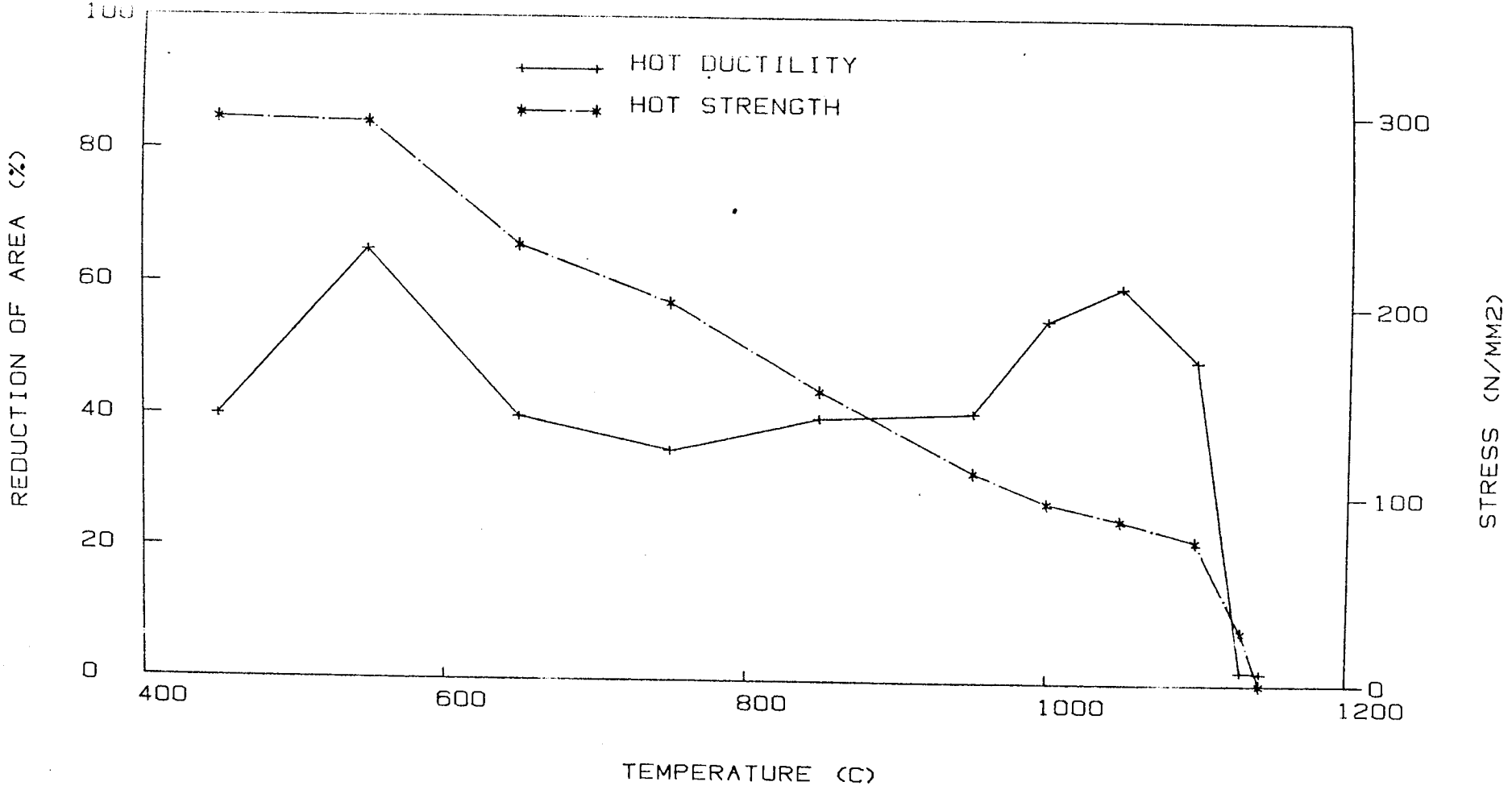

Fig 51. Plot of tensile properties against temperature for alloy H8 on cooling from 1160 C

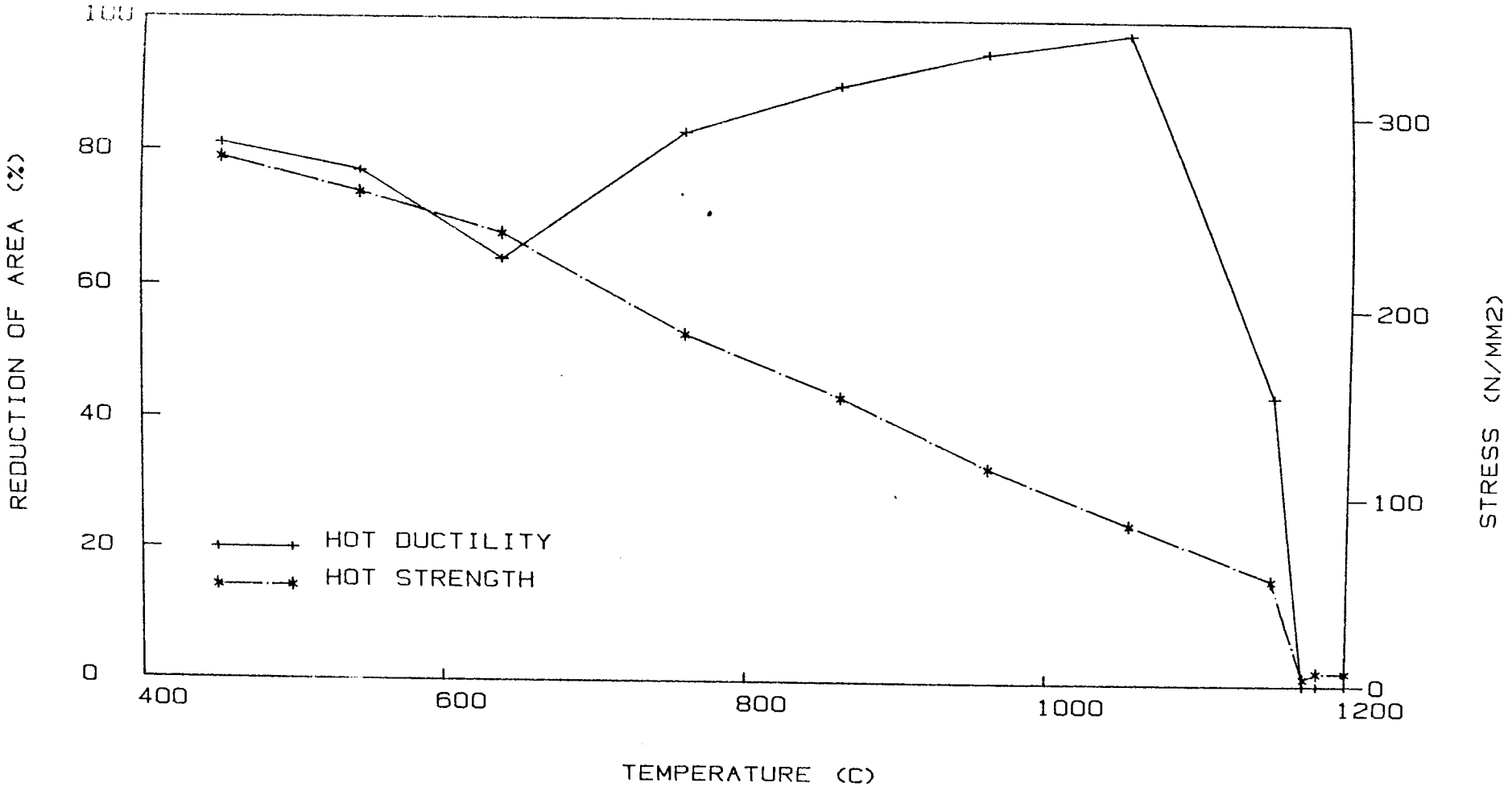

Fig 52. Plot of tensile properties against temperature for alloy H1 on heating

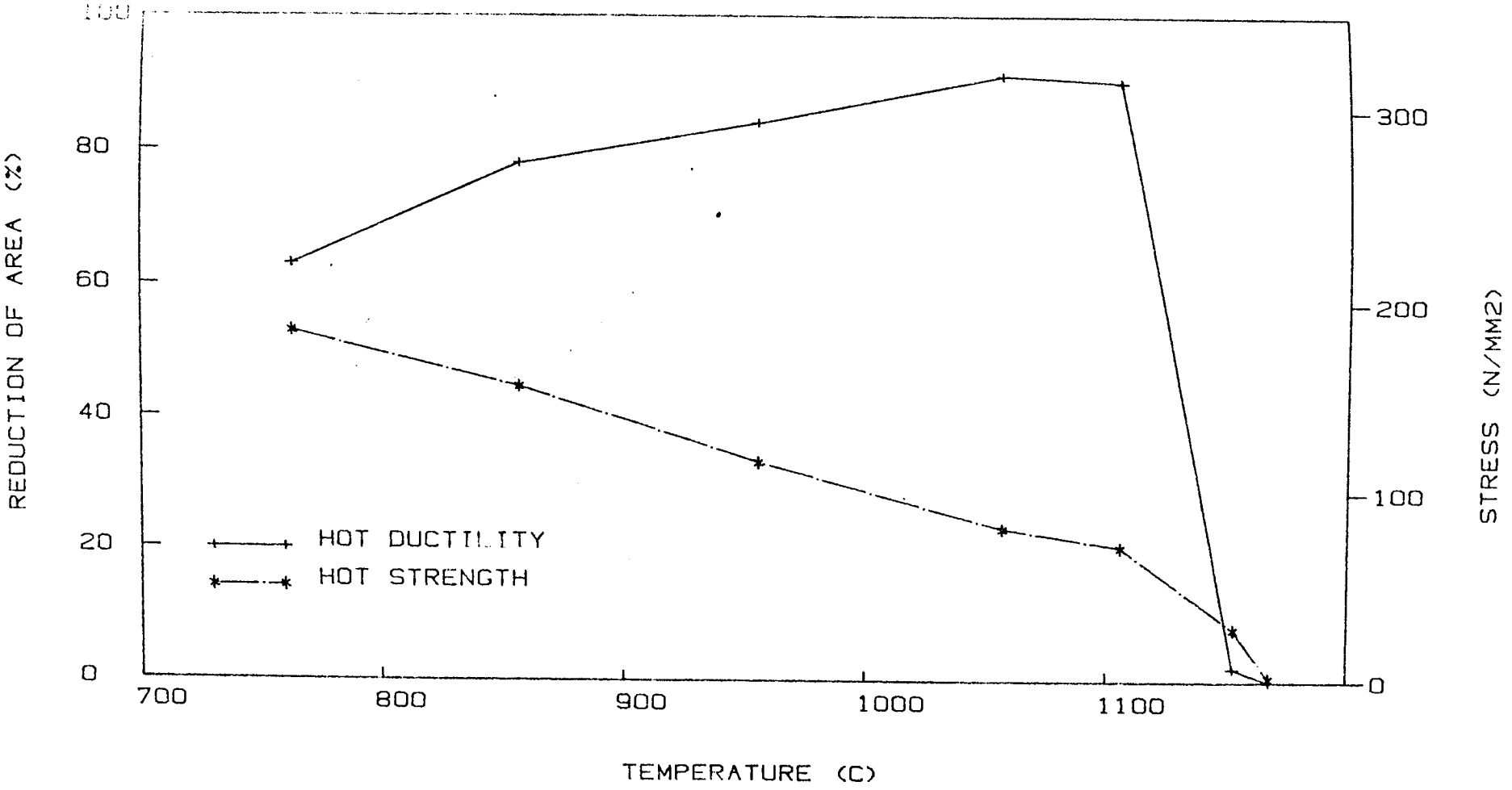

Fig 53. Plot of tensile properties against temperature for alloy H3 on heating

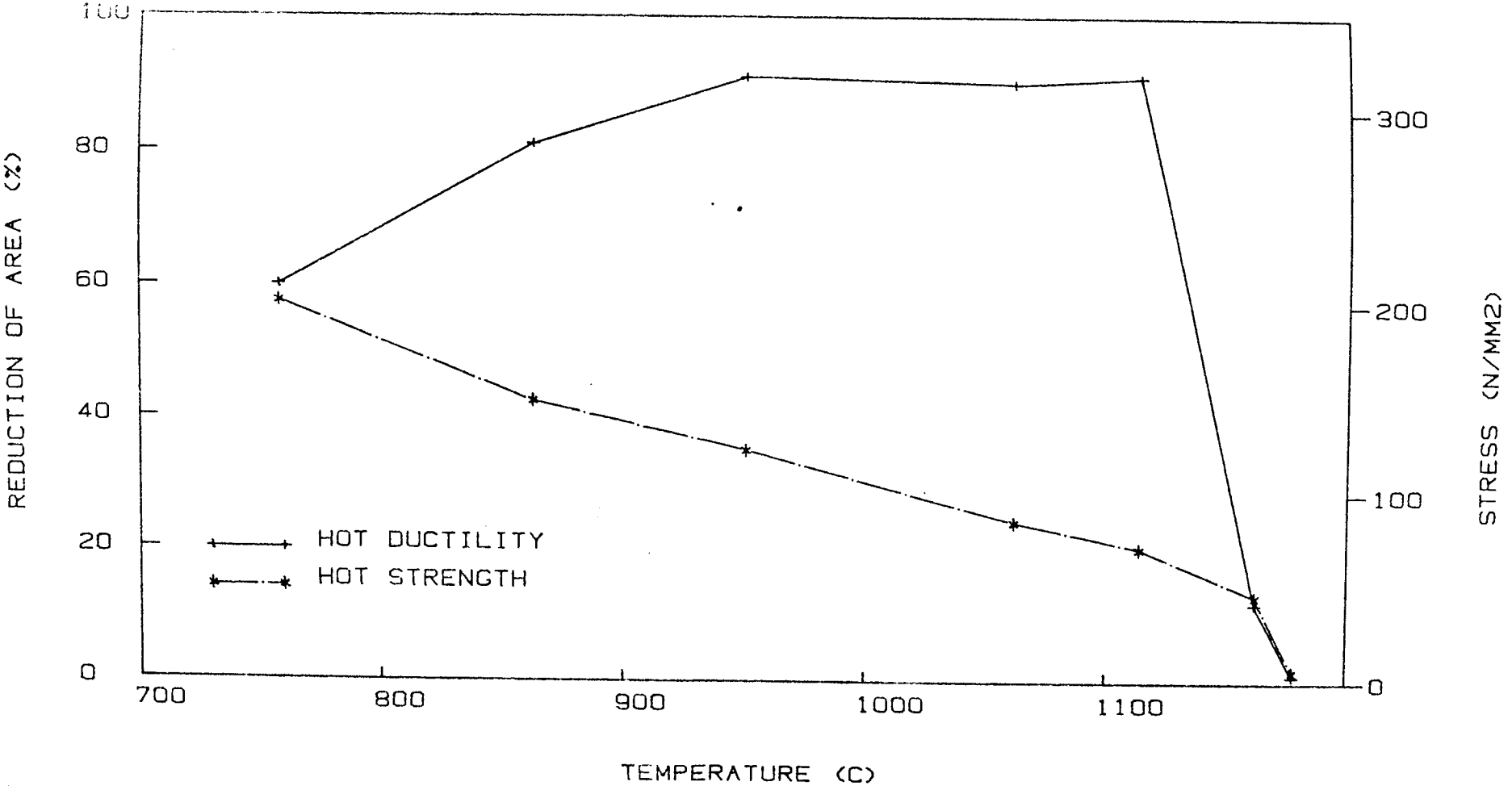

Fig 54. Plot of tensile properties against temperature for alloy H4 on heating

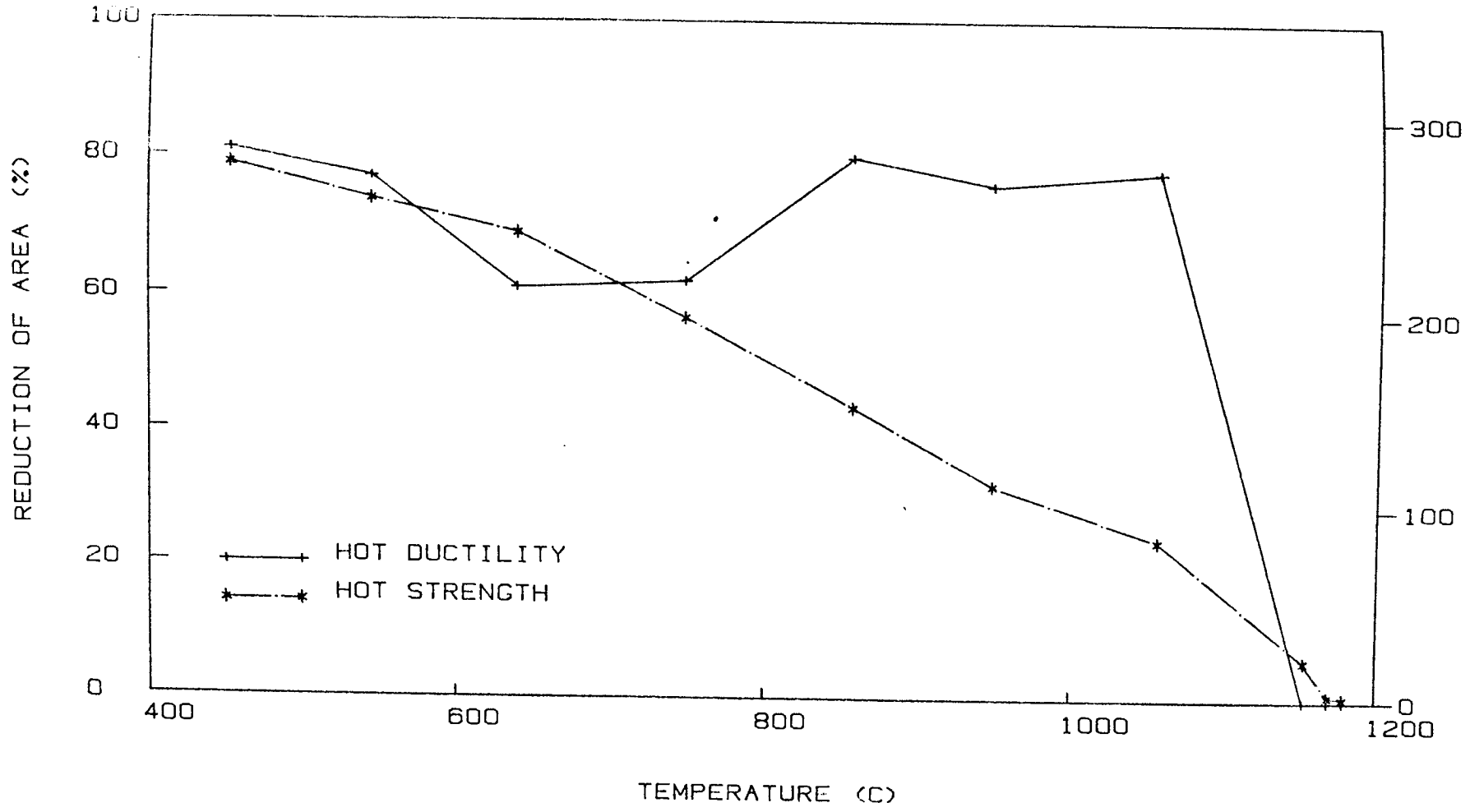

Fig 55. Plot of tensile properties against temperature for alloy H5 on heating

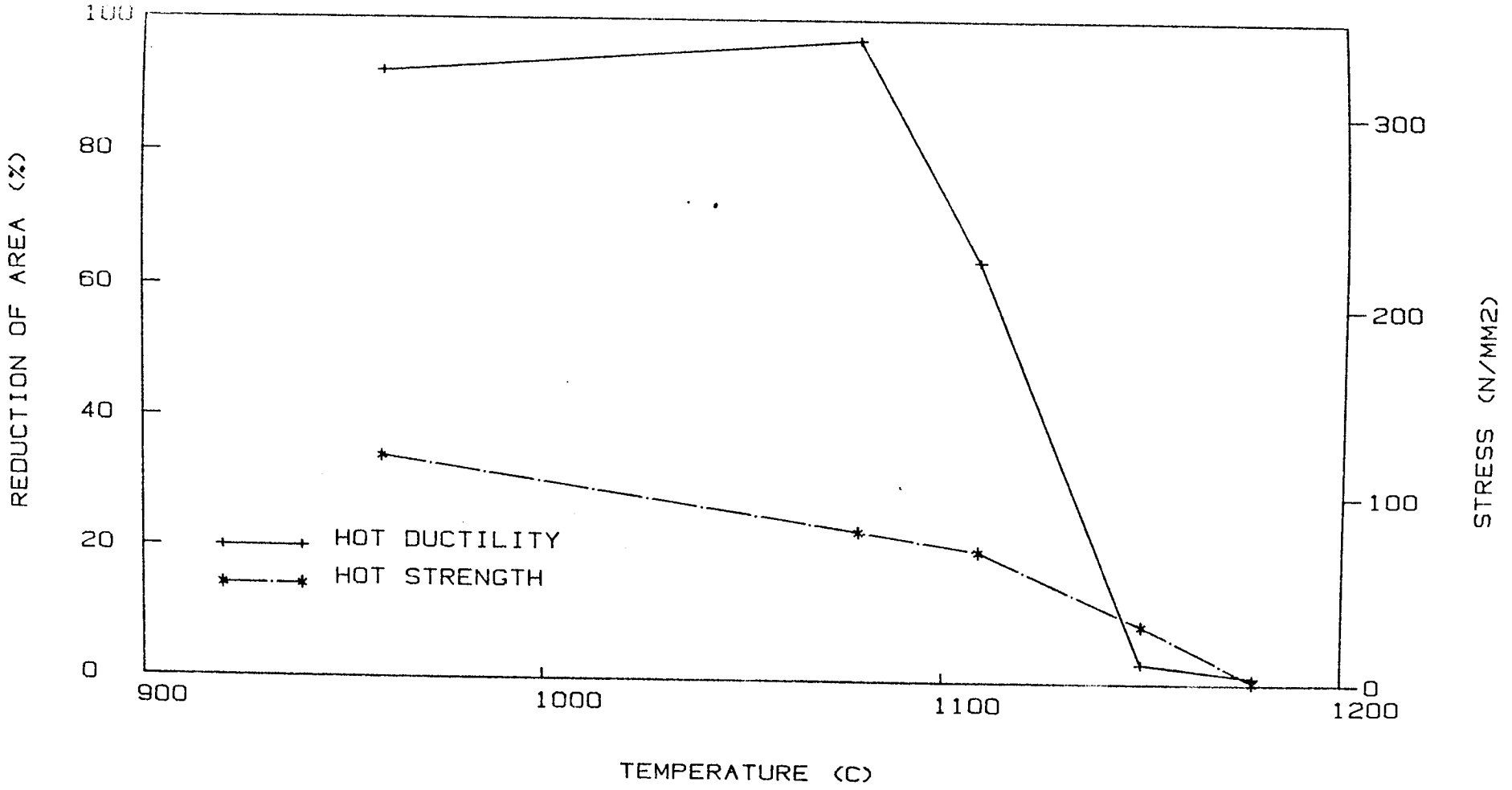

Fig 56. Plot of tensile properties against temperature for alloy H6 on heating

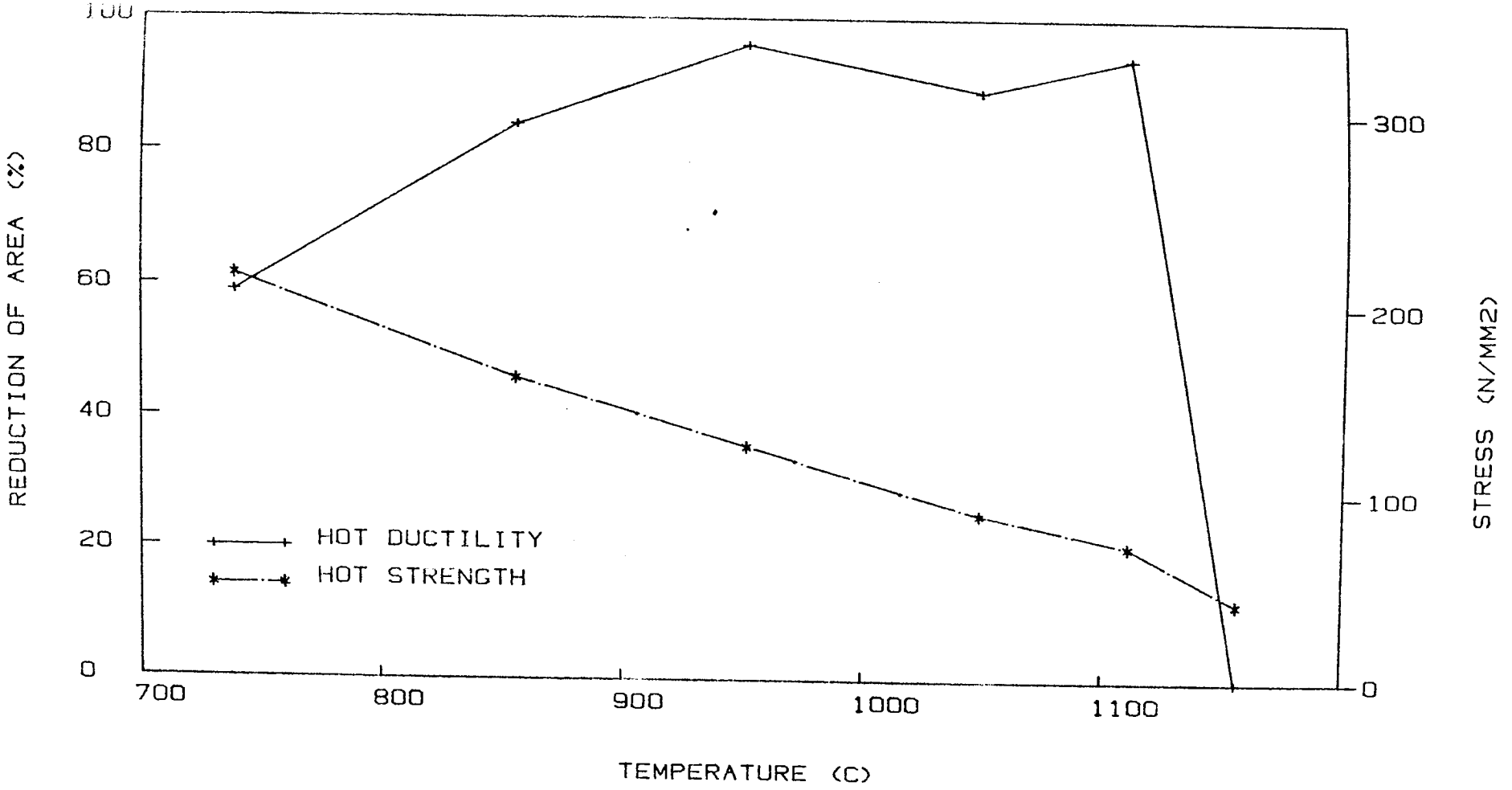

Fig 57. Plot of tensile properties against temperature for alloy H7 on heating

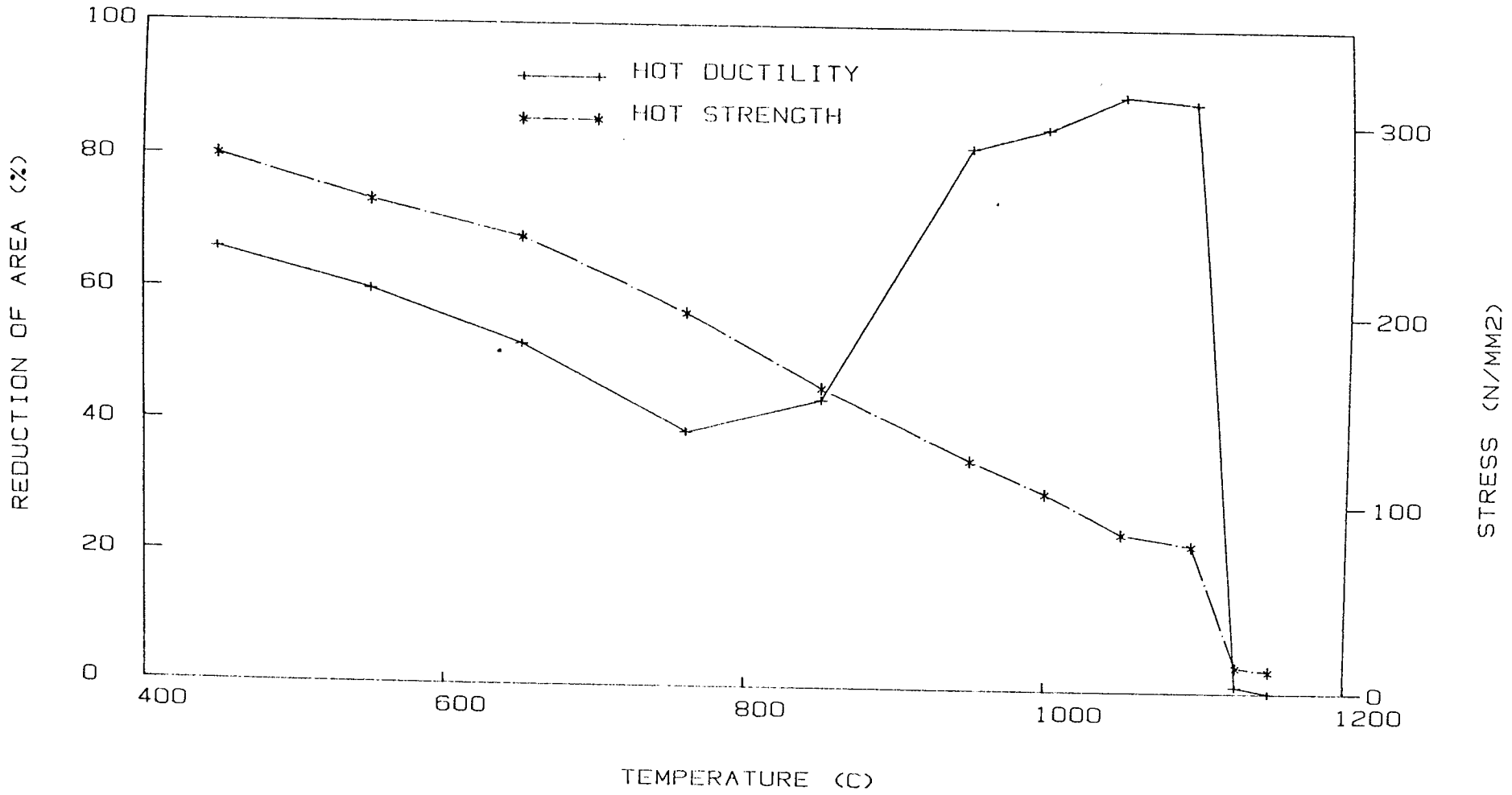

Fig 53. Plot of tensile properties against temperature for alloy S1 on cooling from 1160 C

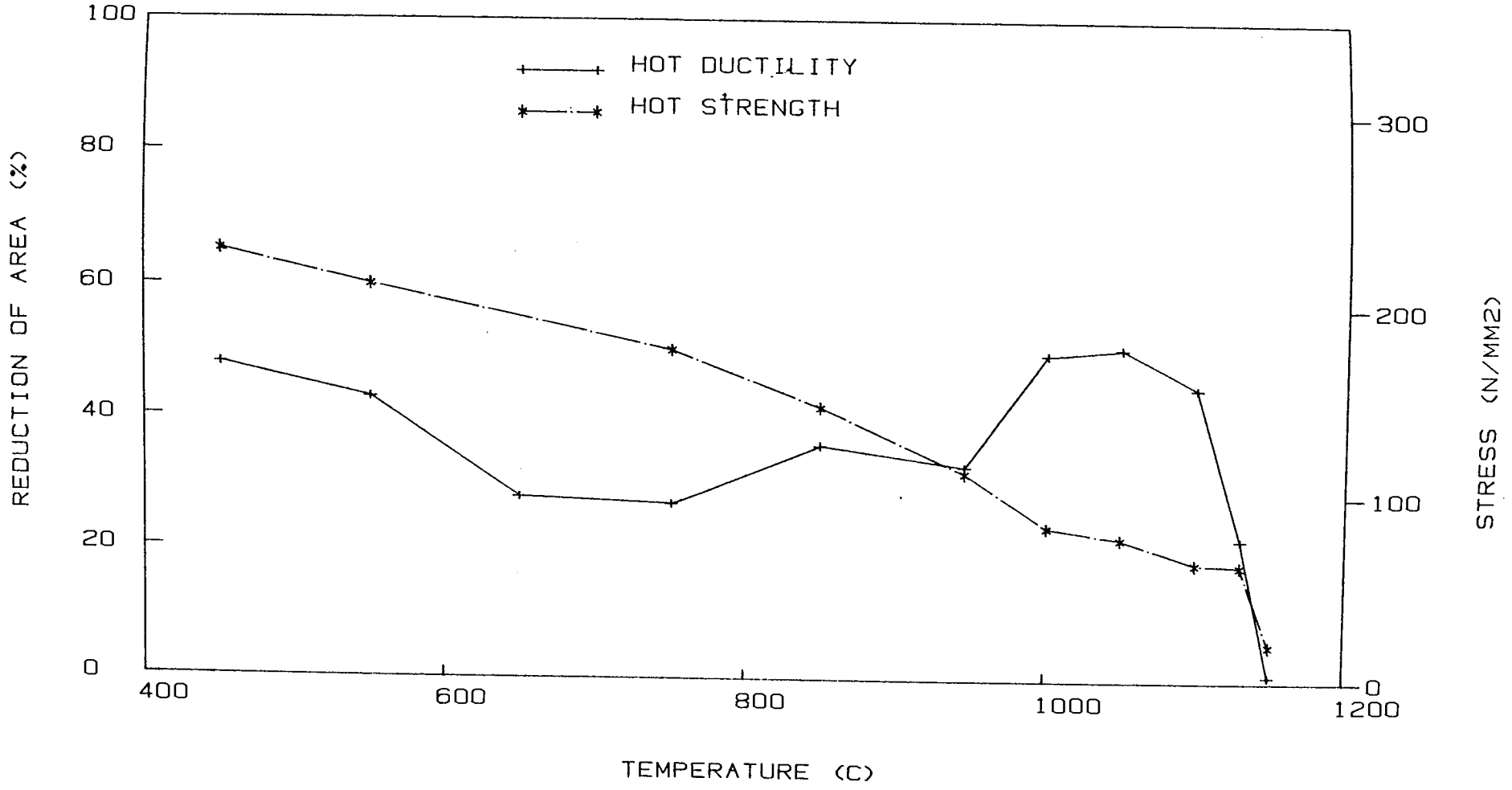

Fig 59. Plot of tensile properties against temperature for alloy S2 on cooling from 1160 C

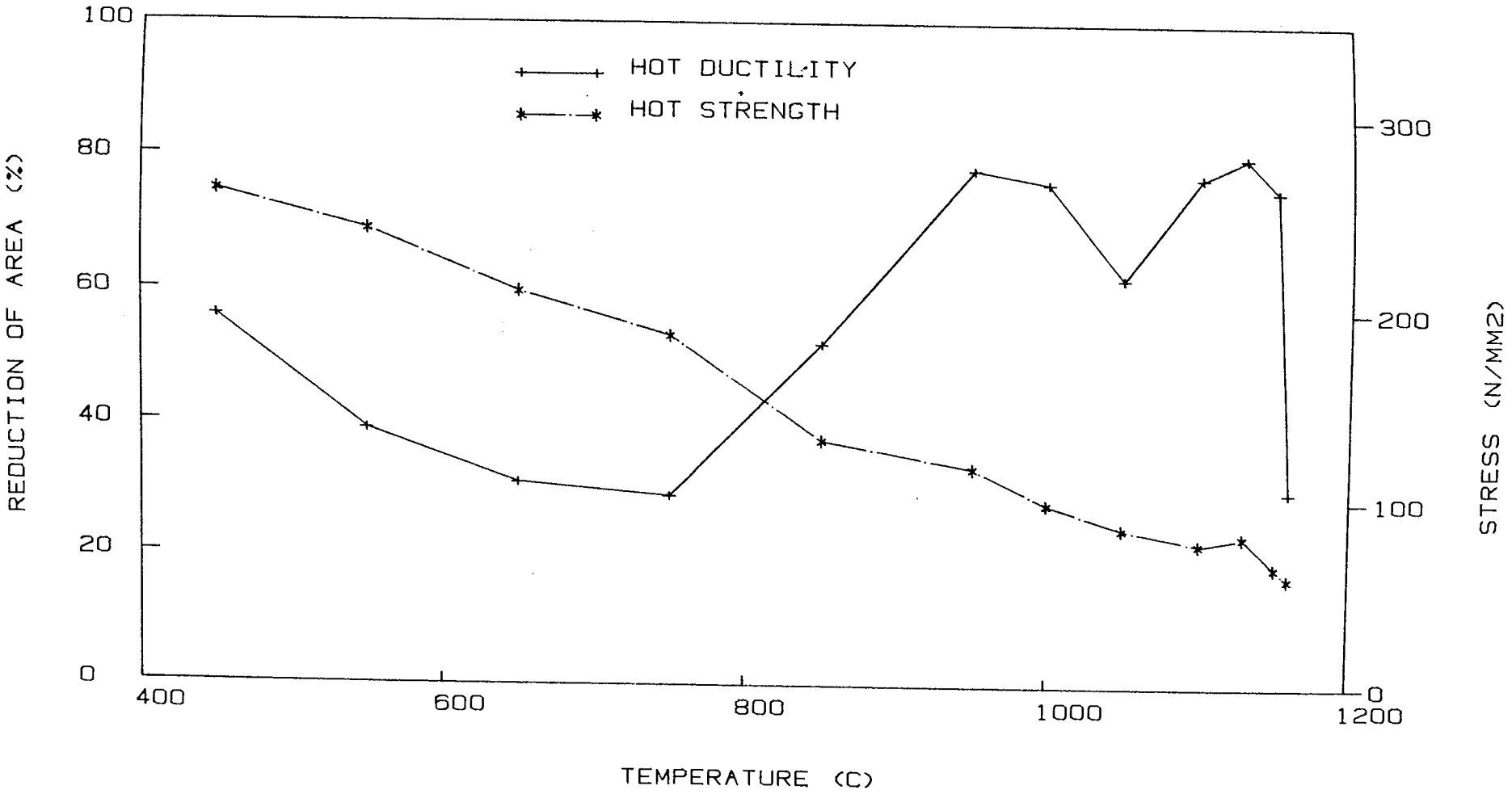

Fig 60. Plot of tensile properties against temperature for alloy S3 on cooling from 1160 C

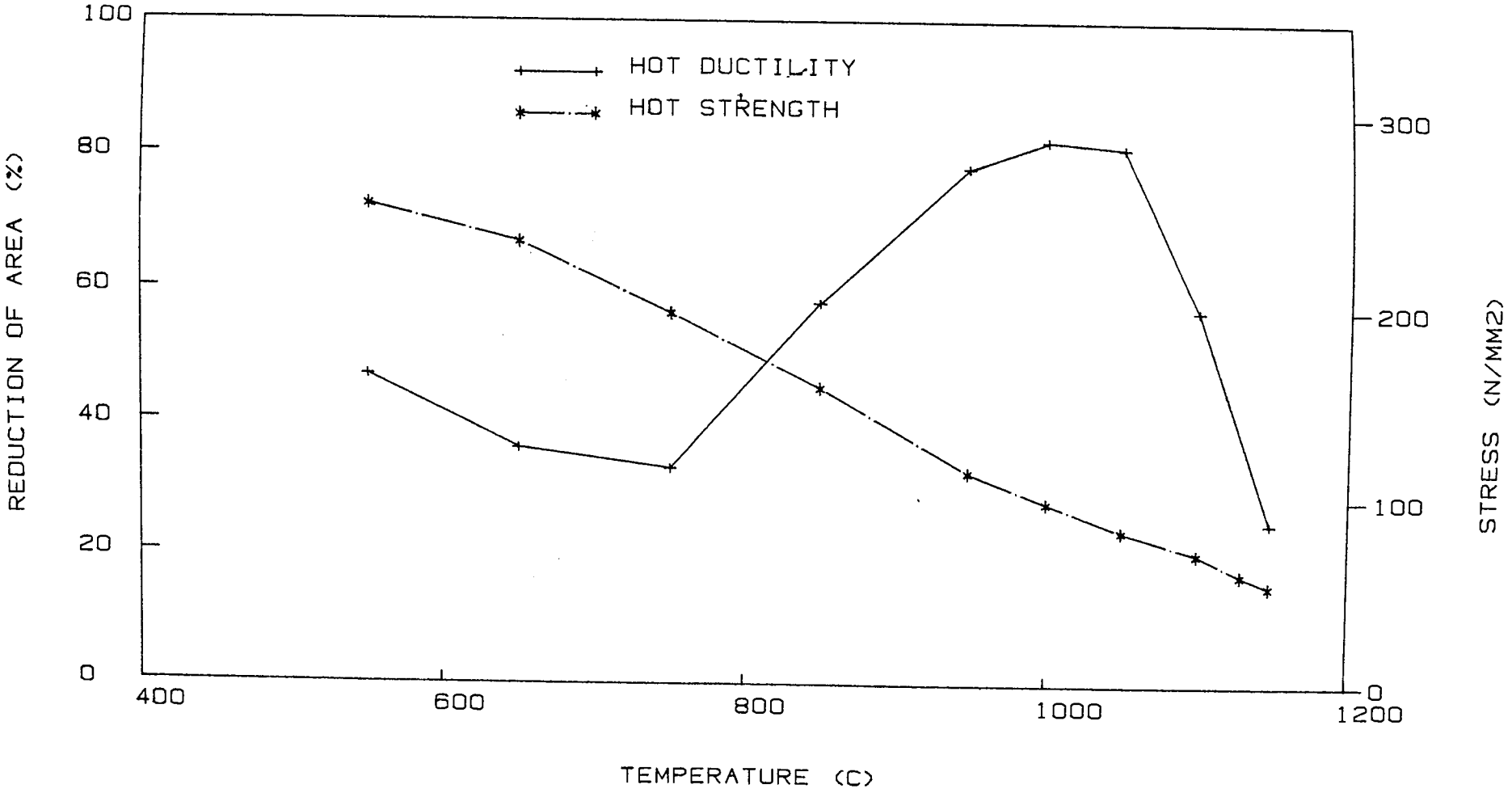

Fig 61. Plot of tensile properties against temperature for alloy S4 on cooling from 1160 C

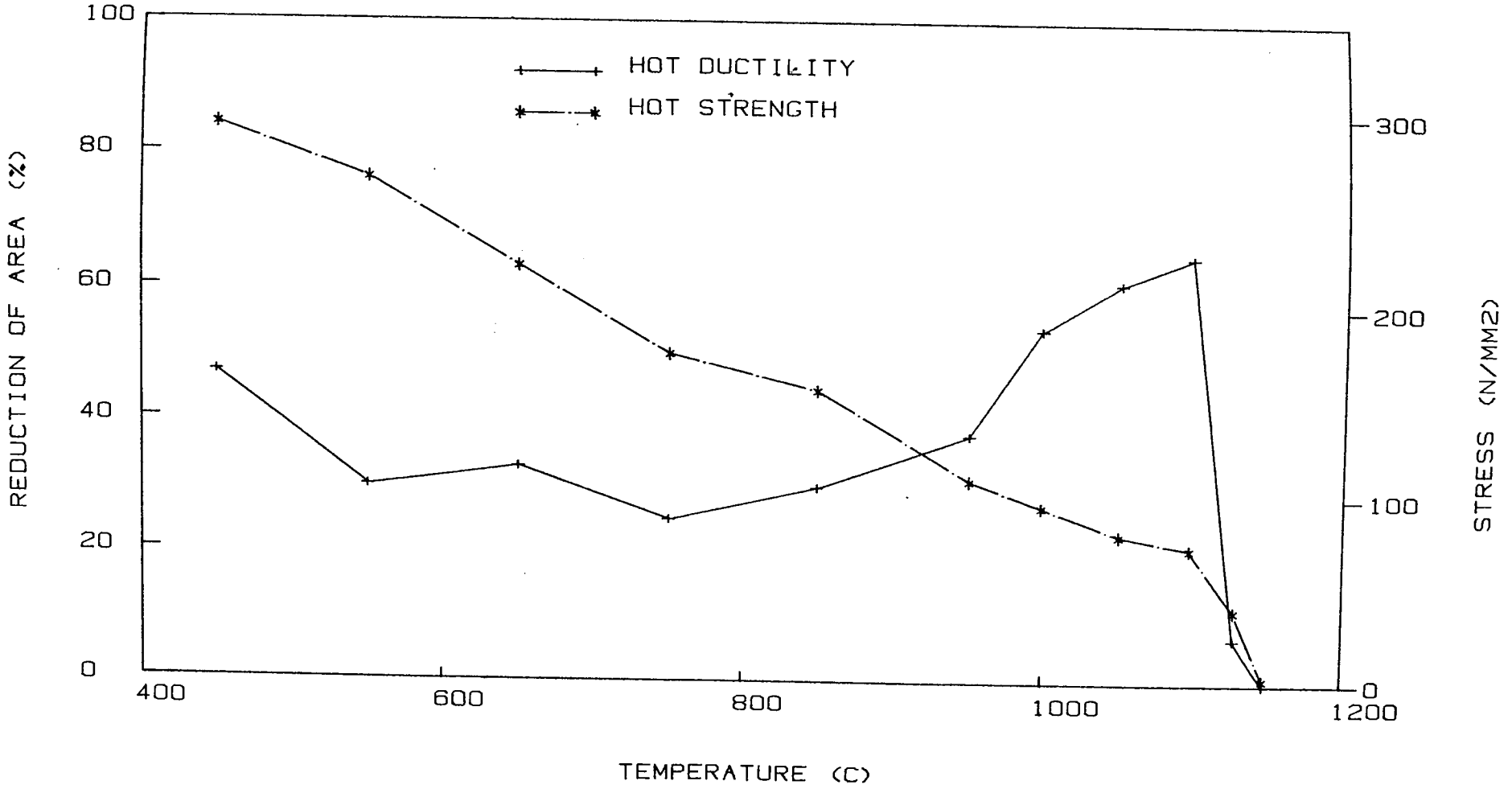

Fig 62. Plot of tensile properties against temperature for alloy S5 on cooling from 1160 C

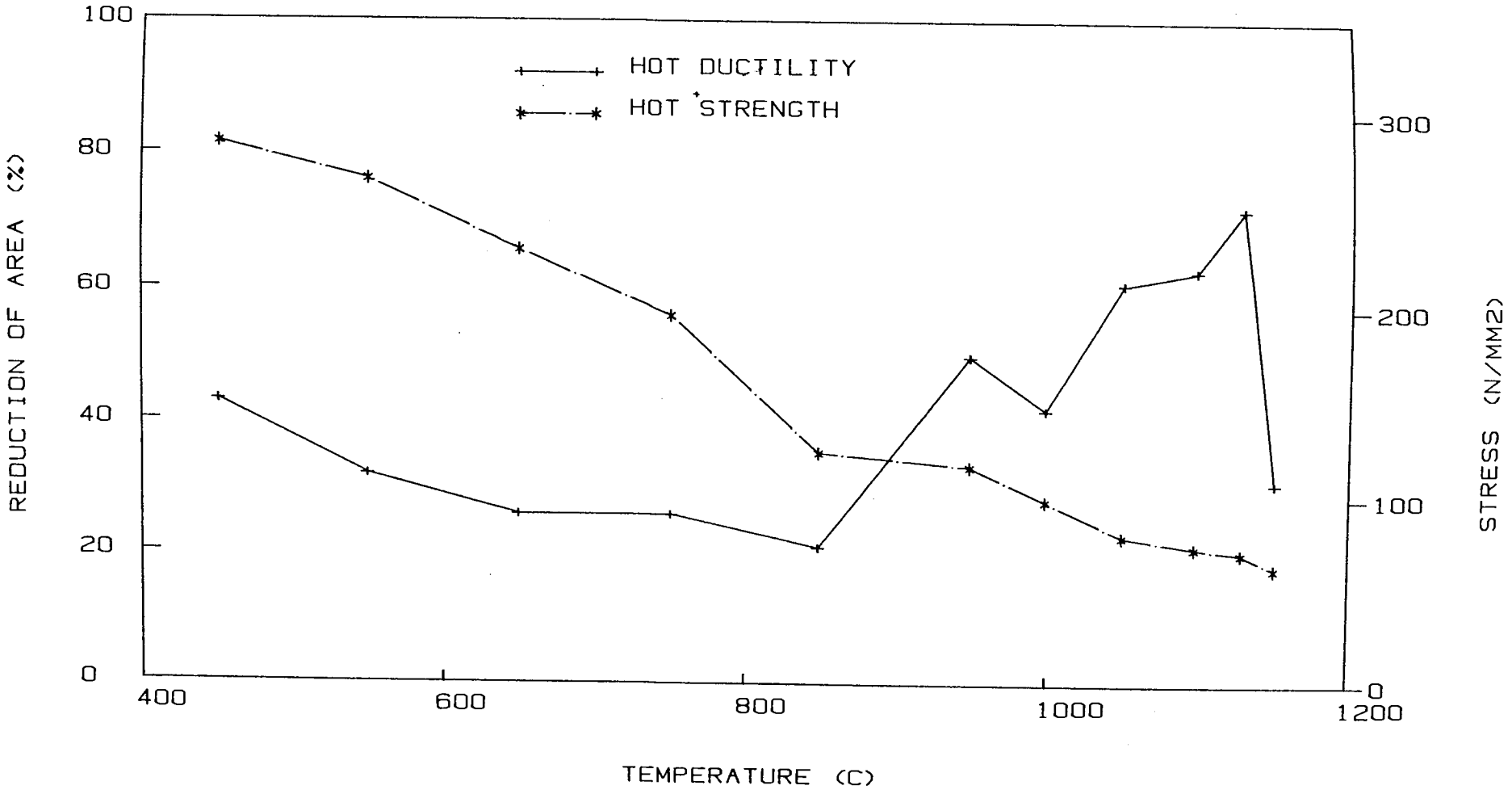

Fig 63. Plot of tensile properties against temperature for alloy S6 on cooling from 1160 C

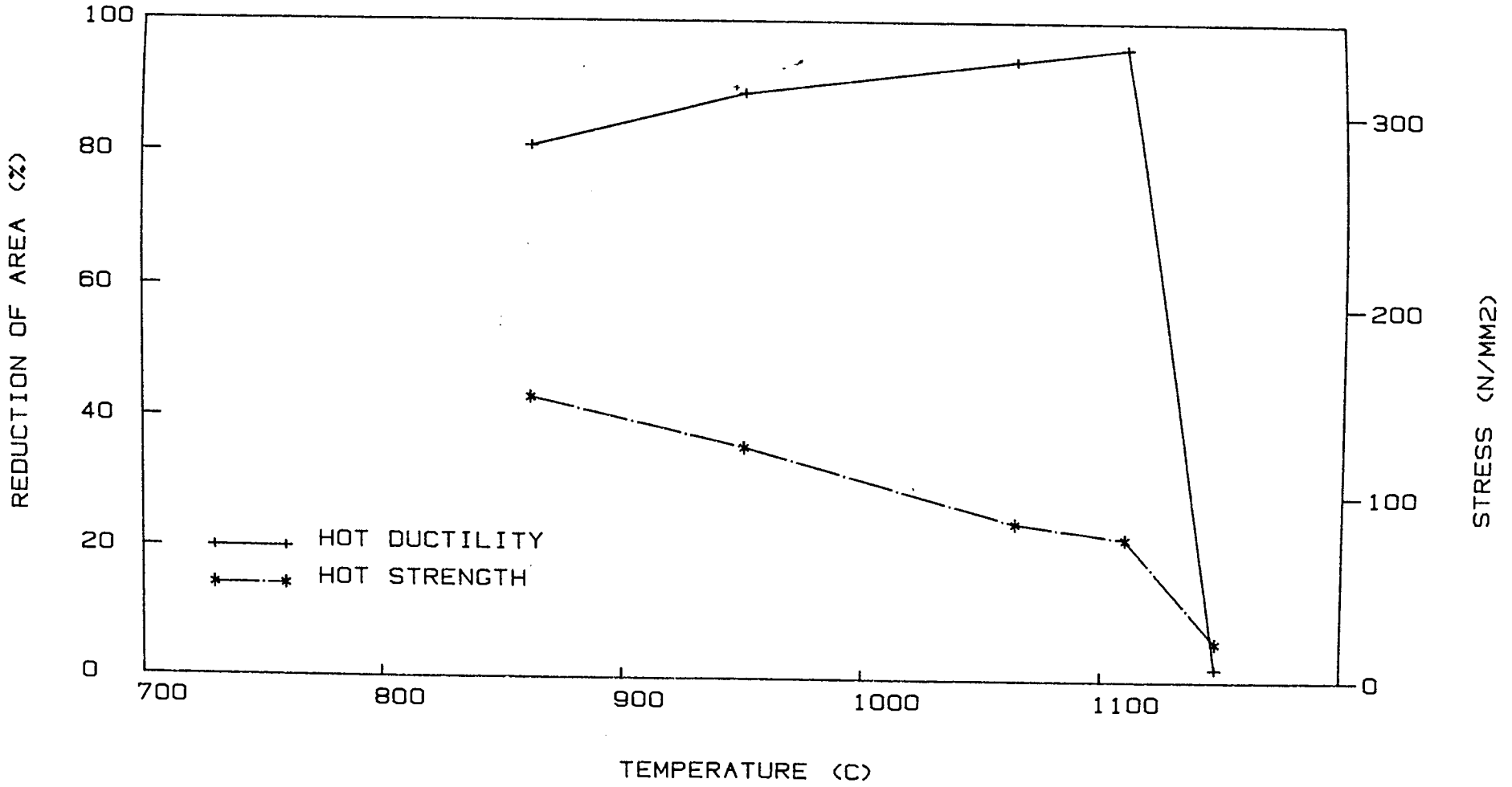

Fig 64. Plot of tensile properties against temperature for alloy S1 on heating

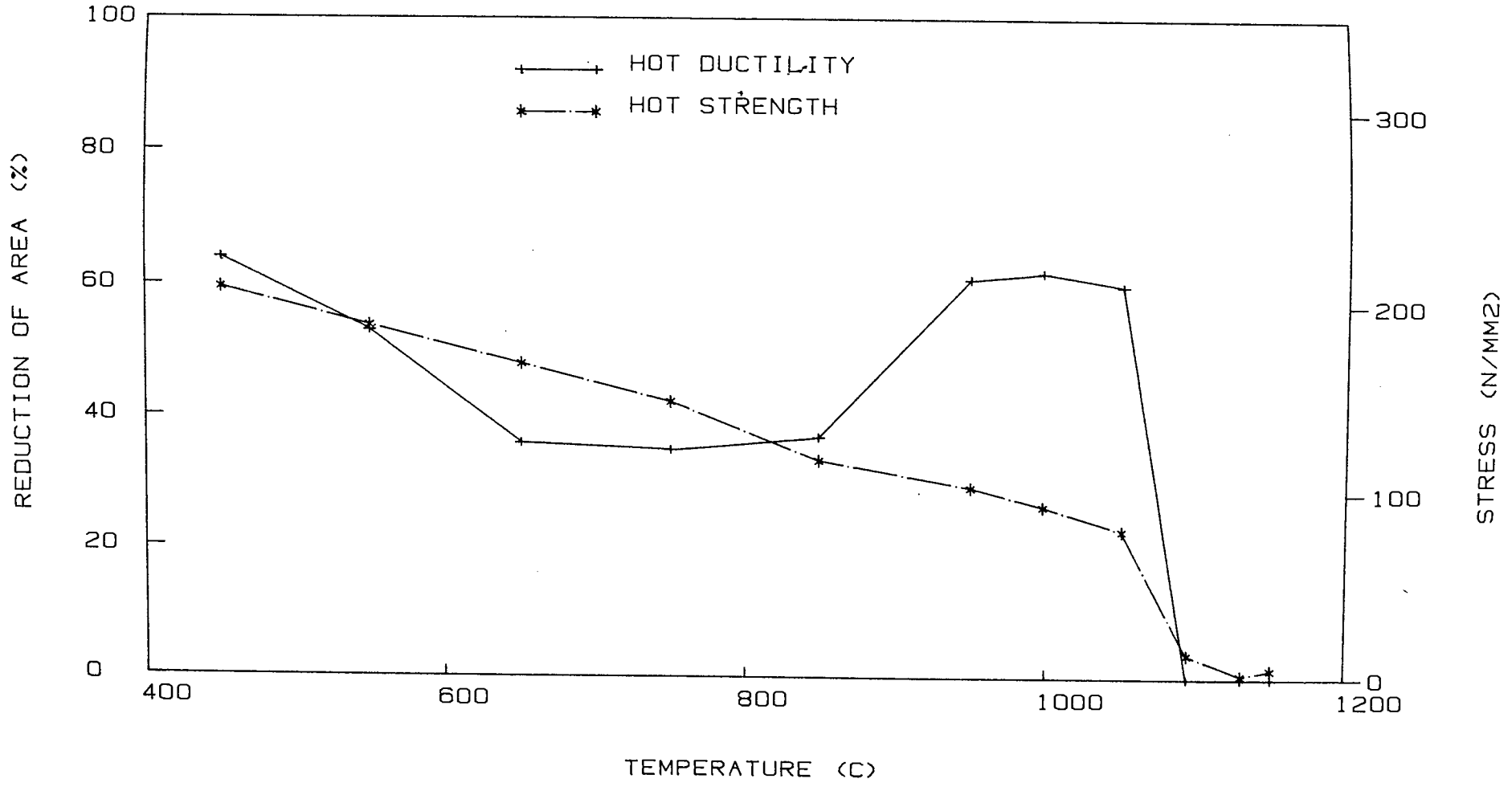

Fig 65. Plot of tensile properties against temperature for alloy R1 on cooling from 1160 C

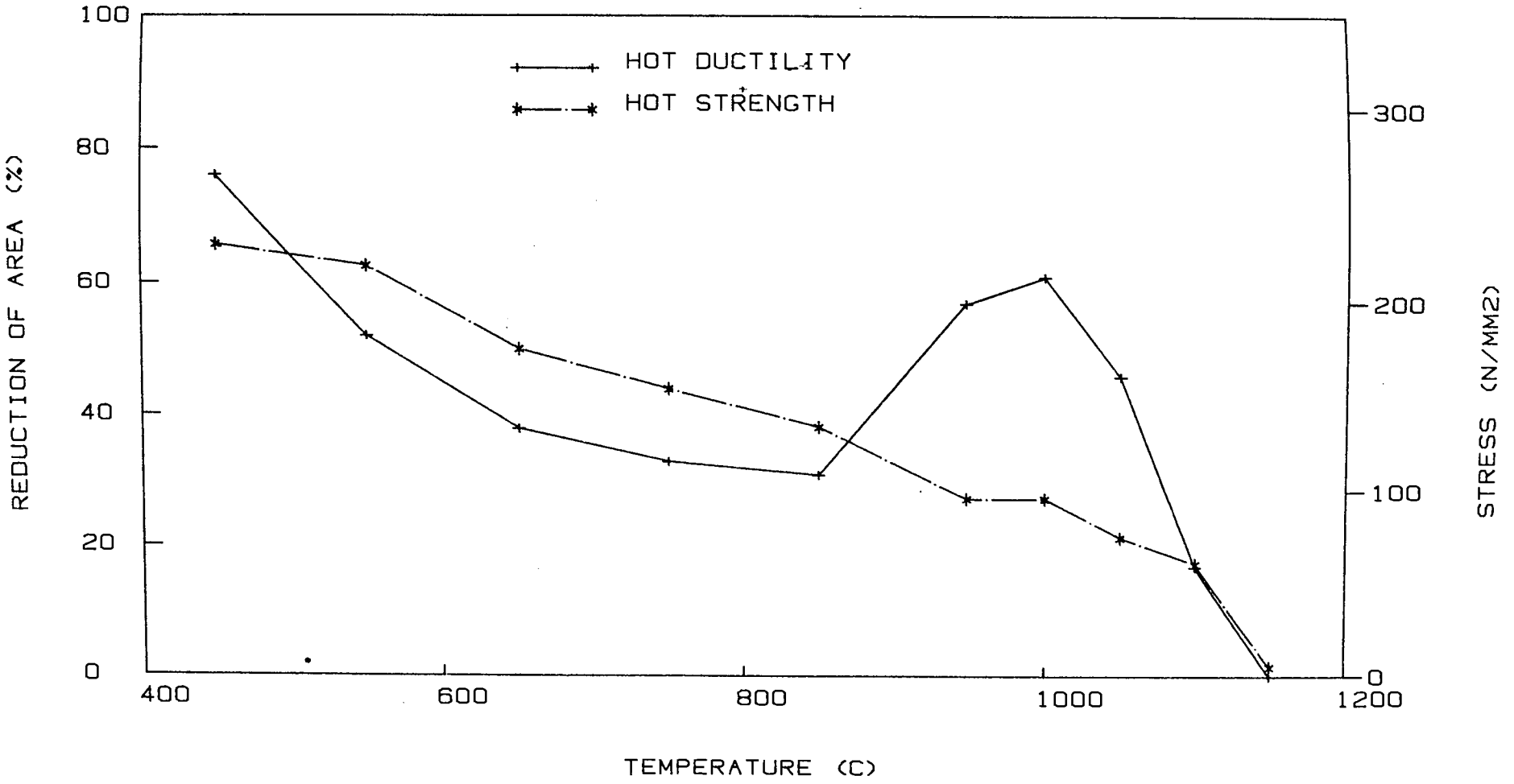

Fig 66. Plot of tensile properties against temperature for alloy R2 on cooling from 1160 C

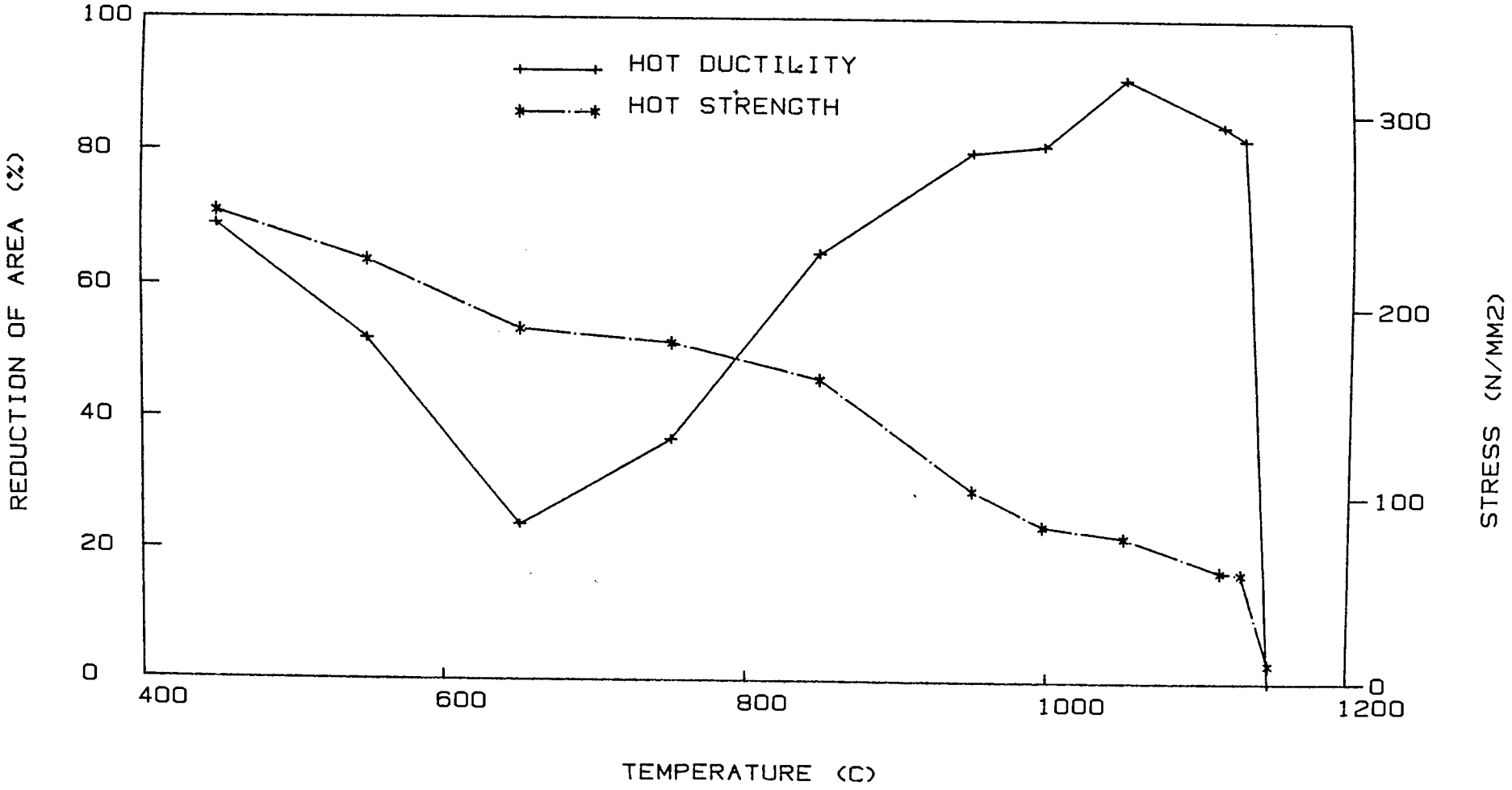

Fig 67. Plot of tensile properties against temperature for alloy R3 on cooling from 1160 C

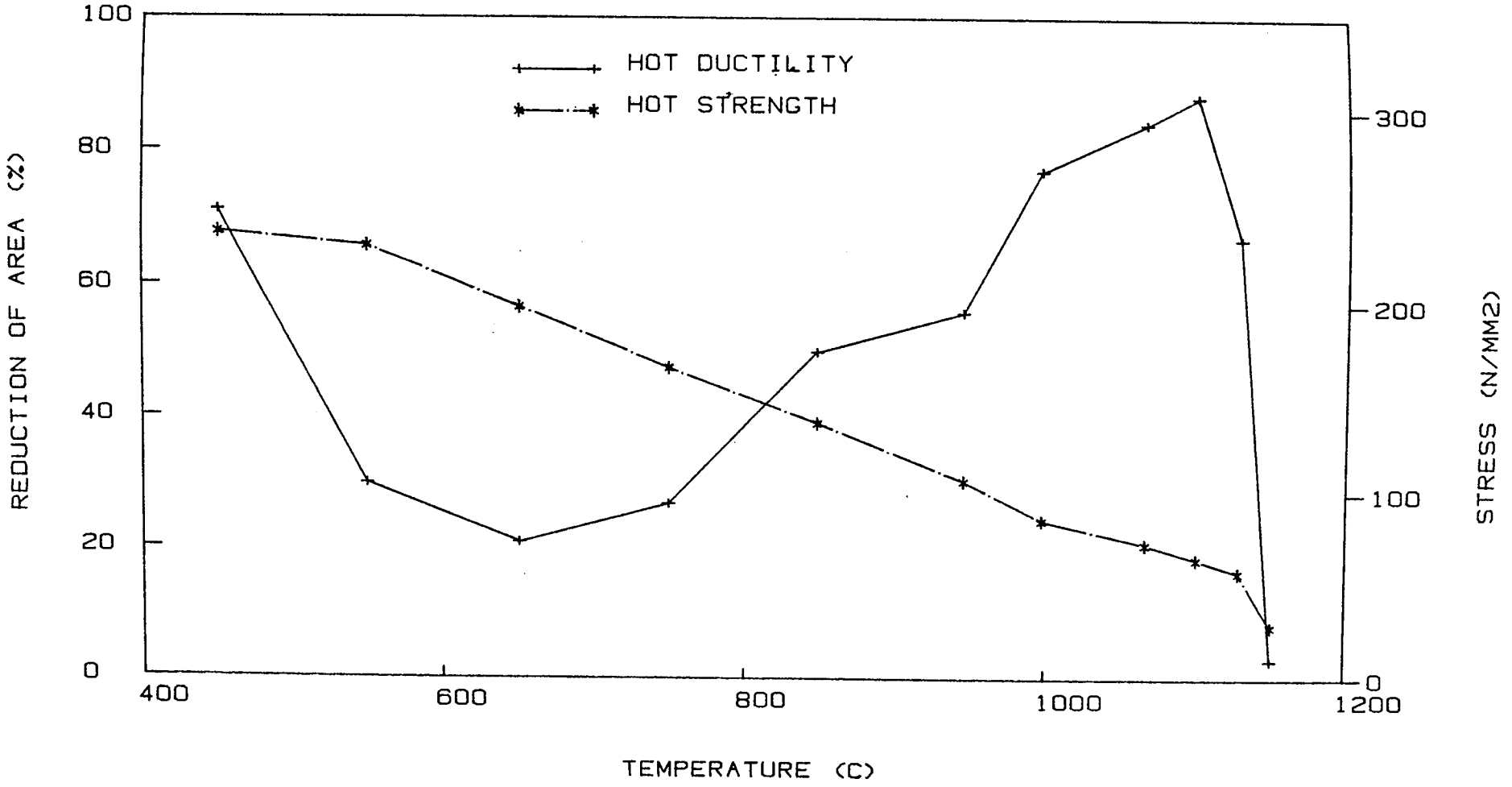

Fig 68. Plot of tensile properties against temperature for alloy R4 on cooling from 1160 C

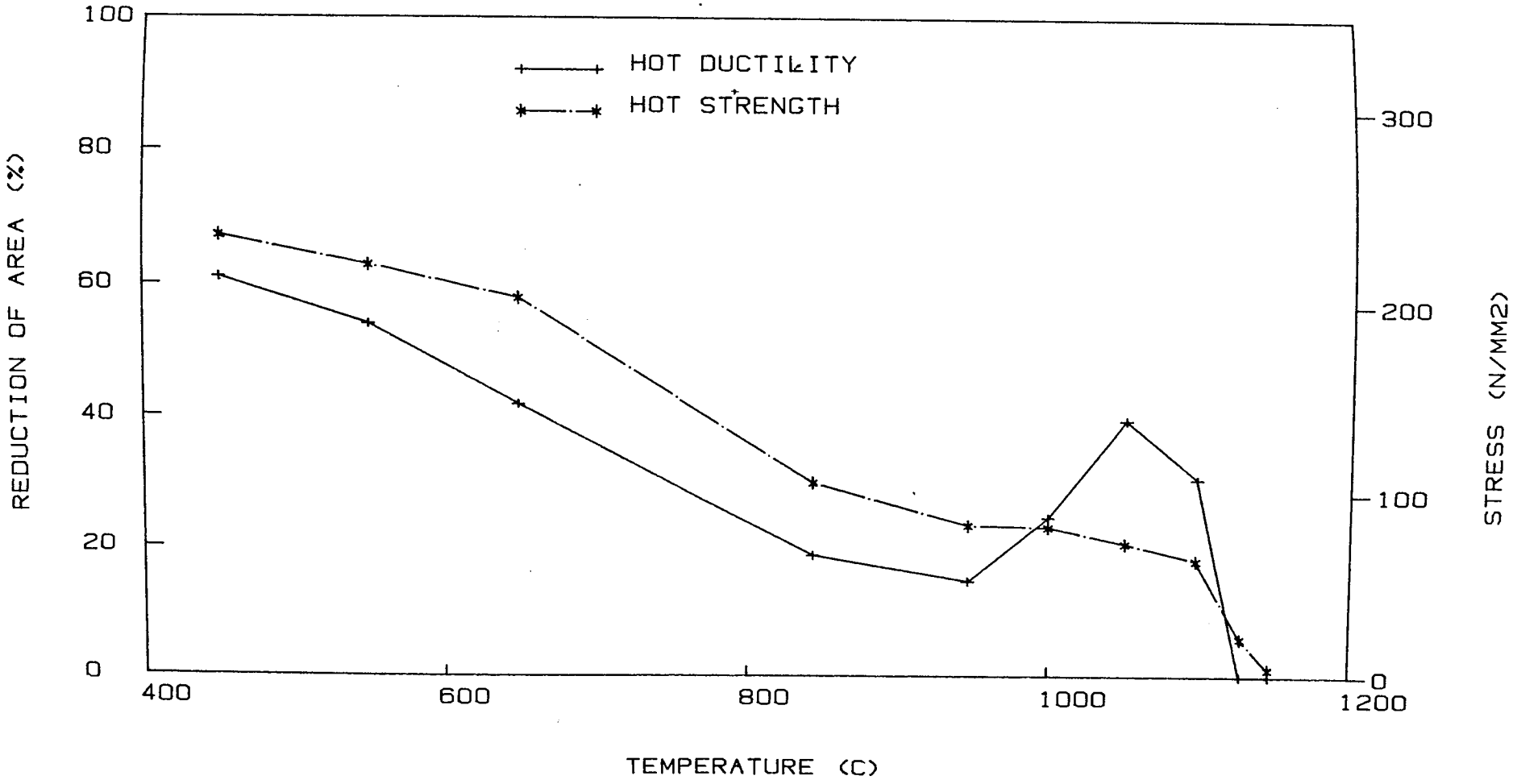

Fig 69. Plot of tensile properties against temperature for alloy R5 on cooling from 1160 C

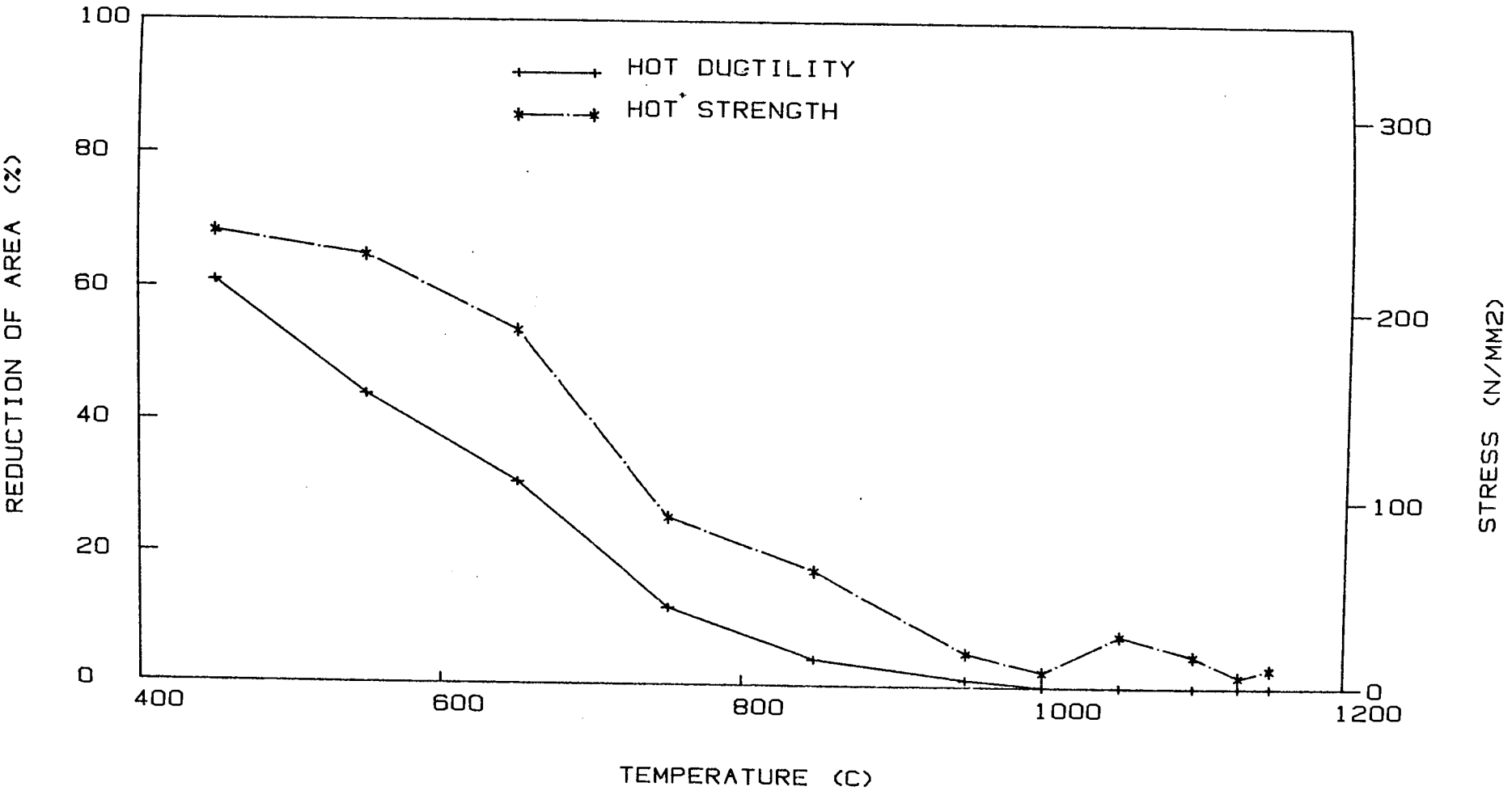

Fig 70. Plot of tensile properties against temperature for alloy R6 on cooling from 1160 C

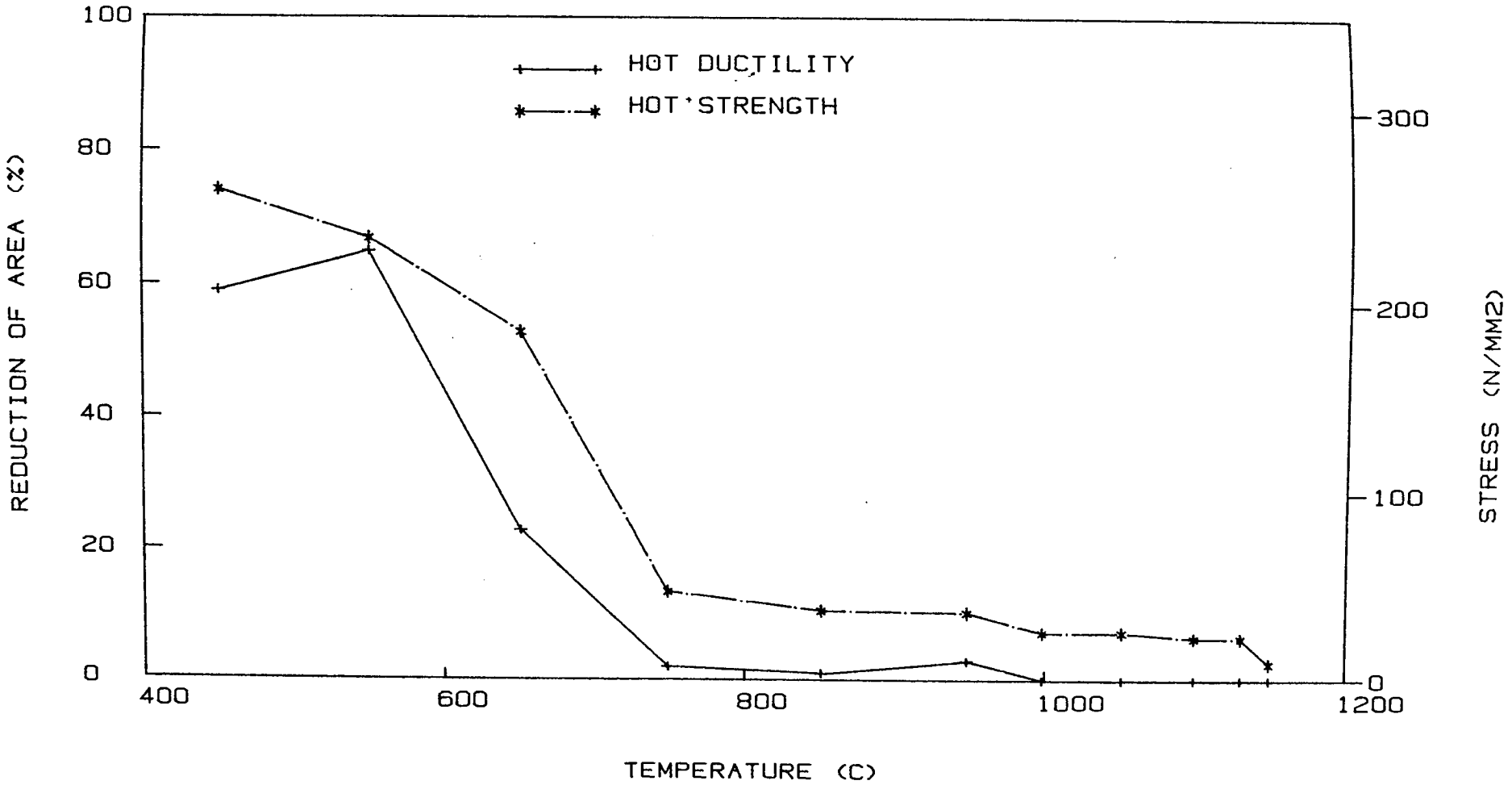

Fig 71. Plot of tensile properties against temperature for alloy R7 on cooling from 1160 C

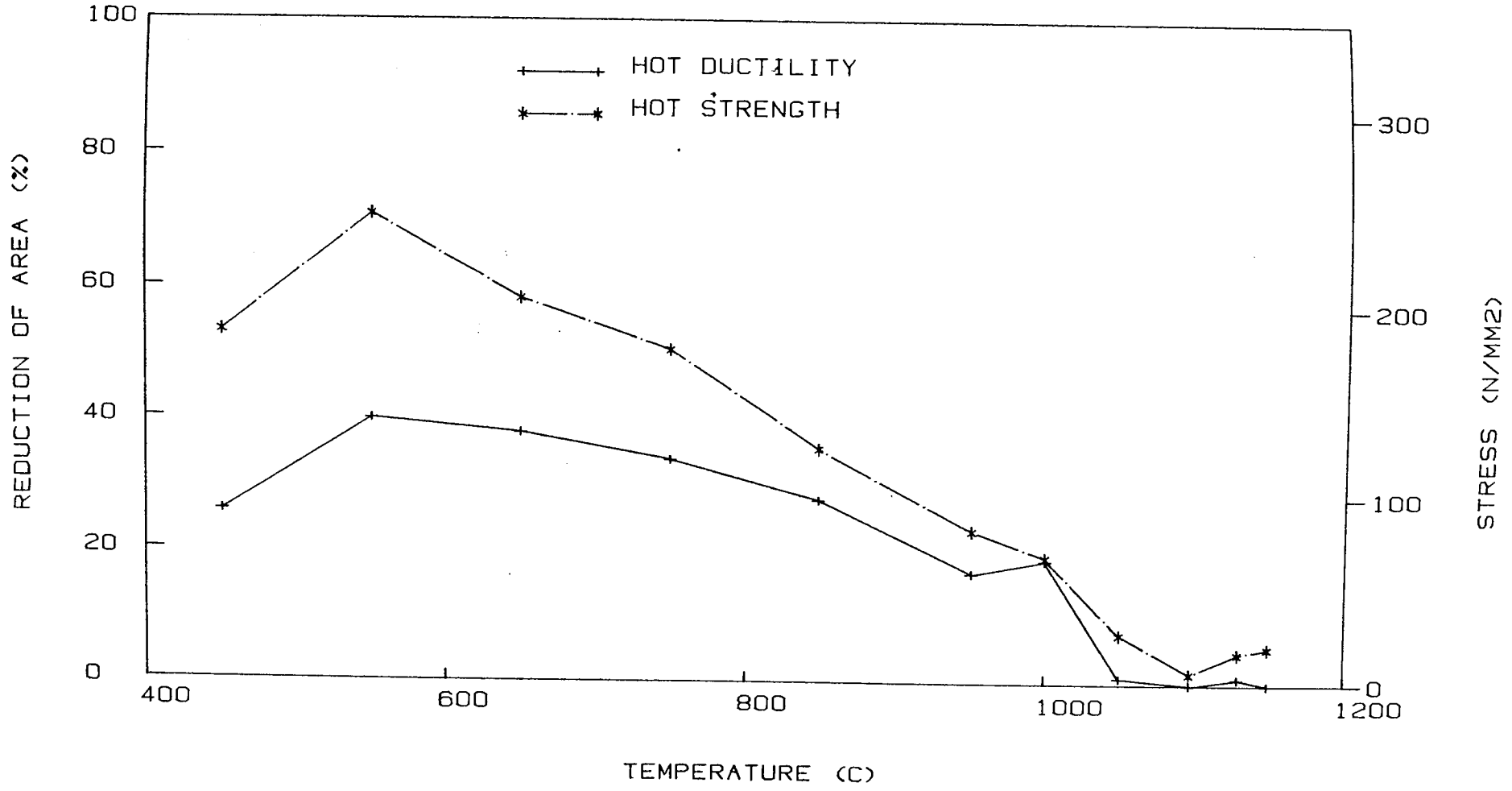

Fig 72. Plot of tensile properties against temperature for alloy R8 on cooling from 1160 C

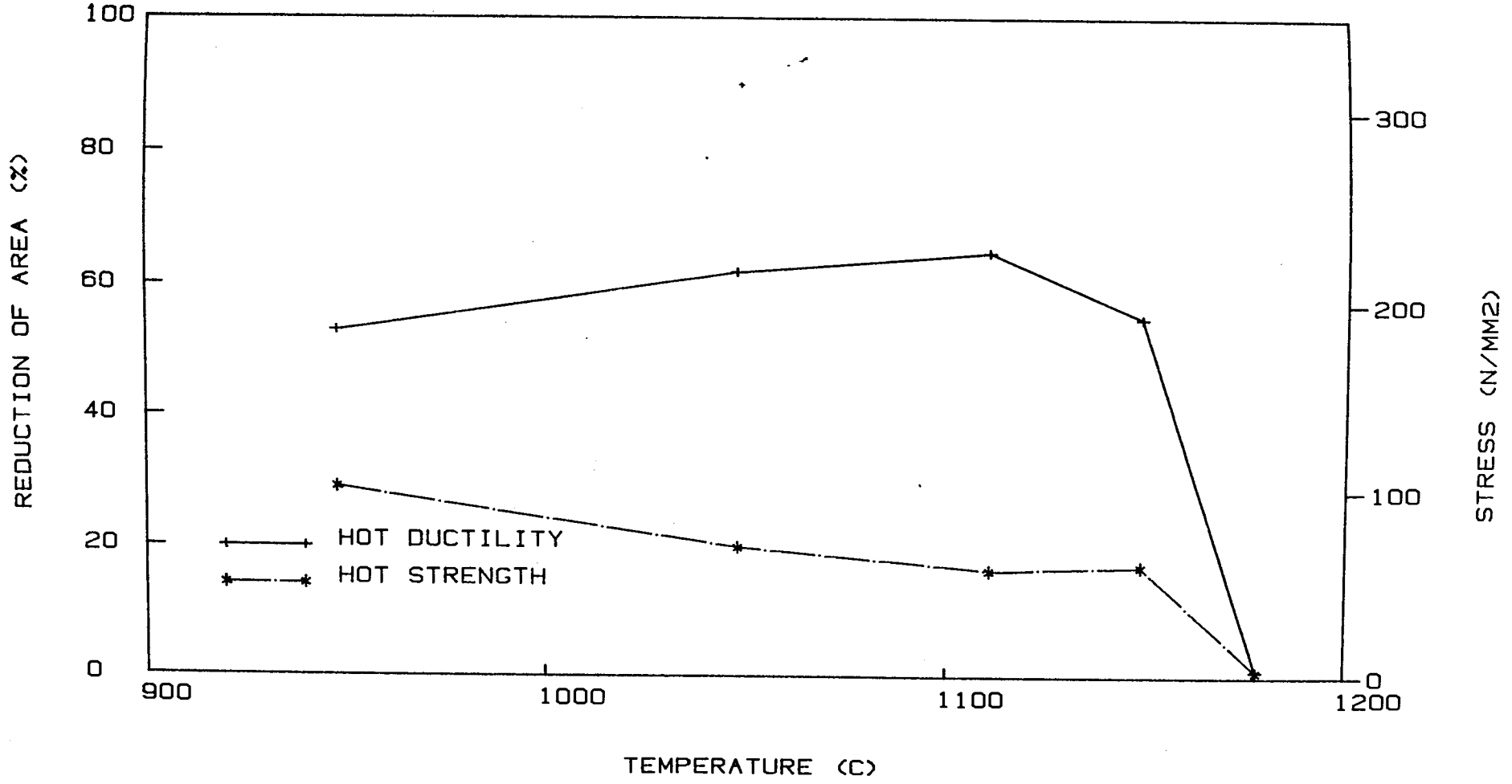

Fig 73. Plot of tensile properties against temperature for alloy R1 on heating

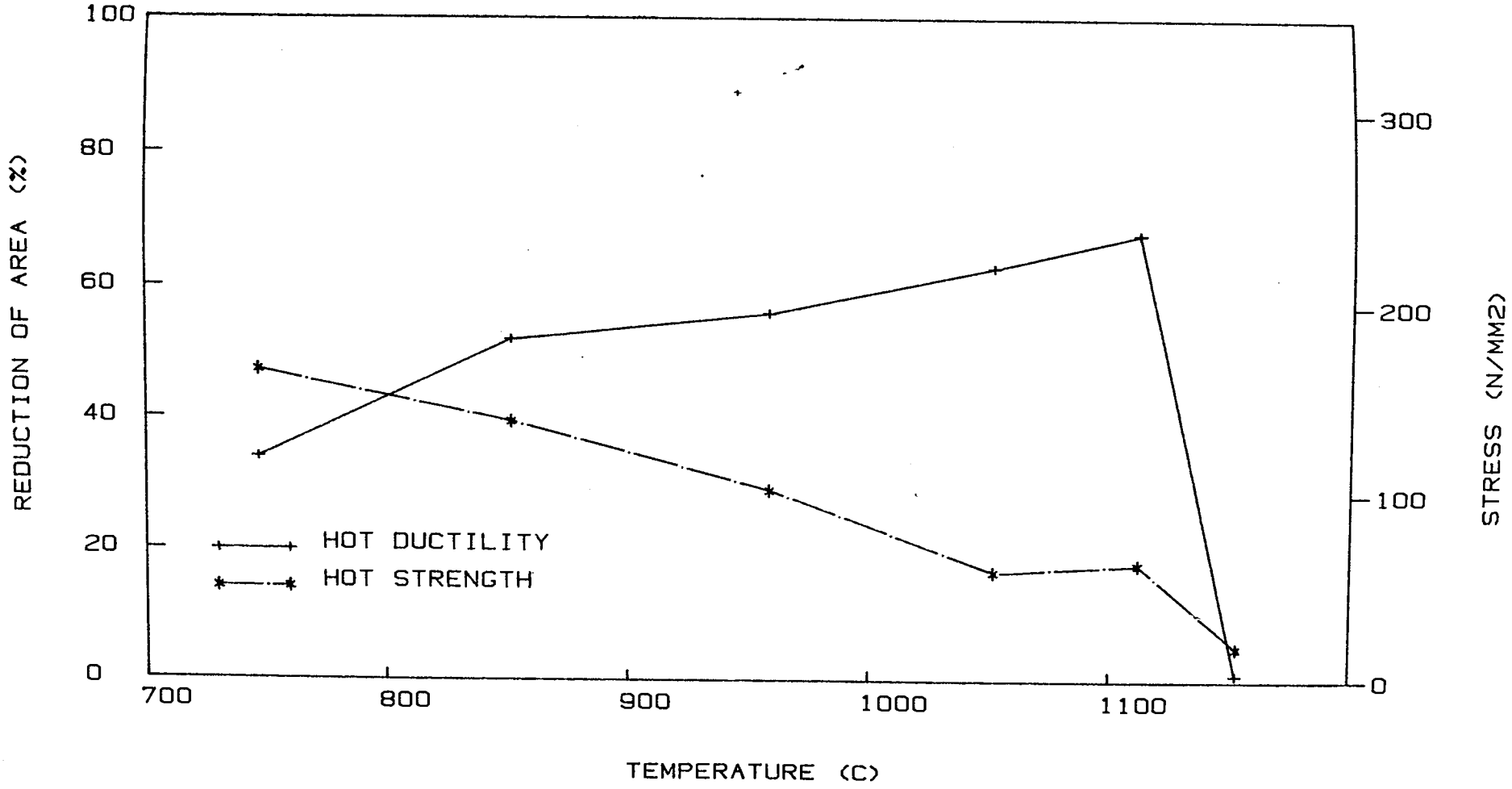

Fig 74. Plot of tensile properties against temperature for alloy R2 on heating

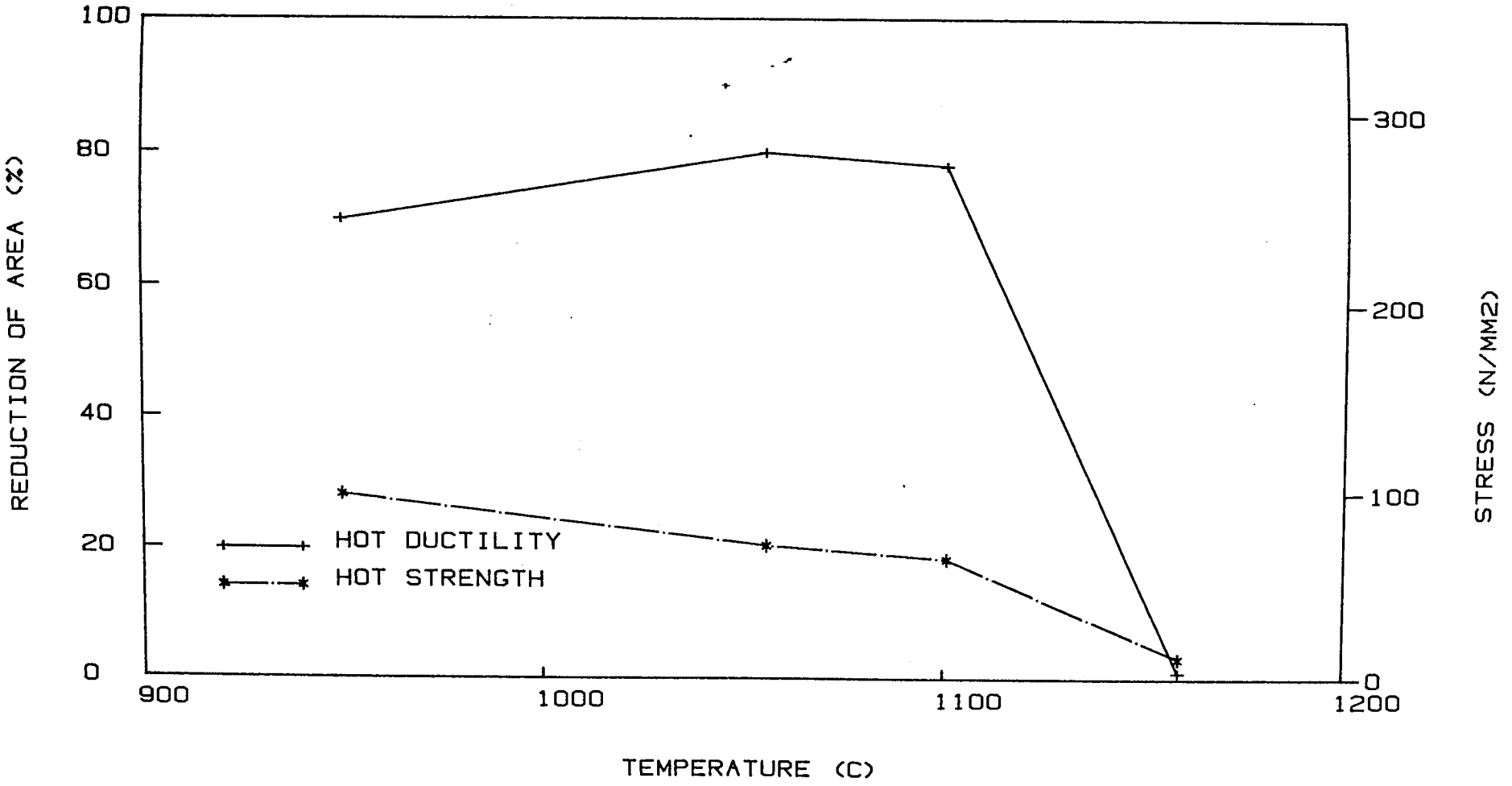

Fig 75. Plot of tensile properties against temperature for alloy R3 on heating

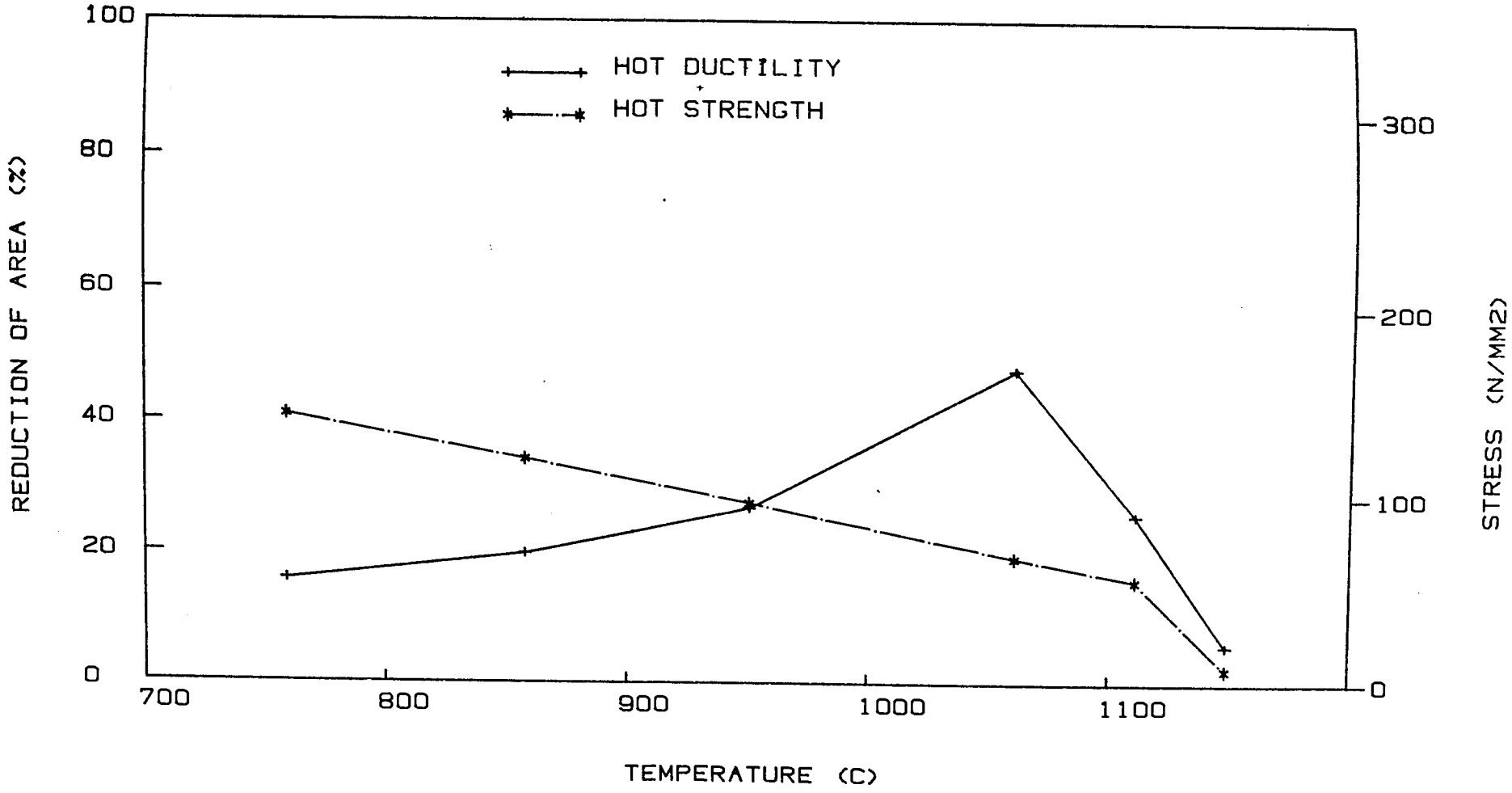

Fig 76. Plot of tensile properties against temperature for alloy R7 on heating

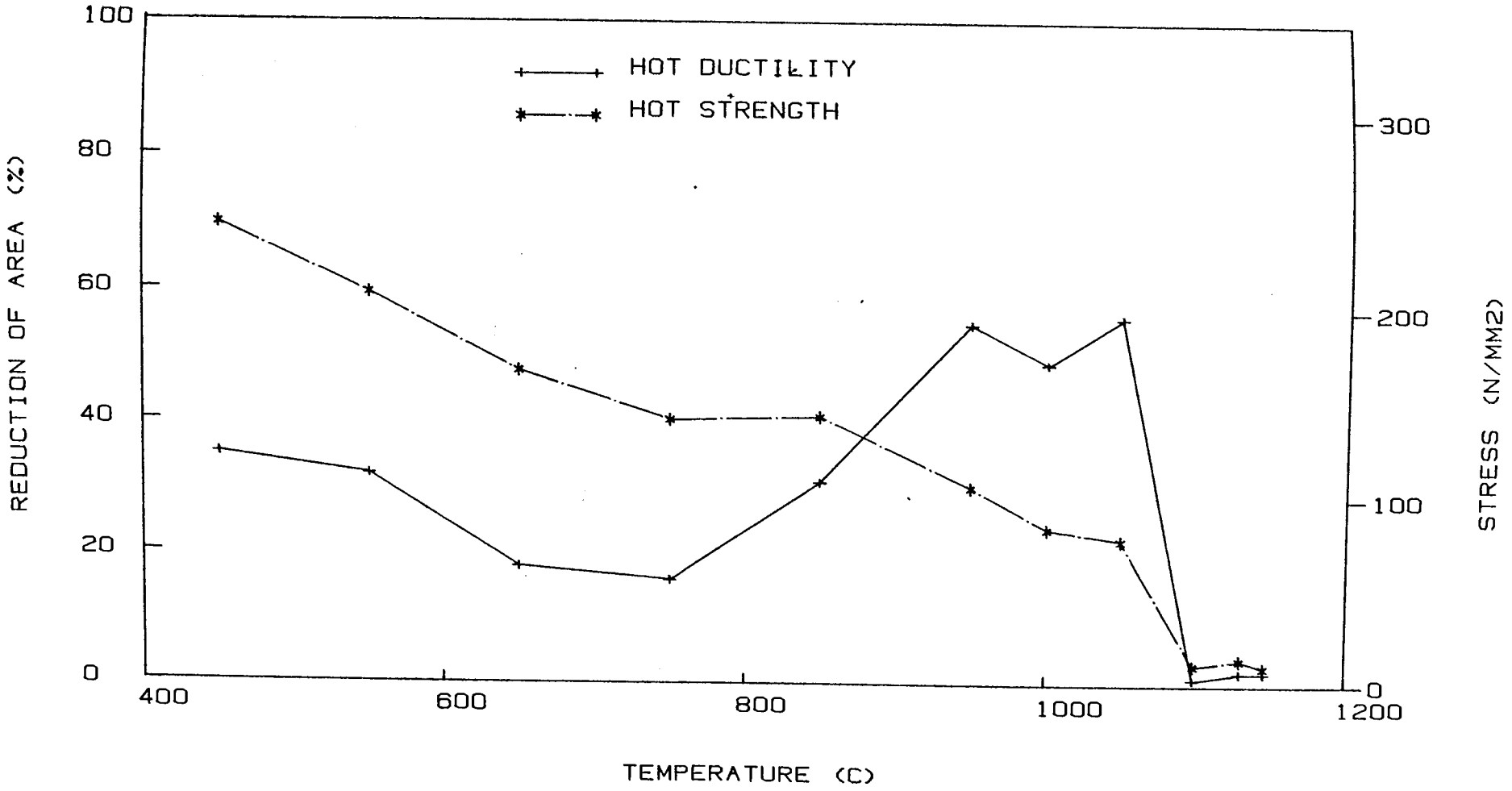

Fig 77. Plot of tensile properties against temperature for alloy T1 on cooling from 1160 C

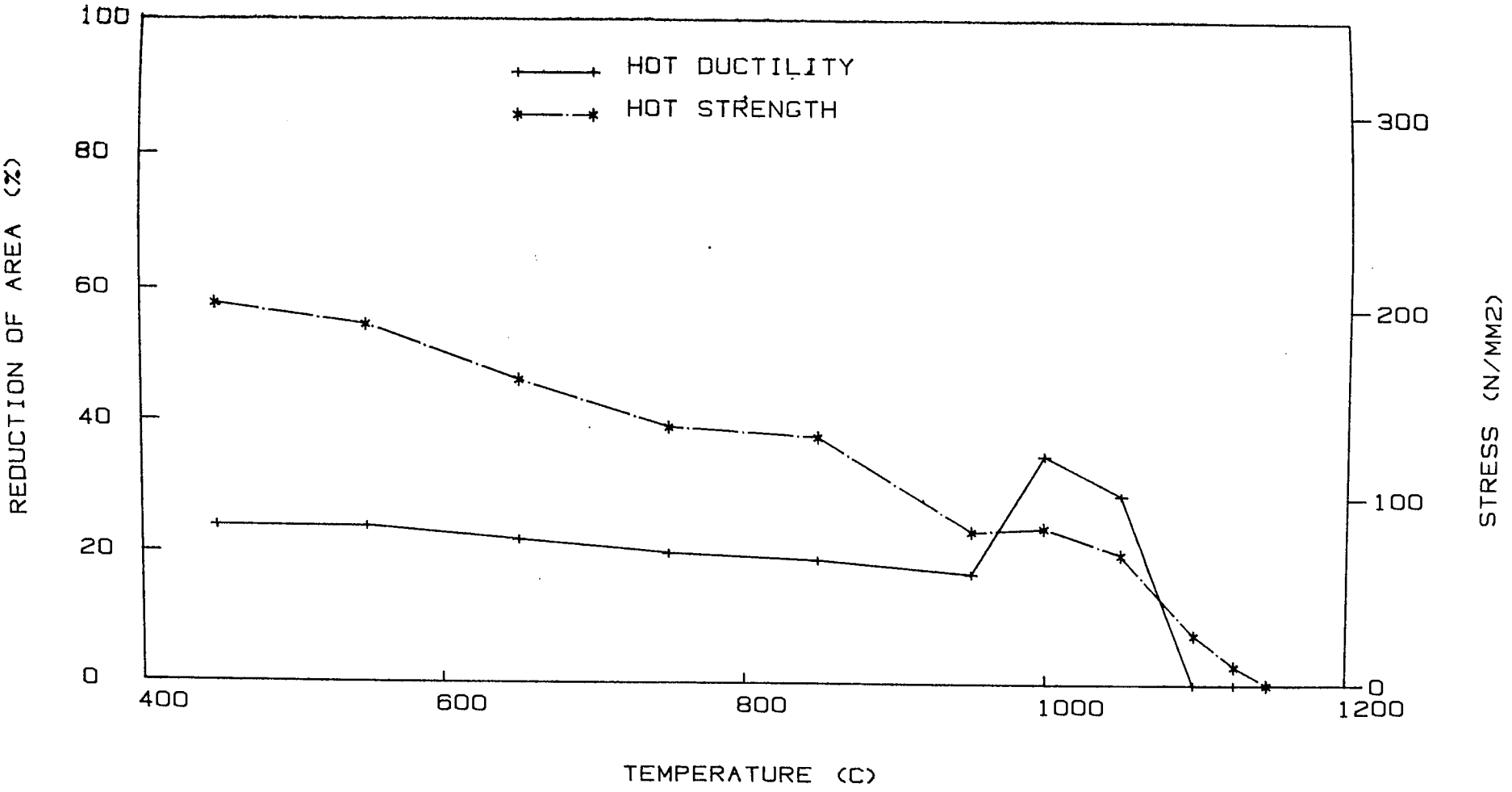

Fig 78. Plot of tensile properties against temperature for alloy T2 on cooling from 1160 C

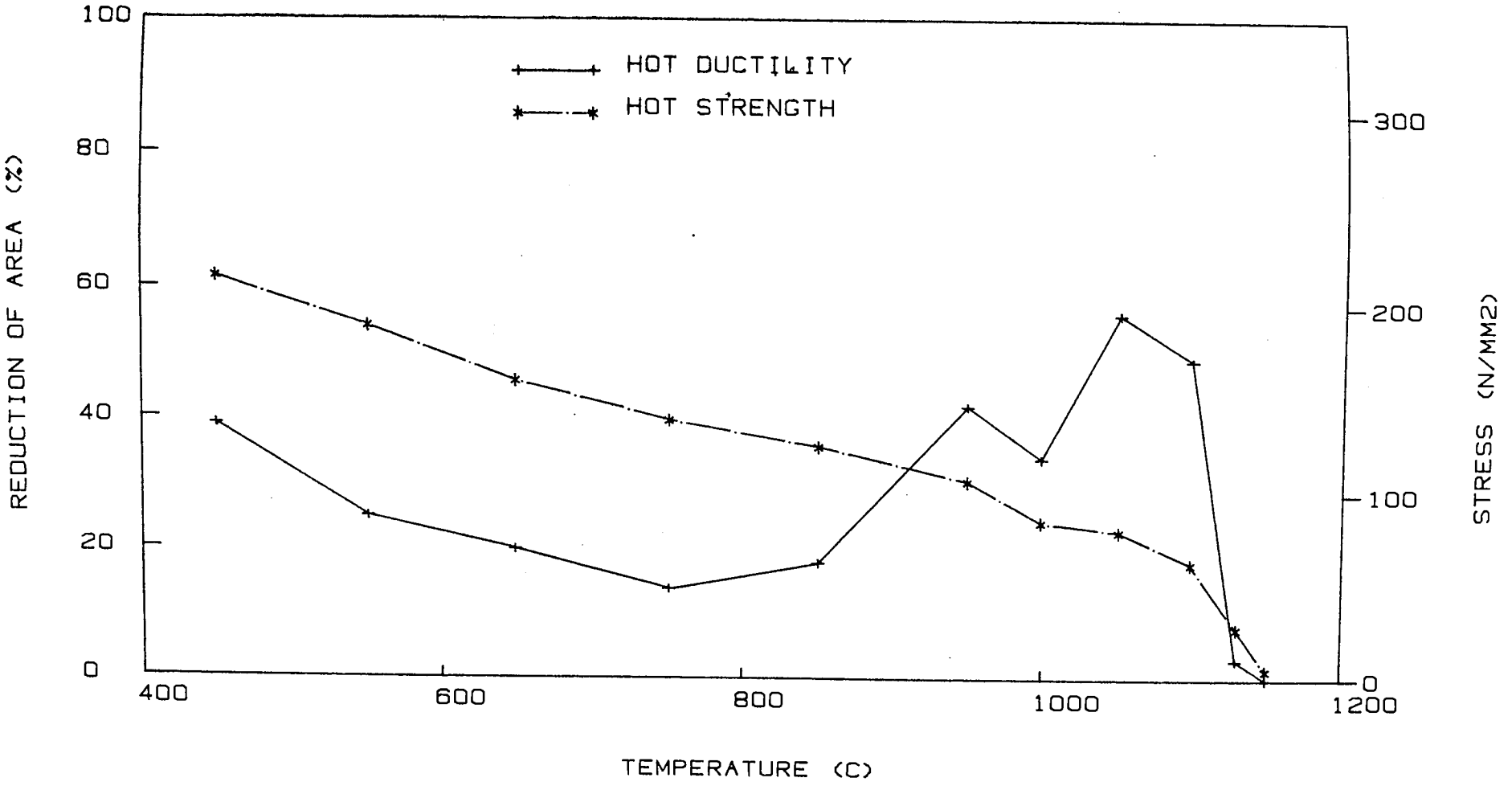

Fig 79. Plot of tensile properties against temperature for alloy T3 on cooling from 1160 C

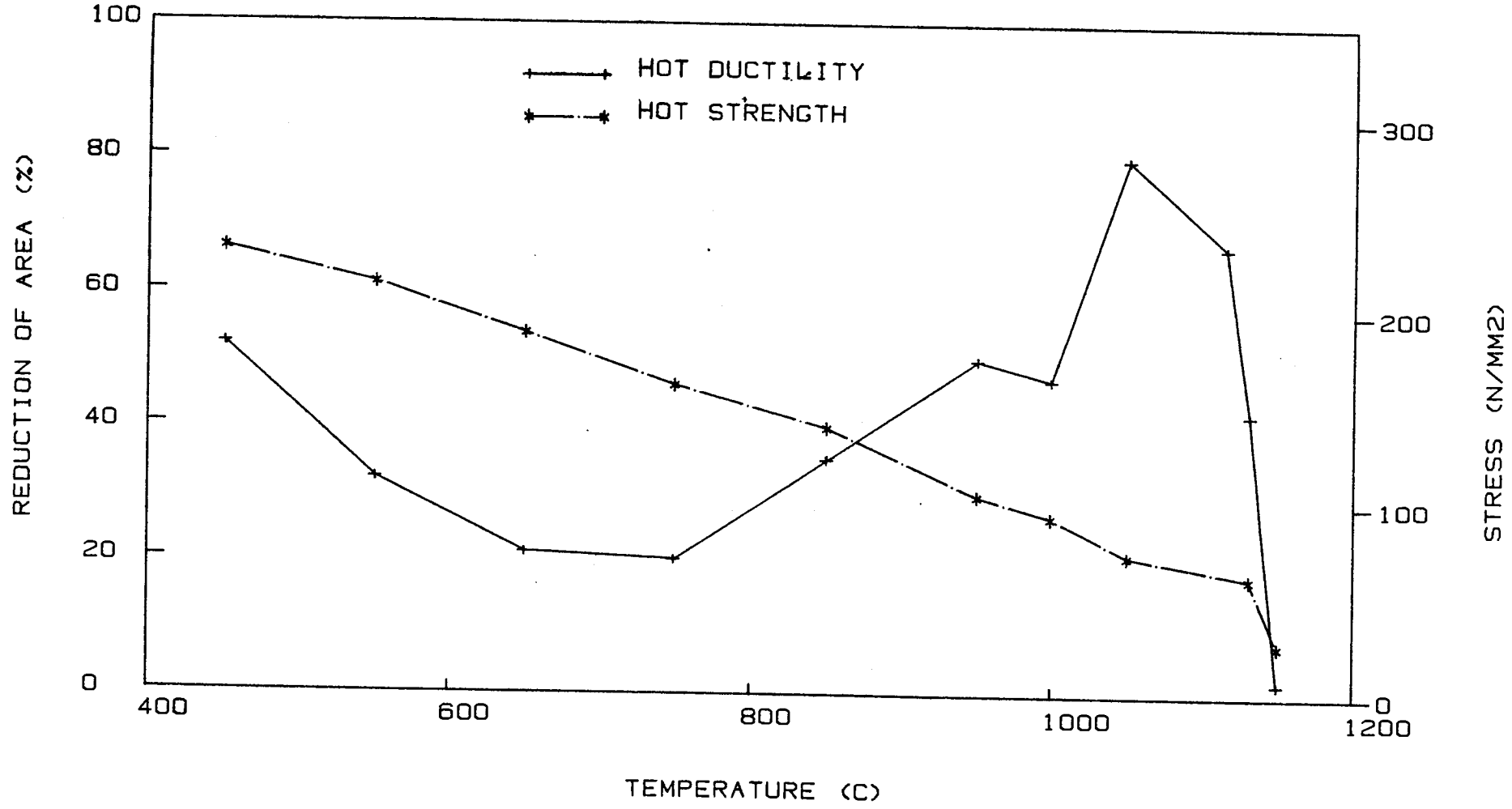

Fig 80. Plot of tensile properties against temperature for alloy T4 on cooling from 1160 C

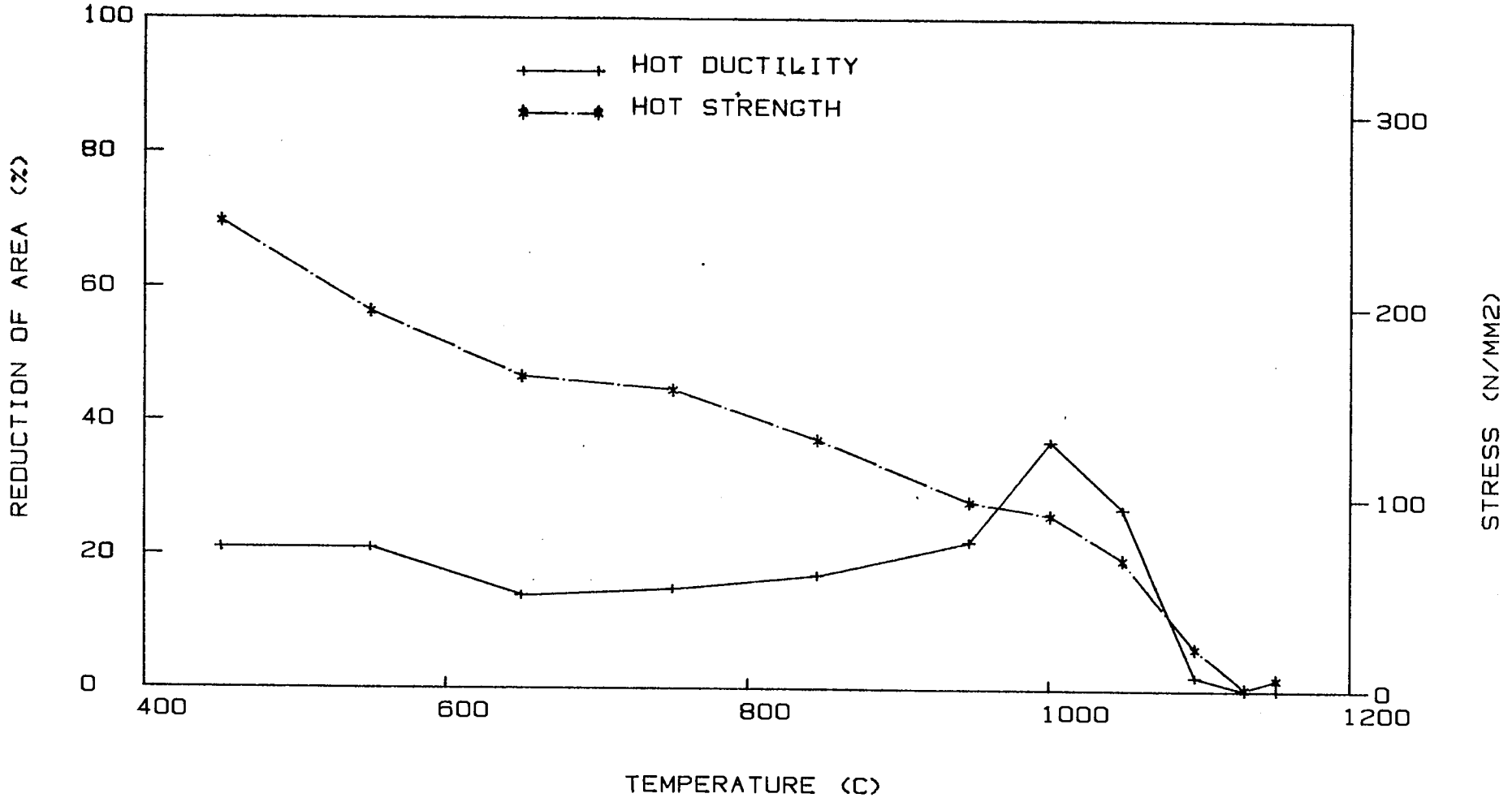

Fig 81. Plot of tensile properties against temperature for alloy T5 on cooling from 1160 C

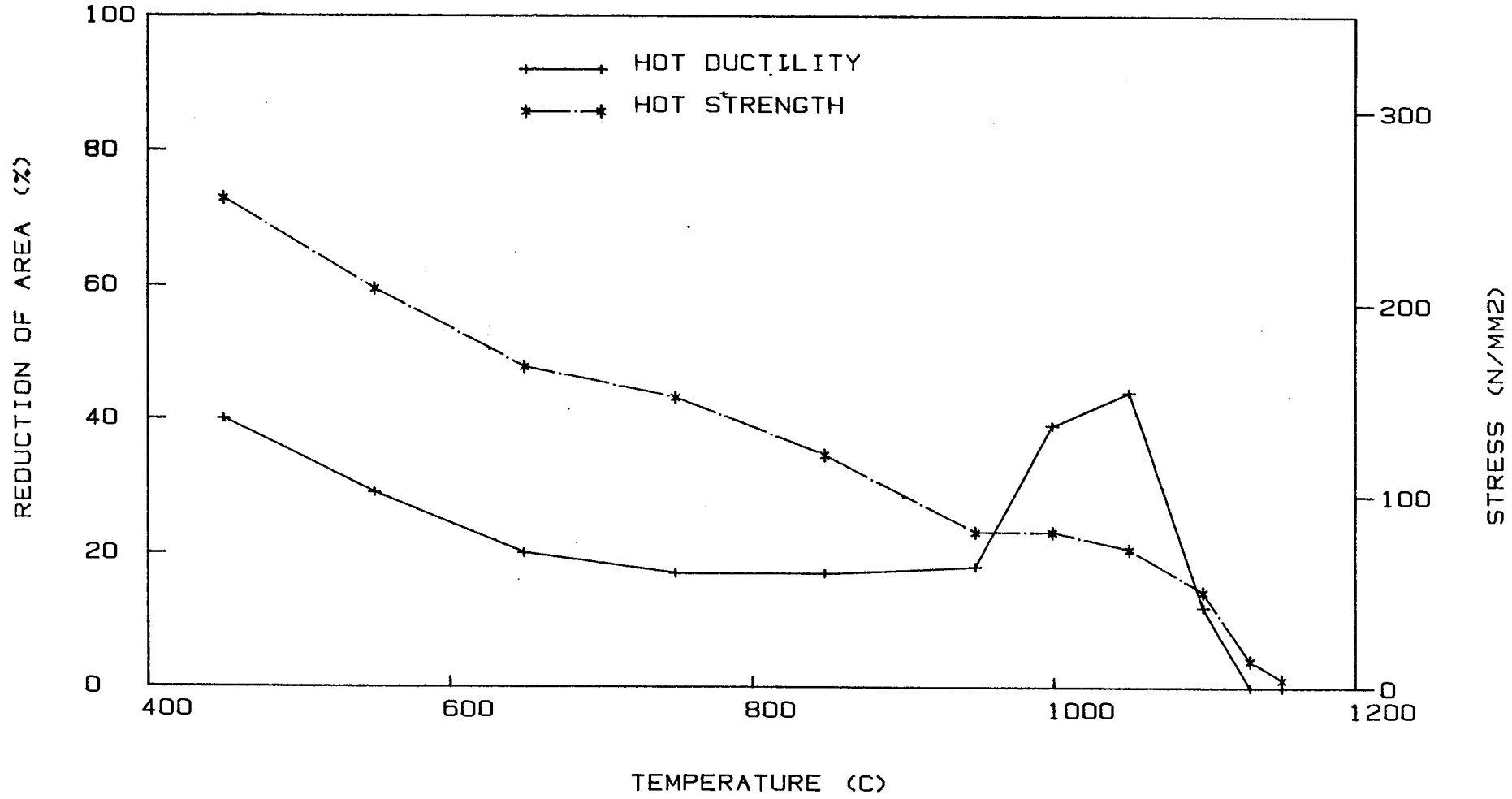

Fig 82. Plot of tensile properties against temperature for alloy T6 on cooling from 1160 C

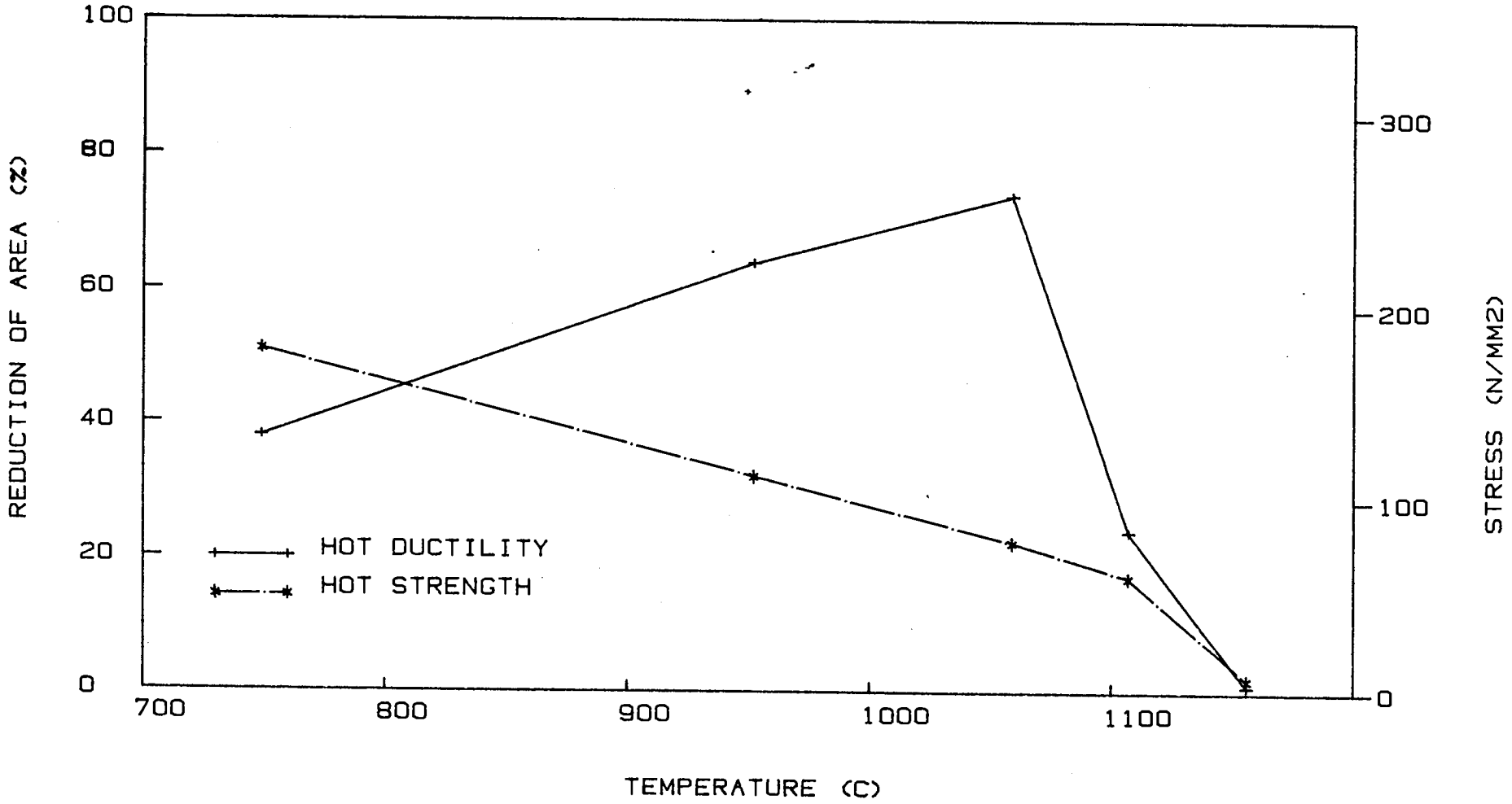

Fig 83. Plot of tensile properties against temperature for alloy T1 on heating

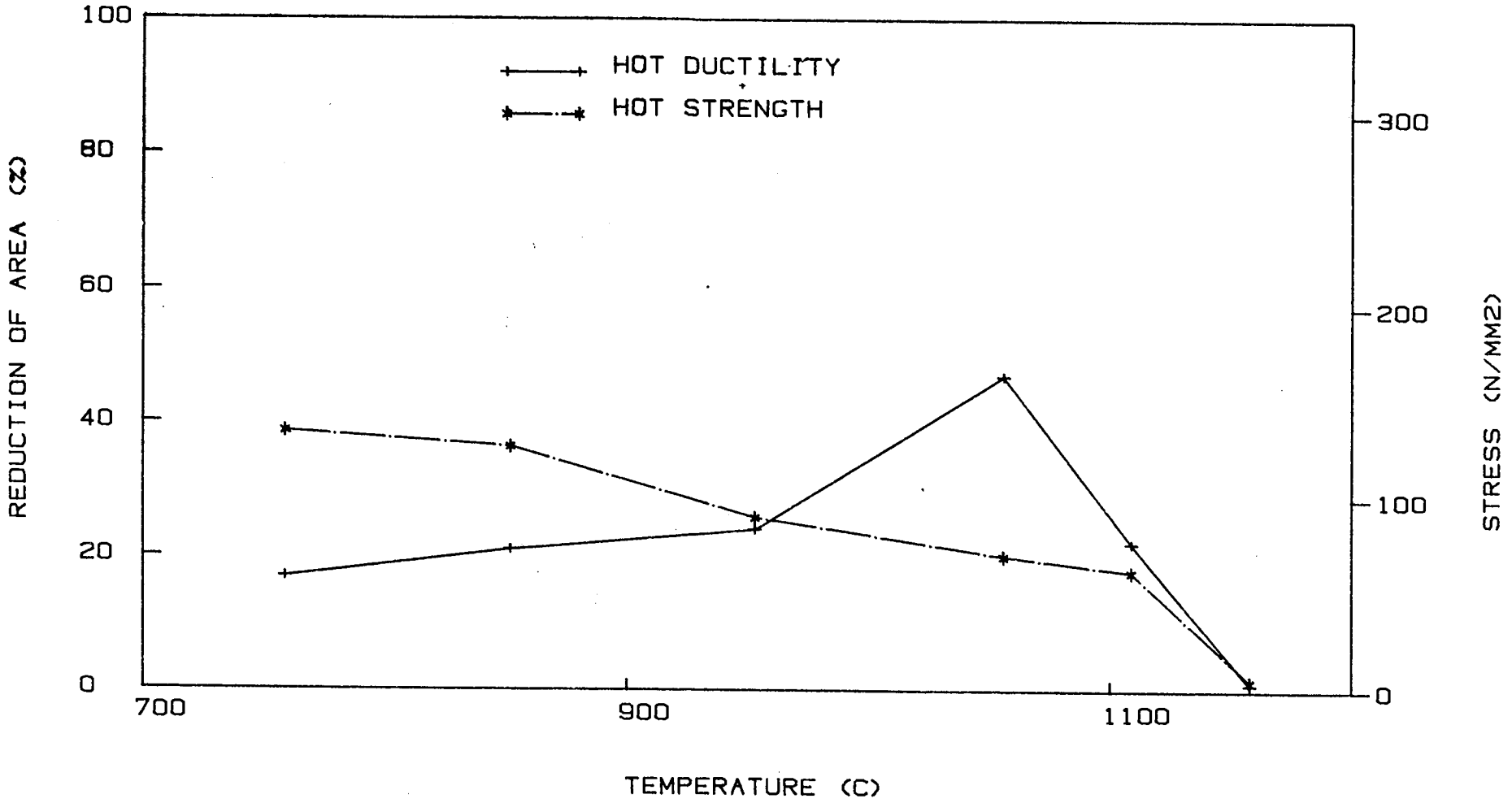

Fig 84. Plot of tensile properties against temperature for alloy T2 on heating

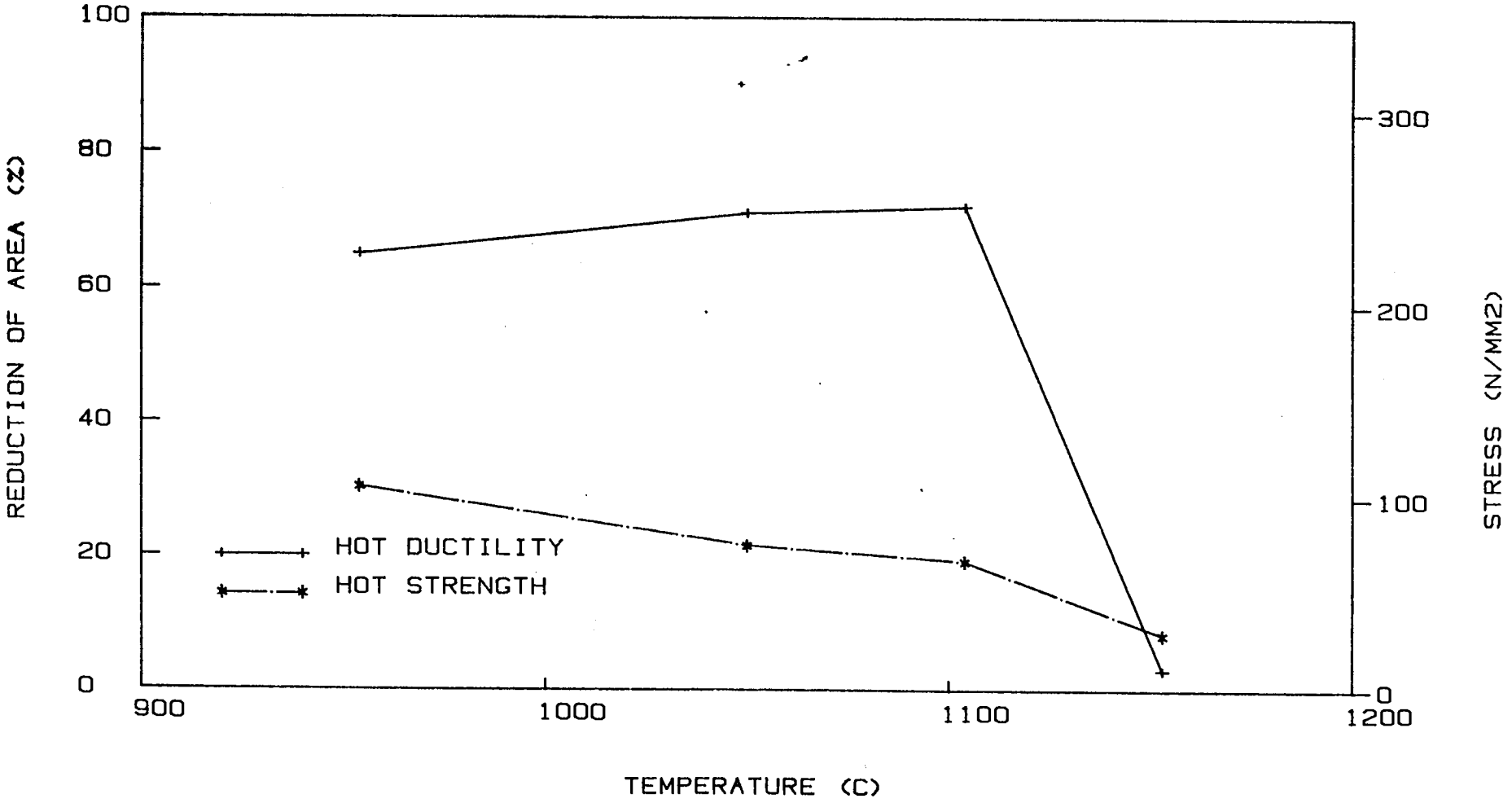

Fig 85. Plot of tensile properties against temperature for alloy T4 on heating

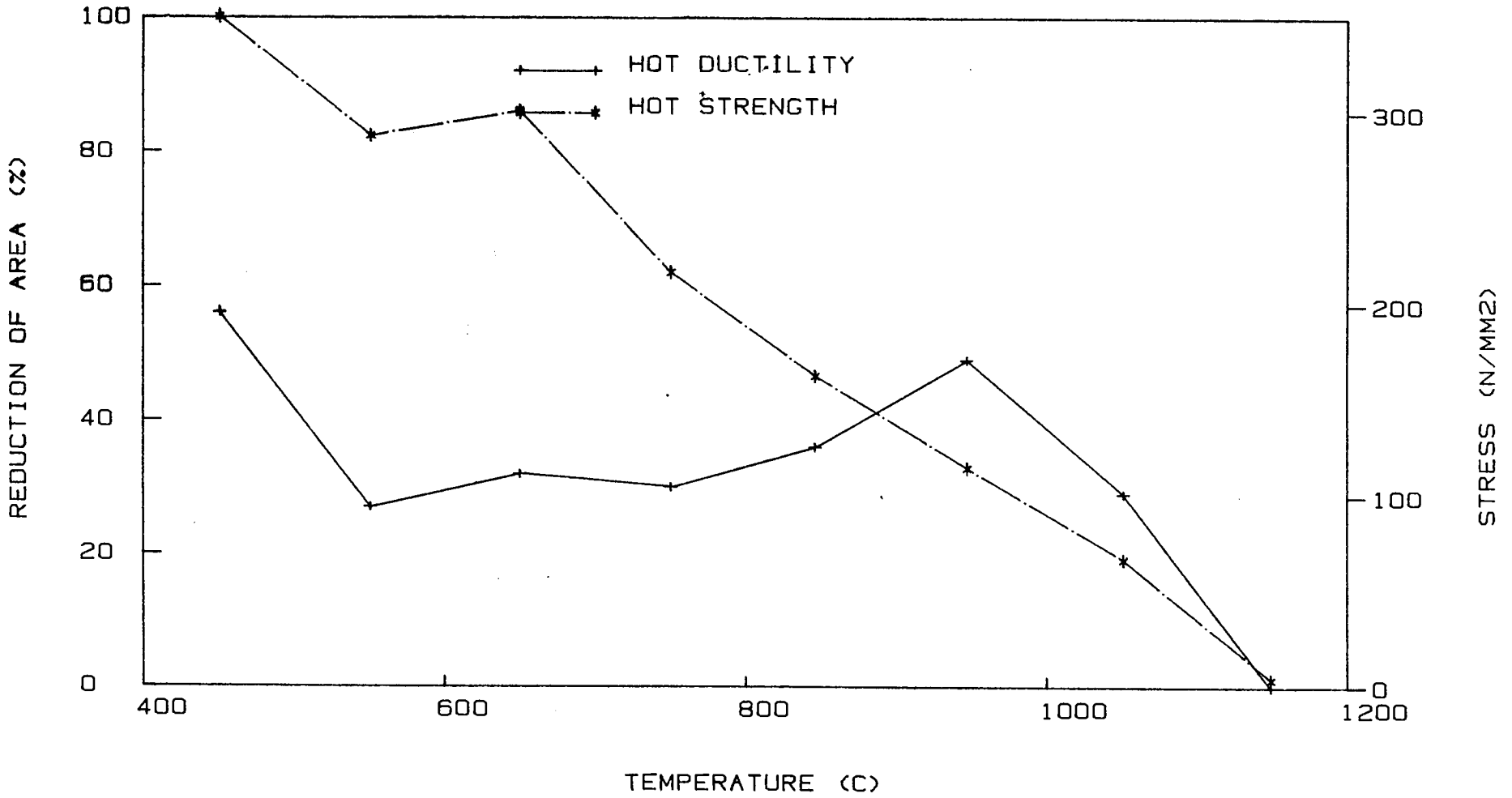

Fig 86. Plot of tensile properties against temperature for alloy K2 on cooling from 1160 C

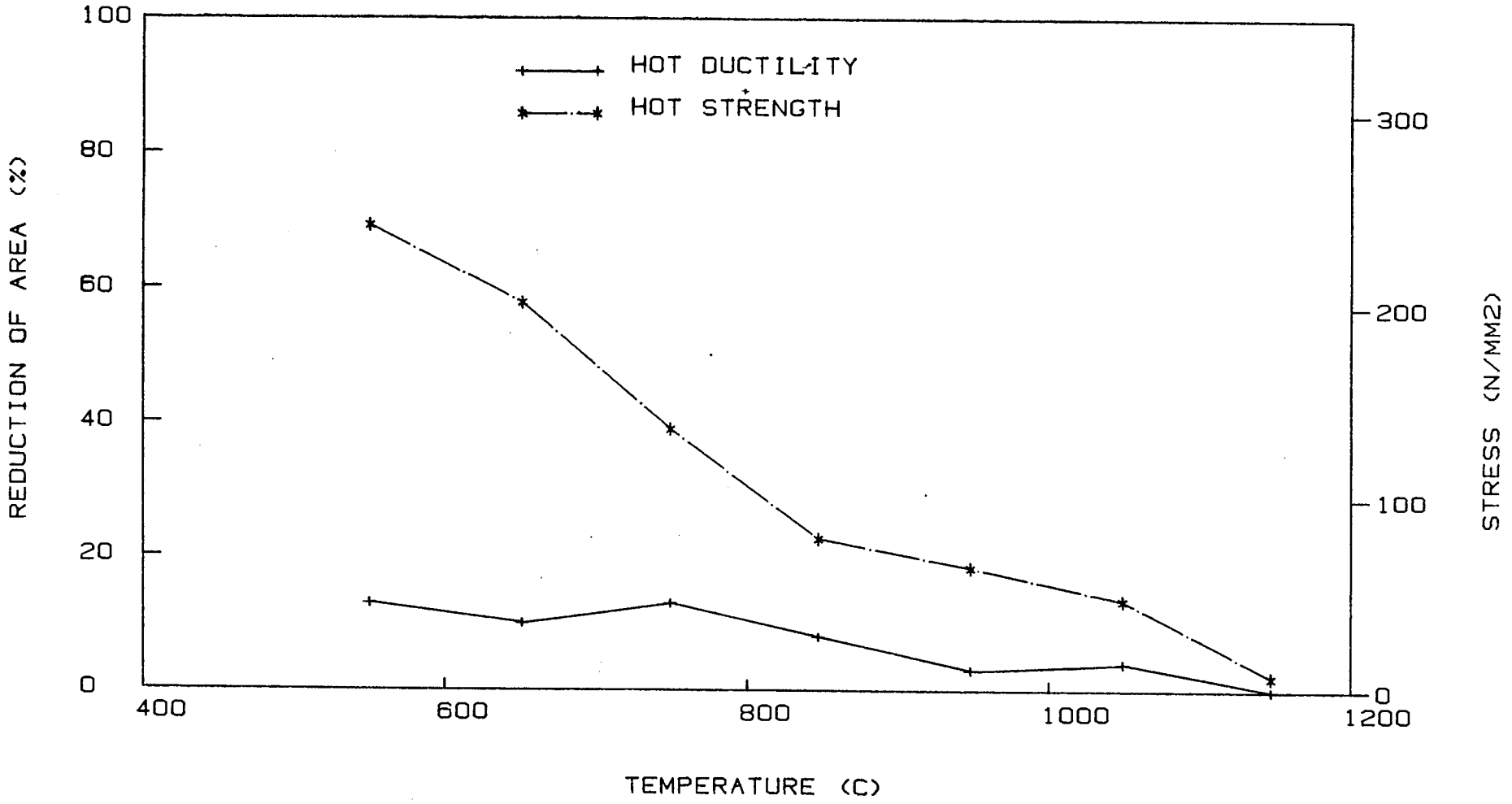

Fig 87. Plot of tensile properties against temperature for alloy K4 on cooling from 1160 C

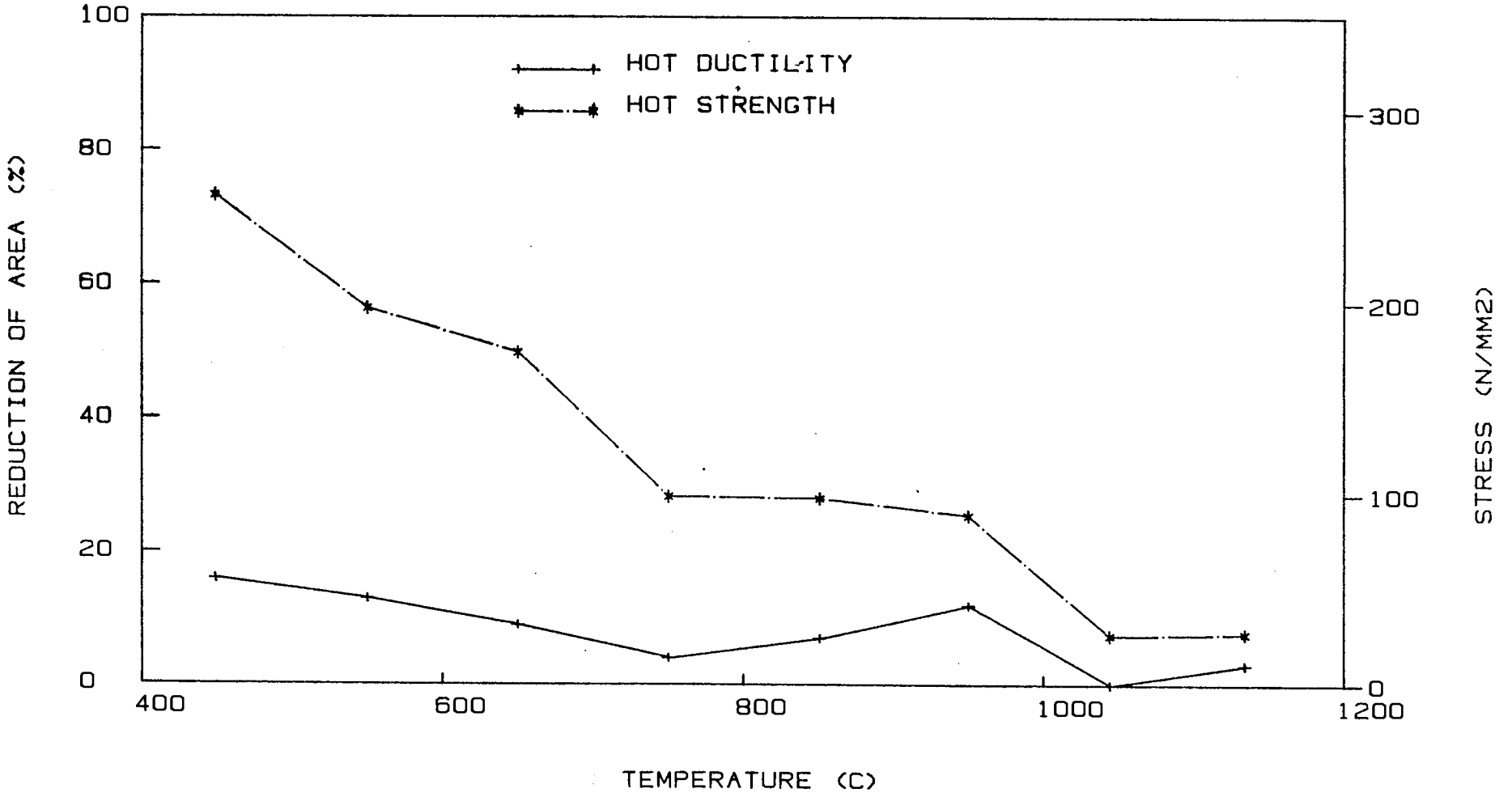

Fig 88. Plot of tensile properties against temperature for alloy K6 on cooling from 1160 C

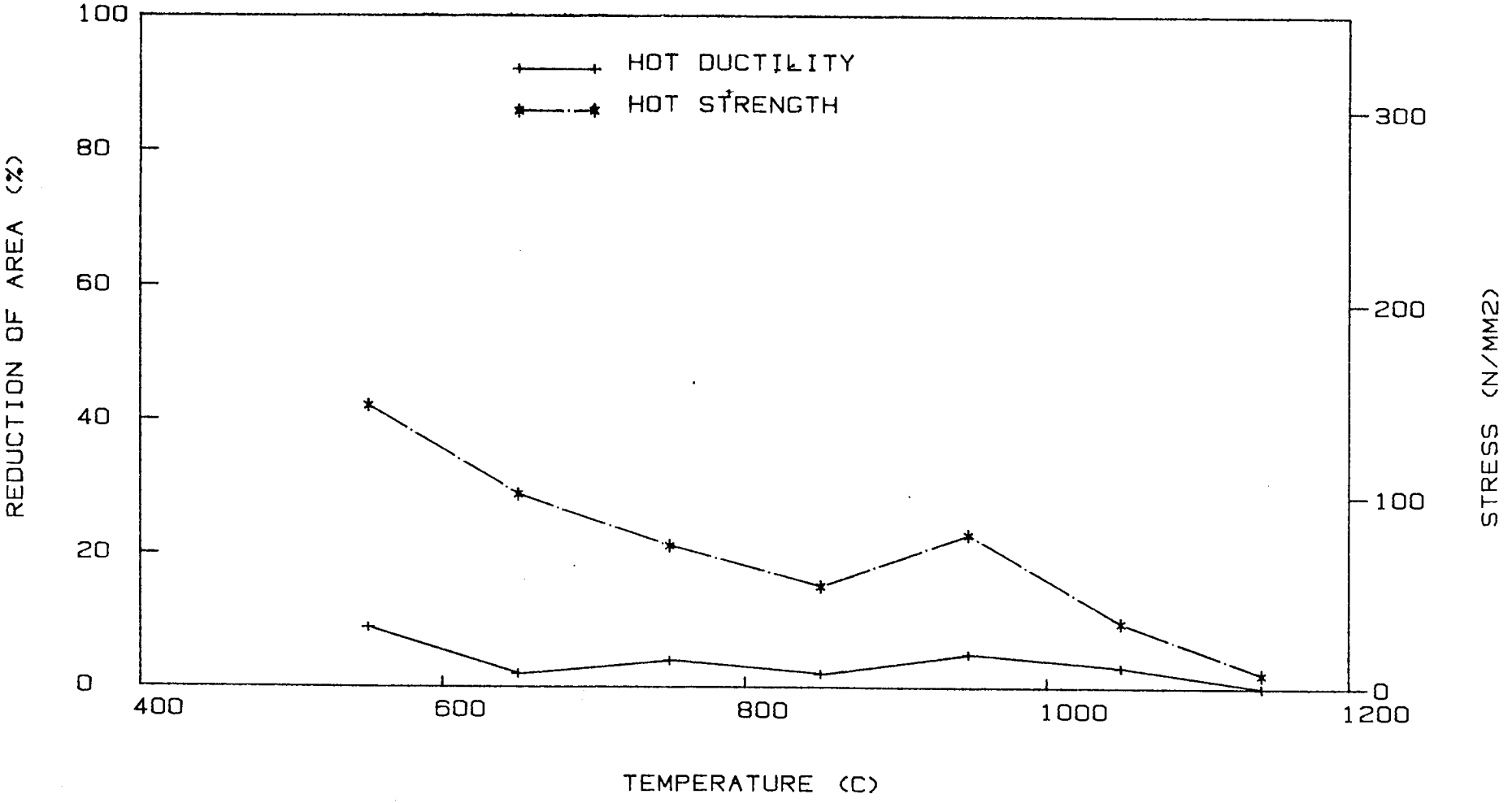

Fig 89. Plot of tensile properties against temperature for alloy K8 on cooling from 1160 C

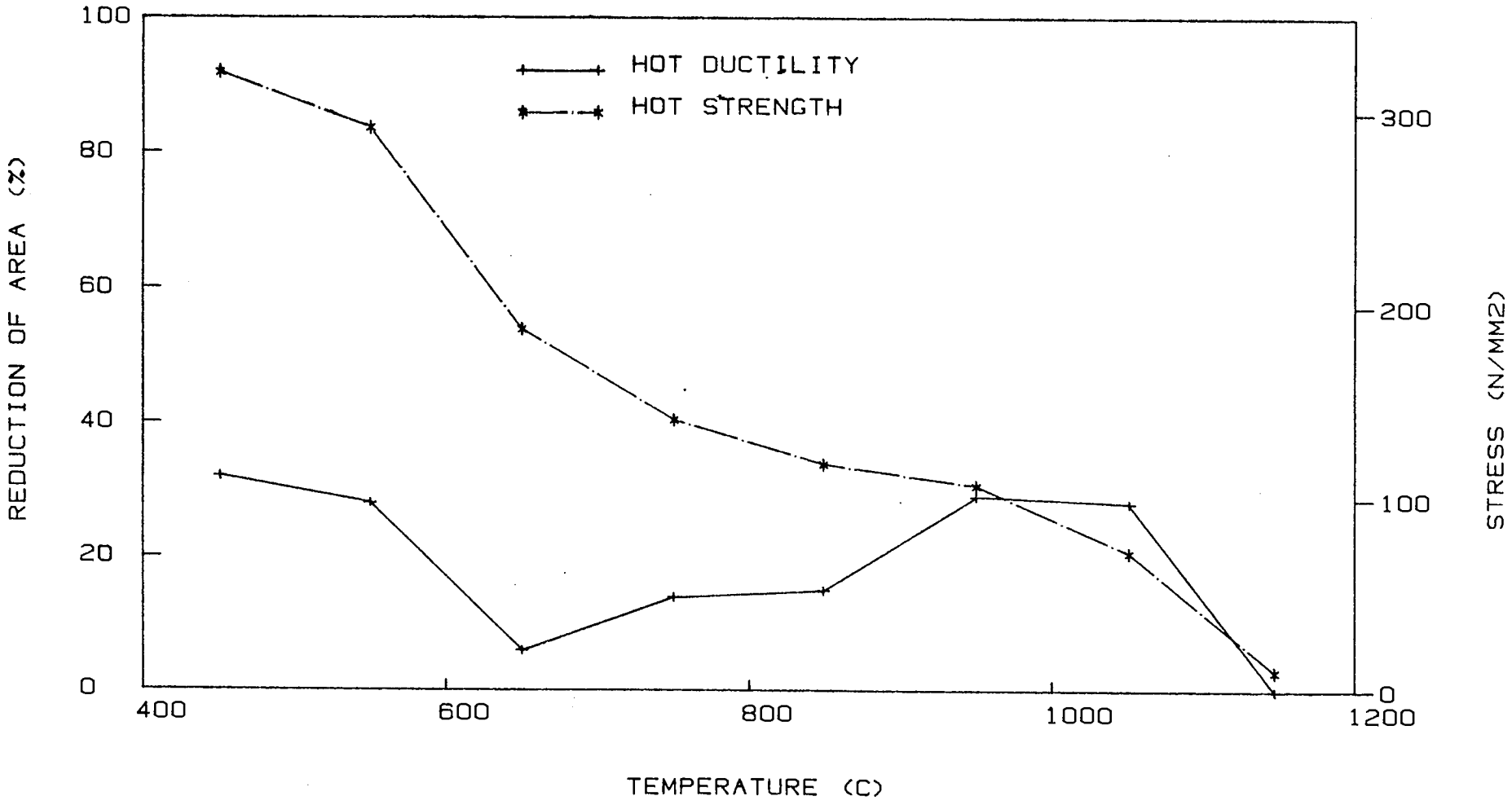

Fig 90. Plot of tensile properties against temperature for alloy L2 on cooling from 1160 C

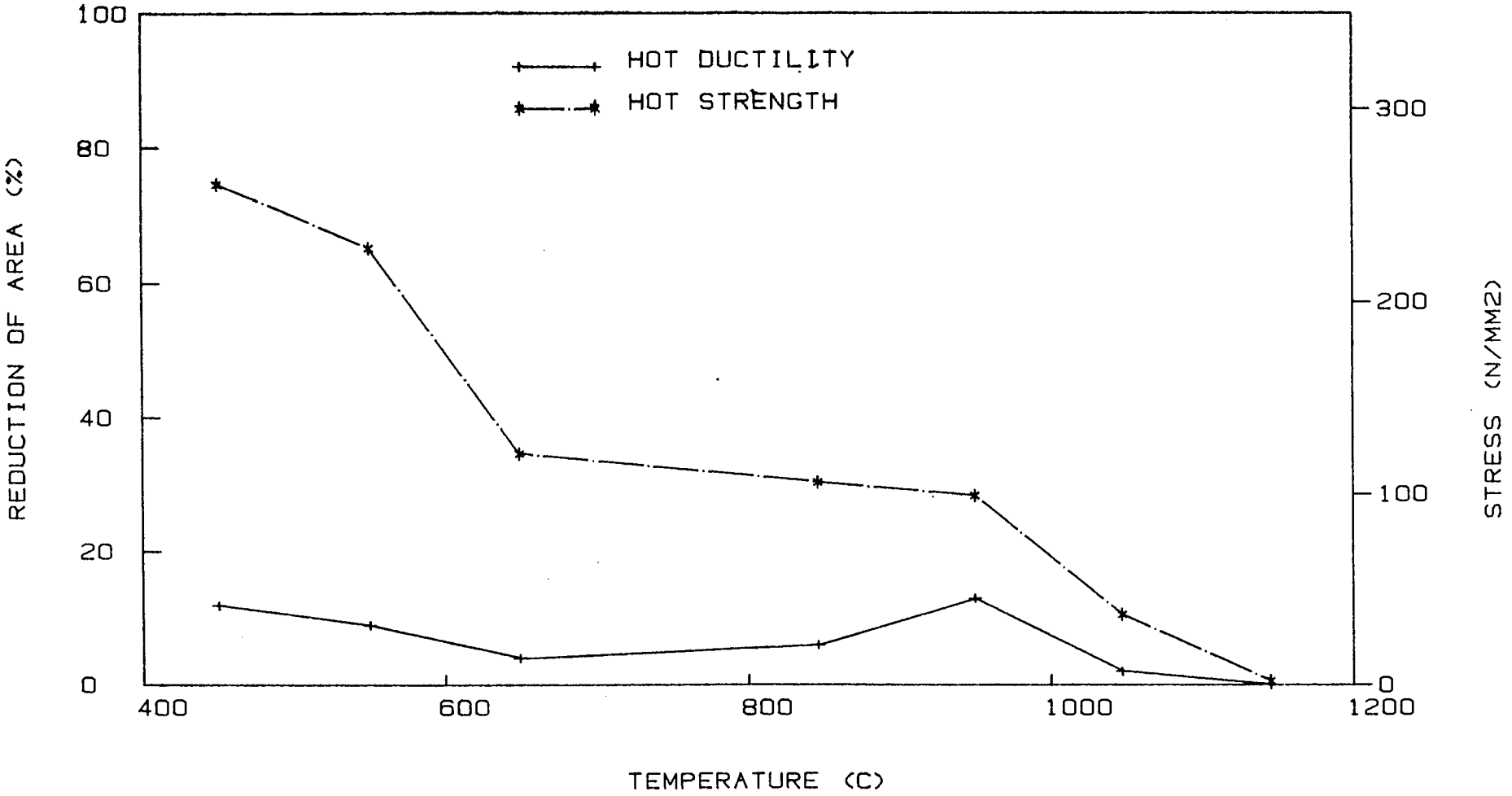

Fig 91. Plot of tensile properties against temperature for alloy L3 on cooling from 1160 C

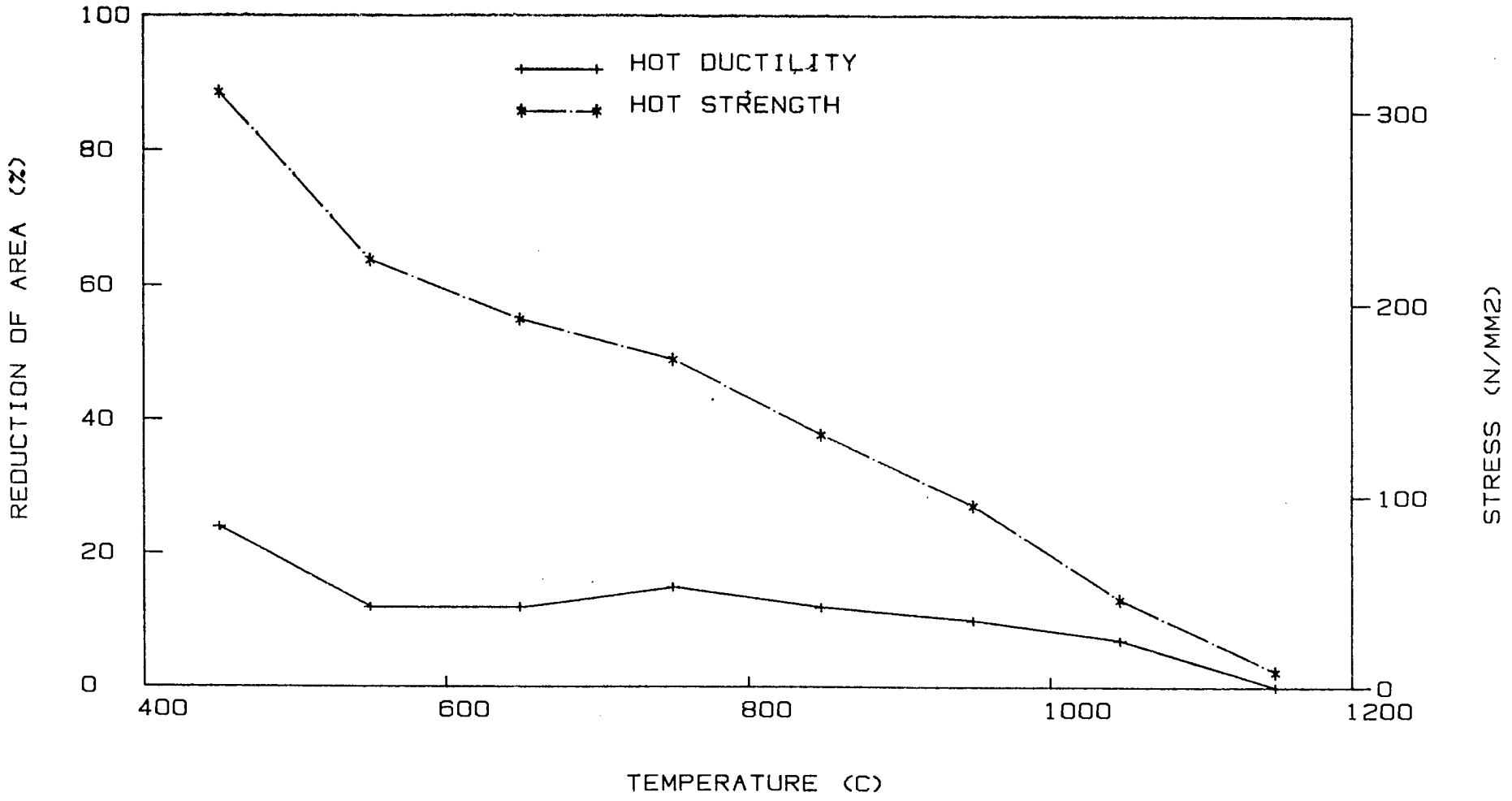

Fig 92. Plot of tensile properties against temperature for alloy M1 on cooling from 1160 C

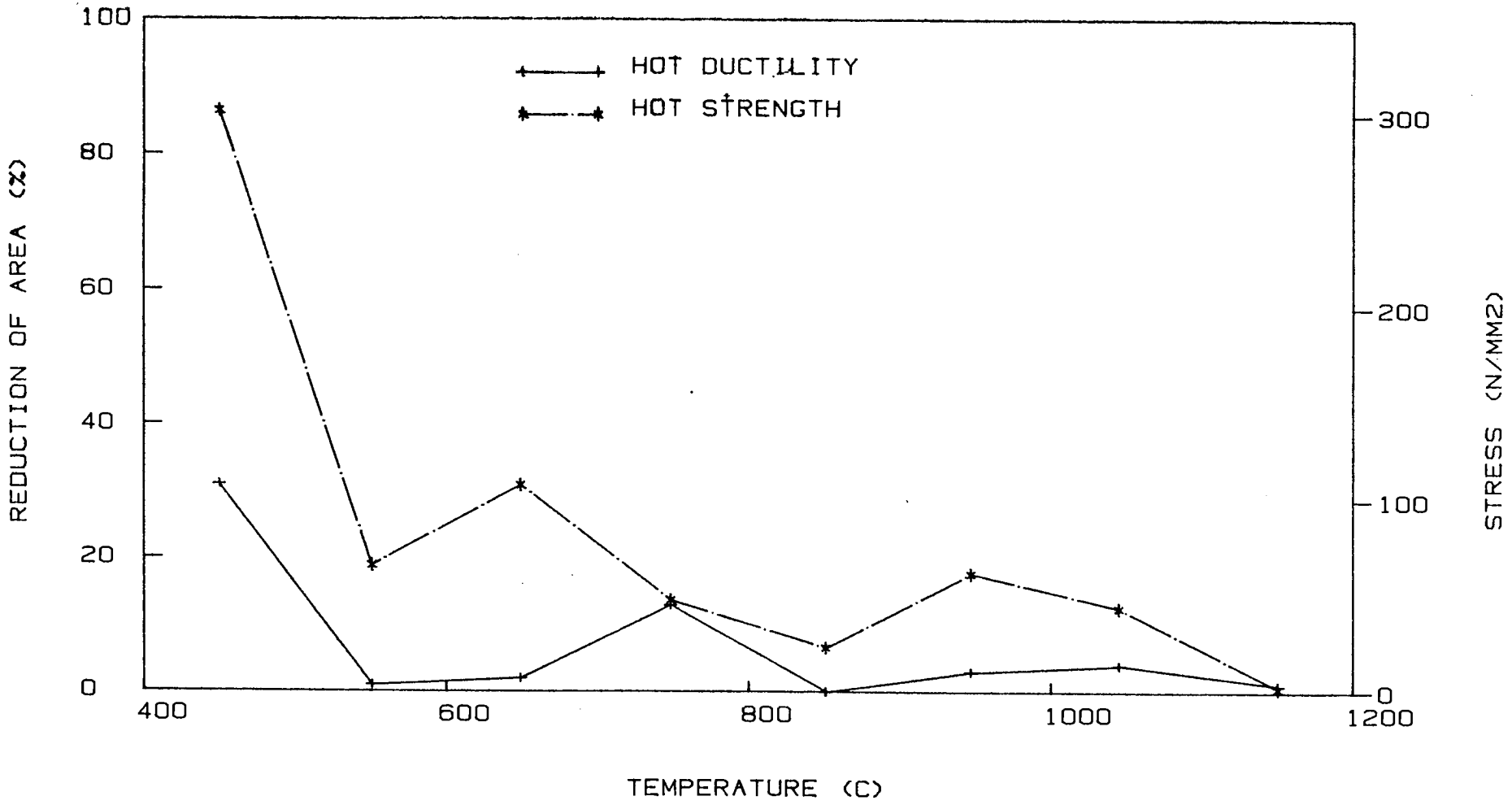

Fig 93. Plot of tensile properties against temperature for alloy M3 on cooling from 1160 C

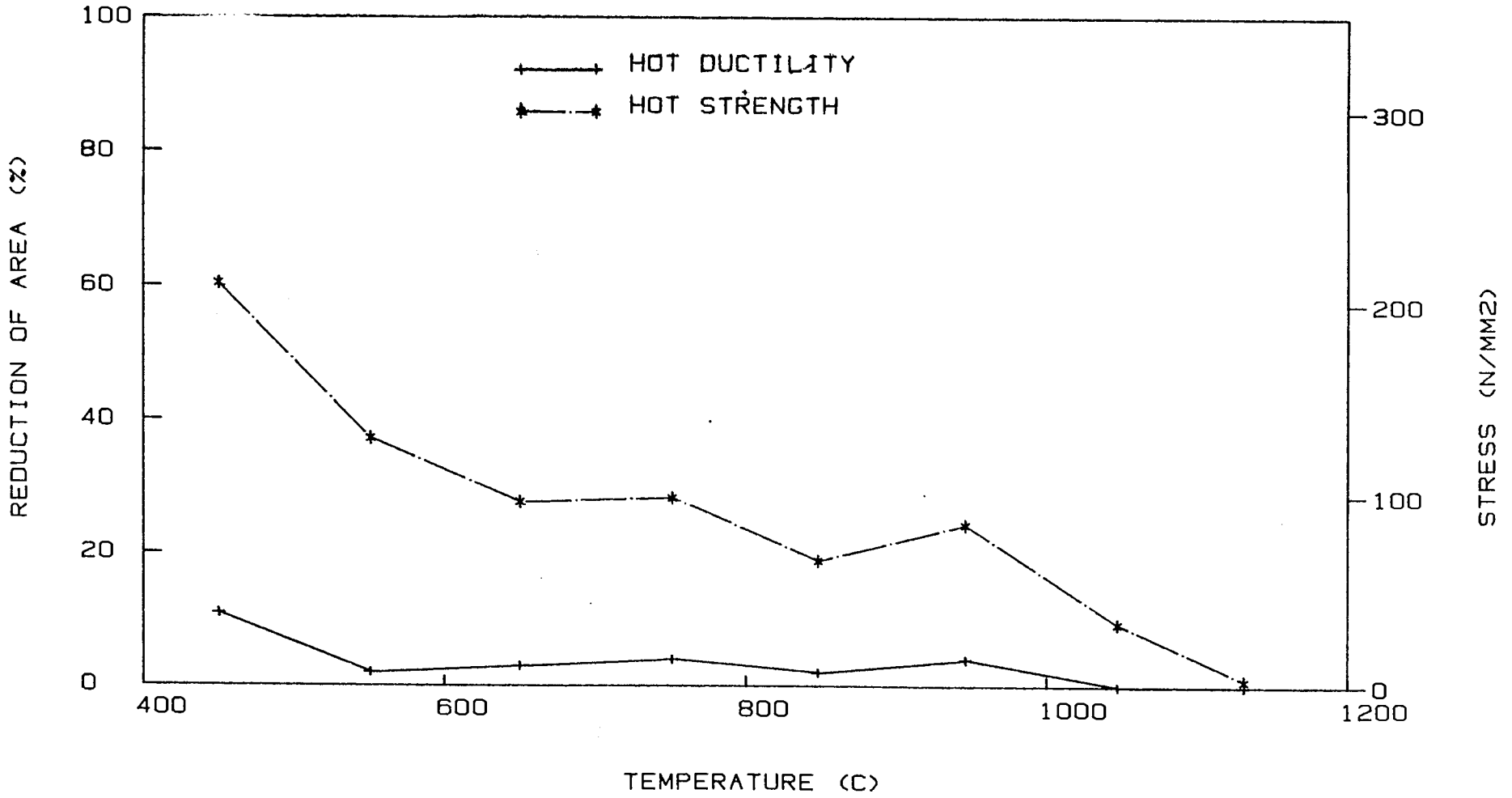

Fig 94. Plot of tensile properties against temperature for alloy N2 on cooling from 1160 C

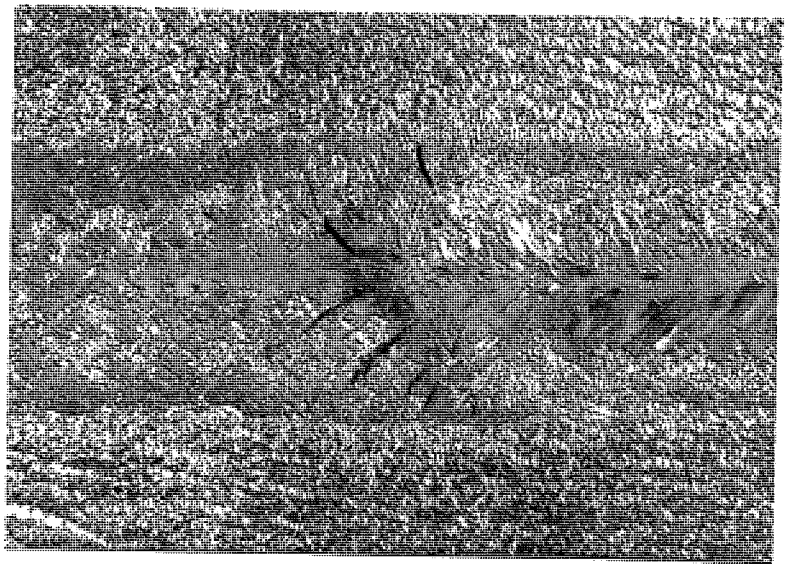

Fig 95. Pattern of cracking in a typical Varestraint test region x3

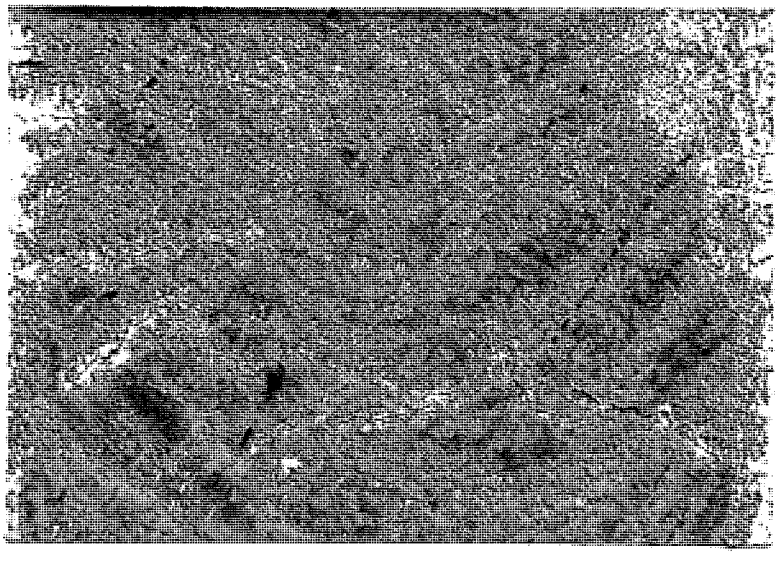

Fig 96. Sub-surface cracking in Varestraint test region x10

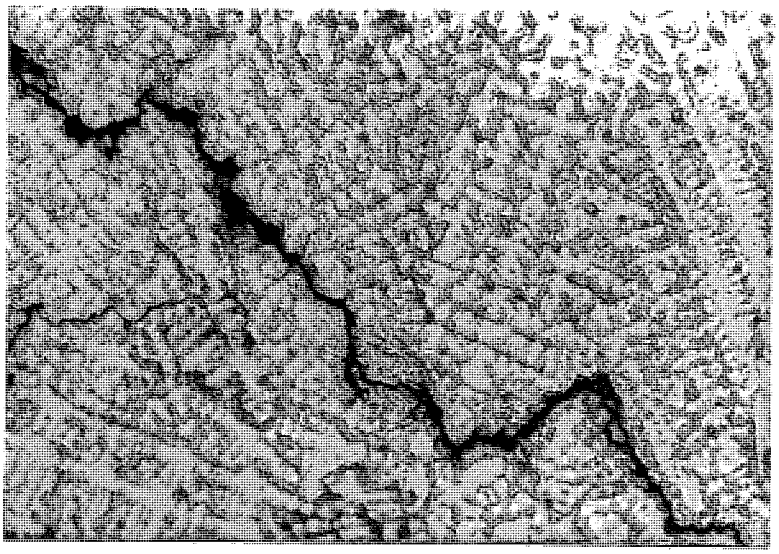

Fig 97. Weld metal cracking in Varestraint test x340

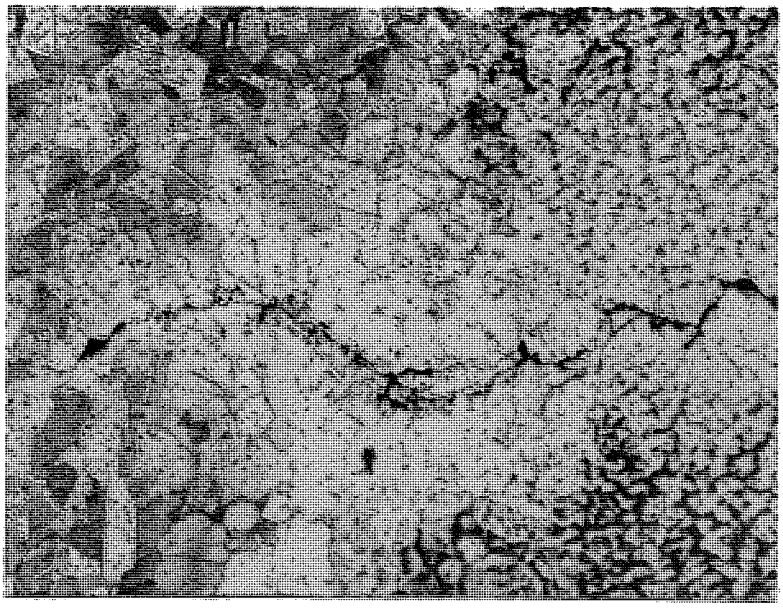

Fig 98. Crack crossing fusionline from weld metal to HAZ x140

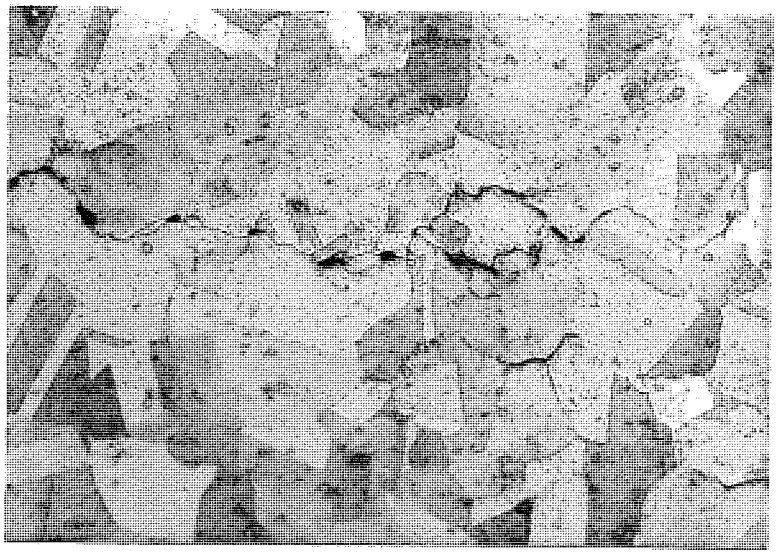

Fig 99. Fine grain boundary cracking in HAZ x340

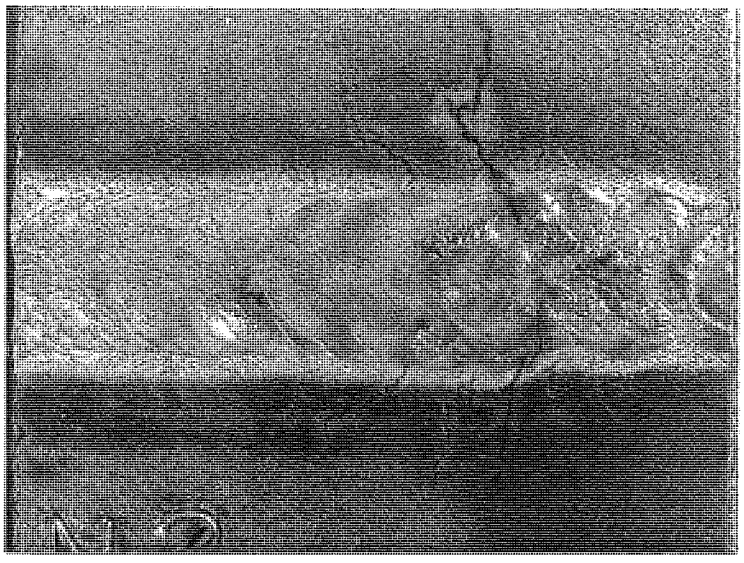

Fig 100. Pattern of cracking in a typical IN768
Varestraint test region x3

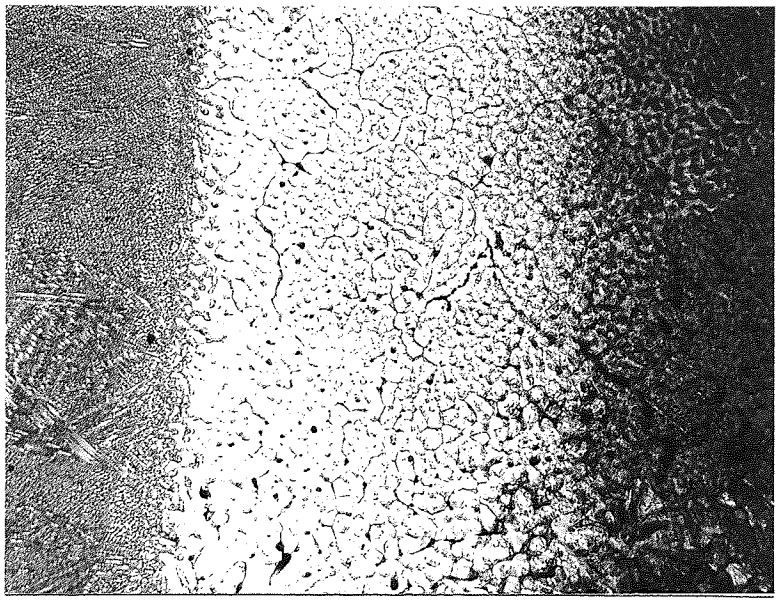

Fig 101. Weld metal and HAZ in IN768 alloy x30

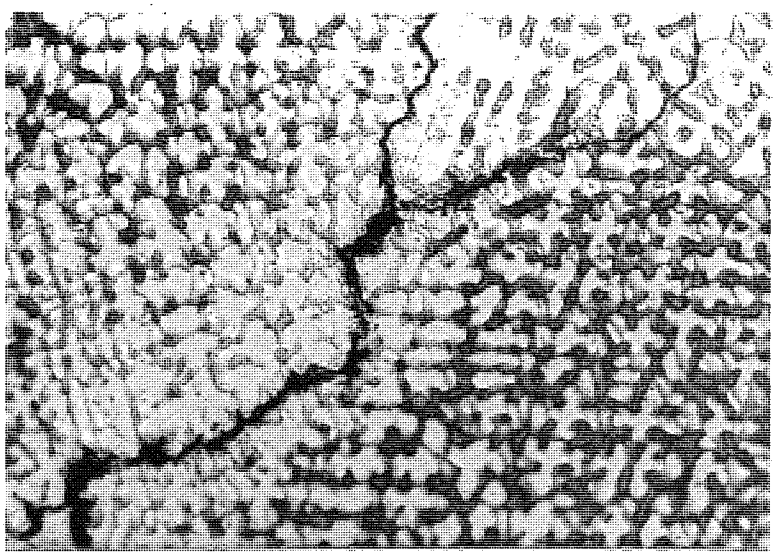

Fig 102. Weld metal cracking in IN768 Varestraint test x340

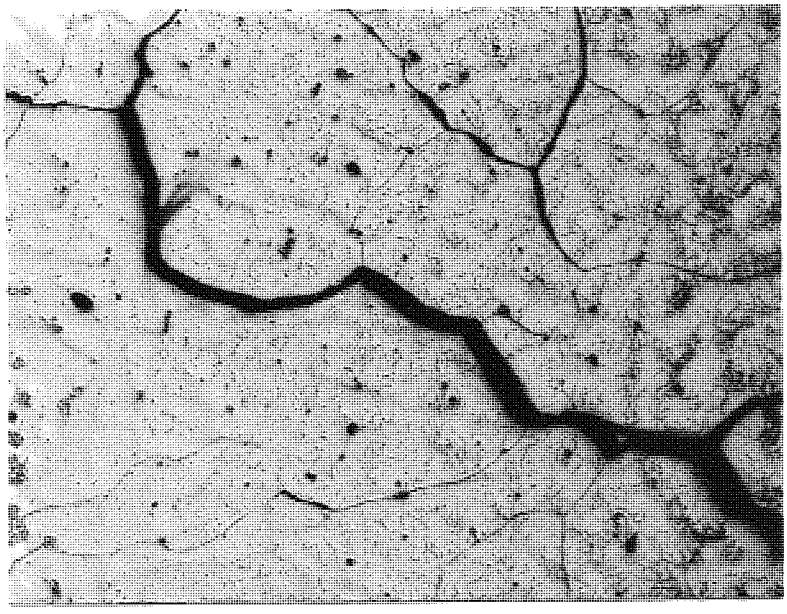

Fig 103. HAZ cracking close to fusion line in IN768 Varestraint test x70

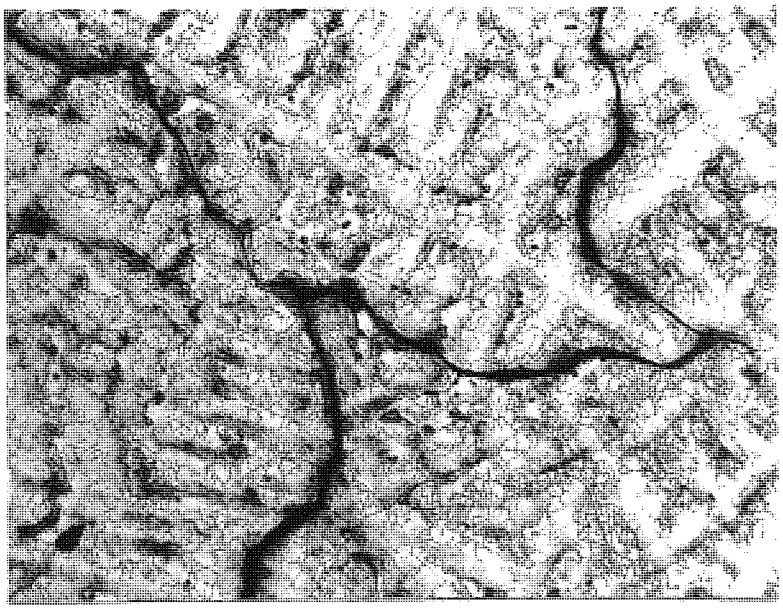

Fig 104. HAZ cracking distant from fusion line in IN768 Varestraint test x70

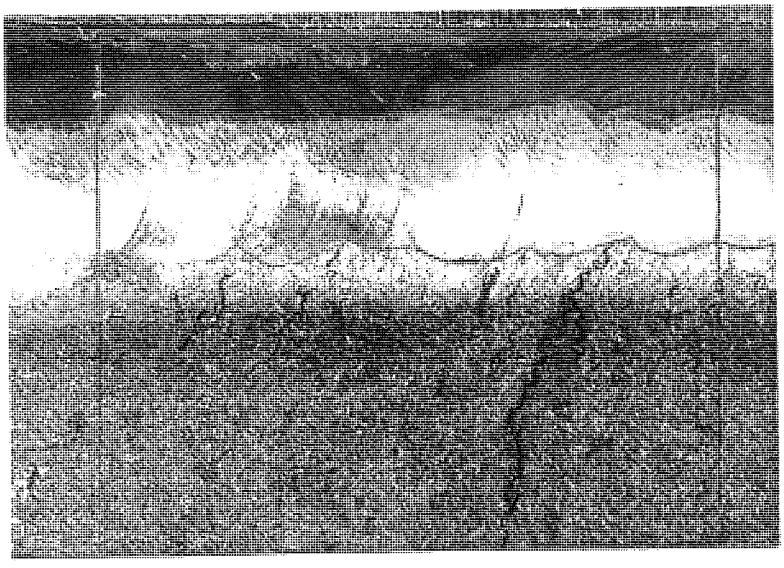

Fig 105. Cracking in butt weld with low crack susceptibility (K2) x3

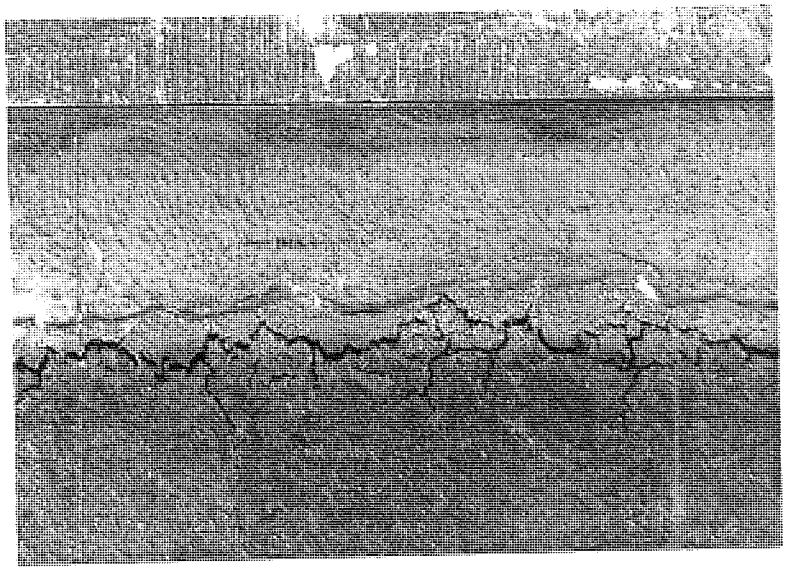

Fig 106. Cracking in butt weld with high crack susceptibility (N2) x3

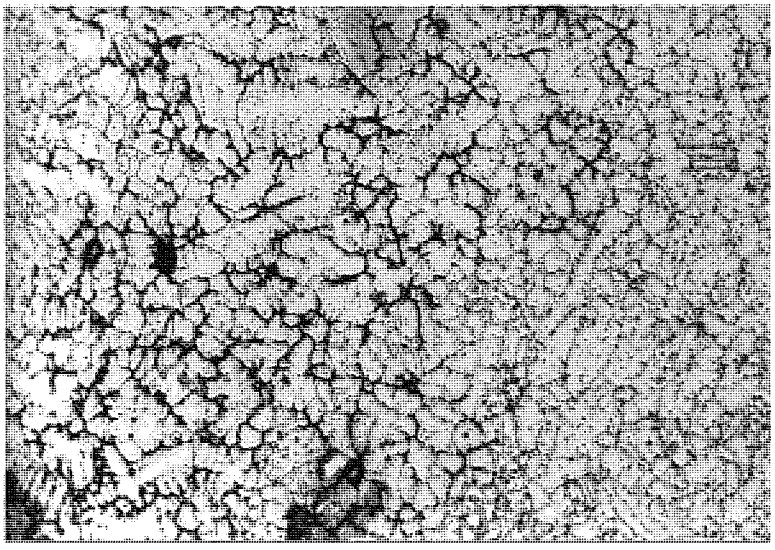

Fig 107. Liquated region near to fracture surface x140

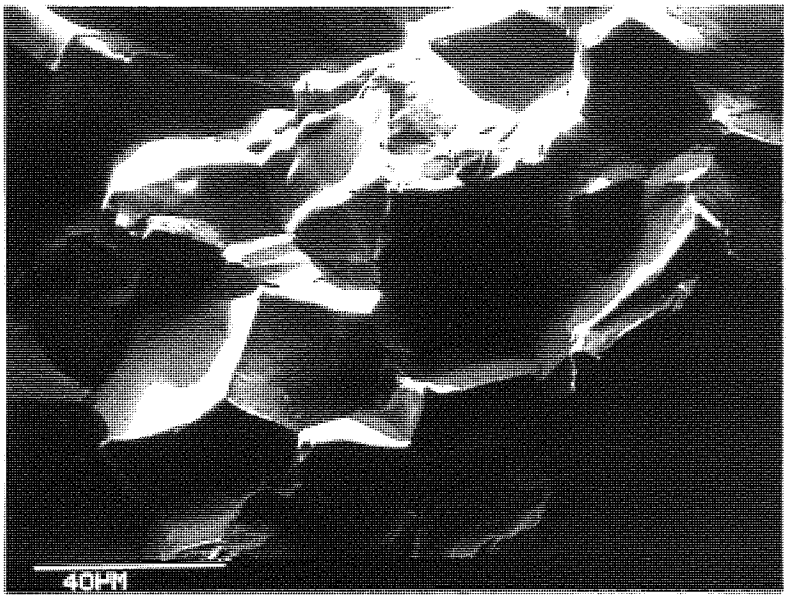

Fig 108. Fracture surface from alloy H6, tested on cooling at 1000 C x500

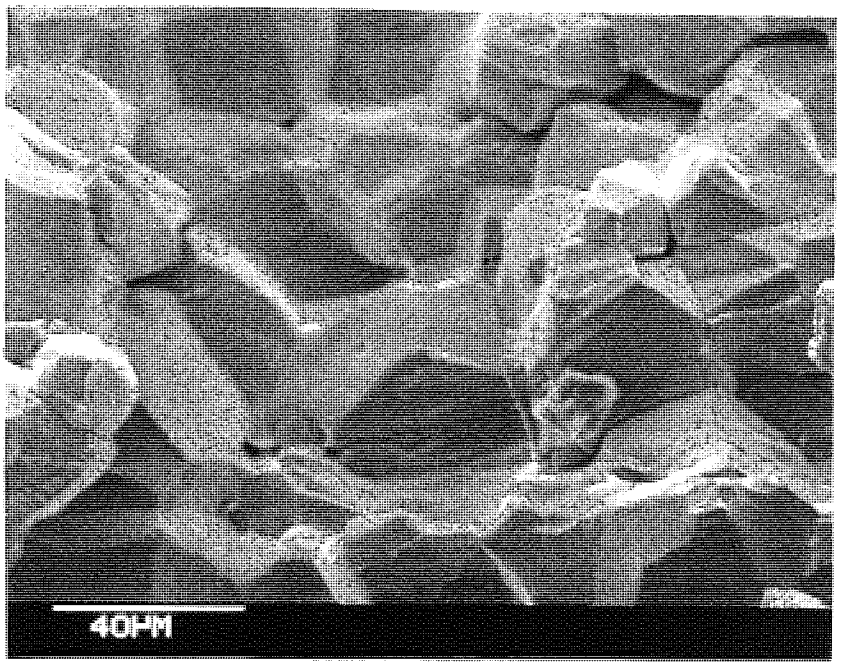

Fig 109. Fracture surface from alloy H6, tested on cooling at 1100 C x500

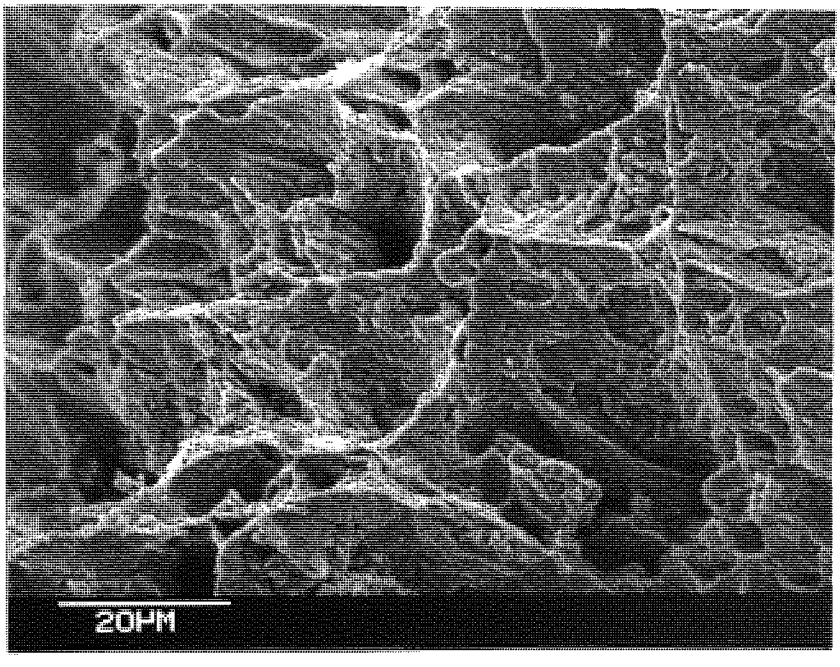

Fig 110. Fracture surface from alloy H5, tested on heating at 1057 C x1K

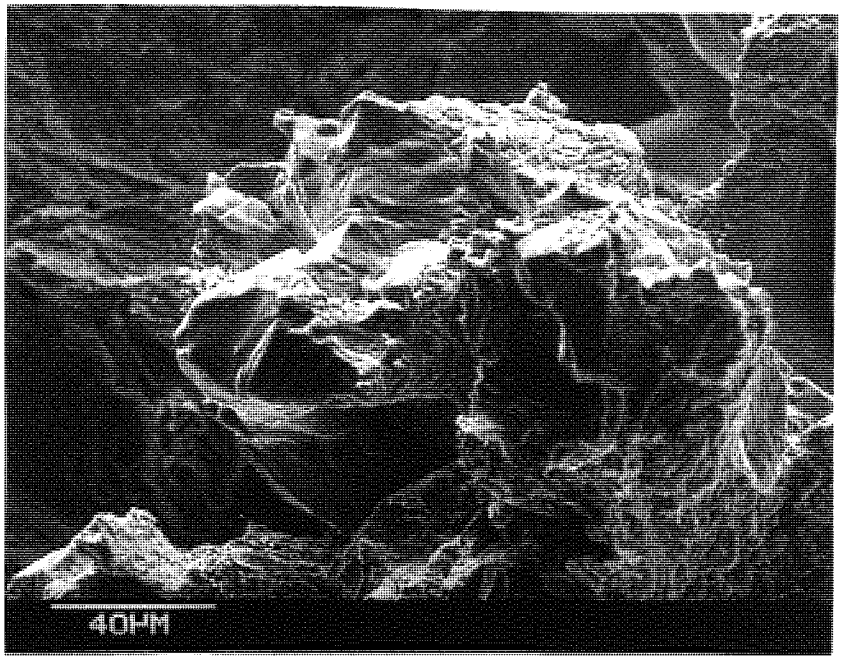

Fig 111. Fracture surface from alloy H1, tested on heating at 1150 C x500

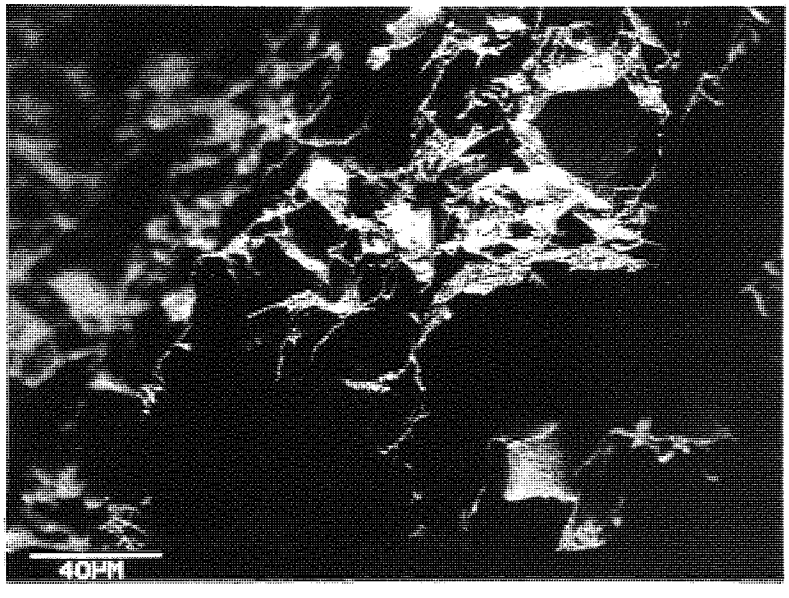

Fig 112. Fracture surface from alloy S3, tested on cooling at 850 C x500

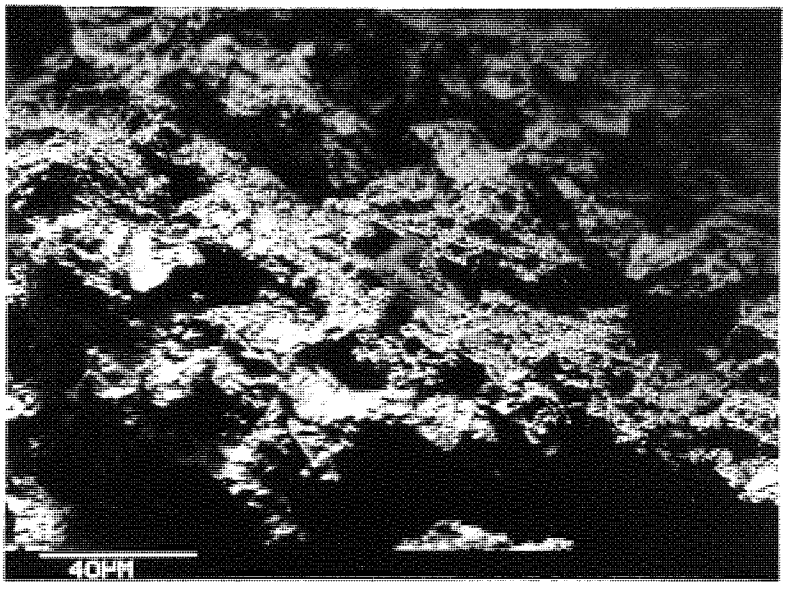

Fig 113. Fracture surface from alloy S3, tested on cooling at 1150 C x500

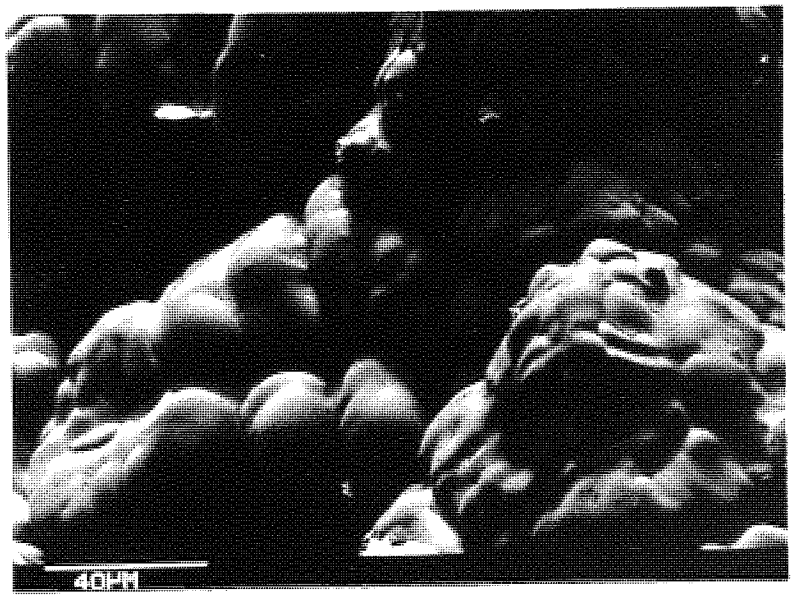

Fig 114. Fracture surface from alloy R1, tested on cooling at 1095 C x500

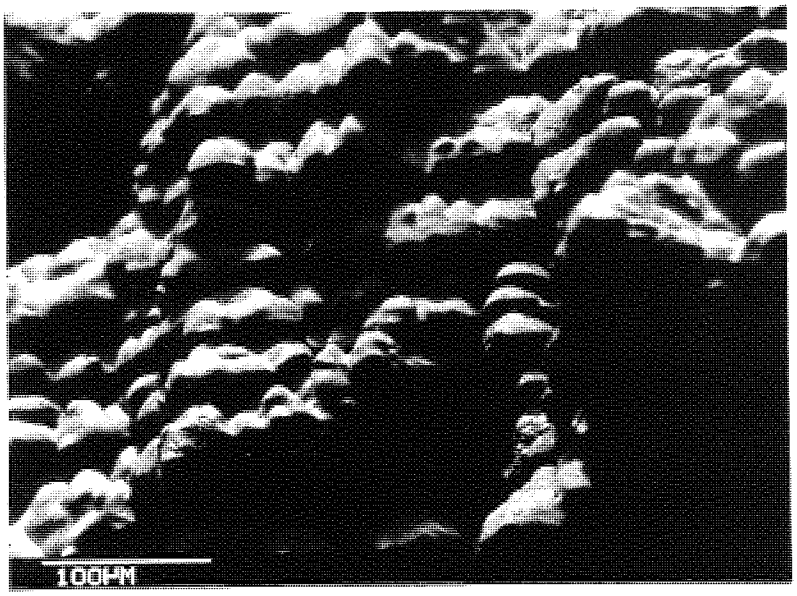

Fig 115. Fracture surface from alloy R1, tested on cooling at 1131 C x200

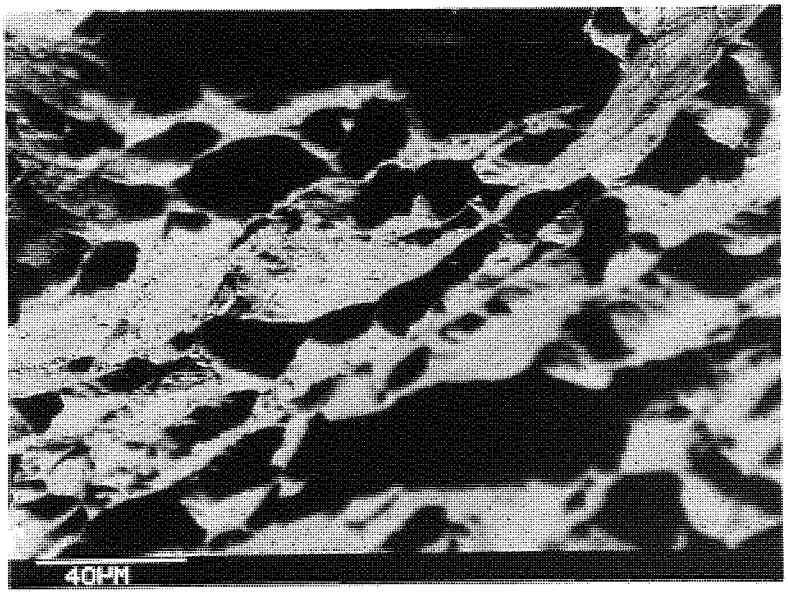

Fig 116. Fracture surface from alloy R1, tested on cooling at 450 C x500

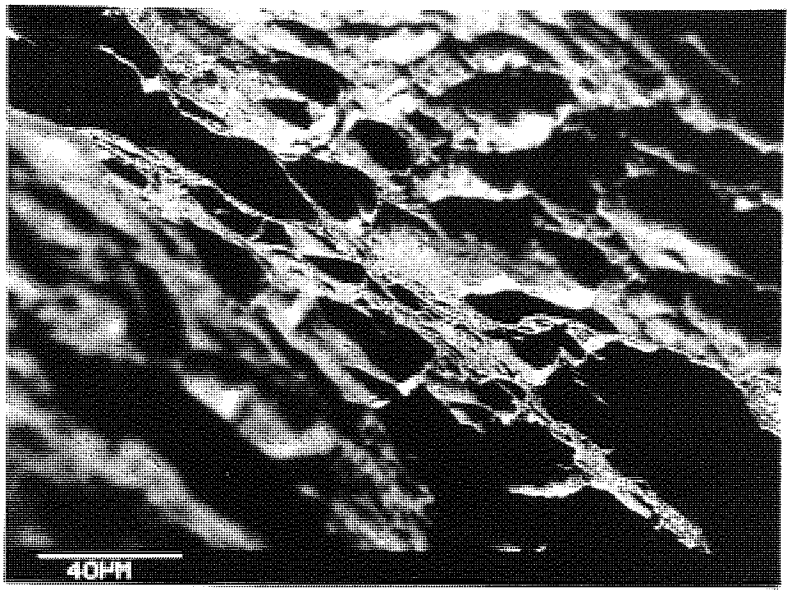

Fig 117. Fracture surface from alloy R1, tested on cooling at 850 C x500

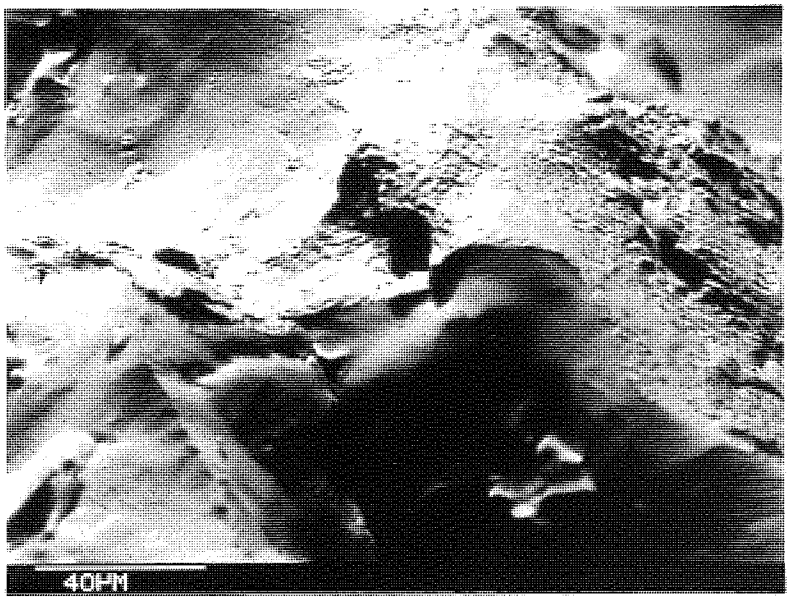

Fig 118. Fracture surface from alloy R7, tested on cooling at 1130 C x500

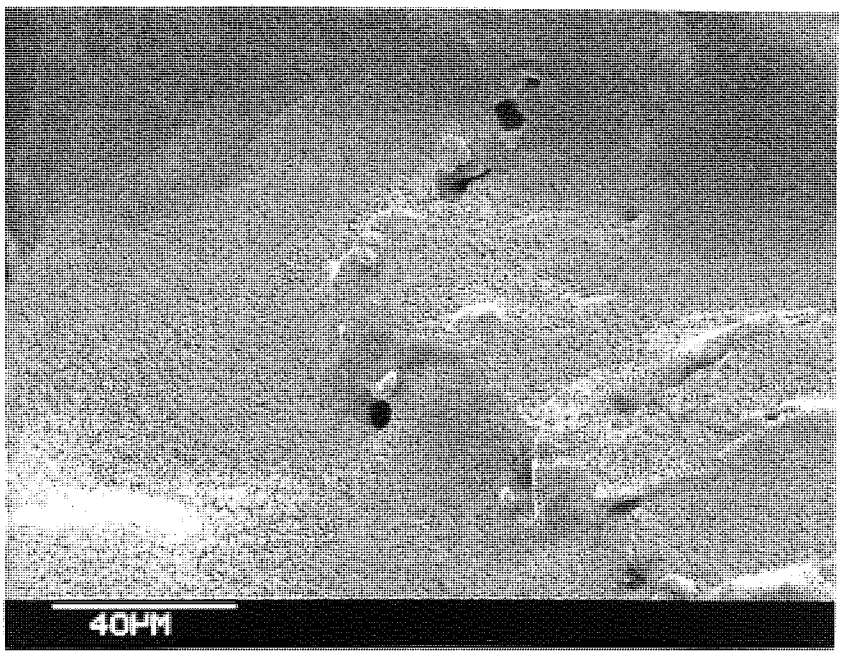

Fig 119. Fracture surface from alloy R7, tested on cooling at 1100 C x500

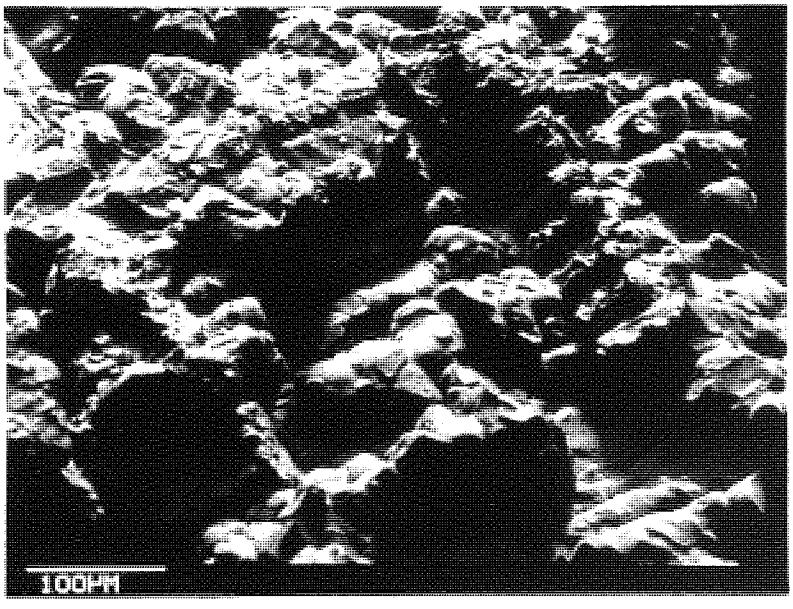

Fig 120. Fracture surface from alloy R7, tested on cooling at 850 C x200

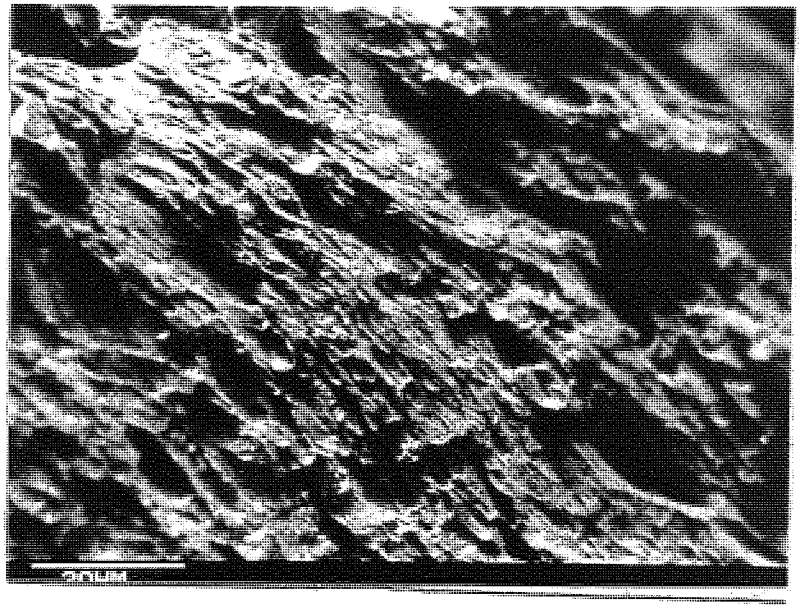

Fig 121. Fracture surface from alloy R7, tested on cooling at 650 C x1K

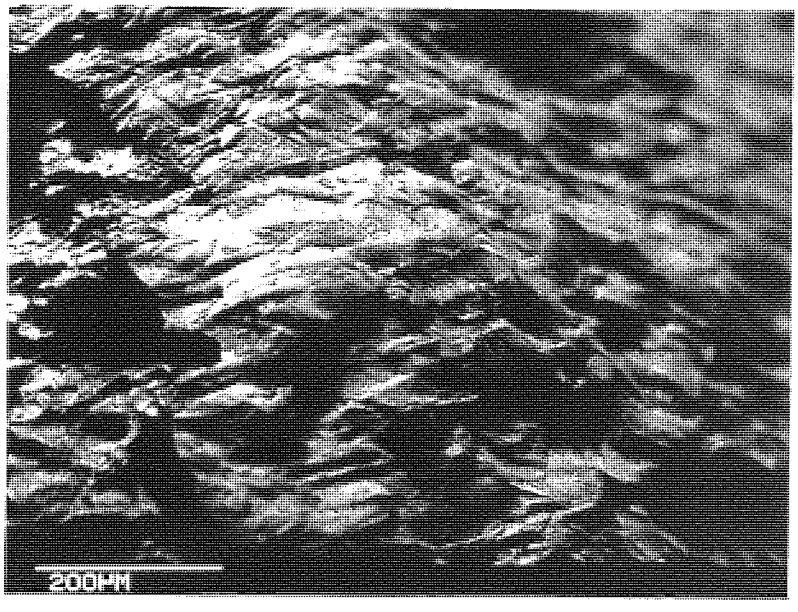

Fig 122. Fracture surface from alloy R7, tested on heating at 860 C x100

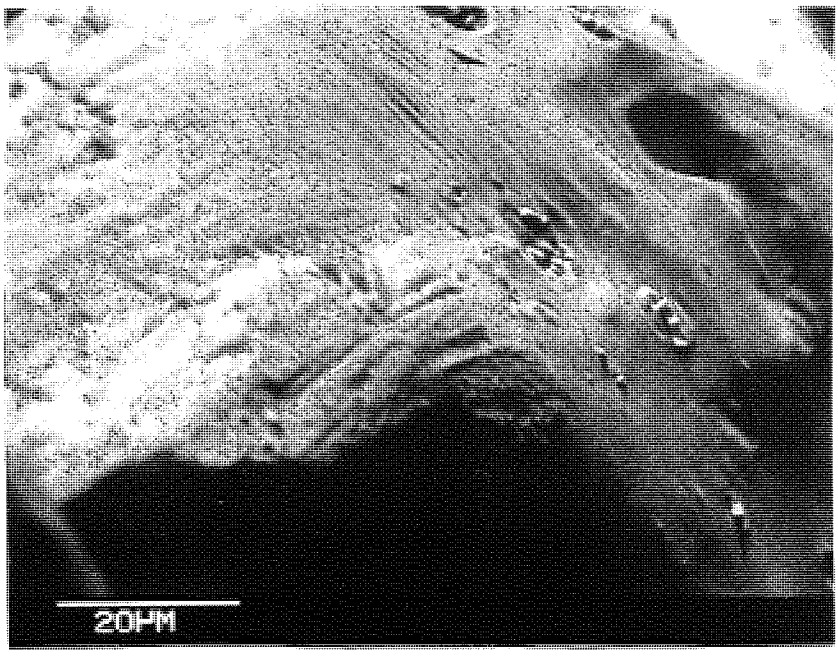

Fig 123. Fracture surface from alloy T4, tested on heating at 1150 C x1K

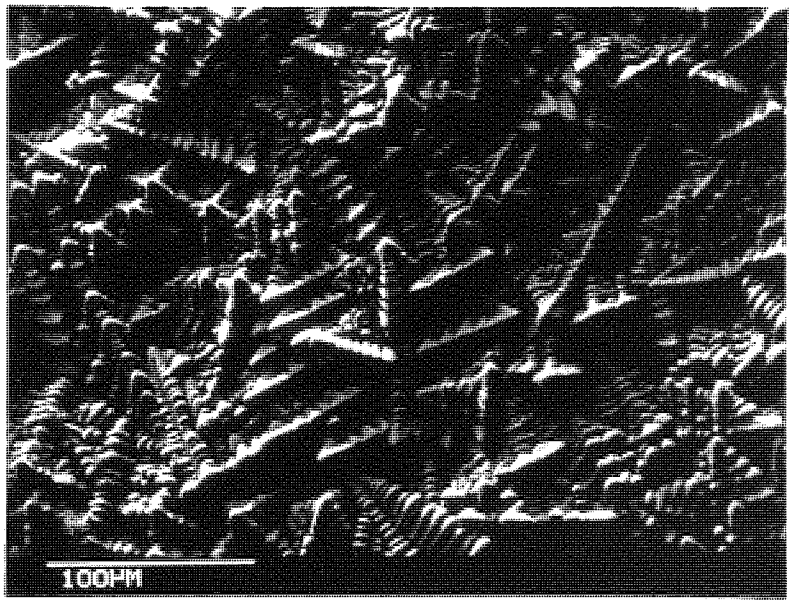

Fig 124. Fracture surface from alloy T6 (bulk melting) x200

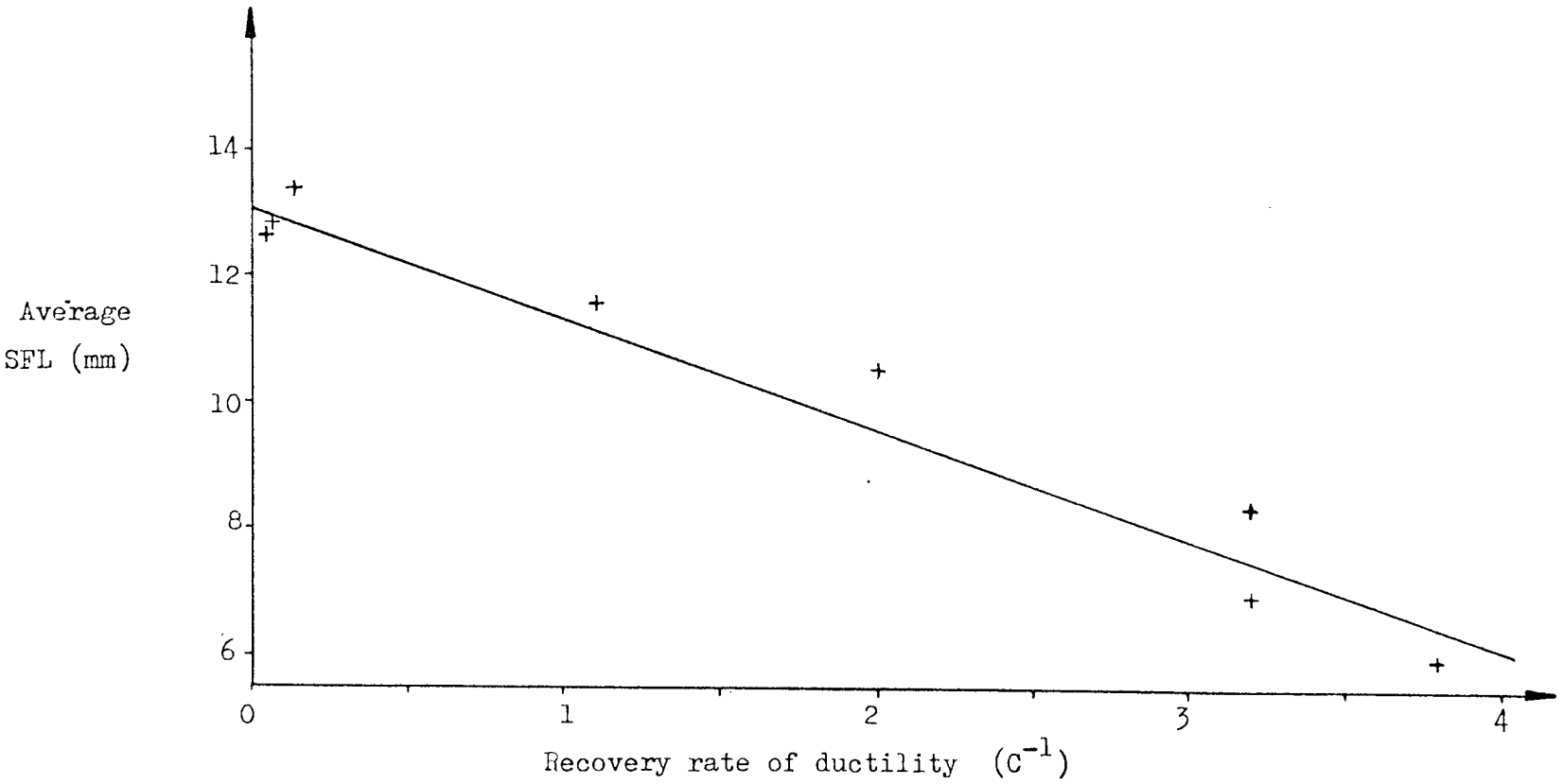

Fig 125. Plot of average sum of five longest cracks against recovery rate of ductility for second series wrought alloys

APPENDIX C
CALCULATION OF REPLICATION REQUIREMENTS

APPENDIX C CALCULATION OF REPLICATION REQUIREMENTS

The method of calculating the number of replicates requires a value for standard deviation, and also decisions regarding the level of significance needed and the smallest change in crack susceptibility which is desired to be detected. As no prior experimental data were available, the results of Lee et al (8) were used for determining the standard deviation. They carried out three replicates of each test, and the standard deviation is calculated from these. The results obtained divide into three groups according to low, medium and high phosphorus, and the high phosphorus group seems to correspond to the results obtained from the current experimental alloys. These results were therefore used for the analysis and are shown in Table C-1, together with the mean and range of each set of three.

From these, the mean range can be calculated, $\bar{R} = 6.322$, and also the grand mean, $\bar{\bar{x}} = 19.362$.

The standard deviation is then given by:-

$$s = \frac{\bar{R}}{d_n}$$

where $d_n = 1.6926$ for $n = 3$

$$s = \frac{6.322}{1.6926} = 3.735$$

The difference being sought is $(\bar{x}_1 - \bar{x}_2)$.

If the largest difference which is allowable is 10% of the mean,

$$\text{then } (\bar{x}_1 - \bar{x}_2) = 19.362 \times \frac{10}{100} \times \frac{5}{3.735}$$

$$(\bar{x}_1 - \bar{x}_2) = 0.518 \text{ s}$$

The comparison of two means is carried out using the t-test,

$$\text{where } t = \frac{\bar{x}_1 - \bar{x}_2}{s\sqrt{\frac{1}{n_1} + \frac{1}{n_2}}}$$

If a significance of 5% is required, and the number of degrees of freedom is assumed to be 30,

$$t = 2.04$$

$$2.04 = \frac{0.518 \text{ s}}{s\sqrt{\frac{1}{n_1} + \frac{1}{n_2}}}$$

The same number of tests will be carried out at both high and low levels, so $n_1 = n_2$

$$2.04 = \frac{0.518}{\sqrt{\frac{2}{n}}}$$

$$\frac{2}{n} = \frac{0.518}{2.04}$$

$$n = \left(\frac{2.04}{0.518}\right)^2 \times 2 = 31$$

Therefore, 31 tests are required at both high and low levels. This will be achieved by four replicates of sixteen experiments.

This calculation is based on weld metal cracking. A similar calculation can be carried out for ductility dip cracking in the base metal. The figures on which this is based are shown in Table C-2.

$$\bar{R} = 5.126$$

$$\bar{\bar{x}} = 9.185$$

$$s = \frac{5.126}{1.6926} = 3.028$$

$$(\bar{x}_1 - \bar{x}_2) = 9.185 \times \frac{10}{100} \times \frac{s}{3.028}$$

$$= 0.303\ s$$

Subjecting this to the t-test

$$2.04 = \frac{0.303\ s}{s\ \frac{2}{n}}$$

$$\frac{2}{n} = \frac{0.303}{2.04}$$

$$n = \left(\frac{2.04}{0.303}\right)^2 \times 2 = 91$$

Ninety-one tests at high and low level requires eleven replicates of the sixteen experiments to be carried out.

Table C-1 Weld Metal Total Crack Lengths in 70/30 Cupronickel after Lee et al (8)

Set of results	Crack Lengths mm				
	Replication			Mean	Range
	1st	2nd	3rd		
A	17.65	18.44	18.08	18.06	0.79
B	21.64	19.18	28.19	23.01	9.01
C	27.94	13.31	17.15	19.71	14.63
D	19.30	19.56	18.92	19.25	0.64
E	18.85	16.46	20.57	18.62	4.11
F	16.26	16.41	22.68	18.44	6.42
G	18.34	12.24	22.43	17.68	10.19
H	19.18	23.37	18.59	20.37	4.78

Table C-2 Base Metal Total Crack Length in Welded 70/30 Cupronickel, after Lee et al (8)

Set of results	Crack Length mm				
	Replication			Mean	Range
	1st	2nd	3rd		
A	11.28	4.78	18.49	11.51	13.71
B	9.91	8.76	11.81	10.16	3.05
C	11.30	10.41	8.31	10.00	2.99
D	5.44	8.69	10.46	8.20	5.02
E	13.03	11.05	11.25	11.79	1.98
F	7.21	11.81	10.21	9.75	4.60
G	3.35	3.66	8.48	5.16	5.13
H	7.62	8.89	4.19	6.91	4.70

APPENDIX D
COMPUTER PROGRAM FOR THERMAL SIMULATION

```
 10 REM **** SELECT PROGRAM SECTION ****
 20 PNT 15
 30 PRINT PRINT "SELECT OPTION"
 40 PRINT PRINT "          1 - TESTING"
 50 PRINT "          2 - LOAD CALIBRATION"
100 PRINT INPUT "  OPTION REQUIRED? "C9
110 ON C9 GOTO 140,3120
120
130 REM **** SET CONSTANTS & DIMENSIONS ****
140 PNT 5
150 PNT 10
160 DIM A(4),B(5)
170 DIM D1(200),C'(200,3)
180 DIM E(100),L(100),L1(100)
190 DIM A$(1),C$(1),Q$(1)
191 DIM N$(2)
192 DIM P$(2)
200 DIM V3(830),E3(830),I3(830),M3(830),T(830)
210 INPUT " INITIAL VOLTAGE " M
220 S=.1 G=.006 C=6
260 R3=3.5 Y=.02 P=.9
270 G3=.56
300 I3(1)=R3/G3
400 S1=.1 T1=.002
420 INPUT "BREAKING TEMPERATURE "T
425 T=T+1.5
430 IF T>1065 GOTO 510
440 IF T>631 GOTO 480
450 V1=5.28913*T+1.39111E-2*T^2-2.40052E-5*T^3
460 V1=V1+3.84977E-14*T^6-1.53726E-17*T^7
470 V1=V1+3.62014E-8*T^4-4.4645E-11*T^5
475 GOTO 540
480 A(1)=-2.6418E2 A(2)=8.04687
490 A(3)=2.98923E-3 A(4)=-2.68761E-7
500 GOTO 530
510 A(1)=1.49017E3 A(2)=2.86399
520 A(3)=8.08236E-3 A(4)=-1.93385E-6
530 V1=POLY(T,A(1),4)
540 V1=V1/1E3
550
560 REM *** SCAN ARRAY ***
570 REM *** CHAN. 0 = LOAD ,CHAN. 1 = POSN. ***
580 FOR B=1 TO 199 STEP 2
590   C'(B,1)=0 C'(B,2)=0 C'(B,3)=0
600   C'(B+1,1)=0 C'(B+1,2)=1 C'(B+1,3)=0
610 NEXT B
620 Z' = 0 M1 = M Q1 = 0
630 Q9=0 F1=0 F3=0
640 ACT(1,1)=M
650
660 REM **** START OF TEST SEQUENCE ****
670 PRINT PRINT "SWITCH TO MACSYM CONTROL"
```

```
 680 INPUT "PRESS 'C' & RETURN TO CONTINUE " C$
690 IF C$<> "C" THEN  END
 700 PRINT PRINT PRINT "                    **** TEST COMMENCED ****"
 720 T3=((AIN(3,15,2)-AIN(3,0,2))/5E-3-273.15)*5.62
 730 T3 = T3/1000
 740
 750 REM **** MAIN TASK ****
 760 TASK 1,860,2
 770 TASK 2,980
 780 TASK 3,1120,2
790 TASK 4,1410,2
 800 TASK 5,1470,2
 805 TASK 6,1950
 810 ACTIVATE 1
 820 ACTIVATE 2
 830 WAIT 1 IF Q9=0 GOTO 830
 840 END
 850
 860 REM **** LOAD CONTROL ****
 870 U1=-AIN(0,0)
 880 E=S-U1
 890 M = M-G*(E+(E-F1)*C)
 900 AOT(1,1)=M
 910 IF Q1 = 1 GOTO 930
 920 IF U1>=S THEN  Q1=1 ACTIVATE 3
 930 F1 = E
 940 WAIT .03
 950 GOTO 870
 960
 970 REM **** SAFE ****
 980 INP I
 990 IF I<>32 GOTO 980
 995 IF TSTATE(3)<>-1 THEN  KILL 3
1000 AOT(1,3)=0
1010 PRINT "PRESS 'E' TO END LOAD CONTROL"
1020 INP A1 IF A1<>69 THEN GOTO 1020
1030 AOT(1,1)=M1 KILL ALL
1040 PRINT
1050 INPUT "IS CONTROL BACK ON MAND? " A$
1060 IF A$="Y" GOTO 1080
1070 GOTO 1050
1080 PRINT PRINT "  TEST HALTED"
1090 Q9=1 KILL SELF
1100
1110 REM **** TEMPERATURE CONTROL ****
1120 PRINT "           **** IN HEATING CYCLE ****" PNT 7
1130 WAIT 10
1140 FOR Z'=2 TO 830
1150   V3(Z')=AVG(3,5,9.40,.00025)*1E3+T3
1160    IF V3(Z')<-.2 THEN  RESET FOR GOTO 1350
1170    IF V3(Z')>13.2 THEN  RESET FOR GOTO 1350
1180    IF Z'<115 GOTO 1200
1190    IF V3(Z')<=V1 THEN  AOT(1,3)=0 SUSPEND 1
1191    ACTIVATE 5 ACTIVATE 4 SUSPEND SELF
```

```
 1200 AOT(1,0)=V3(Z')/2
 1210 E3(Z')=T(Z')-V3(Z')
 1220 I3(Z')=I3(Z'-1)+E3(Z')*Y
 1230 IF E3(Z')<0 THEN  E3(Z')=0
1240 IF Z'>200 GOTO 1260
 1250 IF I3(Z')<I3(1) THEN  I3(Z')=I3(1)
 1260 D3=(E3(Z')-F3)*P
 1270 IF D3<0 THEN  D3=0
 1280 M3(Z')=G3*(E3(Z')+I3(Z')+D3)
 1290 F3= E3(Z')
 1300 IF M3(Z')>5.4 THEN  M3(Z')= 5.4
 1310 IF M3(Z')<2 THEN  M3(Z') = 2
 1320 AOT(1,3)=M3(Z')
 1330 WAIT .03
 1340 NEXT Z'
 1350 AOT(1,3)=0
 1360 PRINT "TEMPERATURE OUT OF LIMITS"
 1370 KILL SELF
 1390
 1400 REM **** STRAIN ****
 1410 FOR Z=M TO M-5 STEP -S1
 1420   AOT(1,1)=Z
 1430 'NEXT Z
 1440 KILL SELF
 1450  '
 1460 REM **** COLLECT DATA ****
 1470 SCAN (C'(1),200,T1) INTO D1(1)
 1480 ACTIVATE 6 KILL 2 KILL SELF
 1500
 1950 REM **** SAVE TEMP. & TENSILE ARRAYS ****
 1952 PRINT PRINT PRINT "SWITCH TO CONSOLE "
 1955 INPUT "TEST NO? " L7
 1960 PRINT PRINT " INSERT DATA TAPE "
 1965 INPUT "TAPE NO? "N5
 1970 INPUT "TEMP. FILE NO? "N1
 1975 INPUT "IS PLOTTER AVAILABLE? " Q$
 1980 INPUT "ALLOY CODE? " F$
 2000 OPENW :6 "MTO:"STR$(N1)
 2010 SAVE ARRAY :6 V3(2),Z'-1
 2015 CLOSE
 2020 N$=STR$(N1+1)
 2030 SAVE ARRAY D1(1) "MTO:"N$
 2040 CLOSE
 2051
 2052 REM **** CALCULATE MAXIMA ****
 2058 D3=0
 2062 FOR B3=1 TO 199 STEP 2
 2064   IF D1(B3)<D3 THEN  D3=D1(B3)
 2065   IF D1(B3)<D3 THEN  D3=D1(B3) B4=B3
 2068 NEXT B3
 2070 K1=1
 2072 FOR K=3 TO 199 STEP 2
 2076   K1=K1+1
```

```
2080 L(K1)=-D1(K)*1E3/(9*PI)
2084 E(K1)=((D1(K-1)+D1(K+1))/2-D1(2))*100/15
2085 E(K1)=E(K1)*10./3
2087 NEXT K
2100 L2=0
2110 FOR K2=2 TO 100
2130   L1(K2)=L(K2)*(1+E(K2)/100)
2133   IF L1(K2)>L2 THEN  L2=L1(K2) K3=K2
2140 NEXT K2
2499
2500 REM **** GRAPH PLOTTING (TENSILE) ****
2510 IF Q$="N" GOTO 2930
2520 OPENW :4 "$QTO:0"
2530 PRINT :4 "IN";
2540 PRINT :4 "DT",CHR$(5);
2550 PRINT :4 "SP1";
2560 PRINT :4 "IP1000,1000,10000,7400";
2570 L6=50*INT(1.2+(-D3*1E3/(50*9*PI)))
2575 L5=40
2580 PRINT :4 "SCO",L5,"0",L6
2590 PRINT :4 "PU";
2600 PRINT :4 "PA 0,0";
2610 FOR I=1 TO 3
2620   PRINT :4 "PD;PA",L5,"0",L5,L6,"0",L6,"0,0"
2630 NEXT I
2640 PRINT :4 "PU";
2650 PRINT :4 "SI.18,.23;TL1.5,0"
2660 WAIT 8
2670 FOR X=0 TO L5 STEP 5
2680   PRINT :4 "PA",X,",0;XT;"
2690   PRINT :4 "CP-.33,-1;LB";X;
2691   PNT :4 5
2700   WAIT .5
2710 NEXT X
2720 WAIT 3
2730 FOR Y6=0 TO L6 STEP 50
2740   PRINT :4 "PA0,";Y6,"YT;"
2750   PRINT :4 "CP-3.5,-.25;LB";Y6;
2751   PNT :4 5
2760   WAIT 1
2770 NEXT Y6
2780 WAIT 3
2790 PRINT :4 "DI0,1;PA0",L6*.45;"CP0,4;LBSTRESS-N/MM2 "
2800 PRINT :4 "DI;PA",L5*.45,"0;CP0,-2.5;LBSTRAIN-% "
2810 PRINT :4 "PA",L5*.12,L6*.85;"LBTEST-";L7;" "
2820 WAIT 8
2830 PRINT :4 "PA0,0;PD"
2840 FOR J=2 TO K3
```

```
 2850 IF L(J)>L6 THEN  L(J)=L6
 2860 IF L(J)<.01 THEN  L(J)=0
 2870 IF E(J)>L5 THEN  RESET FOR GOTO 2910
 2880 IF E(J)<0 THEN  E(J)=0
 2885 IF E(J)=E(J-1) THEN  E(J)=(E(J)+E(J+1))/2
 2890 PRINT :4 "PA",E(J),",",L(J);
 2900 NEXT J
 2910 PRINT :4 "PU";
 2920 CLOSE
 2930 REM **** PRINT RESULTS ****
 2940 OPENW :2 "$QTO:1"
 2950 PRINT :2 "TEST NO. ";L7
 2955 PRINT :2 PRINT :2 " ALLOY CODE ";P$
2960 PRINT USING :2 "STRAIN RATE =-##.## /S",E(98)/T1*1.0202E-4
 2970 PRINT :2 "MAXIMUM STRESS = ";INT(-D3*1E3/(9*PI));" N/MM2"
 2980 PRINT USING :2 " TOTAL ELONGATION =-##.#%",E(K3)*.7267
 2990 V9=0
 3000 FOR B1=1 TO Z'
 3010   IF V3(B1)>V9 THEN  V9=V3(B1)
 3020 NEXT B1
 3030 V7=V9 GOSUB 3190
 3040 'PRINT :2 PRINT :2 " PEAK TEMPERATURE = ";INT(T7);" C"
 3050 V7=V3(Z') GOSUB 3190
 3060 PRINT :2 PRINT :2 " BREAKING TEMPERATURE = ";INT(T7);" C"
 3070 PRINT :2 PRINT :2 " THERMAL TAPE/FILE ";N5;"/";N1
 3080 PRINT :2 PRINT :2 " TENSILE TAPE/FILE ";N5;"/";N1+1
 3083 PRINT :2 PRINT :2 " NO. OF TEMPERATURE POINTS = ";Z'-1
 3090 CLOSE
 3100 Q9=1 KILL ALL KILL SELF
 3110
 3120 REM **** LOAD CALIBRATION ****
 3130 L=-AVG(0,0,3,40)
 3140 PRINT USING " -#.##",L
 3150 WAIT 1
 3160 GOTO 3130
 3170 END
 3180
 3190 REM **** MV TO TEMP. CONVERSION ****
 3200 IF V7<3.407 GOTO 3250
 3210 B(1)=4.83437E1 B(2)=1.10983E-1 B(3)=-2.43539E-6
 3220 B(4)=4.51645E-11 B(5)=1.81726E-16
 3230 T7=POLY(V7*1E3,B(1),5)
 3240 RETURN
 3250 B(1)=0 B(2)=1.52395E-1 B(3)=-1.37557E-5
 3260 B(4)=1.26109E-14 B(5)=-4.42813E-14
 3270 GOTO 3230
 9990
 9991 REM **** LOAD ARRAY ****
 9992 DIM T(830)
 9993 LOAD ARRAY T(1) "MTO:2"
 9994 END
 9995 LOAD ARRAY D(1) "MTO:7"
 9998
 9999 REM **** LOAD ARRAY ****
10000 DIM T(830)
11000 LOAD ARRAY T(1) "MTO:2"
11500 END
12000 LOAD ARRAY D(1) "MTO:7"
```

REFERENCES

1. Witherell, C.E. Weld. J, 1960 39 (9) 411s-416s.

2. Calvert, D. S. The British Foundryman, 1969 42 (1) 1.

3. Petersen, W. A. Weld. J, 1969 48 (10) 425s-430s.

4. Jordan, D. E. Weld and Met. Fabr., 1972 40 (9) 323-327.

5. Pease, G. R. and Kihlgren, T. E., Weld J, 1954, 33 (4) 329-338.

6. Scott, M. H. Met. Constr, 1972, 4 (8) 292-296.

7. Savage, W. F., Nippes, E. F. and Casteras, J. E., Weld J, 1978, 57 (12) 375s-382s.

8. Lee, J. W., Nichols, E. E. and Goodman, S. Weld J, 1968. 47 (8) 371s-377s.

9. Matthews, S. J. Weld. J, 1968, 47 (4) 155s-161s.

10. Hemsworth, B; Boniszweski, T and Eaton, N. F. Met. Constr, 1969. 1 (2s) 5-16.

11. Holsberg, P. W. Weld J, 1970 49 (12) 554s-558s.

12. Chubb, J. P. and Billingham, J. Metals Tech, 1978. 5 (3) 100-103.

13. Chubb, J. P, Billingham, J, Hancock, P, Dimbylow, C and Newcombe, G. J. Metals, 1978. 30 (3) 20-25.

14. Gavin, S.A, Chubb, J. P. and Billingham, J. Grain Boundaries, 1976 Institution of Metallurgists, London, 1976. C25-C30.

15. Gavin, S. A., Billingham, J. Chubb, J. P., and Hancock, P. Metals Tech, 1978, 5 (9) 397-401.

16. Lupton, D. F. and Thompson, J. R. J. Inst. Met, 1972. 100 352-356.

17. Evans, R. W. and Jones, F. L. Metals Tech, 1978. 5 (1) 1-6.

18. Middleton, C. J., Ph.D. Thesis, University of Leeds 1971.

19. Bailey, G. L. J. Inst. Met., 1951 79 243-292.

20. Dimbylow, C. S. High strength copper-nickel casting alloys for pressurised seawater systems. Report AMTE (M)/R78/008.

21. British Standards Institute. BS 2871:Part 3:1972. Standards for copper and copper alloy tubes.

22. Hall, B. N. Metallurgia, 1966. 74 251-254.

23. Dimbylow, C. S. and Dawson, R. J. C. Copper alloys in the marine environment. Paper 5. Copper Development Association, 1978.

24. Gilbert, P. T. Metall. and Mat. Tech, 1978 10 (6) 316-319.

25. Gilbert, P. T., Br. Corr. J, 1979. 14 (1) 20-25.

26. Glover, T. J. Cupro-nickel alloys for anti-fouling. Symposium. 29th Jan. 1980. Paper 1, Copper Development Association.

27. Badia, F. A; Kirby, G. B. and Mihalisin, J. P. Trans. ASM 1967. 60 395-401.

28. Bower, D; Lorimer, G. W., Saunderson, I, and Wilkes, P. Metals Tech, 1980, 7 (3) 120-126.

29. Savage, W. F., Nippes, E. F., and Miller, T. W., Weld J. 1976. 55 (6) 165s-173s.

30. Vanick, J. S. Foundry, 1952. 80 100-105, 246-248, 250-253.

31. Shepherd, B. F. Modern Castings, 1960. 37 (5) 120-130.

32. French, R. S. and Evans, J. K. Modern Castings, 1966. 50 (2) 60-63.

33. Ansuini, F. J. and Badia, F. A. Modern Castings, 1970. 58 (3) 165-168.

34. Townsend, D. W. BNF Research Report A1671. Dec. 1967.

35. Guha. P, Brown, D, and Littlewood, G. J. Inst. Met, 1971. 99 148-155.

36. Dimbylow, C. S. and Jones, R. L. CDL Report 11/75 Dec. 1975.

37. Bagley, D. S. and Brook, G. B. Fulmer Research Institute Report R298/6 May 1977.

38. INCO Europe. Guide to the welding of copper-nickel alloys. INCO Europe, 1979.

39. Banas, C. M. INCRA Project No. 241. Final Report March 1981.

40. Devine, J. and Krause, P. C. INCRA Project No. 295. Annual report July 1980.

41. Newcombe, G; Dimbylow, C and Jones, R. Welding of Castings - An International Conference. Vol. 1, 199-216. The Welding Institute 1976.

42. Copper Development Association. Technical Note. TN2. CDA London, Oct. 1970.

43. Clatworthy, D.S. Met. Constr., 1979. 7 (4) 182-183.

44. Dawson, R. J. C. Weld. Met. Fabr, 1976 44 (10) 703-711.

45. American Welding Society. Welding Handbook, Section 4. Metals and their weldability 6th edition 1972.

46. Henry Wiggin and Co. Publication 3409. August 1979.

47. Anderson, D. K.C. C.M.E., 1981 28 (10) 75-85.

48. Betteridge, W. Nickel and its alloys. Macdonald and Evans 1977.

49. Prager, M and Thiele, E. W., Weld J. 1979. 59 (7) 17-24.

50. Glover, T. J. Br. Corros, J, 1982. 17 (4) 155-158.

51. Banas, C. M. Weld Met. Fabr, 1983. 51 (6) 297-299.

52. Parker, M. N. Assessing Hull Surface deterioration B.S.R.A. Conference on hull surface maintenance. Nov. 1977, London.

53. Glover, T. J. Copper alloys in the marine environment Paper 7. Copper Development Association, 1978.

54. Moreton, B. B. and McDonald, Schectky, L. Copper alloys in the marine environment. Paper 9. Copper Development Association, 1978.

55. Bradley, R. Ph.D. Thesis. University of Leeds. 1975

56. Dimbylow, C. S. Private Communication.

57. Pumphrey, W. F. and Jennings, P. H. J. Inst. Met, 1948. 75, 235 - 256.

58. Pumphrey, W. F. and Lyons, J. V. J. Inst. Met., 1948, 74 439-455.

59. Singer, A. R. E. and Cotterell, S. A. J. Inst. Met, 1947. 73 33-54.

60. Singer, A. R. E. and Jennings, P. H. J. Inst. Met, 1947. 73 273-284.

61. Singer, A. R. E. and Jennings, P. H. J. Inst. Met, 1947. 73 197-212.

62. Pellini, W. S. Foundry, 1952, 80 (11), 124-133.

63. Apblett, W. R. and Pellini, W. S. Weld J, 1954. 33 (2) 83s-90s.

64. Borland, J. C. Brit. Weld J, 1960, 7 (8) 508-512.

65. Rhines, F. N. and Wray, P. J. Trans. ASM, 1961, 54 117-128.

66. Izumi, O and Harada, Y. Trans. J. I. M., 1970 11 292-299.

67. McKeown, D. Weld Inst. Res. Bull, 1974, 15, (3) 59-65.

68. McLean, D. J. Inst. Met, 1956-7. 85 468-472.

69. Powell, B. D. and Mykura, H. Acta Met, 1973. 21 (8) 1151-1156.

70. Yeniscavich, W. Weld. J., 1966. 45 (8) 344s-356s.

71. Krammer, D. A, Masubuchi, E. C. and Monroe, R. E. DMIC Report 197, 7 Feb. 1964.

72. Hawthorne, L. H. Weld J. 1953, 32 (1) 31-36.

73. IIT Research Institute, Report IITRI-B6098-3
14 November 1969.

74. IIT Research Institute. Report IITRI-B6106-9 19 Jan.
1971.

75. Stout, R. D; Tor, S. S; McGeady, L. J. and Doan, G. E.,
Weld J, 1946, 25 (9) 522s-531s.

76. Stout, R. D; Tor, S. S. McGeady, L. J. and Doan, G. E.
Weld J. 1947 26 (11) 673s-682s.

77. Otani, M. and Fujiwara, J. J. Japan, Weld Soc. 1947.
16 (5) 239-242.

78. Ando, S. J. Japan Weld Soc., 1953. 22 (8)
258-262.

79. Luther, C. G. Jackson, C. E. and Hartbower, C. E. Weld
J. 1946, 25 (7) 376s-384s.

80. White, S. S. Moffatt, W. G. and Adams, C. M. Weld
J, 1958, 37 (4) 185s-192s.

81. Houldcroft, P. T. Brit. Weld. J, 1955, 2 (10) 471-475.

82. Garland, J. G., and Davies, G. J. Met. Constr. 1969, 1 (1) 565-568.

83. Huxley, H. V. Brit. Weld. J., 1961 8 (11) 514-519.

84. Rollason, E. C. and Roberts, D. T. F. Brit. Weld. J., 1954 1 (10) 441-447.

85. Nakane, K; Muramoto, T; Kan, H and Yokoi, T. J. Japan Weld Soc., 1959. 28 (4) 229-235.

86. Nakane, K and Muramoto, T. IIW Doc. II-142-60.

87. Savage, W. F. and Lundin, C. D. Weld J. 1965 44 (10) 433s-442s.

88. Savage, W. F. and Nippes, E. F. Weld J. 1966, 45 (11) 497-503s.

89. Jordan, M. F. and Morgan-Warren, E. J. Latin American Congress on Welding Technology, Rio de Janeiro, Brasil. 15-19 Sept. 1975.

90. Cieslak, M. J. and Savage, W. F. Weld J. 1980, 59 (5) 136s-146s.

91. Lundin, C. D, Lingenfelter, A. C. Grotke, G. E., Lessman, G. G. and Matthews, S. J. Welding Research Council Bulletin 280.

92. Scott, M. H. Private Communication.

93. Savage, W. F. and Lundin, C. D. Rensselaer Polytechnic Institute Report, AFML-TR-68-48.

94. Matthews, S. J. Weld J. 1975, 54 (9) 281s-287s.

95. McKeown, D. Met. Constr. 1970, 2 (8) 351-352.

96. Garland, J. G. and Bailey, N. Weld Res. Inst. 1975, 5 (3) 1-33.

97. Brockhurst, P. J. and Muir, H. Weld Fabr. and Des, 1965, 9 (1) 80-86.

98. Taylor, E. A. and Burn, A. H. Inert gas welding of copper and its alloys. Proceedings of 2nd Commonwealth Welding Conference. 1966.

99. Casteras, J. E. INCRA Project No. 58. Final Report.

100. Savage, W. F, Nippes, E. F. and Miller, T. W. Weld J. 1976, 55 (7), 181s-187s.

101. Townsend, D. W. Eng. Mat. and Des. 1969. 12 1703-1706.

102. Dawson, R. J. C. Fusion welding and brazing of copper and copper alloys. Newnes Butterworths, 1973.

103. Bower, W. Private Communication.

104. Copper development Association. Welding brazing and soldering of copper and its alloys. Publication No. 47.

105. Smith, C. S. British patent No. 569 408.

106. Popham, B. J. Metall, 1983, 50 (4) 168-171.

107. McDonald Schectky, L. Memorandum to the committee on the weldability of copper base alloys. Welding Research Council. 4 Dec. 1979.

108. Conde, J. Dimbylow, C. S. and Newcombe, G. Private Communication.

109. The Iron Age, 10 Mar. 1966. 122-123.

110. Sahoo, M and Campbell, W. P. Anmerican Foundrymen's Society. 84th Annual Meeting, Conference Proceedings. 727-736.

111. Dickerson, W. C. and Zanis, C. A. A.F.S. Trans. 1973, 81 388-394.

112. Dimbylow, C. S. and Dawson, R. J. C. Weld Metal Fab. 1978. 46 (7) 461-471.

113. Bradley, J. N. Int. Met. Reviews, 1972, 17 81-99.

114. Nippes, E. F., Savage, W. F. Bastian, B. J. Mason, H. F. and Curran, R. M. Weld J, 1955, 34 (4) 183s-196s.

115. Weiss, B; Grotke, G. E. and Stickler, R. Weld J. 1970, 49 (10) 471s-487s.

116. Clifton, T. E, and George, M. J. Met Constr. 1969. 1 (9) 427-431.

117. Adams, D. F. and Mombrun, A. J. Metall, 1969 80 (10) 131-134.

118. Sopher, R. P. Jacobs, A. J. and Rieppel, P. J. Weld J. 1955 34 (11) 544s-552s.

119. Sopher, R. P. Weld J. 1958, 37 (11) 481s-492s.

120. Cremisio, R. S. and Koffler, W. T. Weld. J. 1967, 46 (6) 259s-265s.

121. Inagaki, M. Trans. Nat. Res. Inst. Metal (Japan), 1964. 6, 39-46.

122. Dimbylow, C. S. The hot tensile behaviour of copper base casting alloys. Report AMTE (M)/R79/007.

123. Gavin, S. A. Ph.D. Thesis Cranfield Institute of Technology 1978.

124. Yeniscavich, W. Welding Research Council symposium, "Methods of high-alloy weldability evaluation" AWS Spring Meeting, 1969.

125. Heuschkel, J. Weld, J. 1956. 35 (12) 569s-581s.

126. Thompson,. R. G. and Genculu, S. Weld J., 1983. 62 (9) 337s-345s.

127. Williams, C. S. Weld J., 1963, 42 (1) 1s-8s.

128. Duvall, D. S. and Owczarski, W. A. Weld J., 1967, 46 (9) 423s-432s.

129. Phillips, R. H. and Jordan, M. F. Metals Tech, 1977. 4 396-405

130. Yorkshire Imperial Metals. British Patent No. 1 040 884.

131. Yorkshire Imperial Metals. British Patent No. 1 144 334.

132. Davies, O. L. Design and analaysis of industrial experiments Oliver and Boyd. 2nd. ed. 1956.

133. Norrish. J. Private Communication.

134. Fenn, R. Ph.D Thesis, University of Aston, 1977.

135. De Perdigao, S. C. Ph.D Thesis University of Aston, 1981.

136. Wilber, C. A. and Bucher, J. H. Electron fractography of high temperature, high strain rate fracture. ASTM STP 493. Applications of electron microfractography to materials research. ASTM, 1971. 80-96.

137. McDonald Schectky. L. Private Communication.

138. Timothy, J. P. M. M.Sc. Thesis University of Aston, 1983.

139. Zenkova, E. K. and Glikman, E. E. Weld. Prod, 1980. 27 (6) 5-6.

ACKNOWLEDGEMENTS

The author wishes to thank Professor R. H. Thornley, Head of the Department of Mechanical and Production Engineering, for the use of experimental facilities throughout this work. I would like to extend my gratitude to the International Copper Research Association who financed the major part of the work, and to the Ministry of Defence (Navy) who supported the work on the IN768 alloys.

I would also extend my thanks to Dr. M. F. Jordan for his helpful supervision; to Mr. C. Smith for many useful discussions; to Dr. J. L. Aston for advice on experimental design and statistical analysis; and to the late Mr. A. Smith and other technical staff of the University for their invaluable assistance with experimental work.

In conclusion, I would like to thank Mrs. V. M. Shaw for carrying out the typing of this thesis; and finally, my wife Beverley, for providing moral support and encouragement throughout the duration of my research.